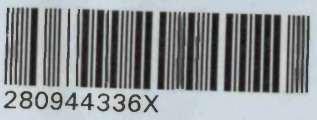

UNIVERSITY OF LONDON THESIS

Degree PhD Year 2007 Name of Author MELANIE DENISE WHITE

RNA INTERFERENCE AS A THERAPEUTIC APPROACH IN PRION DISEASE

Melanie Denise White

MRC Prion Unit

Institute of Neurology

University College London

Submitted for the degree of Doctor of Philosophy to the University of London

2007

Supervisors

Dr Giovanna Mallucci

Prof John Collinge

ProQuest LLC
789 East Eisenhower Parkway
P.O. Box 1346
Ann Arbor, MI 48106-1346

ABSTRACT

Prion diseases are fatal, transmissible neurodegenerative disorders characterised by accumulation throughout the brain of PrP^{Sc}, an abnormally folded isoform of the normal cellular prion protein, PrP^{C}. PrP^{Sc} is associated with infectivity but is not directly neurotoxic and targeting it is of limited efficacy in prion therapeutics. However, PrP-null mice are resistant to prion infection and neurotoxicity. Transgene-mediated depletion of neuronal PrP^{C} in mice with established prion infection reverses early spongiosis, neuronal loss and cognitive deficits, and prevents clinical disease progression. Thus, reducing PrP^{C} expression in the brain through extrinsic means is likely to be an effective therapy for prion diseases.

RNA interference can be exploited to mediate gene silencing and can be stably achieved in non-dividing cells such as neurons by incorporation of the small interfering RNAs into replication-deficient lentiviruses.

The work described in this thesis strongly validates the use of lentiviral-mediated RNA interference as a therapeutic approach in prion disease. Reducing PrP^{C} expression with siRNA duplexes enabled clearance of PrP^{Sc} and infectivity from prion-infected cells *in vitro*. Lentiviruses constructed to express the interfering sequences demonstrated effective reduction of PrP^{C} expression *in vitro*. Stable expression of the interfering RNA molecules *in vivo* through lentiviral transduction of the hippocampus reduced local pathology and significantly prolonged survival in a mouse model of prion disease. This represents an important and novel advance in the treatment of established prion disease with relevance for all prion strains.

TABLE OF CONTENTS

LIST OF FIGURES

LIST OF FIGURES

LIST OF TABLES

ACKNOWLEDGEMENTS

Thanks to the many people who have played an active role in helping and supporting me along the way.

To my supervisor, Dr Giovanna Mallucci for her guidance and enthusiasm, the MRC for funding, and head of department, Prof John Collinge, for making it possible.

Cheers to the other student inmates of the MRC Prison Unit past and present for support and solidarity. In particular, Dr Patrick Lewis, Dr Mark Kristiansen, the legendary Dr Gaia Skibinski, Dr Lisa Stone, Paresh Shah, Ruth Chia, Francesca Achilli, and my conference buddy Pelagia Deriziotis. Special mention to Marie O'Shea, not just a student and a friend, but also a housemate.... Very brave of you indeed!

Thanks to other non-student colleagues too...
Sharon Cooper, Kevin Williams, Dr Tim Szeto and Prof Tony Clarke for general hilarity, letting me rant and aiding my alcohol consumption.
The histology girls, and Catherine Elliot in particular, for much hard work and rewarding gossip. Julie Underwood for her efficient management and endless good cheer in the face of a continually demanding *in vivo* experiment.

Many thanks to Michael Farmer who came on board at a low point of the project and whose hard work and calming influence helped to turn the tide.

Special thanks to Matt Simpson, my long-suffering boyfriend who came along for the rollercoaster ride and took all the accompanying drama in his stride without ever missing a beat.

Finally, special thanks to my Nana, Betty, the most loving person I know and my Grandad, Darcy, the original family star, modest enough to let the rest of us shine. Your unconditional love and support has helped make me the person I am today, so this is for you, Nana and Grandad...

ABBREVIATIONS

All amino acid abbreviations as standard

AEBSF 4-(2-aminoethyl)-benzenesulphonyl fluoride

AHP after-hyperpolarisation potential

bp base pairs

BSE bovine spongiform encephalopathy

CJD Creutzfeldt-Jakob disease

CMV cytomegalovirus

CNS central nervous system

cPPT central polypurine tract

Cre site-specific recombinase from phage P1

CSF cerebral spinal fluid

CWD chronic wasting disease

DMSO dimethyl sulphoxide

Dpl PrP doppel protein encoded by *Prnd*

DNA deoxyribonucleic acid

dpi days post-inoculation

dsDNA double-stranded DNA

dsRNA double-stranded RNA

ECL enhanced chemiluminescence

ELISPOT Enzyme-linked immunosorbent spot assay

EtOH ethanol

FACS fluorescent-activated cell sorting

fCJD familial Creutzfeldt-Jakob disease

FCS foetal calf serum

FDC follicular dentritic cell

FFI fatal familial insomnia

Floxed term describing a DNA sequence flanked by *lox*P sites

gDNA genomic DNA

GFAP glial fibrillary acidic protein

GFP green fluorescent protein

GPI glycosyl phosphatidyl inositol

Grb2 growth factor receptor-bound protein 2

GSS Gerstmann-Sträussler-Scheinker disease

H&E haematoxylin and eosin

Ha hamster

HIV human immunodeficiency virus

HRP horse radish peroxidase

i.c. intracerebrally

iCJD iatrogenic Creutzfeldt-Jakob disease

ID infectious doses

ID_{50} infectious dose with 50 % attack rate

Ig immunoglobulin

IU infectious units

kb kilobase pairs

kDa kilo Daltons

LD_{50} lethal dose with 50 % attack rate

loxP recognition site for Cre recombinase

LV Lentivirus

M molar

MAP2 microtubule-associated protein 2

MEM minimal essential medium

MeOH methanol

M*lox*P construct for expression of the floxed *Prnp* ORF by the CosSHaTet expression vector

Mo mouse

MRI magnetic resonance imaging

mRNA messenger ribonucleic acid

neo neomycin resistance gene amino 3'-glycosyl phosphotransferase

ABBREVIATIONS

NFH neurofilament heavy chain gene

NFH-Cre transgenic construct for the expression of Cre under the NFH promoter and intragenic elements

nNOS neuronal nitric oxide synthase

ORF open reading frame

PAGE polyacrylamide gel electrophoresis

PBS phosphate buffered saline

PBST PBS containing Tween 20

pi post-inoculation

PK proteinase K

PMCA protein misfolding cyclical amplification

PNS peripheral nervous system

PRNP human PrP genetic transcript

Prnp mouse PrP genetic transcript

$Prnp^{0/0}$ transgenic mouse lacking PrP genetic transcript

PrP prion protein

$PrP^{27\text{-}30}$ protease resistant core of PrP^{Sc}

PrP^{C} cellular isoform of prion protein

PrP^{RES} PrP that is partially protease resistant and may or may not be infectious

PrP^{Sc} disease associated prion protein

PVDF polyvinylidene fluoride transfer membrane

PTGS post-transcriptional gene silencing

RML Rocky Mountain Laboratory (mouse adapted scrapie)

RNA ribonucleic acid

RNAi RNA interference

rpm rotations per minute

rPrP recombinant PrP

RT-PCR reverse transcriptase polymerase chain

Sc237 hamster adapted scrapie

SCA scrapie cell assay

sCJD sporadic Creutzfeldt-Jakob disease

SDS sodium dodecyl sulphate

shRNA short hairpin RNA

siRNA short interfering RNA

ssDNA single-stranded DNA

ssRNA single-stranded RNA

SOD superoxide dismutase

Sprn mouse Shadow of Prion gene transcript

STI1 stress inducible 1 protein

TBST tris buffered saline containing tween 20

Tg transgenic

TME transmissible mink encephalopathy

Tris 2,3-dibromopropyl phosphate

TSE transmissible spongiform encephalopathy

TU transducing unit

Tween 20 polyoxyethylene (20) sorbitan monolaurate

U units

v/v volume to volume ratio

vCJD variant Creutzfeldt-Jakob disease

VSV-G vesicular stomatitis virus envelope

wpi weeks post-inoculation

w/v weight to volume ratio

WPRE woodchuck hepatitis posttranscriptional regulatory element

INTRODUCTION

1.1 The prion diseases and the prion protein gene

1.1.1 The prion diseases

Transmissible spongiform encephalopathies (TSEs), more commonly known as prion diseases, are fatal neurodegenerative diseases of humans and animals (Collinge, 1998). They include scrapie of sheep, bovine spongiform encephalopathy (BSE) of cattle (Hope et al., 1989), chronic wasting disease of mule deer and elk (Williams and Young, 1993), and the human diseases Creutzfeldt-Jakob disease (CJD), Gerstmann-Straussler-Scheinker syndrome (GSS), fatal familial insomnia (FFI), kuru and variant CJD (vCJD). Pathologically, they are characterised by spongiform change, neuronal cell loss, astrocyte proliferation, and frequently, deposition of amyloid plaques containing insoluble aggregates of prion protein. They can be transmitted experimentally both within and between mammalian species by inoculation or ingestion of prion-contaminated material and are unique in having sporadic, inherited and acquired origins.

Scrapie; a unique class of transmissible diseases

Scrapie, a TSE of sheep, was first documented in a parliamentary enquiry in 1755 and has been studied extensively as a model of prion diseases. The disease is characterised by a loss of co-ordination, an uncontrollable urge to itch, excitability and progressive

paralysis resulting in death. The neuropathological hallmarks of scrapie include global neuronal loss and cytoplasmic vacuolation: the spongiform degeneration that characterizes the TSEs (Foster et al., 2001).

The first experimental transmission of scrapie was achieved in 1936 through inoculation of healthy sheep with spinal cord from an affected sheep (Cuillé and Chelle, 1936). Accidental transmission occurred when lymphoid tissue used to vaccinate sheep against louping ill virus caused scrapie in the inoculated sheep (Gordon, 1946). This also provided the first demonstration of the unusual resistance of the infectious agent to chemical treatment as the lymphoid tissue used to make the vaccine had been formalin fixed. The observation that formalin failed to inactivate the infectious agent contributed to the proposal of revolutionary new theories that the infectious agent lacked nucleic acid (Alper et al., 1967) and transmission occurred via a protein-only mechanism (Griffith, 1967).

During the 1950s, a fatal neurological disease called kuru reached epidemic proportions amongst the eastern highland Fore people of Papua New Guinea. This was the first human TSE to be defined as such and striking similarities with scrapie pathology were quickly recognised (Gajdusek and Zigas, 1957). These observations prompted the suggestion that kuru, like scrapie, may be an infectious disease (Hadlow, 1959). Inoculation of chimpanzees with brain homogenate from a kuru patient resulted in transmission of the disease, confirming its infectious nature (Gajdusek et al., 1966). The mode of transmission was proposed to be via consumption of contaminated material during ritual cannibalism practiced by the Fore people (Alpers, 1969). Banning the practice in the late 1950s resulted in a near total disappearance of the disease,

substantiating its cannibalistic origin. No new cases have been recorded in people born since 1959 and the 11 cases documented between 1996 – 2004 in people born prior to 1959 reflect the extremes of the incubation period of kuru in some individuals (Collinge et al., 2006).

Another outbreak of prion disease occurred in the mid 1980s amongst the UK cattle population in the form of BSE, stimulating increased research into this unusual family of diseases. The origin of BSE, or 'mad cow disease' as it became commonly known, is unexplained but the impact of the initial infection was amplified by reprocessing of infected carcasses into cattle feed, resulting in a full-scale epidemic. This contaminated fodder was also fed to other animals and led to identification of new TSEs in exotic ungulates (Kirkwood et al., 1990), domestic cats (Wyatt et al., 1991) and zoo animals (Kirkwood and Cunningham, 1994). The neuropathological and molecular characteristics of these TSEs were nearly identical to those of BSE, reflecting a common origin (Collinge et al., 1996;Hill et al., 1997). The transmission of BSE to other species raised concerns about the possibility of an epidemic in humans and in 1996 a new human prion disease, variant CJD, was identified (Will et al., 1996). This aggressive new disease was shown to be due to exposure to BSE (Collinge et al., 1996;Hill et al., 1997;Bruce et al., 1997) and prompted further research into the pathogenesis and aetiology of prion diseases.

The human prion diseases

The human TSEs share many characteristics with their animal counterparts including pathological features and similar disease progression. With an annual incidence of one

to two cases per million worldwide, they are rare, but are well known due largely to the kuru and BSE epidemics. Intense research into the human prion diseases has revealed a range of closely related, yet distinct, disorders. They can be inherited, acquired or sporadic in origin and are traditionally categorised as the clinicopathological syndromes of Creutzfeldt-Jakob disease (CJD), Gerstmann-Straussler-Scheinker syndrome (GSS), fatal familial insomnia (FFI) and kuru.

Sporadic, or classical, CJD accounts for 85% of the human prion diseases and is recognized by occurrence of a rapidly progressive dementia with myoclonus and development of movement disorders such as tremor, spasticity and rigidity. The mean age of onset is 65 years and the clinical course is rapid with an average duration of 7.6 months. Abnormal electro-encephalogram (EEG) recordings are common with characteristic periodic sharp-wave complexes. Definitive diagnosis requires histopathological confirmation of extensive spongiform degeneration and neuronal loss, accompanied by gliosis and deposits of prion protein within the brain. Although sporadic in origin, CJD is also transmissible, as demonstrated by experimental passage to chimpanzees (Gibbs et al., 1968;Gajdusek and Gibbs, 1971), and occasional iatrogenic transmissions to humans (Brown et al., 1985;Billette de Villemeur et al., 1991;Martinez-Lage et al., 1994;Cavanagh and Hogan, 1999).

Around 14% of human prion diseases are inherited and result from coding mutations in the human prion protein gene *PRNP*. These include the diseases traditionally classified as familial Creutzfeld-Jakob disease (fCJD), GSS and FFI. They are autosomal dominant in inheritance and result either from expansion of an octapeptide repeat in the normal sequence of the prion protein, non-conservative point mutations or stop

mutations within the *PRNP* open reading frame (ORF). Over 30 different pathological mutations have been described which produce a wide spectrum of clinical phenotypes but generally have an earlier onset and longer disease duration than sporadic prion disease (reviewed in: Mead, 2006). The core features of the inherited prion diseases include rapidly progressive dementia with myoclonus and pseudoperiodic EEG discharges in fCJD, slow progression of ataxia accompanied by late onset dementia in GSS, and refractory insomnia, dysautonomia and motor signs in FFI, although there can be broad phenotypic and pathological variation between individuals with the same mutation (Collinge et al., 1992;Tranchant et al., 1992;Mallucci et al., 1999).

The acquired human prion diseases include kuru, iatrogenic CJD (iCJD) and variant CJD (vCJD). The name kuru means shaking or trembling and is used by the Fore people to describe the progressive cerebellar ataxia that characterizes this disease. Mood and personality changes are often present and dementia commonly develops during the final stages of the disease (Gajdusek and Zigas, 1957). Death occurs, often through starvation, after a disease course of around one year. Iatrogenic CJD is very rare and results from exposure of patients to prion-infected materials during medical treatment. Transmission has been described in recipients of contaminated growth hormone and gonadotrophin as well as dura mater and corneal grafts (Gibbs et al., 1985). More recently, transfusion of blood from a donor with pre-symptomatic vCJD resulted in transmission of disease to recipients, sparking further public health concerns (Llewelyn et al., 2004;Peden et al., 2004;Wroe et al., 2006). Peripheral inoculation usually results in prolonged incubation times with marked ataxia and late-onset dementia, whereas

intracerebral inoculation causes a rapid disease course with prominent early dementia (Collinge, 1998).

The most recently described acquired human TSE, vCJD, emerged in the mid 1990s in the wake of the UK BSE epidemic (Will et al., 1996). The clinicopathological features were unlike those of sporadic CJD, with a mean age of onset of 29 years and patients as young as 16 being diagnosed. The initial symptoms are mainly neuropsychiatric and behavioural, followed by ataxia and movement disorders. Unlike sCJD, dementia and myoclonus occur during the later stages of disease and EEG abnormalities are frequently absent. The disease course is also longer than that of sCJD, with a mean duration of 14 months (Collinge, 2001). None of the patients had *PRNP* mutations or iatrogenic exposure and the possibility of a new human prion disease resulting from exposure to BSE-contaminated food was considered. Transmission studies performed in mice demonstrated a similar neuropathological profile between BSE and vCJD and molecular studies of PrP^{Sc} from affected bovine and human brains revealed similar biochemical characteristics (Raymond et al., 1997;Lasmézas et al., 1996;Hill et al., 1997;Prusiner, 1997;Manuelidis et al., 1997;Scott et al., 1999). It is now widely accepted that vCJD arose as a result of human infection with BSE prions.

The unusual nature of the scrapie agent and the protein-only hypothesis

The unusual nature of the scrapie agent first recognised by its resistance to formalin (Gordon, 1946), was further demonstrated when its infectivity was also shown to resist inactivation by high temperature and ultraviolet light (Alper et al., 1966). Examination of infected and infectious tissues revealed no evidence of bacteria or virions and it was

proposed that the infectious agent was devoid of nucleic acid (Alper et al., 1967), and composed mainly of protein. That a protein alone might self-replicate and be infectious was first proposed in 1967 by Griffith (Griffith, 1967) and ran counter to the central dogma of molecular biology. The theory did not gain credence until 1982, when Prusiner achieved substantial purification of the scrapie agent and showed its physiochemical properties were characteristic of proteins, not nucleic acids (Prusiner, 1982). In a seminal paper, he coined the term 'prion' to describe the *pro*teinaceous *in*fectious particle of the scrapie agent. Extending Griffith's theory from over a decade before, Prusiner set forth the 'protein-only hypothesis' in which he stated that a protein was capable of self-replication within vulnerable host cells and was the causative agent of scrapie. Shortly after, a scrapie-associated protein which correlated with infectivity was isolated from infected hamster brain (McKinley et al., 1983). This protein was found to be aggregated, highly insoluble in non-ionic detergents and partially protease resistant with a molecular mass of 27 – 30kDa. In accordance with the protein-only hypothesis, it was proposed to be the major constituent of the scrapie agent and was designated the *pr*ion *p*rotein, or PrP.

Purification of PrP to homogeneity allowed determination of its N-terminal amino acid sequence (Prusiner et al., 1984) and led to the recovery of PrP cDNA clones from scrapie-infected Syrian hamster (Oesch et al., 1985) and murine (Chesebro et al., 1985) brain libraries. PrP was shown to be encoded by a host gene, called *Prnp*, which was equally expressed in both infected and uninfected animals (Chesebro et al., 1985). The normal product of *Prnp* was a protease sensitive protein of 33 – 35kDa and was designated PrP^{C}, for cellular prion protein. The previously isolated 27 – 30kDa disease-

specific protein was found to be a protease resistant core of a 33 – 35kDa protein, designated PrP^{Sc} for scrapie-associated prion protein. These two isoforms of PrP had identical primary structures but differed in secondary or tertiary structure, prompting Prusiner to update the protein-only hypothesis by proposing that the central mechanism of infectivity involved a change of the normal cellular isoform, PrP^{C}, into the scrapie-associated isoform, PrP^{Sc} (Prusiner, 1989). This change is thought to be a post-translational conformational alteration which would initiate a catalytic cascade in which new molecules of PrP^{Sc} are able to recruit further PrP^{C} molecules for conversion. This hypothesis neatly provides an explanation for all three categories of prion disease through the same mechanism. In sporadic disease, rare spontaneous conversion of PrP^{C} into PrP^{Sc} would instigate the disease process, whereas familial disease may arise as the result of destabilizing mutations in PrP^{C} facilitating conversion. Acquired prion diseases would arise through introduction of foreign PrP^{Sc} molecules capable of converting host PrP^{C}.

Further support for this notion comes from the field of yeast genetics where propagation of the [PSI+] and [URE] phenotypes occurs through a prion-like mechanism involving conformational templating of proteins in the absence of nucleic acids (reviewed in: Kushnirov and Ter-Avanesyan, 1998;Liebman and Derkatch, 1999). More recently, a normal, physiological function for this mechanism has been proposed for a member of the cytoplasmic polyadenylation element binding protein (CPEB) family, where a conformational change is associated with translation of mRNAs involved in memory storage (Si et al., 2003;Berger-Sweeney et al., 2006).

Two main models have been proposed for the PrP conversion process including a heterodimer model in which PrP^{Sc} binds PrP^{C} and acts as a template, forcing refolding of PrP^{C} (Prusiner, 1991), and a nucleated or seed polymerization model in which the two isoforms normally exist in an equilibrium skewed towards PrP^{C} but mutations or the presence of aggregated seed PrP^{Sc} shifts the equilibrium towards PrP^{Sc} replication (Jarrett and Lansbury, 1993;Caughey et al., 1995).

Conversion of PrP^{C} to PrP^{Sc} has been achieved in cell-free systems *in vitro* but infectivity of the *de novo* generated PrP^{Sc} could not be established (Kocisko et al., 1994;Kocisko et al., 1995;Hill et al., 1999). Recently, a more sophisticated *in vitro* conversion technique called Protein Misfolding Cyclical Amplification has allowed much more efficient replication and detection of PrP^{Sc} (Bieschke et al., 2004;Sarafoff et al., 2005) which is infectious upon intracerebral inoculation of hamsters, although with a significantly prolonged incubation time (Castilla et al., 2005).

The identity of the infectious agent is still debatable and even in highly purified infectious fractions, only one in 10^5 PrP^{Sc} particles is infectious (Bolton and Bendheim, 1991). The most infectious prion protein particles have been shown to be non-fibrillar particles containing 14 – 28 PrP molecules with infectivity significantly reduced in oligomers larger and smaller than this (Silveira et al., 2005). Partial protease resistance is not consistently associated with infectivity and noninfectious protease resistant PrP can be produced (Riesner et al., 1996). In FFI patients, PrP^{Sc} is often not detectable in the brain, yet the disease is transmissible (Tateishi et al., 1995;Collinge et al., 1995). There is, however, compelling genetic and biochemical evidence that some form of PrP

is the essential, and possibly only, component of the infectious agent (Prusiner, 1989;Weissmann, 1996;Legname et al., 2004).

1.1.2 The prion protein gene, *Prnp*, and its product, PrP

Prnp gene organization and PrP biosynthesis

In the mid-1980s, the genes encoding scrapie-associated PrP in mice and hamsters were found to be host specific (Oesch et al., 1985;Chesebro et al., 1985;Basler et al., 1986;Locht et al., 1986). Shortly after, the prion genes of humans, rats, goat, sheep, mink, cattle and chicken were cloned. Human *PRNP* mapped to the short arm of chromosome 20 and the mouse *Prnp* mapped to the homologous murine chromosome 21(Sparkes et al., 1986). Over 85% homology in the amino acid sequence was found between mammalian species and hybridization studies with hamster PrP indicated homologous sequences in Drosophila and yeast (Westaway and Prusiner, 1986). The PrP gene is a single copy gene consisting of two (or three differentially spliced) exons in humans (Puckett et al., 1991) and hamsters (Basler et al., 1986) and three exons in mice (Westaway et al., 1994). The ORF is entirely contained within the second exon in all species examined (Kretzschmar et al., 1986;Puckett et al., 1991), and encodes 253 – 257 amino acids; 254 in the mouse. The primary sequence of PrP contains a hydrophobic signal sequence of 22 – 24 C-terminal amino acids which targets the newly synthesized polypeptide to the endoplasmic reticulum (ER). Here, PrP may be glycosylated on two N-linked glycosylation sites and a single disulphide bond is formed between two C-terminal cysteines (Stahl and Prusiner, 1991;Rudd et al., 2001). Glycosylation of PrP is

variable, resulting in un-, mono-, or diglycosylated species (Haraguchi et al., 1989) and the conservation of both N-linked glycosylation sites in all mammalian PrP genes suggests functional significance of this modification. Subsequent cleavage of the signal sequence precedes addition of a glycosyl-phosphatidyl-inositol (GPI) anchor (Stahl et al., 1987). PrP is then trafficked through the Golgi apparatus where further processing of the N-linked oligosaccharides occurs before the protein is transported to the cell surface. The mature polypeptide is attached to the cell surface by its GPI anchor (Stahl et al., 1993) which localizes the protein predominantly to detergent-resistant microdomains (Vey et al., 1996). From here, the protein may be released through cleavage of the GPI anchor or subjected to endocytosis whereby it can cycle between endocytic vesicles and the cell surface (Shyng et al., 1993).

Prnp expression

Prnp is expressed in the brain, spinal cord, peripheral nervous system, ganglia and nerve trunks of the autonomic nervous system of the developing mouse embryo from 13.5 days (Manson et al., 1992). In the adult mouse, high levels of PrP mRNA have been detected in the brain, with intermediate levels in heart and lung, and lower levels in the spleen (Oesch et al., 1985;Caughey et al., 1988). Post-natally, PrP gene expression is developmentally regulated in the brain (Mobley et al., 1988;McKinley et al., 1988), and in the adult, PrP^C is clustered at the neuronal surface in coated pits, consistent with endocytic trafficking (Madore et al., 1999). Although PrP mRNA is detectable in all neurons, only a subset express PrP^C protein. Neurons in the cerebral cortex generally

direct PrP^C to their soma and dendrites, whilst those in the brainstem and spinal cord direct it to their axons (Madore et al., 1999).

High PrP^C expression is also found in the parasympathetic and enteric nervous systems, the neuroendocrine system, antigen-presenting cells and subpopulations of lymphocytes (Ford et al., 2002).

PrP structure

Expression of recombinant PrP in *E.coli* allowed determination of the three dimensional structure of hamster, mouse and human PrP using nuclear magnetic resonance (Riek et al., 1996;James et al., 1997;Riek et al., 1998;Hosszu et al., 1999;Liu et al., 1999;Zahn et al., 2000). The recombinant protein was shown to consist of a structured C-terminal domain containing three alpha helices and two short beta anti-parallel sheets, plus an unstructured N-terminal domain. The structure of PrP^{Sc} has not been resolved due to its insolubility and tendency to form aggregates. Low resolution studies have indicated that PrP^{Sc} contains ~43% beta sheet and 34% alpha helix, in contrast to the 43% alpha-helical content of PrP^C which contains only 3% beta sheet (Pan et al., 1993). This observation led to the suggestion that the infective process results in a switch from the predominantly alpha-helical PrP^C to the predominantly beta sheet PrP^{Sc} (Caughey et al., 1991;Gasset et al., 1993;Pan et al., 1993). The observed increase in beta sheet content in PrP^{Sc} has been proposed to result from refolding of the flexible tail of PrP^C (Riek et al., 1997).

The N-terminal region of PrP^C contains a series of highly conserved octapeptide repeats which are implicated in copper binding (Brown et al., 1997a) and may play a role in the normal function of the prion protein (Pauly and Harris, 1998;Brown, 1999).

1.1.3 Investigations into PrP function

Prnp knockout models

Despite extensive research, the function of PrP^C is still unknown. The observation that *PRNP* is a highly conserved gene in mammals which is tightly regulated developmentally (Manson et al., 1992) and post-natally (Lazarini et al., 1991) led to the assumption that PrP^C had an essential biological function. Knockout mouse models of *Prnp* were produced by homologous recombination in embryonic stem cells in an attempt to elucidate the function of PrP^C. The first knockout model created was designated $Prnp^{0/0}$ (also referred to as the 'Zurich I' mouse), and was made by replacing codons 4 – 187 of the *Prnp* ORF with a *neo* gene cassette (Bueler et al., 1992). Shortly after, a second line designated $Prnp^{-/-}$ was created by disruption of the ORF by insertion of a *neo* cassette at a unique restriction site (Manson et al., 1994a). In both of these lines, the knockout was restricted to the ORF and the 5' splice site was unaffected, unlike in subsequent models (Sakaguchi et al., 1996;Moore et al., 1999). The mice were created on different genetic backgrounds and did not express detectable PrP^C. Unexpectedly, both lines were developmentally and phenotypically essentially normal. The possibility that functional compensation was occurring developmentally in these knockout models was eliminated by the creation of a conditional, adult-onset *Prnp*

knockout mouse (Mallucci et al., 2002). This model was created by crossing mice carrying a 'floxed' *Prnp* gene on a $Prnp^{0/0}$ background with $Prnp^{0/0}$ mice expressing Cre recombinase under the control of the neurofilament heavy chain (NFH) promoter. The NFH promoter here becomes active at around 9 - 10 weeks of age, leading to Cre-mediated excision of *Prnp* in neuronal cells. The mice remained healthy following ablation of neuronal PrP^{C}, confirming the limited effects of loss of PrP function found in previous models.

Three lines of PrP knockout mice did develop a neurodegenerative phenotype (Sakaguchi et al., 1996;Moore et al., 1999;Rossi et al., 2001), but this was shown to result from ectopic expression of the downstream *Prnd* gene due to deletion of a splice acceptor site 5' to the *Prnp* ORF in exon three. *Prnd* encodes the Dpl protein, and exon skipping leads to splicing of the Dpl-encoding exon to the first two exons of *Prnp*, resulting in expression of Dpl driven by the *Prnp* promoter (Rossi et al., 2001;Flechsig et al., 2003).

Putative functions of PrP

Despite the lack of gross abnormalities in PrP null mice, intensive research has revealed some subtle phenotypic differences. Both synaptic function (Collinge et al., 1994;Manson et al., 1995) and intrinsic features of hippocampal cells (Colling et al., 1995;Mallucci et al., 2002) have been shown to be altered upon PrP knockout. PrP null mice also have altered circadian rhythms (Tobler et al., 1996), an intriguing finding in light of the sleep disturbances characteristic of the human inherited prion disease, FFI. Changes in the membrane localization of neuronal nitric oxide synthase (nNOS) also

occur following *Prnp* knockout, suggesting a role for PrP^C in targeting nNOS to the cholesterol-rich microdomains it usually occupies (Keshet et al., 1999).

PrP binds copper with femtomolar efficiency (Brown et al., 1997a;Brown, 2001;Jackson et al., 2001) and is endocytosed, leading to suggestions that it may act as a copper transporter in the brain (Pauly and Harris, 1998;Brown, 1999).

Reduced Cu^{2+}/Zn^{2+}-dependant SOD activity has been reported *in vivo* in $Prnp^{0/0}$ mice and neurons derived from these mice exhibit increased vulnerability to oxidative stress *in vitro* (Brown et al., 1997b). A neuro-protective role for PrP^C is further supported by the observations that serum-deprivation induced apoptosis is significantly higher in cultured cells in $Prnp^{0/0}$ cell lines (Kuwahara et al., 1999), and PrP^C protects human primary neurons (Bounhar et al., 2001) and yeast (Li and Harris, 2005) against Bax-mediated cell death. Expression of N-terminally truncated PrP in transgenic mice results in extensive degeneration and death of cerebellar granule neurons by 8 weeks of age (Shmerling et al., 1998). That this can be rescued by expression of wild-type PrP^C implies a neuroprotective signaling function of the N-terminal region of PrP.

The cell surface location of PrP^C and its observed recycling between the plasma membrane and endocyctic compartments led to speculations of a role in cell adhesion or cell signaling. Interaction between PrP^C and neuronal cell adhesion molecules (Schmitt-Ulms et al., 2001), and the observation that PrP^C over-expression increases cell aggregation in a neuronal cell line (Mange et al., 2002), tend to support a role in cell adhesion.

PrP^C has been implicated in cell signaling by the demonstrations that binding to stress-inducible protein 1 (STI1) mediates neuro-protection through a cAMP/PKA signaling

pathway (Zanata et al., 2002), and antibody-mediated cross-linking of PrP^C triggers signal transduction through the non-receptor tyrosine kinase Fyn (Mouillet-Richard et al., 2000). PrP^C has also been shown to interact directly with proteins involved in signaling pathways, including Grb2, Synapsin Ib and Pintl (Spielhaupter and Schatzl, 2001) and to mediate neuritogenesis, cell differentiation and memory consolidation through an interaction with laminin (Graner et al., 2000a;Graner et al., 2000b;Coitinho et al., 2006).

Role of PrP in prion disease

A number of key observations highlight the important role the prion protein has in defining the onset and phenotype of prion diseases. The length of prion disease incubation time correlates with two coding mutations in the murine *Prnp* gene at codons 108 and 189 (Westaway et al., 1987), suggesting a link between PrP structure and susceptibility to prion disease. This link is further supported by the observation that amino acid polymorphisms also influence the onset and phenotype of prion disease in sheep and humans (Prusiner, 1998;Collinge, 2001). In sheep, polymorphisms at three PrP codons, 136 (A/V), 154 (R/H) and 171 (R/H/Q), determine incubation time and susceptibility to scrapie (Tranulis, 2002). In humans, codon 129 is polymorphic for methionine (M) or valine (V) and this modulates the protease sensitivity of PrP^{Sc} (Parchi et al., 2000), and the kinetics of amyloid formation (Lewis et al., 2006). Homozygosity at codon 129 for either M or V is associated with increased susceptibility to sporadic CJD (Palmer et al., 1991) and iatrogenic CJD (Collinge et al., 1991), whereas heterozygosity has a protective effect against sporadic, acquired and some of the

inherited prion diseases (Collinge, 2001). All clinical cases of variant CJD studied to date have been homozygous for methionine at codon 129 of *PRNP* (Collinge, 2005) and the valine allele is protective against kuru (Lee et al., 2001).

The octapeptide repeat region of PrP appears to modulate prion replication and pathogenicity (Flechsig et al., 2000), and extension of repeat number is associated with earlier disease onset in a human kindred (Collinge, 2001).

But the most striking confirmation of the role of PrP in prion disease is the absolute requirement of the protein for disease susceptibility. PrP knockout mice are resistant to prion infection and unable to replicate infectivity (Bueler et al., 1993;Manson et al., 1994b) and incubation time is determined by *Prnp* gene dosage (Manson et al., 1994b;Safar et al., 2005). Prion inoculation of $Prnp^{0/0}$ mice with PrP-expressing neuroectodermal grafts results in damage and degeneration only in the PrP-expressing graft whilst surrounding $Prnp^{0/0}$ tissue remains unaffected (Brandner et al., 1996). Furthermore, depletion of neuronal PrP^{C} in mice with established prion infection reverses early spongiform change and prevents disease progression (Mallucci et al., 2003). This is despite continued accumulation of PrP^{Sc} in non-neuronal cells, reinforcing that expression of PrP^{C} is required in neurons for neurodegeneration and clinical disease.

The species barrier

Further emphasizing the central role of PrP^{C} in prion pathology is the finding that transmission of prions from one species to another is much less efficient than transmission within the same species – an effect called the 'species barrier'. This results

in extended incubation times upon passage from the first species into the second. Once transmission has been achieved between species, the barrier has been overcome and subsequent passages of infectivity to homologous hosts occur with normal efficiency and constant incubation times. Wild-type mice are resistant to hamster prions but this barrier can be overcome by the expression of hamster PrP in transgenic mice, demonstrating that the critical determinant of the species barrier is the primary sequence of PrP (Prusiner et al., 1990). PrP glycoform patterns and 3-dimensional structure are also thought to modulate prion species compatibility (reviewed in: Moore et al., 2005).

Subclinical disease

In some circumstances, prion infection may result in a subclinical disease state in which the animal harbours the infection without progressing to clinical symptoms. The species barrier which limits passage of hamster prions to mice results in a subclinical disease state in the inoculated mice (Race and Chesebro, 1998;Hill et al., 2000). The prions continue to replicate in the mice and are infectious upon subsequent passage to both hamsters and mice, but fail to cause clinical symptoms in the incubating mice. Infection of mice with low doses of prions can also result in subclinical disease despite high levels of PrP^{Sc} and infectivity in the brain (Taylor et al., 2000;Thackray et al., 2002;Thackray et al., 2003). Additionally, immunodeficient mice can accumulate PrP^{Sc} and infectivity whilst remaining asymptomatic (Frigg et al., 1999).

Prion strains

One of the most remarkable features of prion disease is the existence of distinct prion strains with well-defined heritable properties. These strains were originally characterized by incubation time and resultant neuropathology (Bruce et al., 1992), but they can additionally be differentiated on the basis of PrP^{Sc} distribution in the brain and physicochemical properties of PrP^{Sc}, including susceptibility to PK digestion, electrophoretic mobility following digestion and glycoform ratios (reviewed in: Bruce et al., 1996). As different prion strains can be serially propagated in inbred mice with the same *Prnp* genotype, they can not be encoded by the primary sequence of PrP. It is now thought that strain specificity is determined by PrP conformation and glycosylation. Different PrP conformers could interact with differing efficiencies and glycosylation may influence the neuropathological targeting of a strain (Collinge et al., 1996;DeArmond et al., 1997). It is known that different cell types may glycosylate proteins differently, therefore particular PrP^{Sc} glycoforms might replicate most favourably in cells expressing a similar PrP glycoform. This regional targeting could also explain the differences in incubation times between various strains with targeting of more critical brain regions resulting in shorter incubation periods.

Prion spread and neuroinvasion

Under natural conditions, prion diseases are usually acquired by oral infection in animals which results in much less efficient transmission and longer incubation times than intracerebral inoculation. Following infection, prions must spread from the periphery to the CNS before causing neurodegeneration. The first phase of infection

involves transport of the prions from the entry site to the lymphoreticular system in a process that involves myeloid dendritic cells (Huang et al., 2002). Prion replication then occurs within the lymphoreticular system (Kitamoto et al., 1991), with B cells playing a vital role in subsequent neuroinvasion (Klein et al., 1998). As PrP expression is not required in B cells, it is thought to be their role in the maturation of follicular dendritic cells (FDCs) that facilitates prion neuroinvasion. FDCs accumulate high levels of PrP^{Sc} during prion infection (Kitamoto et al., 1991), are crucial for efficient disease progression after oral scrapie inoculation (Mabbott et al., 2003) and infection of mice with ME7 prions (Brown et al., 1999), and they mediate faster neuroinvasion if positioned closer to splenic nerves (Prinz et al., 2003). Hence, the topography of lymphoid organs contributes to prion spread, but as there is no physical synapse between FDCs and sympathetic nerves (Heinen et al., 1995), it remains to be determined whether this is a passive process, or relies on active transport via mobile cells.

Following amplification in the spleen, prions are transferred to the CNS, presumably via the main innervation of the lymphoid system, the sympathetic nervous system. This route of spread is supported by the finding that chemical sympathectomy delays the onset of scrapie, whereas sympathetic hyperinnervation promotes splenic replication and neuroinvasion (Glatzel et al., 2001). Once the prions reach the CNS, the typical neuropathological changes associated with prion diseases commence.

Mechanisms of neurotoxicity

Various mechanisms have been proposed to explain neuronal cell death in prion diseases, but it is thought to occur largely by apoptosis (Hetz et al., 2003;Hetz and Soto, 2003;Cronier et al., 2004). Apoptosis has been described in the brains of patients with CJD, FFI and in scrapie-infected hamsters, mice and sheep (Hetz and Soto, 2003). PrP^{Sc}-induced apoptosis has been associated with the induction of ER-stress inducible chaperones and caspase activation both *in vitro* and *in vivo* (Hetz et al., 2003;Kristiansen et al., 2005). Caspases 3 and 8 were also shown to trigger apoptosis in prion-infected cells following mild proteasomal inhibition which resulted in formation of cytosolic PrP^{Sc}-containing aggresomes (Kristiansen et al., 2005). The authors propose it is the presence of these cytosolic aggresomes which is particularly pro-apoptotic. Aggresomes accompanied by proteasomal dysfunction have also been observed in uninfected cells over-expressing cytosolic PrP^{C} (Ma and Lindquist, 2001), but the more recent study suggests any resultant neurotoxicity was due to excessively large doses of proteasome inhibitors (Kristiansen et al., 2005).

Apoptosis may not be the only type of cell death responsible for neuronal loss in TSEs. No morphological evidence of apoptosis was found in prion-infected human biopsies using either ultrastructural (Sikorska et al., 2004) or light (Ferrer, 1999) microscopy and the features of cell death were more consistent with autophagy. More recently, a neuronal marker of autophagy, initially discovered as a gene up-regulated in TSEs, was found to be induced in the neurons of scrapie-infected mice, reinforcing the role of this pathway in neurodegeneration (Dron et al., 2005;Dron et al., 2006).

Although it is still largely unknown how the conversion of PrP^{C} to PrP^{Sc} causes neuronal cell death, the continued extraneuronal PrP^{Sc} accumulation observed in the otherwise healthy conditional knockout mice suggests it is only toxic if it occurs within neurons. Moreover, the finding that removing PrP^{C} expression, even in adult mice, has no gross phenotypic consequences (Mallucci et al., 2002), argues against loss of PrP^{C} being a central cause of the neurotoxicity of prion disease.

Traditionally, it was assumed that PrP^{Sc} itself is the toxic species, but this assumption was based largely on the temporal and anatomical correlation between PrP^{Sc} deposition and neuropathology and there are occasions when this correlation is weak or absent (Chiesa et al., 2001). There are some prion diseases in which PrP^{Sc} levels in the brain are very low, and conversely, subclinical disease states which show extensive PrP^{Sc} deposition without clinical symptoms (Hill et al., 2000;Hill and Collinge, 2003). Purified PrP^{Sc} (Hetz et al., 2003) and shorter fragments corresponding to a putative transmembrane domain (Forloni et al., 1993;O'Donovan et al., 2001) have both shown toxicity *in vitro*, arguing for a toxic gain of function of PrP^{Sc}.

However, PrP^{C} with an altered transmembrane topology, ^{Ctm}PrP, also causes neurotoxicity in a concentration-dependent manner and accumulates in an inherited prion disease, A117V, where PrP^{Sc} accumulation is rare (Hegde et al., 1998;Hegde et al., 1999;Stewart et al., 2005). The concept of a toxic gain of function for PrP^{C} is additionally supported by the finding that accumulation of even small amounts of cytosolic PrP^{C} has been shown to be strongly neurotoxic *in vitro* and *in vivo* (Ma et al., 2002), suggesting a toxicity due to altered trafficking of PrP^{C}. But the data is conflicting, with evidence both for (Rane et al., 2004;Wang et al., 2004) and against

(Drisaldi et al., 2003;Roucou et al., 2003;Fioriti et al., 2005) cytosolic PrP^C being a neurotoxic species.

Whatever the toxic species is, it is clear that the major pathological changes in prion disease do not result from loss of PrP^C, and PrP^{Sc} does not cause neurotoxicity directly but exhibits its toxicity only where PrP^C is also expressed. It has been suggested that a neurotoxic intermediate, termed PrP^L, for lethal, may be formed during the conversion reaction (Hill et al., 2000;Hill and Collinge, 2003), mediating toxicity in a manner similar to Aβ oligomers in Alzheimer's disease (Hardy and Selkoe, 2002) and potential toxic intermediates in other protein misfolding disorders (Kayed et al., 2003). If this is the case, targeting either PrP^C, the substrate for conversion, or the conversion process itself, should both be valid therapeutic approaches.

1.1.4 Therapeutic approaches to prion disease

The uncertainties about the identity of the neurotoxic species and the possible mechanisms of neurodegeneration in prion diseases have complicated therapeutic approaches, meaning that prion diseases are invariably fatal and no therapy is currently available. Additionally, a lack of sensitive preclinical diagnostic tests means that diagnosis of prion disease presently relies on development of clinical symptoms which reflect advanced neurodegeneration. Pathogenesis studies in rodents have indicated that CNS damage and even subtle cognitive and behavioural changes occur long before appearance of conventional clinical symptoms (Cunningham et al., 2003;Mallucci et al., 2007). As neurodegeneration is already established by the time a diagnosis is made, the

therapeutic window is inevitably small, although reversal of early pathological (Mallucci et al., 2003) and cognitive changes (Mallucci et al., 2007) is possible if intraneuronal PrP^{C} conversion is halted.

As PrP^{Sc} is associated with both pathology and infectivity, many potential therapies have targeted this molecule. Several compounds have been identified which reduce PrP^{Sc} accumulation in prion-infected cell models including, Congo red, polyanionic compounds, amphotericin B, porphyrins and quinacrine, but *in vivo* results have been disappointing (reviewed in: Trevitt and Collinge, 2006). Many of these substances only have an effect if administered together with, or soon after, the prion inoculum and may simply reduce the effective titre of the inoculum instead of preventing pathogenesis. Pentosan polysulphate is one of the only agents to lengthen the incubation time in mice inoculated with prions intracerebrally (Doh-ura et al., 2004), but results have been discouraging in human prion disease patients (Todd et al., 2005;Whittle et al., 2006). Although PrP^{Sc} is defined as partially protease resistant, this is only a relative measure and natural clearance mechanisms do exist for this molecule. Compounds such as branched polyamines (Supattapone et al., 1999) and a tyrosine kinase inhibitor (Ertmer et al., 2004) are able to enhance the endogenous clearance of PrP^{Sc} *in vitro*. They do not, however, prevent *de novo* formation of PrP^{Sc}, meaning they will be of limited therapeutic value if the toxic species occurs upstream of PrP^{Sc} in the conversion reaction.

As the conversion process is now known to be central to the pathogenesis of prion diseases, many more recent potential therapeutic agents have aimed to inhibit this reaction either directly, or by targeting the substrate for conversion, PrP^{C}. In theory,

ligands which selectively bind PrP^C may prevent the conversion process by stabilising PrP^C or preventing its interaction with PrP^{Sc}. One recently identified class of molecules thought to act in this manner is degenerate phosphorothioate oligonucleotides which inhibit PrP^{Sc} formation *in vitro* and when delivered prophylactically *in vivo* (Kocisko et al., 2006). Unfortunately, these molecules do not cross the blood-brain barrier and rapid intracerebral infusion was not tolerated *in vivo*. Whilst a gradual infusion might circumvent this limitation, it still remains to be seen if these molecules can be effective when administered later in the course of infection.

Another class of therapeutic agents which seem to act by binding PrP^C and reducing its availability for conversion is anti-PrP antibodies. Antibodies against several PrP epitopes can inhibit PrP^{Sc} replication *in vitro* and transgenic mice expressing anti-PrP μ chains are protected against peripheral, but not central, prion infection (reviewed in: Trevitt and Collinge, 2006). Passive immunisation of peripherally infected mice with anti-PrP antibodies markedly reduced peripheral PrP^{Sc} accumulation but could not treat intracerebrally infected mice due to failure to cross the blood-brain barrier (White et al., 2003). Unfortunately, when administered intracerebrally, anti-PrP antibodies can cause severe neuronal apoptosis showing further investigation of the consequences of PrP binding and refinement of this approach is required (Solforosi et al., 2004).

Active immunisation methods have been limited by the immune tolerance of PrP, but some approaches to overcoming this have reported modest effects (Sigurdsson et al., 2002;Schwarz et al., 2003).

Once severe neuronal loss has occurred, any form of rescue is challenging. Replacement of lost neurons may be possible using embryonic stem cells (McKay, 1997), or neuronal

precursor cells (Gage, 2000;Alvarez-Buylla et al., 2000) but they would need to be *Prnp* null unless the prion infection could be eliminated.

To date, the only approach that is effective for the prevention of clinical disease in animals with established prion neuropathology is the removal of neuronal PrP^C through conditional knockout in transgenic animals (Mallucci et al., 2003). The demonstration that removing neuronal PrP^C is harmless in adult mice (Mallucci et al., 2002), and prevents prion disease progression (Mallucci et al., 2003) has confirmed the rational of therapies based on the removal or elimination of PrP^C. Prion replication continues in non-neuronal cells in these conditional knockout mice, demonstrating that global removal of PrP^C is not required for therapeutic benefit. Depleting neuronal PrP^C in prion-infected mice with early pathology appears to switch the infection to a subclinical state in which prions replicate and remain infectious but further neuropathology does not ensue.

In order to translate this approach into a viable therapy however, an extrinsic means of reducing PrP^C expression must be employed. Recent advances in the field of RNA interference have provided techniques for achieving this extrinsic removal of PrP^C.

1.2 RNA Interference

1.2.1 Post-transcriptional gene silencing

RNA interference is the general term for the process in which double-stranded RNA corresponding to a particular gene prevents or reduces the expression of that gene. It

was originally discovered fortuitously by researchers trying to deepen the colour of petunias through introduction of a pigment-producing gene driven by a powerful promoter (Napoli et al., 1990). Instead of the more intense colour expected, many of the flowers were variegated or even white. The researchers called this phenomenon "cosuppression" because the expression of both the exogenous and the endogenous genes were suppressed (reviewed in: Jorgensen, 1990). Initially, the effect was thought to be specific to petunias, but cosuppression has since been found to occur in many species of plants, nematodes, Drosophila and mammals (Bingham, 1997;Matzke et al., 2001;Vance and Vaucheret, 2001;Waterhouse et al., 2001;Kavi et al., 2005).

The mechanism underlying this was unclear, but evidence from a number of different studies suggested the silencing was at the post-transcriptional level (post-transcriptional gene silencing, PTGS), because although the gene was expressed, the resulting mRNA did not accumulate due to rapid degradation in the cytoplasm of the cell (Ingelbrecht et al., 1994;Baulcombe, 1996;Meyer, 1996).

The first evidence that double-stranded RNA (dsRNA) could be used as a tool for gene silencing came from work in the nematode *Caenorhabditis elegans*. Fire and colleagues showed in 1998 that injection of dsRNA was a much more potent inhibitor of gene expression than single-stranded antisense RNA, the technology of choice at the time (Fire et al., 1998). It was then confirmed that the injected dsRNA silenced gene expression by targeting the endogenous mRNA for degradation through a post-transcriptional mechanism (Montgomery et al., 1998). Researchers rapidly tried to exploit this dsRNA-induced silencing in other model organisms such as *Drosophila melanogaster* (Kennerdell and Carthew, 1998), mouse embryos (Wianny and ernicka-

Goetz, 2000) and mouse oocytes (Svoboda et al., 2000). Before long, cell-free (Tuschl et al., 1999) and cell culture models (Caplen et al., 2000) were established and it was shown that the introduced dsRNA is processed into 21 – 23 nucleotide fragments that guide cleavage of endogenous transcripts in an ATP-dependent and translation-independent manner (Zamore et al., 2000). These fragments are known as short interfering RNAs (siRNAs).

1.2.2 Avoiding the interferon response

Many early attempts at exploiting the endogenous RNAi pathway through the introduction of dsRNA homologous to the gene of interest were problematic in vertebrates due to induction of the interferon response (Caplen et al., 2000;Oates et al., 2000;Zhao et al., 2001). Mammals have evolved defense mechanisms against dsRNA which is a characteristic signature of viruses. The presence of dsRNA > 30bp leads to induction of interferon and transcription of hundreds of interferon stimulated genes that mediate the cellular stress response (reviewed in: Stark et al., 1998). These include a family of oligoadenylate synthase enzymes (OAS), the toll-like receptor and the well characterised dsRNA-dependent protein kinase, PKR (de Veer et al., 2005). Activation of these proteins by dsRNA binding blocks translation of both viral and cellular protein and leads to apoptosis of infected cells (Stark et al., 1998;Williams, 1999;de Veer et al., 2005). The viral dsRNA is rapidly processed into siRNAs by a cellular enzyme (Hamilton and Baulcombe, 1999;Bernstein et al., 2001). The siRNAs then act as guide sequences to direct the sequence-specific degradation of the single-stranded mRNAs of

the invading viral genes (Elbashir et al., 2001b), suggesting viral defence as one plausible reason for the evolution and broad conservation of an endogenous RNAi pathway.

In 2001, Elbashir and colleagues cleverly circumvented induction of the mammalian interferon response by introducing the dsRNA as synthetic 21 or 22 nucleotide siRNAs, thereby preventing cellular detection of the dsRNA and successfully silencing target genes (Elbashir et al., 2001a). This seminal study opened the door for gene silencing by RNAi in mammalian cells.

1.2.3 The mechanism of RNAi

siRNAs

Understanding of the mechanism of RNAi is still growing and many of the key proteins in the pathway have now been identified. Viewed simplistically, the process of RNAi can be divided into an initiation step and an effector step. In the initiation step, long dsRNA is cleaved into siRNAs in the cytoplasm by an RNase III dsRNA ribonuclease called Dicer (Zamore et al., 2000). Together with cytoplasmic proteins, the siRNA now forms the RNA-induced silencing complex (RISC). This is a multi-component nuclease which plays the key role in the effector step in which target mRNA is degraded. The siRNA duplex is unwound and the strand which has the less thermodynamically stable 5' region is loaded into RISC (Khvorova et al., 2003).This strand becomes the 'guide' for locating fully complementary target mRNA within the cell (Martinez et al., 2002). The strand that is not incorporated into RISC is known as the 'passenger' strand and is

cleaved by RISC itself (Matranga et al., 2005;Rand et al., 2005). RISC now becomes activated and can target mRNAs for degradation by endonucleolytic cleavage of the mRNA within the region complementary to the siRNA. The endonuclease responsible for cleavage of both the passenger strand and the target mRNA is termed Slicer and was shown to be a highly conserved protein called Argonaute 2 (Ago-2) (Liu et al., 2004;Song et al., 2004). Although many different proteins may associate with RISC (reviewed in: Sontheimer, 2005). Ago-2 and an siRNA are sufficient for minimal target cleavage activity (Rivas et al., 2005). Cleavage of the target mRNA inhibits translation and protein synthesis, effectively silencing gene expression. A schematic illustrating the basic mechanism of RNAi is shown in Figure 1.1.

Figure 1.1 Illustration of key events in the RNAi pathway

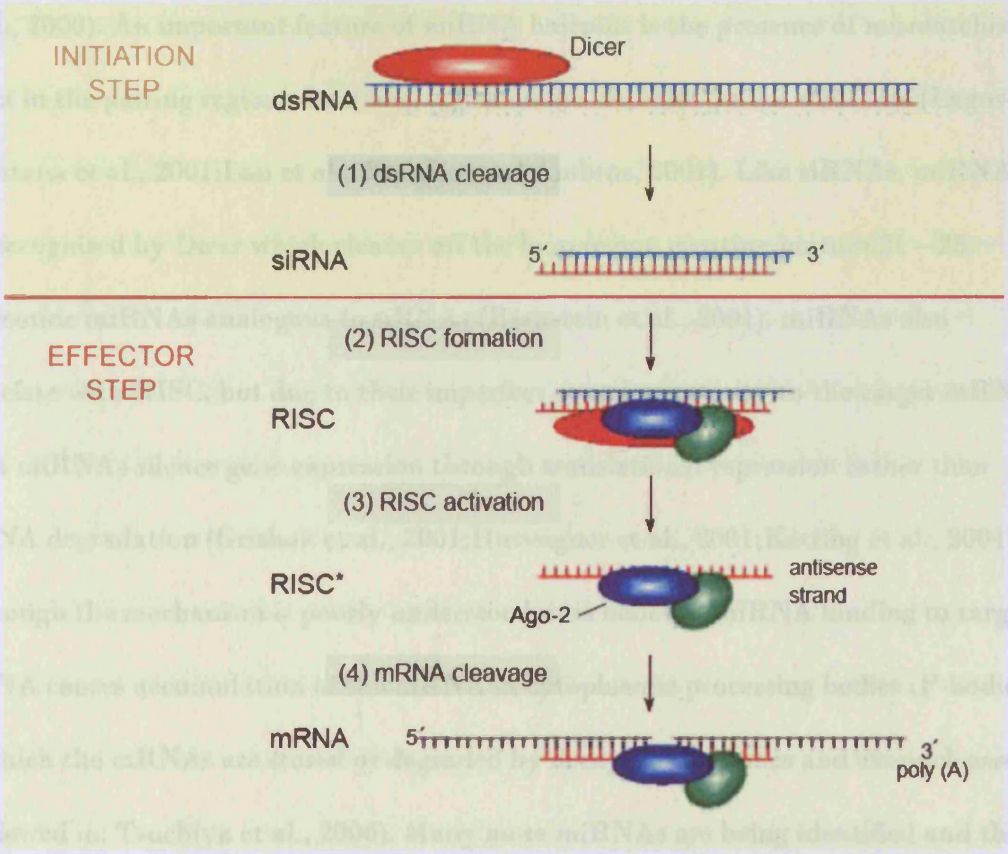

Figure adapted from 'RNA Interference in Functional Genomics and Medicine' (Kim, 2003). During the initiation step of RNAi, Dicer cleaves long dsRNA to generate a siRNA duplex (1). In the effector step, RISC is formed (2), activated by siRNA duplex binding and unwinding (3) and target mRNA is located and degraded (4).

microRNAs

In addition to siRNAs, another class of small RNA molecules called microRNAs (miRNAs) also silence gene expression. Whilst siRNAs are usually produced in a cell upon introduction of long dsRNA from viruses, transposons or transfection, miRNAs are the products of endogenous, non-coding genes whose precursor RNA transcripts contain repeat regions that enable formation of small dsRNA stem-loops. These stem-

loop structures form short hairpin RNA molecules (shRNAs) which can be processed intracellularly to effect silencing of endogenous genes (Pasquinelli et al., 2000;Reinhart et al., 2000). An important feature of miRNA hairpins is the presence of mismatched bases in the pairing regions, or stems, which create 'bubbles' in the structure (Lagos-Quintana et al., 2001;Lau et al., 2001;Lee and Ambros, 2001). Like siRNAs, miRNAs are recognised by Dicer which cleaves off the loop region creating mature 21 – 23 nucleotide miRNAs analogous to siRNAs (Bernstein et al., 2001). miRNAs also associate with RISC, but due to their imperfect complementarity to the target mRNA, most miRNAs silence gene expression through translational repression rather than mRNA degradation (Grishok et al., 2001;Hutvagner et al., 2001;Ketting et al., 2001). Although the mechanism is poorly understood, it is believed miRNA binding to target mRNA causes accumulation of the mRNA in cytoplasmic processing bodies (P-bodies) in which the mRNAs are stored or degraded by decapping enzymes and exonucleases (reviewed in: Tsuchiya et al., 2006). Many more miRNAs are being identified and they have been shown to be important in modulating cellular activities such as morphogenesis, proliferation, differentiation and apoptosis (recently reviewed in: Carthew, 2006).

shRNAs

RNAi induced through transfection of siRNA duplexes into cells is extremely useful for studying gene function, but it is also limited by the efficiency of transfection, dilution of the siRNA below effective levels through cell division and unsuitability for many *in vivo* applications. To generate stable knockdown which could be adapted for *in vivo*

therapeutics, researchers took advantage of the growing understanding of miRNA processing and expressed interfering RNA molecules as hairpins from DNA vectors. Several groups concurrently developed vector systems using the U6 or H1 promoters to drive expression of a shRNA (Brummelkamp et al., 2002;Sui et al., 2002;Paddison et al., 2002). The shRNA consisted of a duplex stem of 19 – 29 nucleotides corresponding to the sense and antisense strands of a 'traditional' siRNA, separated by a short loop sequence. Unlike miRNA precursors however, these shRNAs were generated with perfect complementarity in the stem region to mediate target mRNA destruction. Once expressed within the cell by an endogenous RNA Polymerase, the shRNA is recognised by Dicer which cleaves the loop region off, yielding a functional siRNA (Meister and Tuschl, 2004). The use of vectors to express shRNAs enables long-term silencing through selection of stably transfected cells or through exploitation of recombinant virus techniques to incorporate the shRNA expression cassette into the host cell genome.

1.2.4 Virally-mediated RNAi

The most efficient way to introduce shRNA-expressing vectors into cells is through production of recombinant viruses which efficiently gain access to host cells and exploit endogenous machinery to express the shRNA. Retroviruses, adenoviruses, adeno-associated viruses, herpes-simplex virus and lentiviruses have all been harnessed for this purpose (reviewed in: Thomas et al., 2003). Retroviral vectors are commonly used due to their relatively low immunogenic potential and their ability to integrate into the host

genome facilitating stable shRNA expression. Retroviruses do not, however, transduce post-mitotic cells such as neurons as they are unable to gain access to the nucleus unless the nuclear membrane breaks down during cell division. This limits their utility in neurological systems. Lentiviruses are a member of the retrovirus family which can translocate across the nuclear membrane and transduce non-dividing cells making them an attractive tool for use in the CNS. They have proven to be effective for gene delivery in the brain, resulting in long-term expression in the absence of inflammation (Blomer et al., 1997).

To improve safety and reduce toxicity of lentiviruses, ~95% of the parental genes are deleted from lentiviral vectors, leaving only those necessary for functions such as packaging the vector into viral particles or integrating the expression cassette into the host cell genome. The expression cassette encoding the shRNA can then be cloned into the viral backbone in place of the deleted sequences. Deleted genes which are involved in replication or encode structural and envelope proteins are provided on one or more additional vectors to provide helper functions *in trans*. Co-transfection of the lentivector and helper plasmids into permissive cell lines allows production of recombinant viruses which can transduce target cells, but are unable to replicate themselves.

1.2.5 Precedents for therapeutic RNAi in neurological disease

The use of RNAi as a treatment is of particular interest in neurological diseases which are problematic for traditional small molecule approaches due to the difficulty in crossing the blood-brain-barrier and lack of effective drug binding.

Non-viral delivery of RNAi directly to the nervous system has been achieved successfully with infusion of naked siRNA duplexes alone (Thakker et al., 2004;Dorn et al., 2004), in conjunction with transfection reagents (Hassani et al., 2005;Luo et al., 2005;Tan et al., 2005;Wang et al., 2005;Kumar et al., 2006) and conjugated to a vector peptide, Penetratin-1 (Davidson et al., 2004). Whilst promising results have been attained, current technologies mean clinical translation for treatment of many neurodegenerative diseases would require continuous or repeated long-term infusion of the interfering RNAi directly to the CNS. Stable transduction of cells with virally expressed RNAi does not have this restriction, making it an attractive candidate for treatment for 'non-druggable' targets.

The first proof-of-principle experiment demonstrating the potential of virally-mediated RNA interference as a therapeutic strategy for neurological disorders was performed by Xia and colleagues who silenced EGFP in the brains of transgenic mice using a shRNA expressed from an adenovirus (Xia et al., 2002). Direct injection of the adenovirus into the brain striatal region reduced EGFP expression in the ipsalateral hemisphere within 5 days. The same group then applied this approach to a mouse model of spinocerebellar ataxia (SCA), a progressive neurodegenerative disease caused by a polyglutamine expansion in the ataxin-1 protein. By injecting an adeno-associated virus (AAV) expressing shRNA directed against human ataxin-1 into the cerebellar lobules, they reduced inclusions of the mutant protein in the cerebellum and preserved the cerebellar molecular layer, alleviating clinical symptoms (Xia et al., 2004). Interestingly, the virus was beneficial despite transducing only 5 – 10% of the cerebellar Purkinje cells and reducing ataxin-1 protein by 50 – 60%, suggesting that complete ablation of the mutant

protein was not required for therapeutic benefit. RNAi is also an effective treatment for another polyglutamine expansion disorder, Huntington's Disease. AAVs expressing shRNAs against the coding sequence (Harper et al., 2005) and the 5'-UTR (Rodriguez-Lebron et al., 2005) of mutant huntingtin partially reduced mRNA and protein levels in transduced cells following striatal injection. Huntingtin-reactive inclusions were reduced and motor symptoms were improved up to 4 months post-injection (Harper et al., 2005), again without complete elimination of the mutant protein.

The therapeutic benefit of lentivirally-mediated RNAi in neurological disease has been demonstrated in a transgenic mouse model of amyotrophic lateral sclerosis (ALS). Lentiviruses expressing shRNAs targeting mutant superoxide dismutase (SOD1) were injected into the lumbar spinal cord of transgenic mice (Raoul et al., 2005). Reduction of the mutant protein diminished motoneuron and motor fibre losses, ameliorated neuromuscular deficits and prolonged survival. Likewise, injection of SOD1-targeting lentiviruses into multiple muscle groups of one week old transgenic mice achieved substantial improvement in motor dysfunction and extended lifespan, confirming reduction in SOD1 levels is enough to alleviate disease symptoms (Ralph et al., 2005).

Mouse models of Alzheimer's disease have been effectively treated using a lentivirus directed against the enzyme responsible for cleavage of the amyloid precursor protein, BACE-1 (Singer et al., 2005). Injection of the lentivirus directly into the hippocampus of a transgenic mouse model reduced BACE-1 by ~60%, resulting in reduction of disease-associated Aβ-immunoreactive plaques and improvement in learning and memory tasks.

1.2.6 RNAi directed against the prion protein

As no clear and major phenotypes have been described in *Prnp* knockout mice and removal of neuronal PrP^{C} protects against neurodegeneration despite continued accumulation of non-neuronal PrP^{Sc} (Mallucci et al., 2003), the prion protein is an appealing target for RNAi-mediated therapeutics. In 2003, Daude and colleagues silenced *Prnp* in scrapie-infected neuroblastoma cells using transient transfection of a siRNA duplex (Daude et al., 2003). They showed that reducing PrP^{C} in this manner abrogated accumulation of PrP^{res}, thereby demonstrating the validity of this approach. Although the effect was only transient, they showed it was independent of both host cell type and mouse-adapted scrapie strain. Shortly after, Tilly and colleagues used a vector based system to express a shRNA which silenced ovine PrP, suggesting that retroviral-mediated shRNA expression might be a promising new therapy for prion disease (Tilly et al., 2003). More recently, two groups have used lentiviral-mediated RNAi to reduce expression of PrP^{C} (Pfeifer et al., 2006;Golding et al., 2006). Both of these studies, however, resulted in the production of transgenic animals and neither of them demonstrated a therapeutic use for their lentiviruses in animals with established prion disease.

The recent successes of viral-mediated RNAi in mouse models of other neurological diseases combined with the fact that reducing expression levels of PrP^{C} increases the incubation time in prion-infected mice (Bueler et al., 1994;Fischer et al., 1996;Tremblay et al., 1998) suggests that RNAi could be of great therapeutic benefit in prion disease.

1.3 Aim of the thesis

The aim of this thesis is to evaluate the use of RNA interference to reduce *Prnp* expression as a therapeutic approach in prion-infected mice. It is hoped that reducing PrP^{C} in mice with established prion disease using this extrinsic method will slow disease pathology and generate a subclinical state analogous to that achieved by transgene-mediated depletion of neuronal *Prnp*. Success requires identification of effective target sequences within *Prnp* for silencing of gene expression by RNA interference. Examination of the consequences of RNAi-mediated reduction of *Prnp* on PrP^{Sc} and infectivity in a cell model of prion disease should provide an indication of the validity of the approach. Construction of lentiviral vectors for RNAi will be required to facilitate stable long-term reduction of *Prnp* expression in the target cell type, post-mitotic neurons. Stereotaxic delivery of these lentiviruses into the brains of mice with established prion neuropathology will be used to assess the effects of reducing *Prnp* expression in this manner and evaluate the potential of this approach as a therapy for prion disease.

METHODS AND MATERIALS

2.1 Procedures for analysis of DNA

2.1.1 Preparation of plasmid DNA

Miniprep of plasmid DNA

Qiagen miniprep kits were used to perform preparation of up to 20μg of high purity plasmid DNA. The kit utilises alkaline lysis of bacterial cells followed by adsorption to a silica-gel membrane which selectively binds plasmid DNA under appropriate low-salt and pH conditions. The manufacturer's protocol was followed (Qiagen QIAprep Miniprep Handbook, 2004). 1 - 5ml of saturated LB or TB cultures containing selective antibiotic was centrifuged for 15 minutes at 4°C at 6000g. The supernatant was discarded and the bacterial pellet was resuspended completely in 250μl buffer P1. The cells were lysed under alkaline conditions by addition of 250μl buffer P2 at room temperature for 5 minutes. Genomic DNA was precipitated through the addition of 350μl chilled buffer P3 with immediate inversion of the tube 4 - 6 times to avoid localised precipitation. The lysate was centrifuged at 13,000rpm for 10 minutes, and the supernatant applied to a QIAprep spin column. The column was centrifuged at 13,000rpm for 1 minute to bind the plasmid DNA and the flow-through discarded. Trace nuclease activity was removed by washing the column with 500μl Buffer PB and centrifuging as before for 1 minute. Any remaining impurities were removed by washing

the DNA with 750µl Buffer PE containing ethanol and centrifuging for 1 minute. The flow-through was discarded and the column was centrifuged again at 13,000rpm for 1 minute to remove residual ethanol. The column was placed into a clean 1.5ml tube and 30 - 50µl of Buffer EB was added to the centre of the membrane. The column was incubated at room temperature for 1 minute before centrifuging at 13,000rpm for a final minute to elute the purified plasmid DNA.

Maxiprep of plasmid DNA

Qiagen maxiprep kits were used to prepare up to 750µg of high purity plasmid DNA. The purification protocol is based on a modified alkaline lysis method followed by binding of plasmid DNA to an anion-exchange resin under suitable low salt and pH conditions. The manufacturer's protocol was followed (Qiagen HiSpeed Plasmid Purification Handbook, 2001). 250ml of saturated LB or TB cultures was centrifuged for 15 minutes at 4°C at 6000g. Following removal of the supernatant, the pelleted cells were resuspended in 10ml buffer P1 containing 100µg/ml of RNase A. Lysis was achieved through the addition of 10ml buffer P2 containing NaOH-SDS, followed by thorough mixing and incubation at room temperature for 5 minutes. The SDS disrupts cell membranes releasing DNA and proteins which are then denatured by the NaOH. The lysis reaction was halted by the addition of 10ml chilled neutralisation buffer P3 containing potassium acetate. The high salt concentration of this buffer causes the precipitation of KDS which traps genomic DNA, proteins and cell debris in salt-detergent complexes. The lysates were inverted 4 - 6 times and immediately poured into the barrel of a QIAfilter cartridge. Incubation at room temperature for 10 minutes

allowed the precipitated material to form a layer on top of the solution, preventing clogging of the filter. During this time, 10ml equilibration buffer QBT was added to a HiSpeed Maxi Tip and allowed to drain through the column by gravity flow. The cap was removed from the QIAfilter outlet and the plunger inserted to filter the lysate into the equilibrated Maxi Tip. The cleared lysate entered the anion-exchange resin by gravity flow and plasmid DNA was bound to the resin while degraded RNA, cellular proteins and metabolites passed through. The bound DNA was washed by addition of 60ml wash buffer QC to remove remaining contaminants. 15ml of high salt elution buffer EB was then added to elute the DNA off the resin. The eluted DNA was precipitated by the addition of 0.7 volumes of isopropanol and incubated for 5 minutes at room temperature. The eluate/isopropanol mixture was transferred into a 30ml syringe attached to a QIAprecipitator Maxi Module. Insertion of the plunger into the syringe forced the mixture through the QIAprecipitator which traps the precipitated DNA. 2ml of 70% ethanol was added to the syringe and forced through the QIAprecipitator to wash the DNA. Air was then pressed quickly and forcefully through the syringe to dry the membrane and remove residual ethanol. Finally, a new 5ml syringe was attached to the QIAprecipitator and the purified plasmid DNA was eluted by the addition of 1ml TE. To ensure the maximal recovery of DNA, the eluate was transferred back into the 5ml syringe and pushed through the membrane a second time.

2.1.1 Spectroscopic measurement of nucleic acids

Nucleic acid concentrations were determined by spectroscopic analysis on a NanoDrop ND-1000 Spectrophotometer (NanoDrop Technologies). The Nucleic Acid Measurement module was selected and RNA or DNA was specified. The pedestal was cleaned with dH_2O before measurement of a 1µl blank. 1µl samples of unknown RNA or DNA concentration were then measured and the 260/280 absorbance ratio was also examined for assessment of nucleic acid purity. Samples with a ratio of ~1.8 for DNA or ~2.0 for RNA were considered sufficiently pure.

2.1.2 Restriction enzyme digestion of DNA

Restriction enzyme digestion of plasmid DNA

DNA digestion by specific restriction enzymes (endonucleases) was performed using 1-5 units of enzyme per µg of plasmid DNA at 37°C for a minimum of 1 hour. Restriction enzymes (New England Biolabs) were used with appropriate 10x NEB buffers giving optimal salt and pH conditions for the reaction. The volume of enzyme used was less than $1/10^{th}$ of the total reaction volume to prevent inhibition of the enzyme by high glycerol concentration.

Digestion of DNA by two restriction enzymes

Where 2 restriction enzymes shared the same buffer, digestion was performed with both enzymes simultaneously. When 2 restriction enzymes required different buffers, a

sequential digest was carried out. Following digestion with the 1st enzyme, the DNA was electrophoresed on an agarose gel and the linearised DNA was then purified using a QIAquick Gel Extraction kit (QIAgen) and digested with the 2nd enzyme.

2.1.3 Dephosphorylation of DNA restriction fragments

Antartic phosphatase (New England BioLabs) was used to remove 5' phosphate groups from the termini of DNA fragments following restriction enzyme digestion, to prevent self-ligation. In a microfuge tube containing restriction enzyme digestion products, 5µl of 10x phosphatase buffer (50mM Bis-Tris-Propane-HCl, 1mM $MgCl_2$, 0.1mM $ZnCl_2$, pH 6.0), 1µl Antartic Phosphatase and ddH_2O to a final volume of 50µl were added. The mixture was incubated at 37°C for 15 minutes, and the enzyme was then heat-inactivated at 65°C for 5 minutes. A control reaction was performed in the absence of enzyme. The dephosphorylated vector DNA was extracted from agarose after electrophoresis.

2.1.4 Ligation of DNA

T4 DNA ligase (New England BioLabs) was used for all ligation reactions of DNA fragments. Ligation reactions were set up using a wide range of molar ratios of insert DNA: vector DNA from 0.5:1 to 100:1. Molar ratios were converted to mass ratios using the formula:

$$\frac{\text{vector (ng)} \times \text{size of insert (kb)}}{\text{size of vector (kb)}} \times \text{molar ratio of } \frac{\text{insert}}{\text{vector}} = \text{insert (ng)}$$

Routine controls were performed to check the efficiency of ligation by religating the cut vector alone, and to check complete digestion of the vector by omitting T4 DNA ligase. After pre-treatment of vector DNA by dephosphorylation to prevent intramolecular ligation, vector DNA (usually 100-200ng), insert DNA (as calculated) and ddH_2O to a total volume of 8µl were added to a microfuge tube. The vector and insert DNA mixture was heated to 45°C for 5 minutes to melt any cohesive ends that had annealed. After brief centrifugation, the mixture was placed on ice and 1µl (1-3U/µl) T4 DNA ligase and 1µl 10x ligase buffer (10mM $MgCl_2$, 1mM ATP, 50mM Tris-HCl pH 7.5, 10mM DTT, and 25µg /ml BSA) were added. Ligation was performed at room temperature for 30 minutes or overnight at 16°C.

2.1.5 Transformation of DNA into *E. coli*

Heat-shock transformation of DNA into *E. coli*

100µl competent cells were thawed on wet ice and mixed with 1 - 10µl ligation mix in a chilled 1.5ml microfuge tube. The mixture was incubated on ice for 30 minutes. The cells were heat-shocked by incubation in a 42°C waterbath for 90 seconds, then transferred back to ice for a further 2 minutes. 900µl LB medium was added and the suspension was incubated at 37°C, with shaking at 225rpm for 1 hour to allow the cells to recover. The cells were pelleted by centrifugation at 4,000rpm for 5 minutes and

resuspended in 100µl LB medium before spreading onto LB Agar plates with the appropriate selective antibiotic.

Selection of transformants

The cells plated on LB Agar medium were incubated overnight at 37°C. Colonies evident the following day were picked with a pipette tip and incubated overnight in 5ml of LB containing the appropriate selective antibiotic at 37°C, 225rpm. Cultures were used fresh or stored at 4°C for several days before use in small or large-scale DNA preparation.

Glycerol stocks of transformed *E. coli*

For long-term storage, autoclaved 50% glycerol was added to fresh cultures in the log phase of growth resulting in a 15% v/v solution. The glycerol culture was aliquoted into 1.5ml tubes, snap frozen in dry ice and stored at –70°C.

2.1.6 Agarose gel electrophoresis of DNA

DNA fragments were separated according to size by electrophoresis through agarose gels.

Agarose gel preparation

A 1 - 4% agarose mini-gel was made by heating 1.5 - 6g of electrophoresis-grade agarose (Invitrogen) in 150ml of 1x TAE buffer in a microwave oven until it dissolved. The gel

was cooled to approximately 50°C by stirring and ethidium bromide solution (10mg/ml) was added to a final concentration 0.02% v/v. The molten gel was then poured into a gel tray fitted with the appropriate comb(s) (Hybaid). Gel volumes were varied (mini, midi and maxi) according to number of samples to be loaded and distance required for fragment separation. (Ethidium bromide is a potent carcinogen and was handled carefully according to local safety rules).

Agarose gel electrophoresis

DNA samples were mixed with 1/10th volume of loading buffer (containing Bromophenol Blue as a tracking dye), vortexed and briefly centrifuged. The samples were loaded into individual wells of the gel using a pipette. A molecular weight marker was also loaded on each gel to allow determination of DNA fragment sizes by comparison. Horizontal electrophoresis was performed in appropriate tanks (Hybaid) containing 1x TAE buffer at 2.5-5V/cm until the fragments were adequately separated.

Visualisation of DNA in agarose gels

DNA was visualised by examining the gel on a BioRad Gel Doc 1000 imaging system under UV light. Gels were photographed and analysed using Quantity One software (version 4.5.1, BioRad).

Extraction of DNA from agarose

DNA was electrophoresed on an agarose gel as described above. The gel was placed on a 302nm UV transilluminator (UV products Ltd) and the desired band of DNA excised using a clean scalpel blade. Care was taken to minimise the amount of agarose excised. All DNA extractions from agarose were performed using the QIAquick Gel Extraction Kit (QIAGEN) according to manufacturer's instructions. This kit solubilises the agarose and passes it through a mini column containing a silica membrane. The DNA binds to the membrane in a salt and pH-dependent manner and any contaminants pass through. The DNA can then be washed with ethanol-containing buffer to remove the salt and eluted off using a higher pH buffer.

The gel slice was weighed in a 1.5ml tube and 3 volumes of Solubilisation and Binding Buffer QG were added. If the slice weighed over 400mg, it was split into 2 equal parts and extracted separately to avoid overloading a single column. The agarose was solubilised by heating it in Buffer QG at 50°C for 10min, vortexing every 2 - 3 minutes. 1 gel volume of isopropanol was added to the sample and it was mixed by vortexing briefly. The sample was then loaded onto a QIAquick column in a 2ml collection tube and centrifuged for 1 minute at 13,000rpm to bind the DNA to the membrane. To remove any traces of agarose, 0.5ml of Buffer QG was applied to the column and it was centrifuged again for 1 minute at 13,000rpm. The DNA was washed and any salts quantitatively removed by adding 0.75ml of the ethanol-containing Buffer PE before centrifuging at 13,000rpm for 1 minute. The flow-through was discarded and the column centrifuged again at 13,000rpm for 1 minute to remove residual ethanol which may interfere with downstream applications. To elute the DNA, the column was placed

in a fresh 1.5ml tube and 50µl of Buffer EB was added. The column was incubated at room temperature for 1 minute to allow the increased pH to elute the DNA off the silica membrane. The purified DNA was collected by centrifuging at 13,000rpm for 1 minute.

2.1.7 Polyacrylamide gel electrophoresis of DNA

To more accurately resolve small size differences in DNA fragments, samples were run on a polyacrylamide gel. 100ng of DNA was combined with an equal volume of 2x DNA loading buffer and loaded onto a 6% TBE polyacrylamide gel (Invitrogen). 10µl of 2-log Tri-Dye DNA ladder (New England BioLabs) was loaded into the 1st lane as a size marker. The gel was run at 100V until the Xylene Tylanol dye in the DNA ladder reached the bottom.

To stain the DNA, the gel was incubated in TBE containing 0.1% Ethidium bromide solution (10mg/ml) for 30 minutes at room temperature. Excess buffer was removed by rinsing the gel twice in ddH_20 before visualising the DNA using a BioRad Gel Doc 1000 imaging system as for agarose electrophoresis.

2.1.8 Sequencing of DNA constructs

Standard sequencing

Purified DNA was resuspended in TE buffer pH 8.0 at 50ng/µl and sequenced using an ABI 377 automated sequencer with sequencing primers at 2pmol/µl. Sequencing of all constructs was performed by G. Adamson.

7-deaza-dGTP sequencing

Some DNA structures are refractory to standard sequencing procedures due to the presence of extraordinarily stable base pairing structures which are not fully denatured during electrophoresis. This interrupts migration of DNA bands resulting in compression and loss of sequence information. Substitution of the nucleotide analog 7-deaza-dGTP for dGTP forms weaker secondary structures and allows sequencing of difficult DNA constructs. Lentivector constructs which failed to yield sequences using standard protocols were sequenced by J. Raby at UCL Scientific Support Services using a 7-deaza GTP nucleotide set (Beckman Coulter) on a Beckman Coulter CEQ 8000 genetic analysis system.

2.1.9 Design and preparation of shRNA insert oligonucleotides

To convert siRNA sequences into the required format for expression as shRNA molecules from the pLL3.7 lentivector, the instructions for stem loop design published on the McManus Lab website were followed (http://mcmanuslab.ucsf.edu/protocols/ll37stemloop_design.pdf).

The design of oligonucleotide shRNA-MW1 is shown below. All shRNA oligonucleotides were designed likewise.

siRNA sequence = G(N18)

GTACCGCTACCCTAACCAA

1. Add T to the beginning of G(N18) to recreate -1 in U6 promoter

TGTACCGCTACCCTAACCAA

2. Add loop sequence to end – TTCAAGAGA

TGTACCGCTACCCTAACCAATTCAAGAGA

3. Add reverse complement of G(N18) to end

TGTACCGCTACCCTAACCAATTCAAGAGATTGGTTAGGGTAGCGGTAC

4. Add terminator sequence - 6 Ts

TGTACCGCTACCCTAACCAATTCAAGAGATTGGTTAGGGTAGCGGTACTTTTTT

5. Create antisense strand

TGTACCGCTACCCTAACCAATTCAAGAGATTGGTTAGGGTAGCGGTACTTTTTT
ACATGGCGATGGGATTGGTTAAGTTCTCTAACCAATCCCATCGCCATGAAAAAA

6. Add sticky end to create Xho I site

```
      +1
       |                          Loop                                Terminator
5' – TGTACCGCTACCCTAACCAATTCAAGAGATTGGTTAGGGTAGCGGTACTTTTTTC – 3'
     ACATGGCGATGGGATTGGTTAAGTTCTCTAACCAATCCCATCGCCATGAAAAAAGAGCT
```

All oligonucleotides were ordered from MWG Biotech with a 5' Phosphate and PAGE purification. They were resuspended in ddH_2O ready for annealing.

2.1.10 Annealing shRNA oligonucleotides

60pmol of sense and antisense oligonucleotides were added to 48µl Annealing Buffer (Xeragon) and denatured by heating to 95°C for 10 minutes. The temperature was

reduced to 70°C for 10 minutes and then allowed to cool gradually to room temperature overnight in a waterbath to promote annealing of complementary oligonucleotides.

2.2 Procedures for analysis of RNA

2.2.1 Controlling ribonuclease activity

RNA is rapidly degraded by RNases, which are very stable active enzymes even in minute amounts. Microbiological aseptic technique was used when preparing or working with RNA, sterile RNase-free plasticware was used and solutions were prepared using RNase-free glassware which had been treated with RNaseZAP (Ambion). Dedicated chemicals and pipette tips were reserved for RNA work. Benches, gloves, electrophoresis equipment and pipettes were treated with RNaseZAP and rinsed with DEPC-treated water (Ambion) prior to use. Gloves were changed frequently throughout procedures.

2.2.2 Design and preparation of siRNA duplexes

The ORF of the target gene for RNAi was manually searched for sequences conforming to the following standard rules for siRNA design:

1. GC content of 30 – 50% (Elbashir et al., 2002;Reynolds et al., 2004a)

2. No continuous stretches of 4 or more thymine or adenine nucleotides – a known termination signal for RNA Polymerase III, preventing successful expression of the siRNA sequence as a functional shRNA in future experiments
3. No stretches of more than 3 guanine or cytosine nucleotides due to the potential of these bases to hyperstack
4. Sequence does not contain known Single Nucleotide Polymorphisms
5. No internal repeats or palindromes due to their ability to form internal fold-back structures
6. Less than 15/19 nucleotide matches to any other mouse gene (including known *Prnp* homologs, *Prnd* and *Sprn*) as determined by Blast searching against murine EST libraries and mRNA sequences (www.ncbi.nlm.nih.gov/BLAST)

Desired sequences were ordered as custom RNA duplexes from Invitrogen with a 3' dinucleotide thymine overhang and a 6-carboxyfluorescein tag on the 3' end of the sense strand.

2.2.3 Agarose gel electrophoresis of RNA

RNA agarose gel preparation

All equipment to be used in the preparation and running of the gel was thoroughly cleaned with RNaseZAP (Ambion) and rinsed twice with DEPC-treated H_2O (Ambion) to remove any contaminating RNases. 1.5g of agarose (Invitrogen) was melted in 1x Gel Prep/Gel Running Buffer (Ambion) in the microwave. The solution was allowed to cool

to 50 - 60°C in a waterbath and the gel poured to ~0.6cm depth in a gel tray fitted with appropriate combs (Hybaid). The gel was allowed to solidify at room temperature before removal of the combs to form the wells.

Sample RNA preparation and electrophoresis

1μg total RNA was mixed with an equal volume of Glyoxal Load Dye (Ambion) containing ethidium bromide. The samples were incubated at 50°C for 30 minutes to denature RNA secondary structure and allow binding of ethidium bromide. The samples were then placed on ice or immediately loaded onto the gel.
Horizontal electrophoresis was performed in 1X Gel Prep/Gel Running Buffer (Ambion) at 100V for 90 minutes or until the bromophenol blue dye front had migrated to the bottom of the gel. Bands were visualised as for DNA electrophoresis.

2.2.4 Extraction of total RNA

Brain tissue harvested for RNA analysis was cut into pieces less than 0.5cm thick and immediately submerged in 10 volumes of RNA*later* RNA Stabilization Reagent (QIAgen) to prevent degradation of cellular RNA during storage. Stabilised samples were incubated overnight at 4°C before transfer to -20°C for longer term storage.
RNeasy® Plus Mini kits (QIAgen) were used to extract up to 100μg of total RNA according to manufacturer's instructions (RNeasy® Plus Mini Handbook, Oct 2005). The kit utilises a highly denaturing guanidine isothiocyanate (GITC)-containing buffer, RLT, to inactivate RNases during tissue lysis and homogenisation. Genomic DNA is

removed by passing the lysates through a gDNA eliminator mini column. Samples are then applied to an RNeasy mini column containing a silica-gel membrane that selectively binds RNA molecules longer than 200 nucleotides. This enriches for mRNAs which are then washed before elution off the column.

Sample homogenisation

Brain samples

Brain samples stored in RNA*later*® were placed in 2ml screw-cap tubes containing ~0.5g of ceramic beads. 600µl Buffer RLT was added with 10µl/ml β-Mercaptoethanol to further inhibit RNase activity. The samples were disrupted at 6.5M/s for 45s in a ribolyser (Hybaid).

Cell lines

Prior to extraction of RNA from cell lines, up to 1 x 10^7 cells were washed with PBS and harvested as usual. 350µl Buffer RLT containing β-Mercaptoethanol was added to the pelleted cells and they were resuspended by vortexing. The cells were then passed 5 times through a 20-gauge needle to ensure thorough homogenisation.

Purification of RNA

Homogenised lysates were transferred to a gDNA Eliminator spin column placed in a 2ml collection tube. The columns were spun at 10,000rpm for 30s and the flow-through was retained. An equal volume of 70% ethanol was added and the sample was mixed by

pipetting. 700µl of the lysate was then transferred to an RNeasy spin column and centrifuged at 10,000rpm for 15s. Samples exceeding 700µl were centrifuged in successive aliquots in the same column. The flow-through was discarded and 700µl of Buffer RW1 was added to wash the bound RNA. The column was spun as before and the flow-through discarded. 500µl of Buffer RPE containing 80% ethanol was added to the column as a second wash step and spun as before. Another 500µl of Buffer RPE was added and the column centrifuged for 2min to dry the silica-gel membrane and remove residual ethanol which may interfere with downstream applications. The column was carefully removed from the collection tube without contacting the flow-through and placed in a clean 1.5ml tube. 30 – 50µl of RNase-free water was added directly to the membrane and the column was spun at 10,000rpm for 1min to elute the RNA. A second elution was performed using an additional 30 – 50µl of RNase-free water or the previous eluate if the expected yield was >30µg. Purified RNA was stored short-term at -20°C or long-term at -70°C.

2.2.5 One-step RT-PCR

RT-PCR was performed using the Quantitect® Mulitplex RT-PCR kit according to manufacturer's instructions (Qiagen). The reagents in this kit perform reverse transcription (RT) and polymerase chain reaction (PCR) amplification of a specific target from either total RNA or mRNA. A Passive Reference (ROX) dye is also included to provide an internal reference for normalisation of the reporter dye during data analysis to correct for well-to-well fluorescent fluctuations. The RT-PCR reaction

exploits the 5' nuclease activity of a DNA Polymerase to cleave a TaqMan probe during the PCR phase. The probe is homologous to the target sequence and contains a reporter dye at the 5' end and a quencher dye at the 3' end which suppresses reporter fluorescence when the probe is intact. During the PCR, cleavage of the probe separates the reporter and quencher dyes, allowing reporter fluorescence. Cleavage only occurs if the probe hybridises to its target sequence between the forward and reverse PCR primers. Accumulation of PCR products is detected directly by monitoring the increase in reporter fluorescence during each cycle.

When possible, commercially available, pre-validated sets of primers and probes were used. Otherwise, primer and probe sets were designed using Primer Express software v2.0 (Applied Biosystems).

Duplex reactions for the gene of interest combined with a housekeeping control gene were performed on 25ng of total RNA. Reverse transcription of RNA into cDNA by the Ominscript and Sensiscript Reverse Transcriptases was carried out at 50°C for 20 minutes followed by activation of the DNA polymerase at 95°C for 15 minutes. 40 cycles of target sequence amplification by HotStarTaq DNA Polymerase were performed at 94°C for 45 seconds then 60°C for 45 seconds. Reactions were analysed using the ABI Prism model 7000 sequence detection system (Applied Biosystems). During every run, samples lacking RNA or Reverse Transcriptase were included to control for contamination of reagents and amplification of residual DNA contaminants. mRNA expression of the genes of interest was normalised to the expression of the housekeeping gene amplified within the same well.

2.3 Mammalian cell culture

All work with mammalian cell lines was carried out in a designated tissue culture facility using strict aseptic technique. All media and solutions were bought pre-sterilised or were autoclaved, and sterile plasticware was used. All procedures, including preparation of media, were performed in a tissue culture hood with a laminar flow unit. Water-baths and incubators were cleaned and sterilised regularly. All solutions and media were pre-warmed to 37°C prior to use.

2.3.1 Propagation of adherent cell lines

Mouse cell lines

The N2a, N2a^{MoPrP} and GT1 cell lines were maintained in OptiMEM growth medium (Gibco BRL) containing HEPES buffer, 2400mg/l sodium bicarbonate, hypoxanthine, thymidine, sodium pyruvate, L-glutamine, trace elements, growth factors, and phenol red reduced to 1.1 mg/l, supplemented with 10% v/v foetal calf serum (FCS)(Gibco BRL), and 50U/ml each of penicillin and streptomycin (Sigma). They were maintained in vented plastic flasks (NUNC, Fisher Scientific) in a humidified CO_2 incubator, in an atmosphere of 5-7% CO_2 at 37°C. The nutrient medium was changed every 3 days, and cells were seeded 1:3-1:8 every 5-7 days or when they had reached 85% confluence. To seed the N2a and N2a^{MoPrP} cells, all medium was aspirated from the flask or dish, fresh growth medium was added and the cells were gently triturated from the dish. They were pipetted up and down until a homogenous suspension was attained and then diluted as necessary in fresh medium and transferred to a fresh flask. To seed the GT1 cells, old

medium was aspirated off, the cells were rinsed with sterile PBS and trypsin-EDTA 1x solution (0.05% trypsin, 0.5mM EDTA) (Gibco BRL) was added sufficient to cover the cell monolayer. The flask was placed at 37°C for 2-5 minutes until the cells were seen to be detaching, and an excess volume of growth medium was added, inhibiting further activity of the trypsin. The cell suspension was aspirated, and placed in a polypropylene tube (Falcon) and centrifuged at 1000 x*g* for 5 minutes. The supernatant was discarded and the cell pellet was resuspended in fresh growth medium, taking care to avoid clumping of the cells and transferred to a fresh flask.

When an accurate number of cells had to be seeded they were lifted as usual and counted using a haemocytometer (Hausser Scientific Company) and polarised light microscope, prior to seeding into fresh flasks with an appropriate volume of medium.

Human cell lines

The HEK293FT cell line (Invitrogen) is a fast growing derivative of the Human Embryonic Kidney 293 cell line which stably expresses the SV40 large T antigen for optimal virus production. These cells were propagated in growth medium consisting of Dulbecco's Modified Eagle Medium High Glucose containing 4500mg/l D-glucose and 4mM L-glutamine (Gibco BRL), supplemented with 10% v/v foetal calf serum (FCS)(Gibco BRL), 50U/ml each of penicillin and streptomycin (Sigma) and 50mg/ml Geneticin® (Gibco BRL) to maintain expression of the large T antigen . They were maintained in vented plastic flasks (NUNC, Fisher Scientific) in a humidified CO_2 incubator, in an atmosphere of 5-7% CO_2 at 37°C. The nutrient medium was changed every 3 days, and cells were seeded 1:5-1:10 every 5-7 days or when they had reached

85% confluence. To seed the cells, all medium was aspirated from the flask or dish, and the cells were lifted with trypsin-EDTA as for the GT1 cell line. The HEK293FT cell line was maintained for no more than 20 passages to prevent loss of optimal viral production.

2.3.2 Cryopreservation of cell lines

Low passage cells which were 85% confluent were harvested as above. After centrifugation, the cell pellet was placed on ice and resuspended in DMEM with 20% FCS and 10% DMSO, at a final concentration of 1 x 10^6 cells/ml. 1.0ml aliquots were frozen at a rate of -1°C per minute using a Cryo 1°C freezing container (NALGENE), according to the manufacturer's instructions. These were stored overnight at –70°C before transfer to liquid nitrogen for long term storage at –140°C. When reanimating frozen cells for experimental use, they were thawed at 37°C, then diluted in nine volumes of fresh media. The suspension was then centrifuged at 1000 x*g* for 5 minutes, the supernatant discarded and the cells resuspended in fresh media and seeded in flasks or dishes.

2.3.3 Transfection of mammalian cell lines

Transient transfection of plasmid DNA

All DNA transfections of mammalian cell lines were performed using the FuGENE6 liposomal transfection reagent according to manufacturer's instructions (Roche).

FuGENE6 was used at a transfection reagent:DNA ratio of 3µl:1µg with reactions scaled to use 1µl of FuGENE6 for every 12mm^2 of culture dish. DNA was prepared using miniprep or maxiprep kits (Qiagen)

Briefly, the required volume of FuGENE6 was diluted into warm serum-free Optimem media (Invitrogen) to a final volume of 100µl forl well of a 6-well plate or 1000µl for a T75cm flask. Care was taken when adding the FuGENE6 to pipette directly into the media without touching the sides of the tube. The mixture was incubated at room temperature for 5 minutes. During this time, 1 – 16µg of DNA to be transfected was added to separate 1.5ml tubes. If more than 1 plasmid was to be transfected into the same cells, the DNA was combined at appropriate ratios up to a total of 16µg. The FuGENE6/media mix was added to the DNA dropwise, mixed and incubated at room temperature for 15 minutes. Old media was poured off the cells and replaced with fresh media before the transfection mixture was added dropwise. The culture vessel was swirled to mix the media and the cells were cultured at 37°C, 5% CO_2 until ready for analysis.

Transient transfection of siRNA duplexes

Cells were plated in 6 well plates (NUNC, Fisher Scientific) 24 hours before transfection at a density to provide 40 – 60% confluency at the time of transfection.

The following day, 10 – 400nM of siRNA duplex was added to 225µl OptiMEM (Invitrogen). 5µl of Oligofectamine Transfection Reagent (Invitrogen) was added to 20µl of OptiMEM. Both mixtures were incubated at room temperature for 10 minutes. The2 mixtures were combined and incubated for a further 10 minutes at room

temperature. During this time, the cells were washed twice in 2ml OptiMEM . 1ml of OptiMEM was then added to each well of cells. The siRNA/Oligofectamine complex was added to the wells and swirled to mix. Cells were incubated at 37°C for 4 hours to allow uptake of the transfection complexes. Finally, 625µl of OptiMEM containing 30% FCS was added to each well to adjust the final serum concentration to 10%. Cells were then incubated at 37°C until ready for analysis.

2.4 Procedures for the detection of proteins

2.4.1 Western blotting of proteins

Preparation of cell lysates

4 x 10^5 – 8 x 10^6 cells to be lysed were washed three times with sterile PBS before lifting with 1x Trysin-EDTA (Invitrogen) or by trituration in PBS according to the cell line. Cells were then collected by centrifugation at 1,000rpm for 5 minutes and the supernatant removed. The cell pellet was resuspended in 100 – 300µl ice-cold lysis buffer (TTBS) containing complete protease inhibitors (Roche) and agitated at 4°C in a thermomixer (Eppendorf) for 2 hours. The lysates were centrifuged at maximum speed in a benchtop microfuge (Eppendorf) to pellet cellular debris and the supernatant removed to a clean 1.5ml tube.

Proteinase K digestion of cell lysates

This was performed to detect protease resistant PrP in lysates of prion infected PK1 cells. Proteinase K (VWR) at was added to homogenates at a final concentration of 10μg/ml, and the sample was incubated at 37°C for 45 minutes. The reaction was terminated by the addition of AEBSF (Merck) to a final concentration of 2mM. The samples were then prepared for electrophoresis or frozen overnight at -20°C.

Preparation of brain homogenates

A 10% (w/v) homogenate of either freshly dissected or snap-frozen mouse brain was made using ice-cold sterile PBS containing 2x Complete protease inhibitor tablets (Roche) by disruption at maximum speed for 45 seconds in a Ribolyser (Hybaid). The sample was kept on ice throughout homogenisation and stored at -70°C. When brains from mice inoculated with prions were homogenised, this was done in a designated Class 1 hood according to local safety rules.

Proteinase K digestion of brain homogenates

This was performed to detect protease resistant PrP in homogenates of prion-inoculated mouse brains. Proteinase K (VWR) at was added to homogenates at a final concentration of 50μg/ml, and the sample was incubated at 37°C for 1 hour. The reaction was terminated by the addition of AEBSF (Merck) to a final concentration of 2mM. The sample was then prepared for electrophoresis or frozen overnight at -20°C.

Quantification of protein using BCA assay

All assays were performed using a BCA Protein Assay Reagent kit (Pierce) according to manufacturer's instructions. To conserve lysates, the microplate procedure was used. Briefly, 25µl of each BSA standard (125 – 2000µg/ml) was added to wells in a 96 well microplate (Fisher Scientific). 25µl of at least 2 of the following dilutions of sample lysates were also added to the microplate; 1:10, 1:5, 1:2 or undiluted. Fresh Working Reagent was prepared by mixing 50 parts of BCA Reagent A with 1 part of BCA Reagent B. 200µl of Working Reagent was added to each well and the plate was incubated at 37°C for 30 minutes to allow formation of the purple-coloured reaction product. All assays were performed in duplicate and read at 570nm on a microplate reader (Model 550, Bio-Rad Laboratories).

A standard curve was prepared and unknown protein concentrations calculated using a statistical analysis program (GraphPad Instat Version 3.02, GraphPad Software).

SDS-Polyacrylamide Gel Electrophoresis (SDS-PAGE)

Samples to be analysed were combined with an equal volume of 2x Sample buffer (125mM Tris-HCL, 20% glycerol, 4% SDS, 0.05% bromophenol blue, pH 6.8) and boiled at 100°C for 5 minutes in 1.5ml tubes with a small hole in the lid. Each sample was then loaded onto a 16% polyacrylamide gel (Novex) with 5µl SeeBlue pre-stained molecular weight markers (Novex) in an outside lane. Gels were electrophoresed vertically in Tris-Glycine/SDS running buffer (National Diagnostics) in a XCell *SureLock*™ Mini-Cell (Invitrogen) using a constant current of 15 – 20 mA until the dye front ran off the end of the gel.

Electroblotting of gels

Following SDS-PAGE, electroblotting was performed by transfer onto Immobilon polyvinylidene fluoride (PVDF) membrane (Millipore). Membranes were cut to the same size as the gel and pre-soaked in 100% Methanol for 1 minute to ensure even hydration before transfer into blotting buffer (National Diagnostics). Proteins were transferred from the gel to the membrane in Novex X-Cell II ™ Blot modules (Invitrogen) at either 35V for 90 minutes, or 15V overnight.

Immunoblotting of gels

After electroblotting, membranes were transferred to square tissue culture dishes and washed in phosphate buffered saline, containing 0.05 % v/v tween 20, (PBST). Incubation with blocking solution, 5 % w/v non fat milk powder (Marvel), made up in PBST, was forl hour with gentle agitation. Membranes were rinsed briefly in PBS before incubation with primary antibody diluted in PBST for 1 hour or overnight at room temperature with gentle agitation. The membranes were then washed for at least 1 hour in PBST with a minimum of 5 changes of wash buffer. Incubations with secondary antibodies diluted in PBST were performed forl hour at room temperature as before. To remove unbound antibody, the membranes were washed in PBST for at least 1 hour with a minimum of 5 changes of wash buffer.

Detection of bound antibody was performed with SuperSignal West Pico Chemiluminescent substrate (Pierce) according to manufacturer's instructions. Excess reagents were poured off and the membranes were placed between acetate sheets and transferred to a photographic cassette. Biomax MR films (Anachem) were developed

using Kodak developer and fixative by hand or by using an Xograph imaging machine (Xograph Imaging Systems). Developed films were scanned using an Epson scanner for electronic format and densitometry of digital images was performed using a Kodak Image Station 440 CF (Kodak).

2.4.2 Immunohistochemistry on sections of mouse brain

Preparation of fixed brain sections

Brains from freshly culled mice were fixed in 10% formaldehyde in PBS overnight and processed and paraffin embedded by J. Linehan. 4μm sections were cut and stuck to Super-frost slides and allowed to dry overnight at room temperature, and then for 2 hours at 60°C.

Antibody detection and binding in fixed brain sections

Antigen retrieval in fixed brain sections was accomplished by immersion in a low ionic strength buffer (2.1 mM Tris, 1.3 mM EDTA, 1.1 mM sodium citrate, pH 7.8) and boiling in the microwave for 20 minutes. The slides were dewaxed in xylene (Sigma-Aldrich) and rehydrated through graded alcohols, 100% - 70%, to distilled water. Immunodetection was accomplished on a Ventana automated immunostaining system (Ventana Medical Systems) according to manufacturer's instructions. Slides were mounted in DPX (CellPath) using a Robot coverslipping machine RCM3660 (Hacker-Meisei).

Preparation of frozen brain sections

Frozen sections were prepared as a rapid method of detecting trypan blue injected into the brain when optimising stereotaxic coordinates. The desired section of paraformaldehyde-fixed mouse brain was immersed in Tissue-Tek O.C.T. embedding medium (Bright Instruments Ltd) in a small foil wrapper and placed on dry ice to freeze. 8 - 20μm sections were cut from frozen tissue using a cryostat (Leica) and electrostatically attached to Super Frost glass slides (BDH), then left to dry overnight at room temperature. Sections were fixed in acetone for 10 minutes and stored wrapped in foil at -20°C.

Staining of frozen brain sections

Frozen sections of mouse brains stereotaxically injected with trypan blue were counterstained with Nuclear Fast Red (Vector Labs) to visualize brain structure. Sections were coverslipped by hand using a permanent aqueous mountant (DAKO).

2.4.3 Immunofluorescent staining of cells on coverslips

Cells grown on glass coverslips (VWR) were washed thoroughly in PBS prior to fixation in 4% Paraformaldehyde in PBS, pH 7.4, for 10 minutes at room temperature. The cells were then permeabilised in PBS with 0.1% Triton X (Sigma) for 10 minutes at room temperature and washed three times in PBS. Non-specific binding was blocked with 10% FCS in PBS for 30 minutes at 37°C. The cells were washed three times in PBS and incubated with primary antibody diluted in PBS containing 1% FCS for 1 hour at 37°C.

Excess antibody was removed by washing three times in PBS. The cells were then incubated with secondary antibody diluted in PBS containing 1% FCS for 1 hour at 37°C in the dark. Excess antibody was removed by washing three times in PBS followed by a final three washes in sterile PBS. The coverslips were then mounted upside down on uncoated glass slides (BDH) in fluorescent mounting medium (DAKO) containing 1μg/ml DAPI (Sigma) to stain nuclei and allowed to dry in the dark. Once dry, the edges of the coverslips were sealed with clear nail varnish.

2.4.4 FACS analysis of cell surface PrP

Cells were harvested as usual and washed twice in PBS. The pellets were resuspended in 1ml 4% Paraformaldehdye in PBS and mixed by pipetting so no clumps were visible. They were then transferred to 5ml FACS tubes (Becton-Dickinson) and incubated on ice for 1 hour to allow fixation. 4ml of FACS buffer (PBS containing 2% FCS, 0.1% Sodium Azide) was added to each tube and the cells were spun in a centrifuge at 2000rpm for 5 minutes. The supernatant was removed and the cells were incubated in 300μl of FACS buffer containing ICSM18 at 12μg/ml forl hour on ice. Excess antibody was removed by washing in 1ml FACS buffer three times. Detection of PrP^c labelling used secondary antibody PE-Alexa Fluor® 647 goat anti-mouse IgG at 1:500 dilution (Molecular Probes) forl hour on ice in the dark. The cells were washed three times in FACS buffer to remove any unbound antibody. FACS was performed on a FACSCalibur machine (BD) with fluorescein detection of the siRNA duplexes in the FL1 channel and PrP^c detection in FL3. Analysis was performed using FlowJo software (Tree Star Inc).

2.4.5 Scrapie cell assay

The scrapie cell assay (SCA) is an *in vitro* replacement for bioassays for prion infectivity, in which a cell line that expresses PrP^{c} is capable of propagating PrP^{Sc} and infectivity after infection by certain prion strains. A murine neuroblastoma cell line, N2a, is susceptible to the mouse strain RML, and subclones have been produced that are capable of reporting infectivity at a greater sensitivity than is currently possible using reporter mice (Klohn et al., 2003). The SCA was performed by Dr F. Properzi.
PK1 cells (a highly susceptible subclone of N2a cells) were plated at 20,000 cells per well on a 96 well plate 16 h prior to addition of samples. Samples to be assayed for infectivity were diluted in OptiMEM growth media (Gibco BRL) supplemented with 10% FCS before application of at least 6 replicates in the assay at 300 µl per well. After addition of samples, cells were passaged at 1:10 dilutions three times over a period of 12 days to dilute out initial inoculum and allow propagation of prion infectivity. The cells were then analysed for PrP^{Sc} content by the ELISPOT.

2.4.6 ELISPOT

ELISPOT plates (Multi screen Immobilon-P 96-well filtration plates, Millipore, sterile) were activated with 70% Ethanol and washed twice with PBS by suction prior to addition of cells. 200µl of OptiMEM containing 20,000 uninfected PK1 cells was added to each well to normalise protein content. The OptiMEM was removed by vacuum suction and the cells were adhered to the membrane. A dilution series was prepared for

each sample so that 1,250, 2,500 or 5,000 treated IPK1 cells was added to each well with a minimum of six wells per sample. The media was removed by suction and the plates were dried at 50°C for at least 1 hour and stored at -20°C until ready for use. The remaining procedures in the ELISPOT were performed by A. Badhan and Dr F. Properzi.

60µl of Proteinase K solution (Roche, specific activity 2.2U/mg) at 1µg/ml was added to each well to digest non-resistant proteins and the plate was incubated at 37°C for 30 minutes. The PK was removed by vacuum suction and the wells were washed twice with 160µl PBS. 160µl of 1mM PMSF (Sigma) was added to each well to inhibit the proteinase and the plate was incubated for 10 minutes at room temperature. 120µl of 3 M guanidinium thiocyanate (GSCN) in 10 mM Tris.HCl (pH 8) was added to each well to denature the remaining proteins and the plate was incubated for a further 10 minutes at room temperature before washing 7 times with 160µl PBS. 120µl of Superblock (Pierce) was added to each well and the plate was incubated for 1 hour at room temperature. 60µl of ICSM18 antibody at 1:5,000 dilution in TBST containing 1% milk powder was added to each well and the plate was incubated for 1 hour at room temperature. The plate was washed 5 times with TBST without suction to reduce non-specific binding of the antibody to the membrane. 60µl of Alkaline-Phosphatase conjugated anti-IgG1 antibody (Southern Biotechnology) diluted 1:7,500 in TBST with 1% milk powder was added to each well. The plate was incubated at room temperature for 1 hour before washing 5 times with TBST without suction. The plastic underdrain was removed from the plate and the membrane was dried by pressing onto a clean tissue. 54µl Alkaline Phosphatase dye (Biorad) was added to each well and the plate was

incubated for 16 minutes at room temperature to allow colour development. The supernatant was discarded and the plate was washed twice with water. The plates were dried at room temperature in a hood and stored at -20°C in the dark. PrP^{Sc}-positive cells were counted on a Zeiss KS ELISPOT system (Stemi 2000-C stereo microscope equipped with a Hitachi HV-C20A colour camera and a KL 1500 LCD scanner and WELLSCAN software from Imaging Associates).

2.5 Lentiviral procedures

2.5.1 Recombinant lentivirus production

Low passage number HEK293FT cells in T75cm^2 flasks were transiently transfected at 80% confluency with the lentivector constructs plus the pCMV_dR8_74 and pMD2G helper plasmids. 940µl of warm serum-free DMEM (Gibco BRL) was added to a 1.5ml tube for each transfection. 34µl of FuGENE6 transfection reagent (Roche) was added to this media without touching the sides of the tube and incubated at room temperature for 5 minutes. During this time, 5µg of the lentivector construct was combined in a 1.5ml tube with 3.75µg of pCMV_dR8_74 and 2.5µg pMD2G for each flask to be transfected. The media/FuGENE6 mix was then added to the DNA in slow drops and incubated at room temperature for 15 minutes. During the incubation, the old media was aspirated from the cells and replaced with fresh growth media. The transfection mixture was then added dropwise to the flasks and swirled over the cells. The flasks were incubated overnight to allow uptake of the DNA and the media was replaced with

10ml serum-free OptiMEM (Gibco BRL) for viral collection. Four days post-transfection, the media was harvested and the lentiviruses were concentrated. Two transfections were typically done for each virus and the media pooled prior to concentration.

2.5.2 Concentration of lentiviruses by centrifugal filtration

Lentiviruses were concentrated by centrifugation through sterile disposable filter devices. A filter membrane with a molecular weight cut-off of 100kDa was used to retain the virus whilst allowing contaminating proteins and impurities to pass through. Culture media from lentiviral-producing cells was harvested and centrifuged at 3000rpm at 4°C for 15 minutes to pellet cell debris. The supernatant was collected and filtered through a sterile low protein-binding 0.45μm PVDF filter (Millipore) to remove any remaining debris. In order to prevent loss of virus through non-specific binding to the membrane, the filter unit was primed before use. 10ml of OptiMEM containing 1% Foetal Calf Serum (Invitrogen) was added to each Centricon Plus-20 filter device and they were spun at 2,500rpm for 20 minutes or until the media spun through.
Up to 20ml of pre-cleared culture media was then transferred into a primed filter unit and spun at 2,500rpm at 4°C until it passed through. Any remaining culture supernatant was added and spun through the same filter unit to produce the highest titre possible for each virus.
A sterile retentate cup was then fitted to the top of the filter unit and the entire device was inverted. The concentrated virus was collected by centrifugation at 1000rpm at 4°C

for 3 minutes. A typical yield was approximately 150µl. The concentrated virus was then aliquotted and frozen immediately at -70°C prior to titration.

2.5.3 Determination of lentiviral titre

Transduction of HEK293FT cells

A serial dilution method was used to determine the titre of each lentivirus. 2 x 10^5 HEK293FT cells were plated in each well of a 6 well plate and incubated overnight. The following day, the lentiviral stock was thawed and ten-fold serial dilutions ranging from 10^{-2} to 10^{-6} were prepared in 1ml complete culture medium. Polybrene was added to the dilutions at a final concentration of 8µg/µl to neutralise the charge of the plasma membrane and promote interaction with the virus. The culture media was removed from the cells and the viral dilutions added. One well received polybrene only as a control for any effects of this agent on the cells. The plates were incubated at 37°C overnight and the culture medium was replaced the following day. Four days post-transduction, the cells were examined for GFP expression by fluorescence microscopy and harvested for FACS analysis.

FACS analysis of GFP expression

Cells were harvested as usual and washed twice in PBS. The pellets were resuspended in 1ml 4% paraformaldehdye in PBS and mixed by pipetting so no clumps were visible. They were then transferred to 5ml FACS tubes (Becton-Dickinson) and incubated on ice for 1 hour to allow fixation. 4ml of FACS buffer (PBS containing 2% FCS, 0.1%

Sodium Azide) was added to each tube and the cells were spun in a centrifuge at 2000rpm for 5 minutes. The supernatant was removed and the cells were resuspended in 300µl of FACS buffer.

Analysis of GFP expression was performed on a FACSCalibur machine (Becton-Dickinson) running CellQuest software (Becton-Dickinson). The cells that received polybrene only were used as a negative control to gate for living GFP-negative cells. GFP-positive cells in the transduced samples were detected in FL1 and gated to show percentage of total population. At least 20,000 cells were counted.

Calculation of titre

The following equation was used to correct for the viral dilution factor and the number of cells plated:

Titre = (% GFP-positive) x (virus dilution factor) x (number of cells plated)

The dilution which gave between 1 – 10% GFP-positive cells was used to minimise the chance of underestimating titre by counting cells transduced more than once. Titre was expressed as number of Transducing Units per ml (TU/ml).

2.6 Animal procedures

2.6.1 Scrapie transmissions

Inoculation of RML

Prion inoculation of mice was performed by designated staff, according to established local protocols. One week old mice were anaesthetised with isofluorane in an inhalation chamber until pinch reflexes were absent. They were then inoculated with 20µl of 1% brain homogenate of RML (Rocky Mountain Laboratory) mouse-adapted scrapie strain (I2425) in PBS using a 1ml insulin syringe and a 26-gauge hypodermic needle inserted 3-4 mm into the right parietal lobe. Mice were allowed to recover in a cage placed on a heated pad prior to being replaced in their home cage.

Diagnosis of scrapie symptoms

Mice were examined daily for appearance of scrapie symptoms or other illness. Disease in wild-type animals is diagnosed when at least three of the following symptoms are present: foot clasping of hind legs when mice were lifted by the tail; tail rigidity; decreased motor activity; mincing gait, disorientation; mild hind leg paresis, ataxia; kyphosis. All symptoms were recorded on videotape prior to culling of the animal.

Removal of brains from scrapie sick animals

Terminally scrapie-sick animals or animals sick for other reasons were culled and the brains were removed according to local safety regulations in class I cabinet within the secure pathogen-free facility.

2.6.2 Stereotaxic surgery

All animal experiments conformed to United Kingdom regulations and institutional guidelines and were performed under Home Office project license. Mice were bred in-house and were housed in a temperature and light-controlled mouse colony room (12 hr light/dark cycle) in groups of 4 - 6. All mice had free access to food and water. All cages contained Perspex boxes ('igloos'), cylindrical cardboard tubes and shredded paper in view of the positive effects of such enrichment on cognition in rodents. For surgery, animals were anesthetized with 100mg/kg ketamine (Pharmacia & Upjohn) + 10mg/kg xylazine (Bayer PLC) intraperitoneally and positioned in a small animal stereotaxic head frame (ASI). The skull was exposed by a small midline incision and a hole was drilled at the appropriate coordinates, using bregma as the reference point. Using a 26 gauge 700 series Hamilton syringe (Hamilton) trypan blue or highly concentrated lentivirus was delivered at a rate of approximately 0.5µl/minute. After injection, the needle was left in place for a further 5 minutes. The midline incision was closed with Vetbond (3M) and animals were monitored on heat pads until they woke up and were mobile.

2.7 Materials

2.7.1 Commercial kits

Bicinchoninic (BCA) assay (Pierce Biotechnology)

Plasmid Mini kit (Qiagen)

Plasmid Maxi kit (Qiagen)

Quantitect® Mulitplex RT-PCR (Qiagen)

RNeasy® Mini prep (Qiagen)

SuperSignal® West Pico Chemiluminescent Substrate kit (Pierce)

2.7.2 Equipment

ABI-377 sequencer (Applied Biosystems)

ABI Prism model 7000 sequence detection system (Applied Biosystems)

Allegra 25R Centrifuge (Beckman Coulter)

AxioCam MRm camera (Zeiss)

Axioplan 2 MOT microscope (Zeiss)

Beckman Coulter CEQ 8000

BioMax-MR-I-Film (Anachem)

Centrifuge Universal 32R (Sartorius)

CM1850 Cryostat (Leica)

DH Autoflow CO_2 Air-Jacketed Incubator (Nuaire)

Eppendorf Centrifuge 5415C (Cambridge Scientific)

FACSCalibur (Becton-Dickinson)

Gel Doc EQ UV-transilluminator (Bio-Rad Laboratories)

Haemocytometer (Hausser Scientific Company)

Kodak Image Station 440 CF (Kodak).

LSM 510 META confocal microscope (Zeiss)

Microplate reader Model 550 (Bio-Rad Laboratories)

NanoDrop ND-1000 Spectrophotometer (NanoDrop Technologies)

Novex X-Cell II ™ Blot modules (Invitrogen)

Raven Incubator (LTE Scientific LTD)

Robot coverslipping machine RCM3660 (Hacker-Meisei)

UV transilluminator (UVP)

Ventana automated immunostaining system (Ventana Medical Systems)

Video printer (Bio-Rad Laboratories)

XCell *SureLock*™ Mini-Cell (Invitrogen)

Zeiss KS ELISPOT system (Zeiss)

Xograph imaging machine (Xograph Imaging Systems)

2.7.3 Reagents

16% pre-prepared polyacrylamide Tris-glycine mini-gel (Invitrogen)

1kb Plus DNA ladder (Invitrogen)

2-log Tri-Dye DNA ladder (New England BioLabs)

6% TBE polyacrylamide gel (Invitrogen)

Alkaline Phosphatase dye (Biorad)

Ampicillin (Sigma)

Annealing buffer (Xeragon)

Antartic Phosphatase (New England BioLabs)

Antartic Phosphatase Buffer (New England BioLabs)

Developer and fixer (Sigma)

Dimethyl sulphoxide (Sigma)

DPX (CellPath)

ELISPOT plates (Multi screen Immobilon-P 96-well filtration plates, Millipore, sterile)

Ethanol (Sigma)

Ethidium bromide (Sigma)

Fluorescent mounting media (DAKO)

FuGENE6 (Roche)

Geneticin® (Gibco BRL)

Glycerol (Sigma)

Hyperladder IV (Bioline)

Immobilon polyvinylidene fluoride (PVDF) membrane (Millipore).

Laemmli sample buffer (Bio-Rad Laboratories)

Lipofectamine (Invitrogen)

Mini EDTA free protease inhibitors (Roche)

NEBuffer 3 (New England BioLabs)

Non-fat milk powder (Marvel)

Not I (New England BioLabs)

Nuclear Fast Red (Vector Labs)

Oligofectamine (Invitrogen)

Optimem (Invitrogen)

Paraformaldehyde (PFA) (Sigma)

PMSF (Sigma)

Proteinase K solution (Roche, specific activity 2.2U/mg)

RNaseZAP (Ambion)

SeeBlue Plus 2 (Invitrogen)

Sodium dodecyl sulphate (Sigma)

ß-mercaptoethanol (Sigma)

Superblock (Pierce)

T4 DNA ligase (New England BioLabs)

T4 DNA ligase buffer (New England BioLabs)

Tissue-Tek O.C.T. embedding medium (Bright Instruments Ltd)

Transfer buffer (National diagnostics)

Tris-glycine/SDS (National diagnostics)

Triton-X-100 (Sigma)

Trypan blue (Sigma)

Trypsin-EDTA (Invitrogen)

Ultra Pure Agarose (Invitrogen)

Whatman filter paper (Sigma)

Xba I (New England BioLabs)

Xho I (New England BioLabs)

2.7.4 Vectors

pLL3.7 (ATCC)

pCMV_dR8_74 (kind gift of Trono Lab)

pMD2G (kind gift of Trono Lab)

2.7.5 Bacterial strains

JS4 Competent *E. coli* (kind gift of Professor Jat)

STBL2 Competent *E. coli* (Invitrogen)

2.7.6 Mammalian cell lines and cell media

Mouse neuroblastoma cell line, N2a (ATCC)

N2aMoPrP

Mouse hypothalamic cell line, GT1

Human Epithelial Kidney cell line, fast-growing clone 293FT (Invitrogen)

DMEM containing 4500mg/L-glucose, 4mM L-glutamine, (Gibco BRL)

OptiMeM (Gibco BRL)

10% FCS (Gibco BRL)

10% Penicillin/Streptomycin (Sigma)

Geneticin® (Gibco BRL)

2.7.7 Antibodies

Alexa Fluor 488 goat anti-rabbit IgG_1 (Molecular probes)

Alexa Fluor 546 goat anti-mouse IgG_1 (Molecular probes)

Alexa Fluor 568 goat anti-mouse IgG_1 (Molecular probes)

Alkaline-Phosphatase conjugated anti-IgG1 antibody (Southern Biotechnology)

Anti-GST rabbit polyclonal (Abcam)

Anti-VSV-G mouse IgG_1 (Roche)

Goat anti-mouse IgG (Fab specific) peroxidase conjugated (Sigma)

HIV1 p24 mouse IgG_1 (Abcam)

PE-Alexa Fluor® 647 goat anti-mouse IgG (Molecular Probes)

2.7.8 Prepared solutions

TE (1 litre)

100ml 1M Tris-HCl (pH 7.0, 100mM) (Sigma)

20ml 0.5M EDTA (pH8.0, 10mM) (Sigma)

1 litre with ddH_20

Luria Broth (LB)

25g Luria broth (Sigma)

1 litre with ddH_20

Sterilise by autoclaving

Terrific Broth (TB)

47.5 g Terrific broth, modified (Sigma)

8ml glycerol (Sigma)

1 litre with dd H_20

Sterilise by autoclaving

Luria Agar

40g Miller's LB Agar (Sigma)

1 litre ddH_20

Sterilize by autoclaving

After moderate cooling 100μg/ml ampicillin was added

DNA loading buffer

0.75g Ficoll 400 (Amersham)

0.005g bromophenol blue (Sigma)

5ml with ddH_20

Sample buffer

0.5ml 1M Tris-HCl pH 7.6

25ml glycerol (Sigma)

0.5ml 10% SDS (Sigma)

0.05g bromophenol blue (Sigma)

Make up to 50ml with ddH_20

PBST

0.1% Tween20 (Sigma) in 1 litre of PBS

TTBS

0.1% Tween20 (Sigma) in 1 litre of TBS

Blocking buffer

5% Milk powder (Marvel)

50ml PBST

2.7.9 Computer Programs and Web pages

ABI Prism 7000 SDS Software (Applied Biosystems)

Adobe Photoshop 6 Version 6 (Adobe)

Axiovision control software Version 3.2 (Zeiss)

Ensembl http://www.ensembl.org

FlowJo software (Tree Star Inc)

Genscan Version 3.1 (Applied Biosystems)

GraphPad InStat Version 3.05 (GraphPad Software)

Microplate Manager® Version 4.0 (Bio-Rad Laboratories)

NCBI http://www.ncbi.nlm.nih.gov

Primer Express software v2.0 (Applied Biosystems)

Sequence Analyser Version 3 (Molecular Dynamics)

UniSTS http://www.ncbi.nlm.nih.gov/entrez/query.fcgi?db=unists

siRNA KNOCKDOWN OF *Prnp* EXPRESSION *IN VITRO*

3.1 Introduction

Depletion of neuronal PrP^C in mice with established prion infection reverses early spongiform degeneration of neurons and prevents clinical disease progression (Mallucci et al., 2003). Consequently, reducing PrP^C expression in the brain through extrinsic means is likely to be an effective therapy for prion diseases. One technique for achieving this exogenous knockdown in mammalian systems, both *in vitro* and *in vivo* is through RNA interference (RNAi). This chapter describes the identification and validation of target sequences within *Prnp* for RNAi-mediated knockdown of expression.

3.1.1 Use of cell lines as models to study PrP^C and prion propagation

Although traditionally studies of prion infection have been performed *in vivo,* their prohibitive cost and complexity has led to many attempts to establish cell lines for the study of PrP^C and prion propagation. Many cell lines, however, are resistant to prion infection for unknown reasons (Rubenstein et al., 1984;Butler et al., 1988). Only a few lines have been established which support stable propagation and of these, the mouse neuroblastoma cell line, N2a, has been most widely used. N2a cells were first shown to propagate prions in 1988 (Butler et al., 1988) and became the first clonal line capable of

chronic infection. Populations of N2a cells exhibit heterogeneous susceptibility to prion infection (Bosque and Prusiner, 2000;Enari et al., 2001;Klohn et al., 2003) which is not stable over prolonged periods of propagation (Klohn et al., 2003) and may be due to epigenetic features. Therefore, they are often cloned and highly susceptible sublines selected for further study. As the siRNA duplexes described here were ultimately intended for use in prion-infected N2as, this cell line was also used to evaluate their efficacy.

The level of expression of PrP^C in standard N2as is not high enough to allow easy detection of the protein by all techniques, so for some experiments a PrP^C overexpressing N2a line, $N2a^{MoPrP}$, was used which expresses full-length mouse PrP^C at ~3-fold wild-type levels (Kristiansen et al., 2005).

3.1.2 siRNA design features

siRNAs are the specificity determinants of the RNAi pathway with a defined structure that enables them to direct cleavage of the target mRNA. Prototypical siRNAs are 21nt dsRNAs that contain 19 base pairs and 2 nucleotide 3' overhanging ends (Nykanen et al., 2001;Elbashir et al., 2001a;Chiu and Rana, 2002). It is proposed that during siRNA production, the RNaseIII domains of Dicer act as a pseudo-dimer, each hydrolysing 1 strand of the substrate dsRNA (Zhang et al., 2004). The alignment of the pseudo-dimer results in the 2 nucleotide overhang and cleavage of the dsRNA produces 5' phosphates and 3' hydroxyls. These structural features are important for loading of the siRNA duplex into RISC and determining the cleavage site of target mRNA (Elbashir et al.,

2001b;Tomari et al., 2004) so they must also be preserved when utilising synthetic siRNAs. The 3' overhang of synthetic siRNAs usually consists of two thymine bases for ease of manufacture combined with effective silencing ability (Elbashir et al., 2001b). The siRNA duplexes used here were manufactured to conform to this structure to provide the best chance of being effective.

3.1.3 Comparison against sequences previously shown to silence *Prnp*

The previously published examples of RNAi against the prion protein provide a benchmark against which future silencing attempts can be measured (Daude et al., 2003;Tilly et al., 2003). Although both studies demonstrated successful reduction of *Prnp* expression, advances in the understanding of RNAi since their publication mean more effective sequences may now be possible. For this reason, new sequences were investigated and compared to the previously published ones which are henceforth referred to as the 'Daude' and 'Tilly' sequences.

3.2 Selection of target sequences within *Prnp*

siRNA sequences targeting the mouse prion gene were designed according to established guidelines (Reynolds et al., 2004). As the current sequence design software packages were not available at the time, 19 nucleotide target sequences within the coding sequence of *Prnp* that conformed to generally accepted rules for design of successful siRNA sequences were identified manually. Six sequences (Seq 1 - 6) were identified

that met these guidelines and were then scored in line with the more stringent Reynolds criteria for effective siRNAs. The previously published Tilly and Daude sequences were also scored for comparison, see Table 3.1.

Table 3.1 Scores of the potential siRNA sequences according to the Reynolds criteria

Criterion		Tilly et al	Daude et al	Seq 1	Seq 2	Seq 3	Seq 4	Seq 5	Seq 6
GC = 36 – 52%	(+1)	0	1	0	0	0	1	1	1
A /U positions 15 – 19	(+1 ea)	3	3	2	2	2	3	2	4
A at 19	(+1)	0	0	0	1	0	1	1	1
A at 3	(+1)	0	0	0	1	0	1	0	0
U at 10	(+1)	1	0	0	0	0	0	0	1
Tm less than 20°C	(+1)	0	0	0	0	0	0	0	0
G or C at 19	(-1)	-1	-1	-1	0	0	0	0	0
G at 13	(-1)	0	0	0	-1	0	0	0	-1
TOTAL		**3**	**3**	**1**	**3**	**2**	**6**	**4**	**6**

According to Reynolds et al, a sequence scoring 6 or above is a good candidate for an effectual siRNA. Interestingly, both the Tilly and Daude sequences attain a relatively low score of 3, suggesting that the other sequences may be more effective for silencing *Prnp*. The 3 highest scoring sequences, Seq 4, 5 and 6 were chosen and referred to as MW1, MW2 and MW3 respectively. MW1 and MW3 were commercially synthesised and supplied as duplexes with a 3' dinucleotide thymine overhang. Due to financial

constraints, the lower scoring MW2 duplex was not acquired. The Daude and Tilly sequences were obtained as positive control duplexes. All duplexes were labelled with 6-carboxyfluorescein (6-FAM) on the 3' end of the sense strand facilitating easy detection *in vitro* and monitoring of transfection efficiencies. The sequences and positions within the *Prnp* open reading frame are shown in Figure 3.1:

Figure 3.1 Position of candidate siRNA sequences within the open reading frame of the murine *Prnp* gene

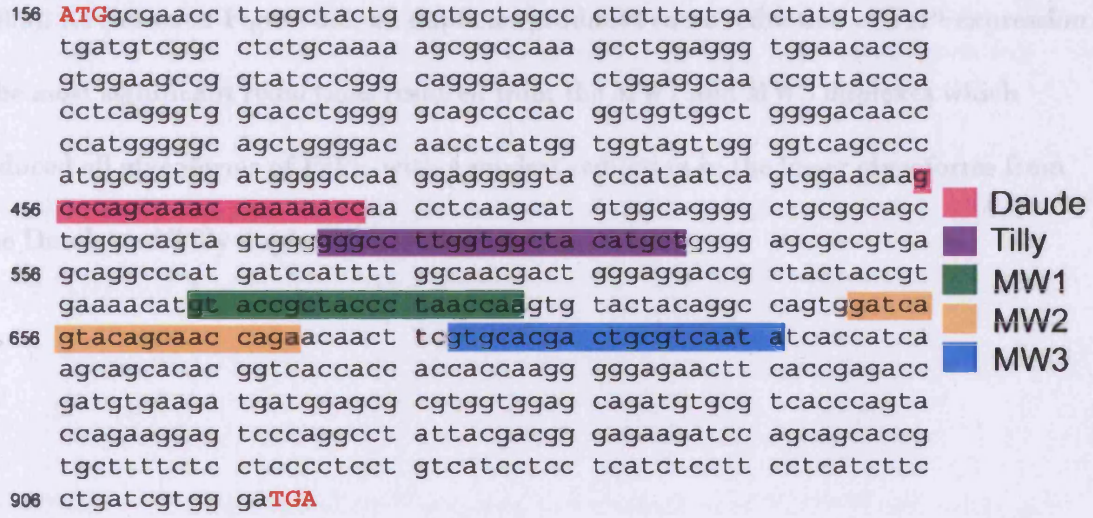

The position of each candidate siRNA sequence within the *Prnp* ORF is highlighted. Numbers of basepairs refer to position within the full-length mRNA sequence, NM_011170.

3.3 Quantification of knockdown of PrP^C expression

3.3.1 Quantification of knockdown of PrP^C in $N2a^{MoPrP}$ cells

To determine if any of the siRNA duplexes reduced *Prnp* expression, 400nM of each was transfected into the PrP-overexpressing cell line, $N2a^{MoPrP}$, allowing direct comparison with the results of Daude et al. According to their protocol, the cells were harvested four days later and lysates made for analysis by western blotting. PrP^C was detected with the ICSM18 antibody which recognises all glycoforms of PrP (Khalili-Shirazi et al., 2005). As shown in Figure 3.2, all duplexes produced some reduction of PrP^C expression. The most significant reductions resulted from the MW1 and MW3 duplexes which reduced all glycoforms of PrP^C, with a modest reduction in the lower glycoforms from the Daude and Tilly duplexes.

Figure 3.2 **PrP^C expression is reduced in a population of $N2a^{MoPrP}$ cells transfected with siRNA duplexes**

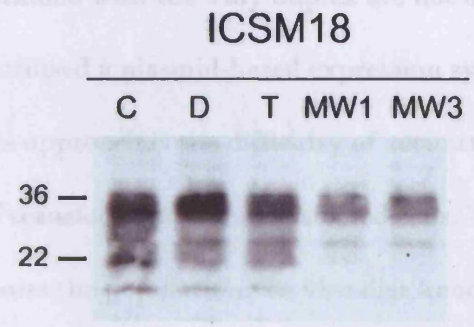

$N2a^{MoPrP}$ cells transfected with 400nM of siRNA were harvested after four days and lysates made. 15µg of total protein was loaded per lane and immunoblotted. Untransfected cells were loaded as a positive control (C) for PrP^C expression in lane 1. The membrane was incubated with ICSM18 at 0.5µg/ml and HRP-conjugated secondary antibody. The signal was visualised with high sensitivity ECL. A duplicate membrane incubated with secondary antibody only was blank. D = Daude duplex, T= Tilly duplex.

Allowing for a 70% transfection efficiency (estimated by visualisation of fluorescein-tagged duplexes under UV light), densitometric analysis revealed each sequence gave the following knockdown of total PrP^C, (Table 3.2).

Table 3.2 **Knockdown of PrP^C obtained by transfection of $N2a^{MoPrP}$ cells with each siRNA duplex**

Duplex	Knockdown of PrP^C
MW1	51.4%
MW3	56.6%
Daude	8.3%
Tilly	19.3%

These results however, are in contrast to the published findings in which cells transfected with 400nM of the Daude duplex produced no detectable PrP^C (Daude et al., 2003). The results obtained with the Tilly duplex are not directly comparable to the original research as this utilised a plasmid-based expression system (Tilly et al., 2003). A major limitation of this approach is the difficulty of accurately measuring knockdown in a mixed population of transfected and untransfected cells. The knockdown measured represents an average across the population. To visualise knockdown in individual positively transfected cells within the population, immunofluorescent histochemistry for PrP^C was performed following transfection of the duplexes.

In addition, 400nM is a very high concentration of siRNA, so the potential for off-target cellular effects is increased (Jackson et al., 2003). To determine the effectiveness of the siRNA at a lower concentration, 200nM of each duplex was transfected into $N2a^{MoPrP}$ cells seeded on glass coverslips. Three days post-transfection, the cells were fixed and immunostained to detect PrP^C expression in positively transfected cells.

Figure 3.3 PrP^C expression is reduced in individual $N2a^{MoPrP}$ cells transfected with 200nM of each siRNA duplex

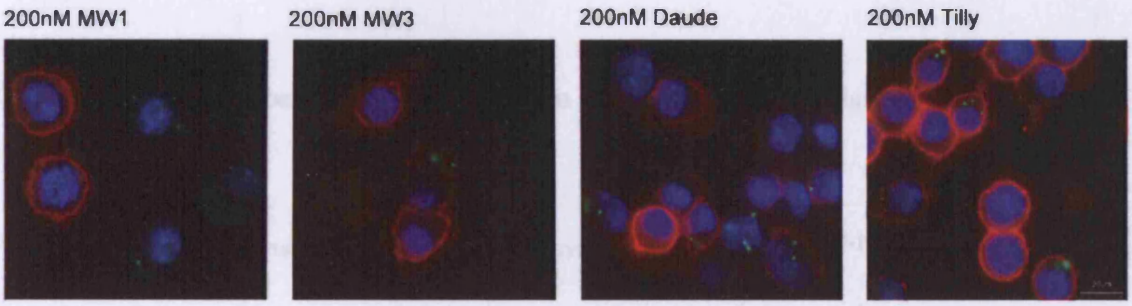

Three days post-transfection with 200nM of each siRNA duplex, $N2a^{MoPrP}$ cells on glass coverslips were fixed and immunostained with primary antibody ICSM18 at 10μg/ml. Detection of antibody binding was performed with secondary antibody, Alexa Fluor®568 goat anti-mouse IgG (H+L) (Molecular Probes) at 1:800 dilution. Coverslips were mounted onto slides with DAKO fluorescent mounting medium containing 1 μg/ml 4',6-diamidino-2-phenylindole (DAPI; Sigma) and cells were viewed on an Axioplan 2 MOT microscope (Zeiss) with an AxioCam MRm camera and Axiovision Control software (Zeiss). The cell nuclei are shown in blue, the green signal represents the fluorescein tag on the siRNA duplexes and red labelling indicates PrP^C staining.

As shown in Figure 3.3, PrP^C labelling was considerably reduced in the cells transfected with the MW1 and MW3 duplexes. The Daude duplex gave markedly less knockdown at this lower concentration and the effects of the Tilly duplex were negligible under these conditions.

As successful knockdown of PrP^C had been achieved, a commercially available negative control duplex was obtained to facilitate a more rigorous investigation of the sequences. This control duplex consisted of a scrambled sequence with approximately the same GC content as the experimental duplexes and no significant matches to any known mouse gene (Invitrogen).

Transfection with a scrambled duplex provides a control for the effects of activating the intracellular RNAi pathway and all future studies were performed with this additional control.

3.3.2 Quantitation of PrP^C knockdown in standard N2a cells

Previous experiments were performed in the overexpressing $N2a^{MoPrP}$ cells for easy detection of the prion protein by western blotting. To examine the efficacy of the siRNA duplexes at a more physiologically relevant PrP^C level, 200nM of each was transfected into the N2a cell line which expresses PrP^C at wild-type levels. 48 hours later, the cells were fixed and immunostained with ICSM18 followed by a fluorescently labelled secondary antibody. FACS was performed to allow a more sensitive analysis based on detection of the fluorescein tag in positively transfected cells. PrP^C expression levels were compared to cells transfected with the scrambled duplex control.

Figure 3.4 FACS analysis demonstrates reduced cell surface PrP^C following transfection of N2a cells with 200nM siRNA duplexes

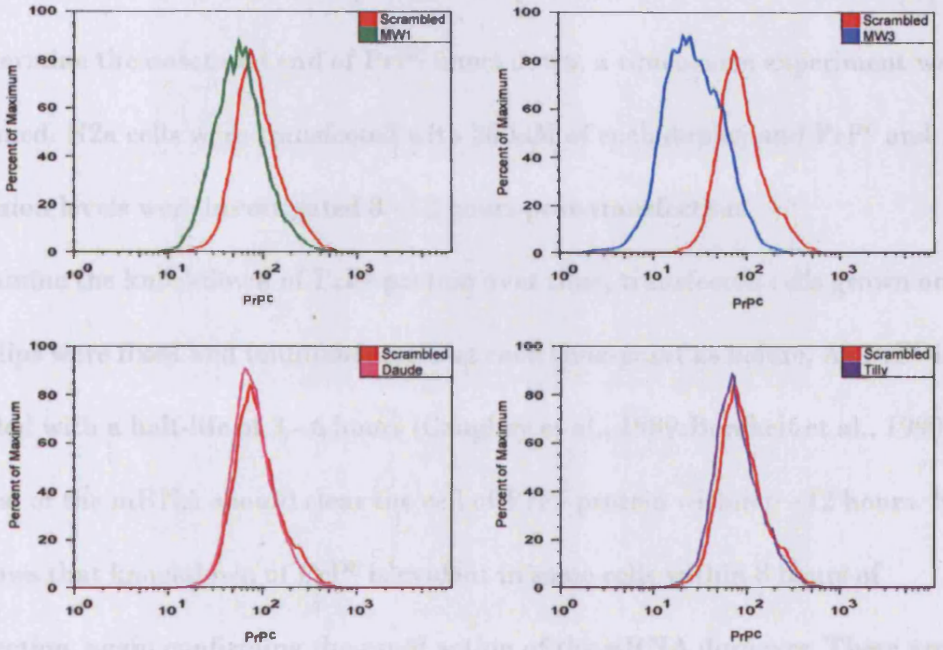

N2a cells transfected with 200nM of siRNA duplexes were harvested 2 days post-transfection. They were fixed and immunostained for FACS analysis. FACS was performed on a FACSCalibur machine (Becton Dickinson) with fluorescein detection of the siRNA duplex in the FL1 channel and PrP^C detection in FL3. Analysis was performed using FlowJo software (Tree Star Inc). A left shift of the histogram indicates a reduction of expression.

Cell surface PrP^C was reduced by 69, 96, 11 and 29% for the MW1, MW3, Daude and Tilly duplexes respectively (relative to PrP^C expression in cells transfected with the scrambled control). These data corroborated the previous observations that the MW duplexes were substantially more effective at silencing *Prnp*.

The knockdown attained with the Daude and Tilly sequences was deemed too low to be useful and these duplexes were not used in further experiments.

3.4 Timecourse of PrP^C knockdown by siRNA duplexes

Due to dilution below functional levels during cell division and degradation by cellular nucleases, effects of the siRNA duplexes are only transient (McManus and Sharp, 2002). To determine the onset and end of PrP^C knockdown, a timecourse experiment was performed. N2a cells were transfected with 200nM of each duplex and PrP^C and *Prnp* expression levels were investigated 8 - 72 hours post-transfection.

To examine the knockdown of PrP^C protein over time, transfected cells grown on coverslips were fixed and immunostained at each time-point as before. As PrP^C is degraded with a half-life of 3 - 6 hours (Caughey et al., 1989;Borchelt et al., 1990), removal of the mRNA should clear the cell of PrP^C protein within 6 - 12 hours. Figure 3.5 shows that knockdown of PrP^C is evident in some cells within 8 hours of transfection, again confirming the rapid action of the siRNA duplexes. There are also, however, transfected cells which still stain positively for PrP^C, presumably because the protein present prior to transfection has not all been degraded yet.

Figure 3.5 Timecourse of PrP^C knockdown in individual N2a cells transfected with siRNA duplexes

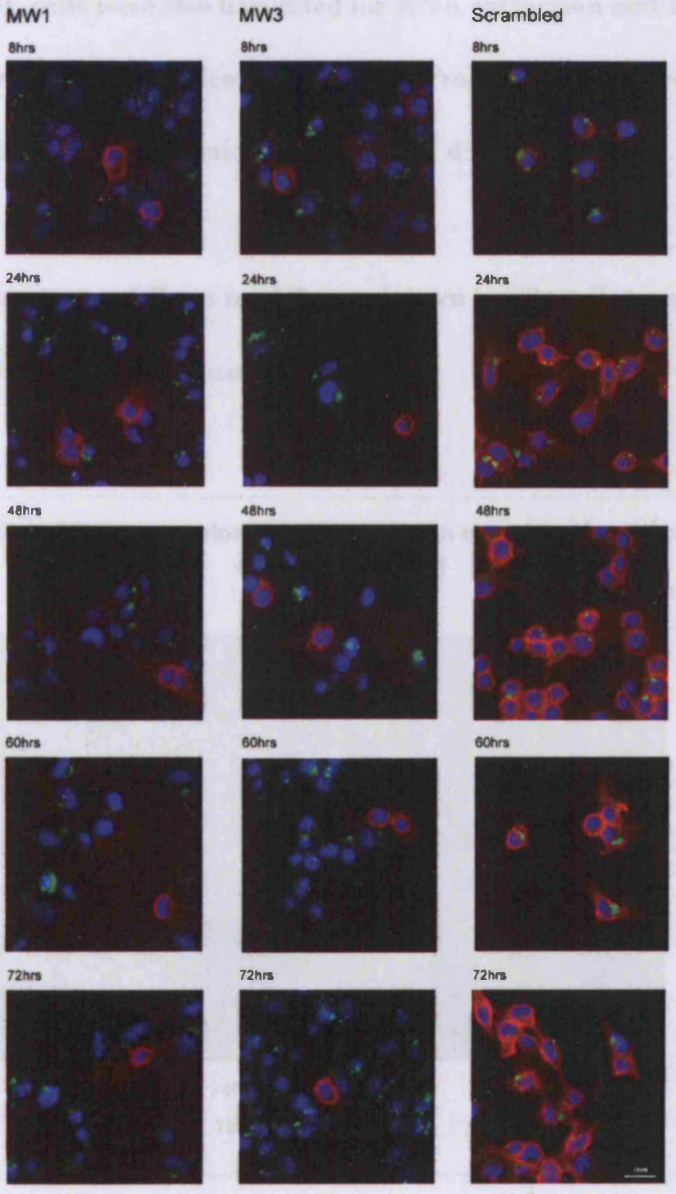

At indicated time-points after transfection with 200nM of each siRNA duplex, $N2a^{MoPrP}$ cells on glass coverslips were fixed and immunostained with ICSM18 at 10µg/ml and secondary antibody, Alexa Fluor®568 goat anti-mouse IgG (H+L) (Molecular Probes) at 1:800 dilution. Coverslips were mounted and viewed as before. The cell nuclei are shown in blue, the green signal represents the fluorescein tag on the siRNA duplexes and red labelling indicates PrP^C staining.

The scrambled duplex did not knockdown PrP^C and in fact, the staining appeared subjectively to be more intense, possibly indicating up-regulation of PrP^C.

At each time-point, cells were also harvested for RNA extraction and RT-PCR analysis. The results, shown in Figure 3.6 demonstrate that *Prnp* expression is reduced very rapidly, within 8 hours of transfection with the MW duplexes.

Figure 3.6 Timecourse of *Prnp* mRNA knockdown in N2a cells transfected with 200nM siRNA duplexes

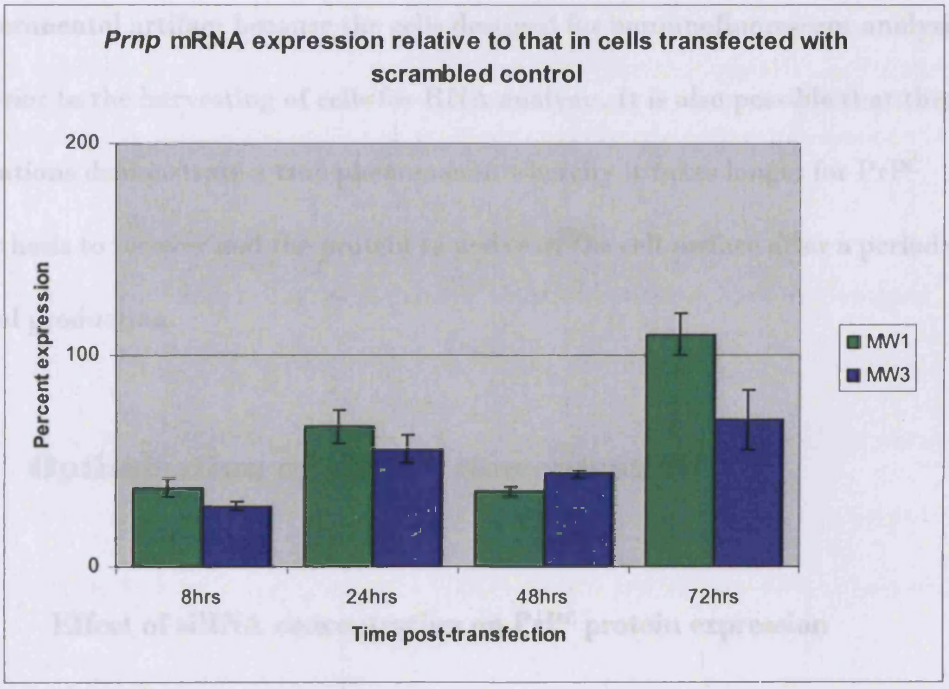

Triplicate wells of N2a cells transfected with 200nM of siRNA duplex were harvested at indicated time-points and total RNA extracted. One-step RT-PCR amplification of *Prnp* and β-actin was performed on a PRISM® 7000 Taqman machine (ABI). Primers and probes used were commercially available ABI assays: Mm00448389_m1 (with FAM labeled probe) for *Prnp* and Mouse ACTB Endogenous control, VIC® labeled MGB probe. All reactions were performed in triplicate and negative controls included H_2O only and omission of Reverse Transcriptase. *Prnp* expression was normalized to β-actin and knockdown is shown as a percentage of expression in N2a cells transfected with scrambled control siRNA duplex. Error bars = s.e.m.

Prnp expression remained low for at least 48 hours, recovering to normal levels by 72 hours for the MW1 duplex. The MW3 duplex may have a longer lasting effect, but the large variation at the 72 hour time-point suggests that at least some of the cells have regained expression by this time.

In light of these results, it is perhaps surprising that the knockdown of the PrP^C protein persists for over 72 hours. As PrP^C has been shown to be transported to the cell surface within an hour of biosynthesis (Caughey et al., 1989) and *Prnp* mRNA levels are recovering by this time, a proportion of cells would be expected to have recovered some cell surface PrP^C. The lack of PrP^C staining at 72 hours post-transfection could reflect an experimental artifact because the cells destined for immunofluorescent analysis were fixed prior to the harvesting of cells for RNA analysis. It is also possible that these observations demonstrate a true phenomenon whereby it takes longer for PrP^C biosynthesis to recover and the protein to arrive at the cell surface after a period of minimal production.

3.5 Optimisation of siRNA concentration

3.5.1 Effect of siRNA concentration on PrP^C protein expression

To evaluate the impact of siRNA concentration on PrP^C knockdown, the MW duplexes were transfected into N2a cells at 50nM, 100nM or 200nM. 66 hours post-transfection, the cells were immunostained for PrP^C and analysed by FACS.

Figure 3.7 Increasing concentrations of MW3 but not MW1 siRNA duplex result in higher knockdown of cell surface PrP^C expression in N2a cells

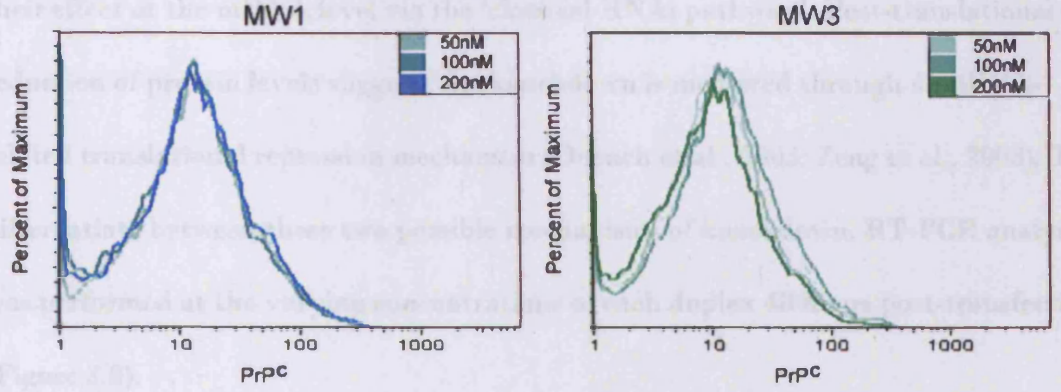

N2a cells transfected with 50 - 200nM of siRNA duplexes were harvested 66 hours following transfection and fixed in 4% PFA. Staining and detection of cells was performed as in Figure 3.4. Histograms for each concentration of the duplex were overlaid for comparison and a leftwards shift indicates reduced expression of PrP^C.

Overlaying the histograms obtained for PrP^C expression revealed that changing concentration had little effect on PrP^C knockdown for the MW1 duplex (Figure 3.7). This indicates that the MW1 duplex reaches its maximal effect at concentrations of 50nM. There was, however, a dose-dependant increase in knockdown for higher concentrations of the MW3 duplex with 200nM producing the greatest reduction in PrP^C expression.

3.5.2 Effect of siRNA concentration on *Prnp* mRNA

FACS analysis measures protein expression but desirable siRNA sequences mediate their effect at the mRNA level via the 'classical RNAi pathway'. Post-translational reduction of protein levels suggests the knockdown is mediated through a miRNA-related translational repression mechanism (Doench et al., 2003; Zeng et al., 2003). To differentiate between these two possible mechanisms of knockdown, RT-PCR analysis was performed at the varying concentrations of each duplex 48 hours post-transfection (Figure 3.8).

Figure 3.8 *Prnp* mRNA knockdown does not vary with siRNA concentration

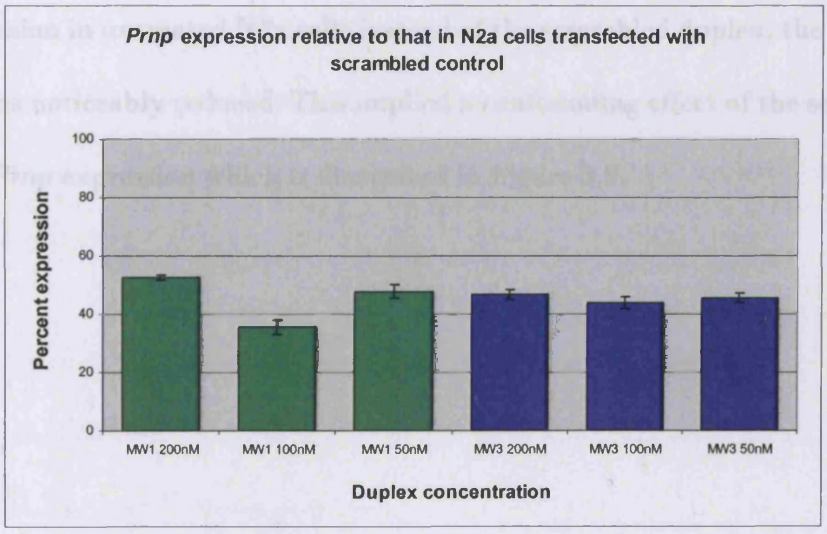

Triplicate wells of N2a cells transfected with 50 - 200nM of siRNA duplex were harvested and total RNA extracted. One-step RT-PCR amplification of *Prnp* and β-actin was performed as before. All reactions were performed in triplicate and negative controls included H_2O only and omission of Reverse Transcriptase. *Prnp* expression was normalized to β-actin and knockdown is shown as a percentage of expression in N2a cells transfected with scrambled control duplex. Error bars = s.e.m.

The reduction in PrP^C mRNA obtained for the MW1 duplex was very similar to the knockdown in protein previously shown by FACS and western blotting, indicating this duplex acts primarily through the classical RNAi pathway. Conversely, the reduction in PrP^C mRNA obtained for the MW3 duplex was significantly less than that seen by FACS analysis, suggesting this duplex may achieve some of its effect through a post-translational mechanism.

3.6 Unexpected effect of transfection on PrP expression

3.6.1 *Prnp* mRNA expression following transfection

Surprisingly, if the previous RT-PCR results (Figure 3.8) were expressed relative to *Prnp* expression in untreated N2a cells instead of the scrambled duplex, the knockdown obtained was noticeably reduced. This implied a confounding effect of the scrambled duplex on *Prnp* expression which is illustrated in Figure 3.9.

Figure 3.9 The scrambled siRNA duplex increases *Prnp* mRNA expression in transfected N2a cells at all concentrations

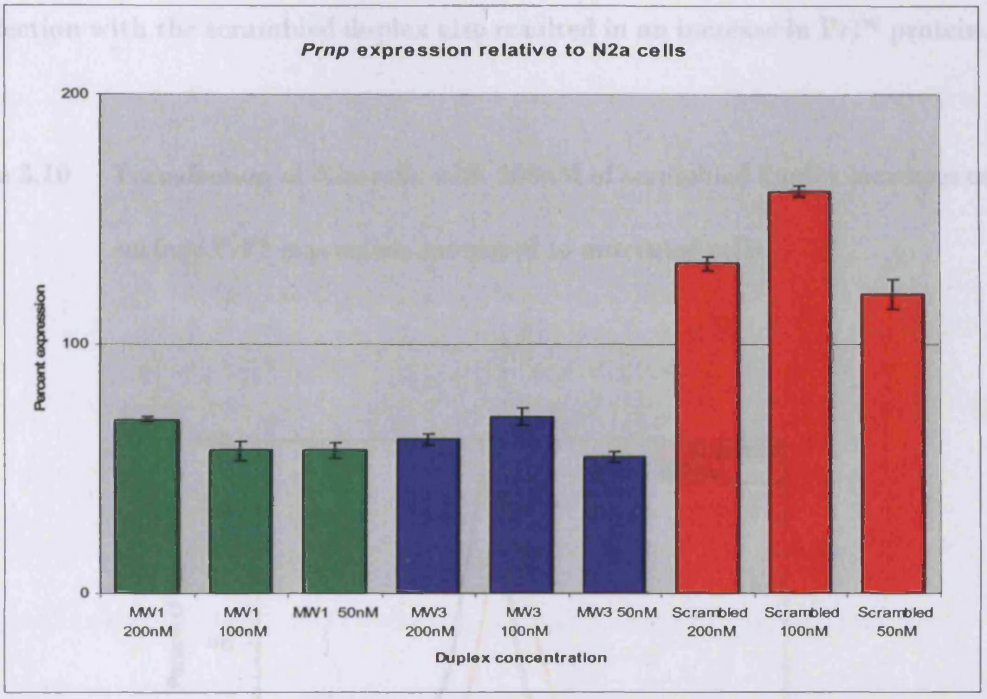

Triplicate wells of N2a cells transfected with 50 - 200nM of siRNA duplex were harvested and total RNA extracted. One-step RT-PCR amplification of *Prnp* and β-actin was performed as before. All reactions were performed in triplicate and negative controls included H_2O only and omission of Reverse Transcriptase. *Prnp* expression was normalized to β-actin and knockdown is shown as a percentage of expression in untreated N2a cells. Error bars = s.e.m.

At all concentrations, the scrambled duplex resulted in a mean increase in *Prnp* expression compared to untransfected N2a cells suggesting this effect could not be avoided by lowering siRNA concentration.

3.6.2 PrP^C protein expression following transfection

FACS analysis was performed to determine if the increase in PrP^C mRNA produced by transfection with the scrambled duplex also resulted in an increase in PrP^C protein.

Figure 3.10 Transfection of N2a cells with 200nM of scrambled duplex increases cell surface PrP^C expression compared to untreated cells

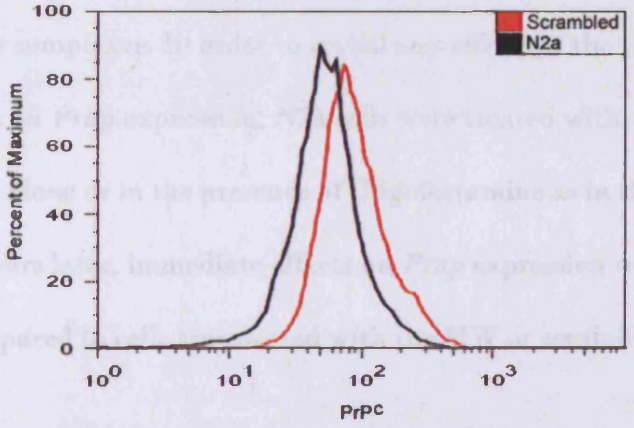

N2a cells transfected with 200nM of scrambled siRNA duplex were harvested 2 days following transfection. They were fixed and immunostained with primary antibody, ICSM18 at 12μg/ml and secondary antibody PE-Alexa Fluor® 647 goat anti-mouse IgG at 1:500 dilution (Molecular Probes) and analysed by FACS as before. A right shift of the histogram indicates increased expression.

Transfection with the scrambled duplex resulted in a 66% increase of cell surface PrP^C compared to untransfected N2a cells (Figure 3.10), implying that the additional mRNAs produced were not degraded but were translated into protein.

In order to determine if this unanticipated effect on PrP^C expression was specific to the scrambled sequence, an effect of transfection or due to activation of the RNAi pathway, further experiments were conducted.

3.6.3 Investigating the cause of *Prnp* overexpression following transfection with the scrambled duplex

The siRNA transfection protocol uses Oligofectamine as a transfection reagent and requires a 4 hour incubation of the cells in serum-free medium following administration of the transfection complexes. In order to reveal any effects of the Oligofectamine and serum deprivation on *Prnp* expression, N2a cells were treated with 4 hours of serum deprivation either alone or in the presence of Oligofectamine as in the transfection protocol. Eight hours later, immediate effects on *Prnp* expression were examined by RT-PCR and compared to cells transfected with the MW or scrambled duplexes (Figure 3.11).

Figure 3.11 ***Prnp*** **mRNA overexpression is stimulated by transfection conditions not the scrambled duplex itself**

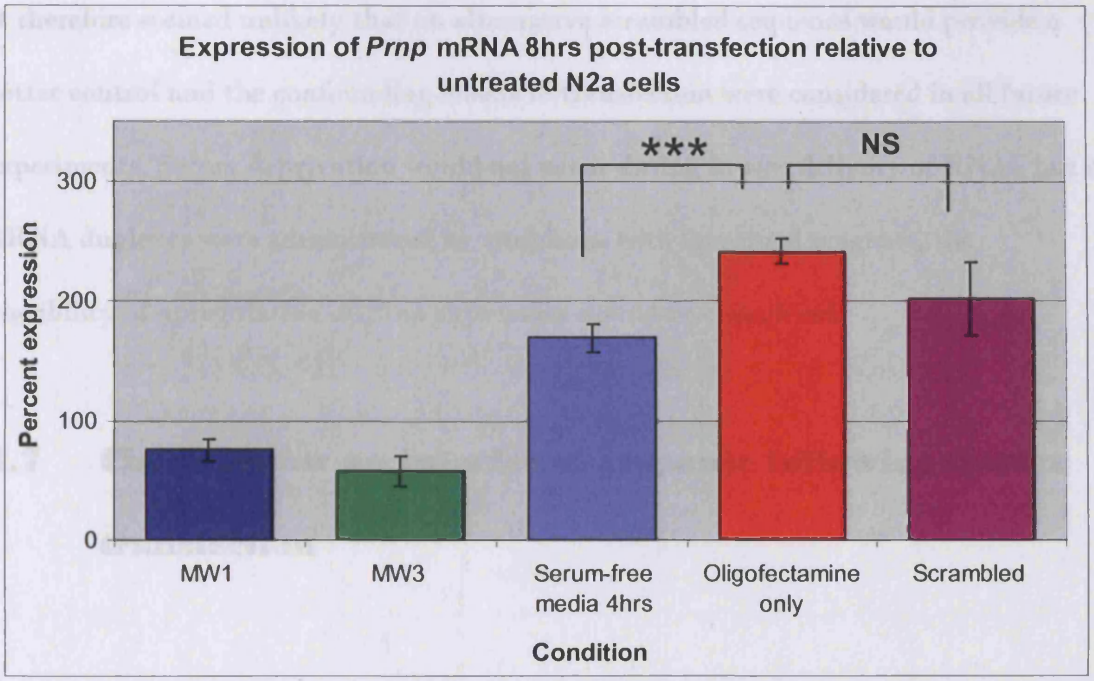

Triplicate wells of N2a cells were exposed to varying stages of the transfection process: serum-deprivation for 4 hours and then a return to normal serum levels, serum-deprivation with addition of Oligofectamine for 4 hours before returning to normal medium or standard transfection of 200nM siRNA duplexes. 8 hours after the start of treatment, cells were harvested, total RNA was extracted and RT-PCR analysis was performed as before. All reactions were performed in triplicate and negative controls included H_2O only and omission of Reverse Transcriptase. *Prnp* expression was normalized to β-actin and knockdown is shown as a percentage of expression in untreated N2a cells. Error bars = s.e.m.

Removal of serum from the media for 4 hours was sufficient to stimulate ~69% increase in *Prnp* mRNA relative to untreated cells. Adding Oligofectamine as well caused a further ~72% increase which was highly significant ($p = 0.0006$, 2-tailed Student's *t*-test). There was no significant difference between cells treated with Oligofectamine only and cells that also received the scrambled duplex ($p = 0.21$, 2-tailed Student's *t*-test).

These results suggested the transfection procedure itself increased *Prnp* expression rather than the specific scrambled duplex sequence or activation of the RNAi pathway per se.

It therefore seemed unlikely that an alternative scrambled sequence would provide a better control and the confounding effects of transfection were considered in all future experiments. Serum deprivation would not occur during *in vivo* delivery of RNAi, but if siRNA duplexes were administered as complexes with liposomal reagents, the possibility of upregulation of *Prnp* expression should be considered.

3.7 Checking for an interferon response following duplex transfection

It was recently discovered that in addition to gene-silencing effects, siRNA can also induce non-specific effects including activation of the interferon response (Bridge et al., 2003;Sledz et al., 2003;Persengiev et al., 2004;Scacheri et al., 2004;Pebernard and Iggo, 2004). Oligoadenylate synthetase 1 (OAS1) is an interferon-stimulated gene which recognizes dsRNA and polymersies ATP (Merlin et al., 1983). This results in downstream activation of a latent endoribonuclease that degrades viral and cellular RNAs (Samuel, 2001). RNA interference has been shown to induce OAS1 expression by 50 – 500 fold (Bridge et al., 2003). Expression levels of *Oas1* were examined following siRNA transfection to look for evidence of an interferon response.

Healthy N2a cells were transfected in triplicate wells with each of the siRNA duplexes at 50, 100 or 200nM. 48 hours post-transfection, the cells were harvested and total RNA

extracted. RT-PCR analysis was performed to detect expression levels of the interferon gene *Oas1*.

Figure 3.12 ***Oas1*** **expression in N2a cells transfected with 50 – 200nM siRNA duplexes**

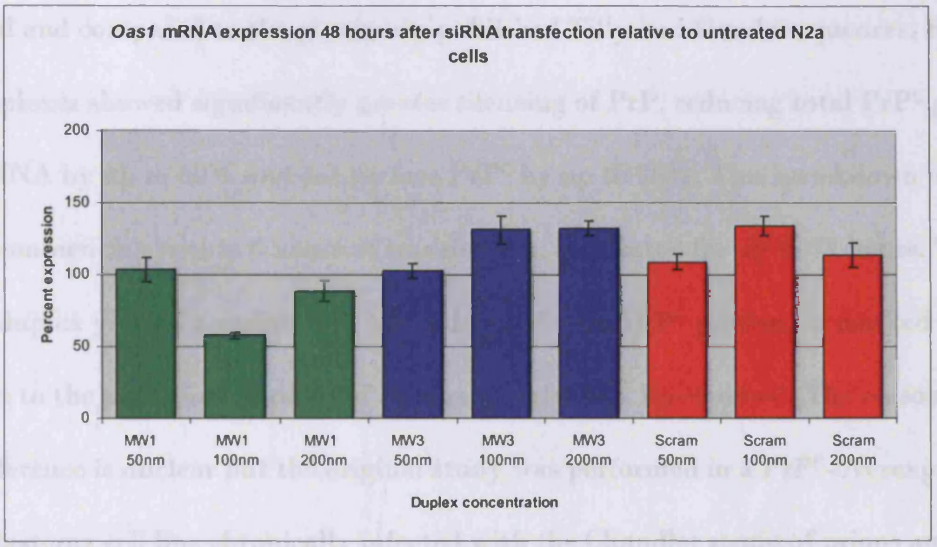

Triplicate wells of N2a cells were transfected with 50 - 200nM siRNA duplex or left untreated. Two days after transfection, the cells were harvested, total RNA extracted and RT-PCR analysis performed as before. All reactions were performed in triplicate and negative controls included H_2O only and omission of Reverse Transcriptase. *Prnp* expression was normalized to β-actin and *Oas1* expression is shown as a percentage of expression in untreated N2a cells. Error bars = s.e.m.

As shown in Figure 3.12, transfection with the duplexes at any of the concentrations tested did not lead to a marked increase in *Oas1* expression. There is a small elevation of expression levels for the MW3 and scrambled siRNAs when compared to untransfected controls but this does not approach the levels of induction seen following a classical interferon response.

Due to the lack of evidence for an interferon response, no further interferon-stimulated genes were examined.

3.8 Discussion

siRNA sequences targeting the mouse prion gene were designed and evaluated for their ability to silence murine PrP mRNA and protein. Two sequences, MW1 and MW3 were designed and compared to the previously published Tilly and Daude sequences. Both MW duplexes showed significantly greater silencing of PrP, reducing total PrP^C protein and mRNA by up to 60% and cell surface PrP^C by up to 96%. This knockdown was rapid, commencing within 8 hours of transfection, and lasted for up to 72 hours. The Daude duplex yielded a modest 8% knockdown of total PrP^C protein, in marked contrast to the published findings of approximately 95% knockdown. The reason for this difference is unclear but the original study was performed in a PrP^C-overexpressing neuroblastoma cell line chronically infected with the Chandler strain of prions and a hypothalamic cell line infected with 22L prions. It is not known how prion infection may affect the RNA interference pathway and the kinetics of knockdown, but it is possible this contributed to the discrepancy.

Under the present conditions, the Tilly duplex also produced substantially less than the 81 – 88% knockdown of PrP^C reported previously. This is not entirely surprising, as methodological differences render a direct comparison inappropriate. In the original study, the Tilly sequence was expressed from a plasmid vector and directed against exogenously introduced PrP^C. Whereas here, a duplexed RNA molecule has been utilised to knockdown endogenous PrP^C, so the kinetics of knockdown are quite different between the 2 studies.

Transfection of the scrambled siRNA duplex increased *Prnp* expression and a closer examination revealed this to be due to the transfection procedure itself. Removal of serum from the culture medium for 4 hours resulted in a 69% increase in PrP mRNA and FACS analysis revealed this mRNA was translated into PrP^C protein. Although this effect was not reported in the original study by Daude and colleagues, their western blotting clearly shows up-regulation of PrP^C following transfection with all concentrations of the scrambled duplex tested. A role for PrP^C in serum-deprivation induced apoptosis has been demonstrated previously (Kuwahara et al., 1999) and the cellular response to this stressor was shown to be fairly rapid (Kim et al., 2004). In this context, it is unsurprising that *Prnp* mRNA expression levels change significantly within 4 hours of serum removal, possibly reflecting an up-regulation of PrP^C in response to apoptotic stimuli.

A further significant increase in *Prnp* mRNA expression was observed upon addition of the transfection reagent Oligofectamine. As this was able to up-regulate *Prnp* expression in the absence of any siRNA, the effect seems to be due to the presence of the cationic lipids or other unidentified components of the reagent mix. It is possible that the resultant overexpression of *Prnp* is due to perturbation of the plasma membrane through lipid binding and/or stimulation of the endocytic pathway during the transfection procedure. Either of these options seem possible since PrP^C is known to be found on the plasma membrane (Stahl et al., 1987), where it is localized to detergent-resistant membrane rafts (Gorodinsky and Harris, 1995;Vey et al., 1996) and is recycled through the endocytic pathway (Shyng et al., 1993).

The addition of the scrambled siRNA duplex had no further effect on *Prnp* expression suggesting activation of the intracellular RNAi pathway does not alter expression of the prion gene.

Although the MW duplexes showed no evidence of an early increase in *Prnp* expression and in fact had reduced it within 8 hours, it remains possible that the knockdown obtained with these duplexes (and indeed, any sequences transfected in this manner) may be limited by the opposing effects of transfection on expression. This may account for why the knockdown obtained was not as high as may have been expected based on the sequence design and high scores on the Reynold's criteria. The true silencing potential of these sequences may be partially obscured in this system and could perhaps be revealed by administration in a different manner.

The knockdown obtained with the MW duplexes is not total but they may still be useful in treating prion-infected cells as the incubation time of prion-infected mice is known to be correlated to expression levels of PrP^{C} (Bueler et al., 1994;Fischer et al., 1996;Tremblay et al., 1998). Further experimentation is required to determine if the knockdown attained is sufficient to allow prion-infected cells to clear PrP^{Sc} and infectivity.

siRNA KNOCKDOWN OF *Prnp* AND CLEARANCE OF PrP^{Sc} AND INFECTIVITY *IN VITRO*

4.1 Introduction

The siRNA duplexes described in Chapter 3 were shown to effectively reduce *Prnp* expression in neuronal cell lines. Previous research has shown that reducing *Prnp* expression in neurons *in vivo* is protective in prion disease and allows long term survival of prion-infected mice (Mallucci et al., 2003). This chapter details an experiment designed to examine whether RNAi-mediated knockdown of *Prnp* can reduce PrP^{Sc} formation and infectivity in a cell model of prion disease.

4.1.1 Clearance of PrP^{Sc}

Inhibition of prion propagation by anti-PrP antibodies revealed an apparent half-life of ~30 hours for PrP^{Sc} in scrapie-infected N2a cells (Peretz et al., 2001). This indicates that it is degraded, albeit slowly, by endogenous mechanisms. From *in vitro* studies it seems likely that PrP^{Sc} is hydrolysed in acidic endosomes and lysosomes (Caughey et al., 1990;Taraboulos et al., 1992). An endogenous clearance mechanism involving lysosomes is further supported by the demonstration that the tyrosine kinase inhibitor, STI571, clears prion-infected cells in a c-Abl-dependent manner (Ertmer et al., 2004). This clearance can be abrogated by raising the lysosomal pH which blocks degradation in

lysosomes. Interestingly, clearance of PrP^C is unaffected by these treatments indicating separate degradation pathways exist for the 2 isoforms. The proteases responsible for degradation of PrP^{Sc} within lysosomes include cysteine proteases (Luhr et al., 2004b) such as cathepsin B and L (Luhr et al., 2004a) which have been shown to degrade PrP^{Sc} in scrapie-infected cells.

Most recently, bigenic mice in which PrP^C expression is regulated by doxycycline administration were utilized to demonstrate that clearance of PrP^{Sc} also occurs *in vivo*. Supression of PrP^C by ~95% in prion-infected mice revealed a half-life for PrP^{Sc} in the brain of ~1.5 days, in accord with previous *in vitro* findings (Safar et al., 2005). That the brain is able to clear PrP^{Sc} implies that inhibiting the conversion reaction should enable endogenous clearance mechanisms to slowly degrade existing PrP^{Sc}.

4.1.2 Measuring prion infectivity with the Scrapie Cell Assay

Infectivity of prion-infected samples has traditionally been measured by injecting the samples intracerebrally into indicator animals and determining the time until appearance of clinical symptoms. This is a very time-consuming and costly assay for infectivity. Recently, a highly sensitive, quantitative *in vitro* assay for prion infectivity called the Scrapie Cell Assay (SCA) was developed (Klohn et al., 2003). It is 2 orders of magnitude cheaper than the animal bioassay, detects infectivity at dilutions beyond the range of the standard mouse bioassay and can be automated. In the SCA, prion-susceptible neuroblastoma cells are exposed to prion-infected samples for 3 days, grown to confluence and split 1:10 3 times to dilute out the initial inoculum. The proportion of

PrP^{Sc}-containing cells is then determined by automated counting of PK-resistant material using a modified ELISA technique called the ELISPOT. The proportion of PrP^{Sc}-containing cells can be directly correlated with the starting infectivity of the samples by comparison to a serial dilution of a prion-infected brain homogenate of known bioassay titre. In this way, the equivalent *in vivo* LD50 units for a sample can be calculated.

4.1.3 Treating infected cells with siRNAs against PrP^{C}

Reducing *Prnp* expression aims to cure a cell by lowering the level of PrP^{C}, the substrate for conversion to PrP^{Sc}. This is intended to prevent further accumulation and allow clearance of existing PrP^{Sc}. The approach has been used successfully before, but the analysis was limited (Daude et al., 2003;Luhr et al., 2004b). In order to more closely examine the consequences of reducing *Prnp* expression on the formation and clearance of PrP^{Sc} as well as effects on infectivity, a more detailed study was performed.
The experiment was designed to knockdown *Prnp* expression in a population of prion-infected PK1 cells (IPK1) over 3 days as they grew to full confluence. Once the cells became confluent, they ceased to divide due to contact inhibition, producing a static population. This makes it possible to measure the production and turnover of PrP^{Sc} and infectivity without the confounding effects of cell division. It was anticipated that removing PrP^{C} would reduce levels of both PrP^{Sc} and infectivity, lending support to the use of RNAi as a therapy in prion disease.

IPK1 cells were plated at approximately 25% confluence in 6 well plates. The following 3 days, they were transfected in triplicate every 24 hours with 200nM MW1 or scrambled siRNA duplex or left untreated. Plating at low confluence allows high efficiency transfection of the duplexes and transfecting on successive days targets the highest number of cells possible to ensure knockdown of *Prnp* for the duration of the experiment. Before each transfection, the media was replaced to ensure the cells remained as healthy as possible.

Following 3 days of *Prnp* knockdown, the proportion of cells containing PK-resistant prion protein (referred to as PrP^{Sc} for the purposes of this chapter) was determined on days 4 - 7 using an ELISPOT, an immunological assay adapted from the traditional ELISA. Cells were lifted each day for assessment of PrP mRNA and protein knockdown and to make homogenates for subsequent analysis of intracellular infectivity by SCA. A schematic detailing this experimental design is shown in Figure 4.1.

Figure 4.1 **Schematic of experimental design for siRNA knockdown of *Prnp* in prion-infected cells**

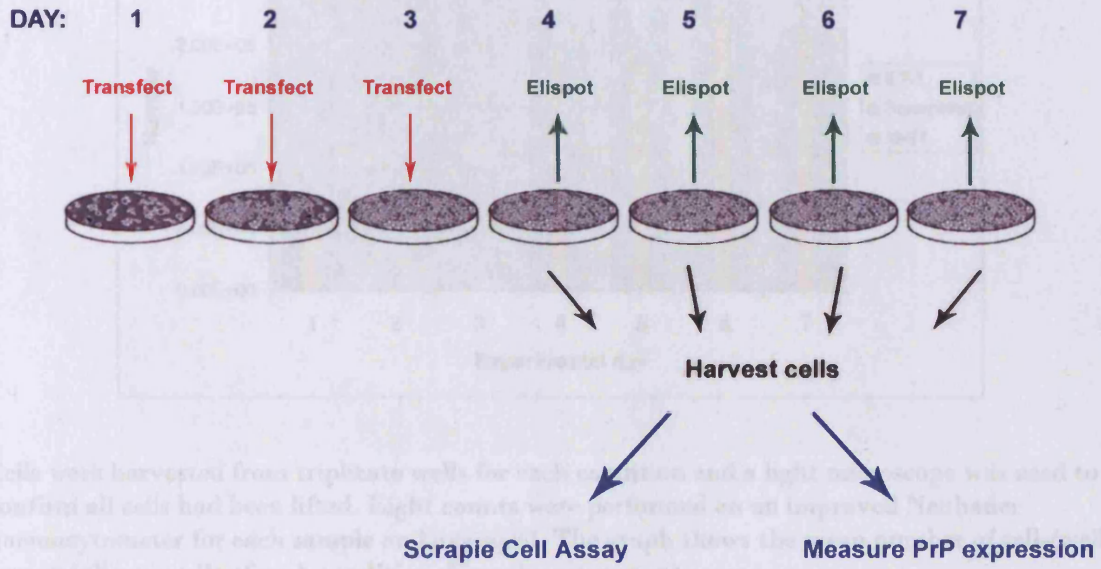

To exclude differences due to alterations in total cell number, cells were counted in triplicate wells for each condition on the final four days of the experiment. Figure 4.2 shows that the cells had reached confluency by the 4th day and numbers remained relatively constant for the rest of the experiment. Furthermore, there was no significant difference between the cells treated with the MW1 or scrambled duplexes and the untreated IPK1 cells at any point, indicating no adverse effects of the siRNAs on cell growth (Student's *t*-test, paired 2 sample for means).

Figure 4.2 Cells reach confluency and cease dividing by day 4 of the experiment

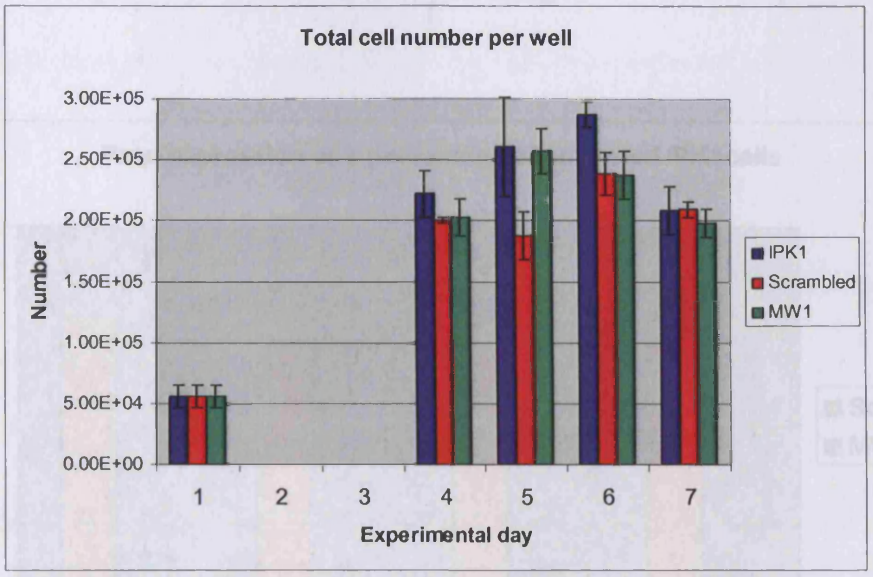

Cells were harvested from triplicate wells for each condition and a light microscope was used to confirm all cells had been lifted. Eight counts were performed on an improved Neubauer haemocytometer for each sample and averaged. The graph shows the mean number of cells/well from triplicate wells of each condition. Error bars represent s.e.m.

4.2 *Prnp* mRNA levels in IPK1 cells following siRNA treatment

RNA was extracted from triplicate wells of each condition harvested on days 4 -7 and RT-PCR analysis was performed to determine the level of *Prnp* expression in the siRNA-treated cells (Figure 4.3).

Figure 4.3 ***Prnp*** **mRNA expression is reduced in IPK1 cells transfected with the MW1 duplex and increased in cells containing the scrambled duplex**

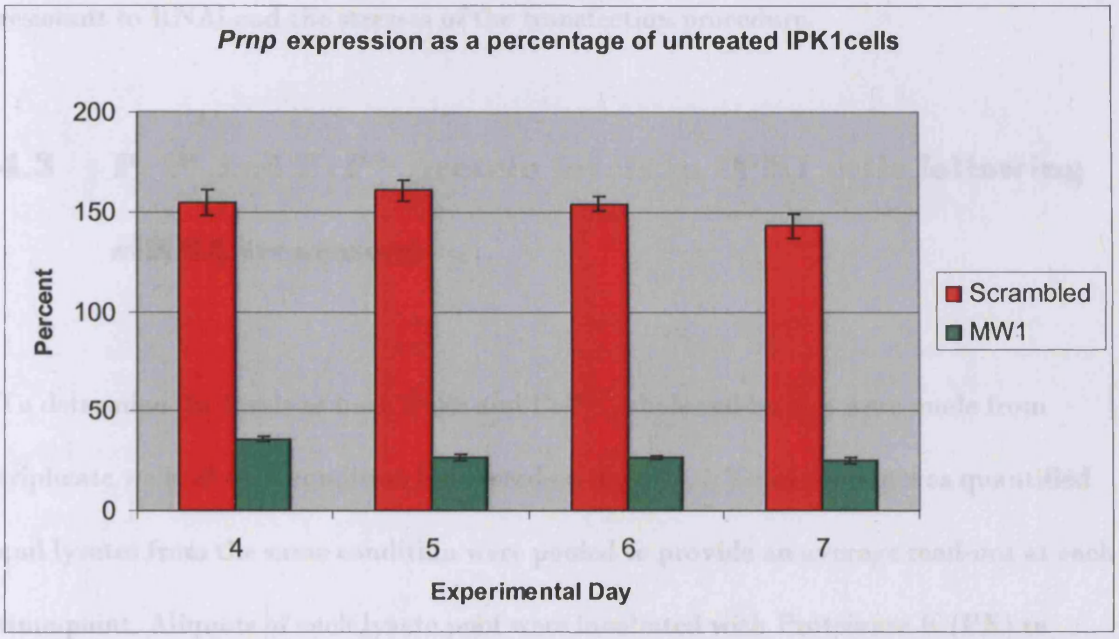

Triplicate wells of IPK1 cells transfected with 200nM of siRNA duplex were harvested on indicated days and total RNA extracted. One-step RT-PCR amplification of *Prnp* and β-actin was performed using commercially available ABI assays: Mm00448389_m1 (with FAM labeled probe) for *Prnp* and Mouse ACTB Endogenous control, VIC® labeled MGB probe. All reactions were performed in triplicate and negative controls included H_2O only and omission of Reverse Transcriptase. *Prnp* expression was normalized to β-actin and expression is shown as a percentage of that in untreated IPK1cells. Error bars represent s.e.m.

By the 4th day of the experiment, PrP mRNA expression in the MW1 treated cells was 36% ± 4 of the expression in untreated IPK1 cells. This expression had fallen to 25% ±4 of the control by the end of the experiment. In contrast, the expression levels in the cells treated with the scrambled duplex were 155% ±20 on the 4th day and remained around this level for the duration of the experiment in agreement with previous observations (see Chapter 3.6). Both the extent and the longevity of knockdown

attained was greater in the IPK1 cells than in the PK1 cells used previously. This is not due to performing successive transfections as the same trend was observed following a single transfection (data not shown), suggesting that prion-infected cells are less resistant to RNAi and the stresses of the transfection procedure.

4.3 PrP^{C} and PrP^{Sc} protein levels in IPK1 cells following siRNA treatment

To determine the levels of both PrP^{C} and PrP^{Sc}, whole cell lysates were made from triplicate wells of each condition harvested on days 4 - 7. Total protein was quantified and lysates from the same condition were pooled to provide an average read-out at each time-point. Aliquots of each lysate pool were incubated with Proteinase K (PK) to digest all non-resistant proteins and reveal the PrP^{Sc} content. Samples of the lysates with and without PK digestion were western blotted and the membranes were overexposed to allow visualization of very faint bands. As shown in Figure 4.4, there was substantial knockdown of PrP^{C} expression relative to untreated IPK1 cells following treatment with the MW1 duplex. PrP^{C} levels diminished from days 4 - 7 and no PrP^{Sc} was detectable by blotting at any stage in these cells.

Figure 4.4 PrP^{C} and PrP^{Sc} protein levels are reduced following *Prnp* knockdown

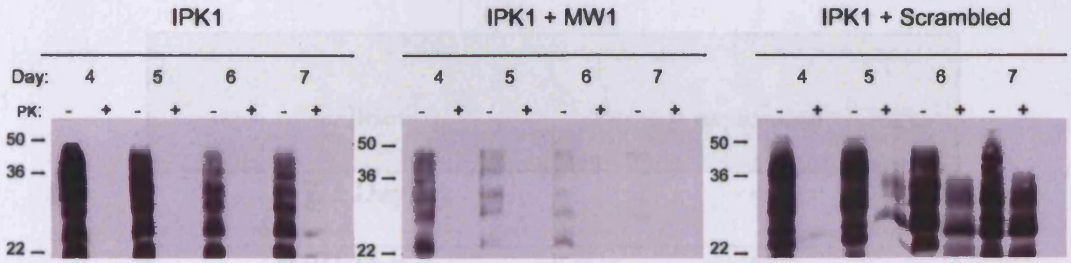

50µg of total protein from each pooled lysate was loaded per lane and immunoblotted. The membrane was incubated with ICSM18 at 0.5µg/ml and HRP-conjugated secondary antibody. The signal was visualised with high sensitivity ECL. Duplicate membranes incubated with secondary antibody only were blank. Quantitation of total PrP protein was performed on a Kodak digital science image station 440CF using Kodak 1D analysis software (v.3.6.3). Identical regions of interest were defined in each lane to encompass all glycoforms and degradation products of PrP. Molecular weight is indicated in kDa.

PrP^{Sc} only became faintly visible in the untreated IPK1 cells on day 7 but it was easily detectable from day 5 onwards in the cells treated with the scrambled duplex. The earlier appearance of PrP^{Sc} in the latter cells probably results from the increased expression of PrP^{C} due to the transfection process (see Chapter 3.6). This would lead to excess PrP^{C} substrate available for conversion. Densitometry on each PK- lane revealed the changes in total PrP expression compared to IPK1 cells at the same time-point (see Table 4.1 where a negative value indicates knockdown and a positive value indicates over-expression)

Table 4.1 **Changes in total PrP expression following transfection with siRNA duplexes**

Condition	Percent expression change
MW1 Day 4	- 42
MW1 Day 5	- 85
MW1 Day 6	- 86
MW1 Day 7	- 96
scrambled Day 4	+ 16
scrambled Day 5	+ 14
scrambled Day 6	+ 16
scrambled Day 7	- 15

Western blot analysis of the whole cell lysates provides information on the total quantity of a protein in a population of cells but does not reveal how many cells contain detectable levels of that protein. When the protein in question is a marker of infection such as PrP^{Sc}, it is also important to know the proportion of cells that are infected. Additionally, the levels of PrP^{Sc} in the IPK1 cells were not high enough for detection by western blotting until the 7^{th} day meaning changes that occurred below this threshold will not be observed.

To visualise and determine the proportion of cells containing intracellular PrP^{Sc}, an ELISPOT was performed. Triplicate wells of each condition were harvested on days 1

and 4 - 7 and a dilution series of 5,000 - 1,250 cells per well were seeded into ELISPOT plates. Cells were dried onto the membrane, non-resistant proteins were digested with PK and the residual PrP^{Sc} was detected using an adapted ELISA technique. The proportion of cells containing PrP^{Sc} in each condition is shown in Figure 4.5.

Figure 4.5 Treatment with MW1 siRNA significantly reduces the proportion of cells containing PrP^{Sc}

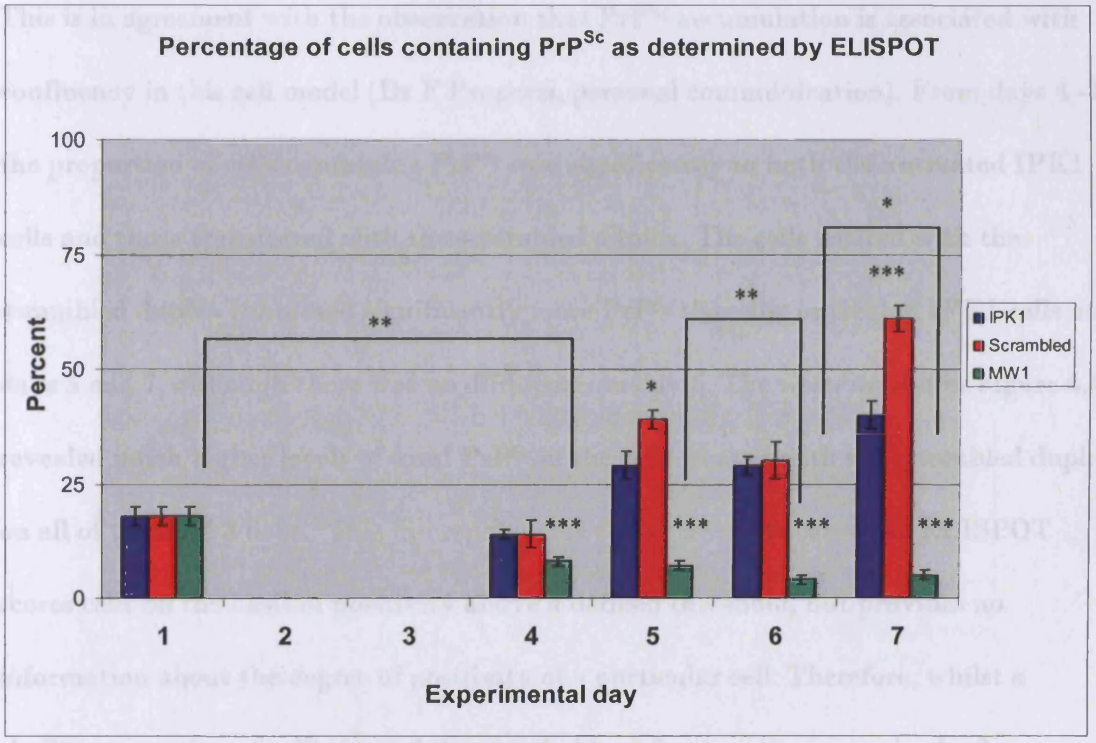

Triplicate wells of IPK1 cells from each condition were harvested on the indicated days and plated into ELISPOT plates (Millipore) with 6 replicates for every sample. The cells were dried onto the plates and stored at 4°C until all plates were ready for analysis. Dr F Properzi performed the ELISA detection of PK-resistant material and counted positive cells using a Zeiss KS ELISPOT system (Stemi 2000-C stereo microscope equipped with a Hitachi HV-C20A colour camera and a KL 1500 LCD scanner and WELLSCAN software from Imaging Associates). Proportions of positive cells were averaged for each condition and the errors bars represent s.e.m.

The proportion of cells containing PrP^{Sc} reduced throughout the experiment in the cells transfected with the MW1 duplex. This decrease was significant between days 1 – 4 ($p = 0.003$, Student's paired *t*-test), 5 - 6 ($p = 0.003$) and 6 - 7 ($p = 0.03$). In addition, transfection with the MW1 duplex yielded a highly significant drop in PrP^{Sc}-positive cells compared with untreated IPK1 cells on days 4 - 7 (Day 7, $p = 7.2 \times 10^{-11}$, Student's paired *t*-test). The proportion of PrP^{Sc}-positive cells remained relatively constant over days 1 - 4 in the untreated IPK1 cells and those transfected with the scrambled duplex. This is in agreement with the observation that PrP^{Sc} accumulation is associated with confluency in this cell model (Dr F Properzi, personal communication). From days 4 -7, the proportion of cells containing PrP^{Sc} rose significantly in both the untreated IPK1 cells and those transfected with the scrambled duplex. The cells treated with the scrambled duplex contained significantly more PrP^{Sc} than the untreated IPK1 cells on days 5 and 7, although there was no difference on day 6. The western blot in Figure 4.4 revealed much higher levels of total PrP^{Sc} in the cells treated with the scrambled duplex on all of the final 3 days. This discrepancy may have arisen because the ELISPOT scores cells on the basis of positivity above a defined threshold, but provides no information about the degree of positivity of a particular cell. Therefore, whilst a similar proportion of cells crossed the threshold set for a positive score in the 2 conditions, the cells transfected with the scrambled duplex may have been 'more positive' and contained higher levels of PrP^{Sc} which is only revealed by western blotting.

4.4 Infectivity of IPK1 cells following siRNA treatment

As the identity of the infectious agent has not been established in prion disease, it is important to examine infectivity levels in addition to PrP^{Sc} when evaluating a potential therapeutic compound. To determine the intracellular infectivity following siRNA treatment, cells were harvested from triplicate wells of each condition on days 4 - 7 and homogenised. The samples were examined using the SCA and the starting infectivity was calculated from the number of PK1 cells positive for PrP^{Sc} 3 passages after exposure to the homogenates. As shown in Figure 4.6, reducing PrP^{C} expression also reduced intracellular infectivity of the MW1 treated IPK1 cells.

Figure 4.6 Knockdown of PrP^{C} reduces intracellular infectivity of IPK1 cells

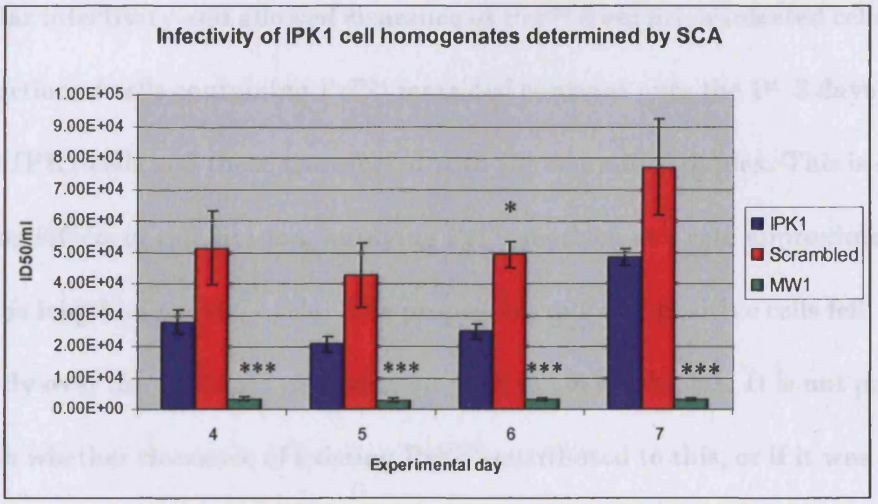

Triplicate wells of IPK1 cells were harvested on the indicated days and homogenates made. Total protein was determined by BCA and the concentrations were adjusted to 200µg/ml. A 1:50 dilution of each homogenate was applied to 6 wells of uninfected PK1 cells for the SCA by Dr F Properzi. The cells were passaged at 1:10 dilutions 3 times over 12 days before 25,000 cells from each well were transferred to an ELISPOT plate for detection of PK-resistant material. Infectious units (ID50/ml) were calculated from a standard curve of an RML-infected brain homogenate of known prion titre. Error bars represent s.e.m.

The reduction in intracellular infectivity following treatment with the MW1 duplex was highly significant with a p value of 4.6×10^{-6} by day 7 (Wilcoxon-Mann-Whitney U Test, used due to differing numbers of data points between some groups). Interestingly, the cells treated with the scrambled duplex had the same level of intracellular infectivity as the untreated IPK1 cells except for day 6 when they were more infectious ($p = 0.02$). It is possible that this inconsistency may have arisen due to contamination in 5/18 wells of the IPK1 condition on day 6, meaning some of the data had to be excluded.

4.5 Discussion

Removing PrP^{C}, the substrate for prion conversion, by RNAi effectively reduced intracellular infectivity and allowed clearance of PrP^{Sc} from prion-infected cells. The proportion of cells containing PrP^{Sc} remained constant over the 1st 3 days in the untreated IPK1 cells and those transfected with the scrambled duplex. This is despite the diluting effects of cell division, implying PrP^{Sc} doubled at a rate approximately equal to the length of the cell cycle. The proportion of PrP^{Sc}-positive cells fell significantly over the 1st 3 days of treatment with the MW1 duplex. It is not possible to distinguish whether clearance of existing PrP^{Sc} contributed to this, or if it was simply due to prevention of further accumulation and dilution below the detection limit as a result of cell division. There was however, a further significant drop in the percentage of PrP^{Sc} positive cells over the last 4 days of the experiment following treatment with MW1. As the cells had ceased dividing by this point, it suggests that removal of the

endogenous PrP^{C} not only prevented further conversion, but also allowed clearance of existing PrP^{Sc} in these cells.

The infectivity of the cells treated with the MW1 duplex had reached its lowest point by day 4 and did not change significantly over the next 3 days of the experiment. This is the 1st demonstration that exogenous knockdown of PrP^{C} results in a rapid loss of infectivity in prion-infected cells. The loss of infectivity in MW1-treated cells preceded clearance of PrP^{Sc} by several days and then infectivity levels remained constant as residual PrP^{Sc} slowly reduced over the last 3 days. This suggests that infectivity is not proportional to PrP^{Sc} levels and the infectious agent is an early product of the conversion reaction. One caveat of these results is that the levels of infectivity in the MW1-transfected cells may have been near the lower limit of detection in this system. Repeating the experiment with more concentrated homogenates could resolve this. Also supporting the interpretation, however, is the observation that both total levels of PrP^{Sc} and the proportion of PrP^{Sc}-containing cells were significantly higher following transfection with the scrambled duplex than in untreated IPK1 cells, yet the intracellular infectivity levels were remarkably similar in the 2 conditions. Furthermore, on day 4 only twice as many of the untreated IPK1 cells and those receiving the scrambled duplex were positive for PrP^{Sc} than the cells treated with MW1, but the intracellular infectivity of the MW1-treated cells was lower by one log.

These results are consistent with a model of prion infection in which the infectious agent is an intermediate formed during the conversion reaction and PrP^{Sc} aggregation within the cell would act to limit the number of molecules available to act as a template for further conversion of PrP^{C}. Whatever the mechanism of conversion, the results detailed

here show that removal of endogenous PrP^{C} by exogenous means allows clearance of PrP^{Sc} and more importantly, infectivity from prion-infected cells *in vitro* and suggests that this may be a valuable therapeutic approach *in vivo*.

CONSTRUCTION OF LENTIVIRUSES EXPRESSING shRNA SEQUENCES TARGETING *Prnp*

5.1 Introduction

Results of experiments detailed in Chapter 4 indicated that RNAi-mediated reduction of *Prnp* expression may be of benefit in prion disease as both PrP^{Sc} accumulation and intracellular infectivity are reduced *in vitro*. In order to validate this approach further, a strategy for delivering interfering RNA molecules to the brain of prion-infected animals is required. This chapter describes the construction and validation of lentiviruses expressing shRNAs targeting the prion gene as a potential tool for stable exogenous knockdown of *Prnp*.

5.1.1 Lentiviruses

Lentiviruses belong to the large family of retroviruses which includes the human immunodeficiency virus, HIV-1. HIV-1 primarily uses receptor-mediated fusion at the plasma membrane to enter a cell in a process mediated by the envelope (Env) protein (Gomez and Hope, 2005). Following fusion between the viral and plasma membranes, the viral capsid containing the RNA genome and various enzymes required for replication is released into the cytoplasm (Chan and Kim, 1998). Once inside the cell, the viral reverse transcriptase enzyme copies the HIV-1 sense RNA strand into viral

cDNA which is converted to dsDNA by host DNA polymerase and can then stably integrate into the host cell genome (Zheng et al., 2005) (see Figure 5.1).

Figure 5.1 Lentiviral infection of a target cell

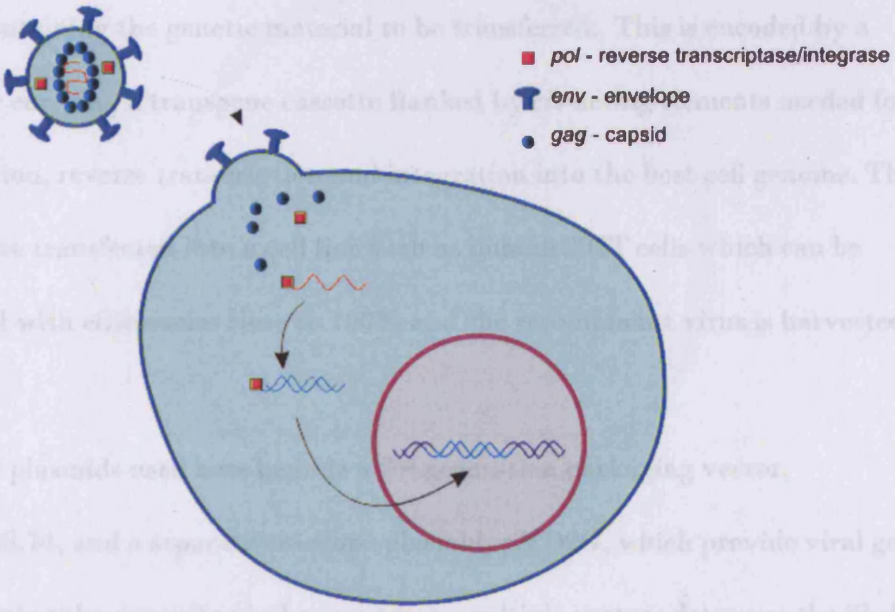

Schematic depicting key events during lentiviral infection of a target cell. Envelope protein mediates lentivirus fusion with the target cell plasma membrane allowing intracellular release of viral capsid contents. The viral RNA (shown in orange) is reverse transcribed into DNA (pale blue) and transported to the nucleus where it integrates into the host cell genome (purple).

Integration is mediated by the viral integrase enzyme, requires the presence of long terminal repeats (LTRs) at the ends of the viral genome and occurs in random places in the host cell genome. This integration is the basis for persistent infection and allows long-term expression of genes contained within the viral genome without provocation of

an immune response, making lentiviruses an attractive tool for gene therapy applications.

5.1.2 Production of lentiviruses in vitro

In vitro production of lentiviruses requires transient transfection of helper plasmids encoding the genes required for virus production and packaging, in addition to the plasmid containing the genetic material to be transferred. This is encoded by a lentivector carrying a transgene cassette flanked by *cis*-acting elements needed for encapsidation, reverse transcription and integration into the host cell genome. The plasmids are transfected into a cell line such as human 293T cells which can be transfected with efficiencies close to 100% and the recombinant virus is harvested from the media.

The helper plasmids used here include a 2nd generation packaging vector, pCMV_dR8.74, and a separate envelope plasmid, pMD2G, which provide viral genes in *trans*. Splitting the requisite viral genes across multiple vectors decreases the likelihood of inadvertently generating replication-competent virus through adventitious recombination of the lentiviral genome. The 2nd generation packaging vectors are additionally deleted in all viral auxiliary genes (vpr, vif, vpu and nef). The pCMV_dR8.74 plasmid (Figure 5.2) uses the human cytomegalovirus promoter (CMV) to drive high level expression of the HIV-1 *gag* and *pol* genes. *Gag* encodes the viral core proteins required for forming the structure of the lentivirus including the viral capsid, nucleocapsid and protective matrix. *Pol* encodes the reverse transcriptase and integrase

enzymes necessary for replication and integration of the lentivirus. Efficient expression of *gag* and *pol* requires a post-transcriptional regulator called *rev* which promotes export of viral mRNA containing a Rev response element (RRE) from the nucleus.

Figure 5.2 Vector map of the pCMV_dR8.74 packaging plasmid

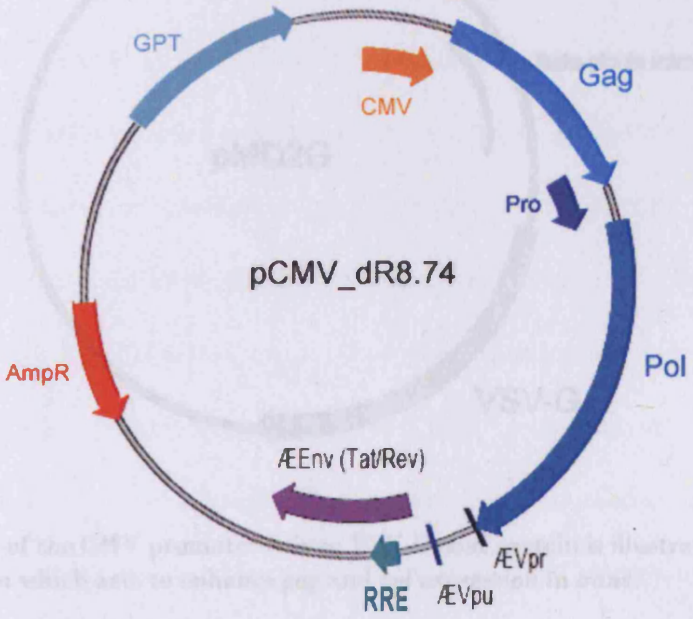

Vector map showing major coding regions of the pCMV_dR8.74 packaging plasmid. The vector is deleted in viral accessory genes Env, Vpu, Nef and Vpr and guanine phosphoribosyltransferase (GPT) replaces the Env gene for historical reasons.

Although the packaging plasmid contains the minimal genes necessary to produce a virion, it has been rendered replication defective by the mutation of viral regulatory genes and replacement of the envelope protein. The HIV-1 virus is able to change its cell binding specificity by combining with envelope proteins from other viruses in a process

known as pseudotyping. The envelope protein used here, VSV-G, is provided in *trans* on another helper plasmid, pMD2G (Figure 5.3).

Figure 5.3 Vector map of the envelope plasmid pMD2G

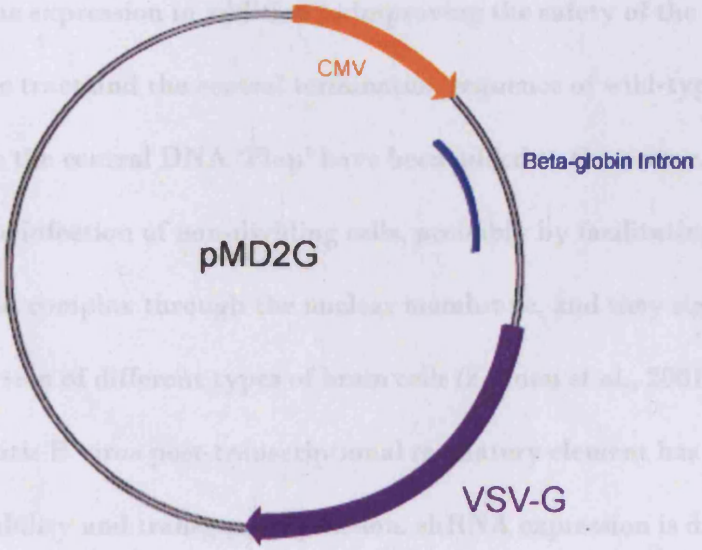

The coding region of the CMV promoter-driven VSV-G coat protein is illustrated in addition to the β-globin intron which acts to enhance *gag* and *pol* expression in *trans*.

VSV-G is the coat protein from the Vesicular Stomatitis Virus which confers broad tropism to the lentivirus and makes the viral particles more stable. VSV-G pseudo-typed lentiviruses also appear to preferentially infect neurons over glia making them an attractive tool for use in neurodegenerative disease (Duale et al., 2005). In addition to the VSV-G protein, the pMD2G vector contains the human β-globin intron which enhances expression of the *gag* and *pol* genes in mammalian cells.

The lentiviral expression vector utilized here, pLL3.7, is derived from the pHR' vectors first described by Naldini and colleagues (Naldini et al., 1996a;Naldini et al., 1996b) with some modifications. The U3 region of the 3' LTR was deleted (Sirven et al., 2001), rendering the integrated viral DNA replication incompetent and preventing interference of the LTR with the transgene promoter (Miyoshi et al., 1998). This modification increases transgene expression in addition to improving the safety of the vector. The central polypurine tract and the central termination sequence of wild-type HIV-1 which together comprise the central DNA 'Flap' have been added to the vector. These sequences enhance infection of non-dividing cells, probably by facilitating transport of the pre-integration complex through the nuclear membrane, and they significantly improve transduction of different types of brain cells (Zennou et al., 2001). Finally, the woodchuck hepatitis B virus post-transcriptional regulatory element has been added to improve RNA stability and transgene expression. shRNA expression is driven by a murine U6 promoter and a separate CMV promoter drives expression of the GFP reporter protein to facilitate identification of transduced cells. A map of the pLL3.7 vector is shown in Figure 5.4.

Figure 5.4 Vector map of pLL3.7 lentivector

A.

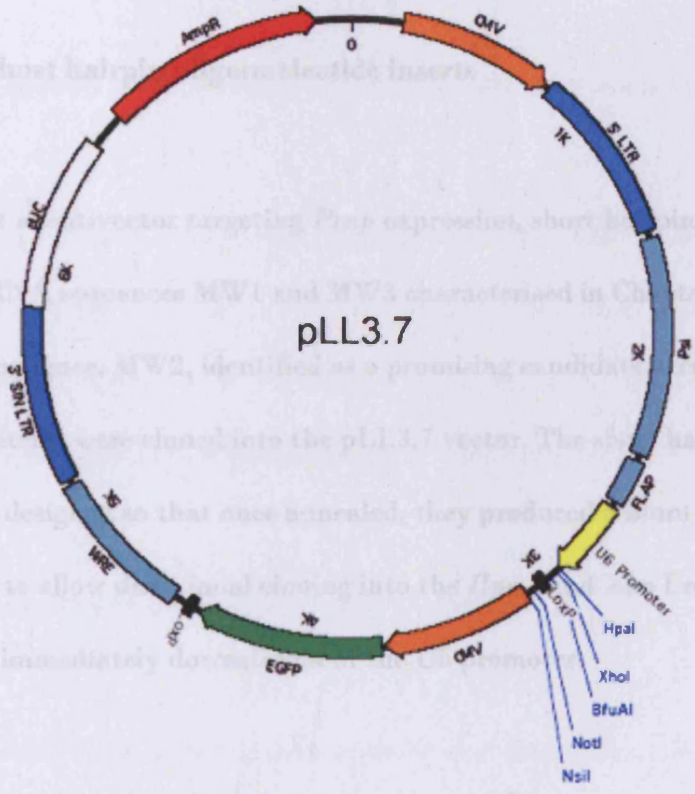

B.

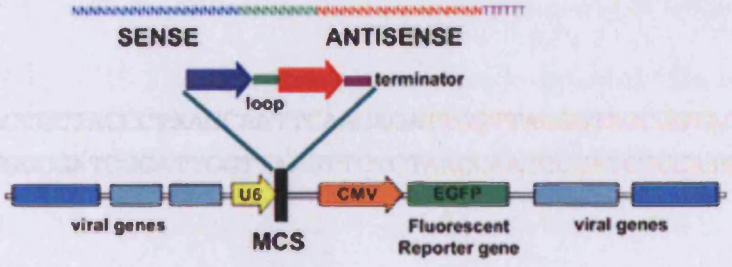

A. Vector map illustrating major features of pLL3.7. Viral accessory genes are indicated in blue and the restriction sites in the multiple cloning site (MCS) are shown. B. Schematic depicting expression cassette for shRNA and cloning of oligonucleotide insert into MCS.

5.2 Construction of lentivectors for expression of shRNAs directed against *Prnp*

5.2.1 Short hairpin oligonucleotide inserts

To construct a lentivector targeting *Prnp* expression, short hairpin sequences derived from the siRNA sequences MW1 and MW3 characterised in Chapter 3, plus an additional sequence, MW2, identified as a promising candidate according to the Reynolds criteria were cloned into the pLL3.7 vector. The short hairpin oligonucleotide inserts were designed so that once annealed, they produced a blunt 5' end and a sticky 3' overhang to allow directional cloning into the *Hpa* I and *Xho* I restriction sites of the lentivector, immediately downstream of the U6 promoter.

The sequences of the short hairpin inserts were as follows:

MW1:

5' – TGTACCGCTACCCTAACCAATTCAAGAGATTGGTTAGGGTAGCGGTACTTTTTTC – 3'
ACATGGCGATGGGATTGGTTAAGTTCTCTAACCAATCCCATCGCCATGAAAAAAGAGCT

MW2:

5' – TGATCAGTACAGCAACCAGATTCAAGAGATCTGGTTGCTGTACTGATCTTTTTTC – 3'
ACTAGTCATGTCGTTGGTCTAAGTTCTCTAGACCAACGACATGACTAGAAAAAAGAGCT

MW3:

```
5' - TGTGCACGACTGCGTCAATATTCAAGAGATATTGACGCAGTCGTGCACTTTTTTC - 3'
     ACACGTGCTGACGCAGTTATAAGTTCTCTATAACTGCGTCAGCACGTGAAAAAAGAGCT
```

5.2.2 Ligation of oligonucleotide inserts into lentivector

Ligation reactions were set up using molar ratios of insert DNA : pre-digested pLL3.7 vector DNA ranging from 0.5:1 – 5:1. Screening of hundreds of resultant colonies by diagnostic digest failed to yield the desired constructs so the efficacy of oligonucleotide annealing was examined to ensure the inserts were double-stranded.

5.2.3 Confirming annealing of shRNA inserts

Double-stranded DNA molecules can be denatured through heating. Raising the temperature of the solution above the melting temperature of the DNA strands causes them to dissociate. Rapid cooling on ice prevents efficient re-annealing so that the majority of the DNA remains single-stranded. This property of DNA was exploited to determine if the shRNA inserts were double or single-stranded following annealing. Annealed and heat-denatured aliquots of oligonucleotides were examined for size differences by non-denaturing polyacrylamide electrophoresis. Under these conditions, dsDNA migrates relative to its size whilst single-stranded DNA often runs anomalously. As shown in Figure 5.5, the migration of the annealed oligonucleotides was equivalent to a 60bp sequence. The single-stranded oligonucleotides migrated further through the

gel and appeared as a double band due to the extra 4bp on the anti-sense strand. Heat denaturation resulted in the reduction of the dsDNA band and an increase in the ssDNA bands. This suggested that the difficulty cloning the inserts into the lentivector was not due to a failure of the oligonucleotides to anneal.

Figure 5.5 Heat denaturation of oligonucleotide inserts confirms annealing

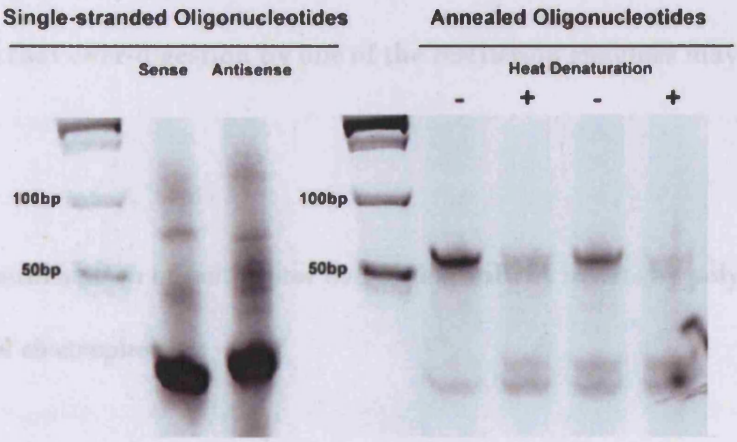

Following heat denaturation of annealed oligonucleotides, 100ng of dsDNA was run on a 10% TBE Polyacrylamide gel. Single-stranded oligonucleotides were loaded onto the gel to provide a comparison. As ssDNA binds ethiduim bromide less efficiently than dsDNA, 1µg samples were loaded. dsDNA markers were loaded to estimate the size of the annealed oligonucleotides. Bands were viewed under UV light on a Biorad Gel Doc 1000 using Quantity One software (version 4.5.1).

5.2.4 Cloning of short hairpin inserts into the lentivector

Following confirmation of oligonucleotide annealing, further ligation reactions were set up for the MW1 shRNA insert at a wider range of molar ratios from 0.5:1 – 100:1. Screening for inserts by diagnostic digests revealed a slight increase in band size in 2 colonies resulting from a 10:1 ligation.

The resolution offered by agarose gel electrophoresis was not sufficient to be certain these bands contained the desired insert, so the digests were run on a polyacrylamide gel to provide better separation of the small DNA fragments. As shown in Figure 5.6, there was a clear size difference of approximately 60bp between the fragments obtained from digestion of the empty vector and those believed to contain the shRNA insert. Throughout the screening, it was observed that bands occasionally appeared to be smaller than that obtained from the empty vector. The reason for this was unclear, but it was suspected that over-digestion by one of the restriction enzymes may have been the cause.

Figure 5.6 Confirmation of lentivector containing shRNA inserts by polyacrylamide gel electrophoresis

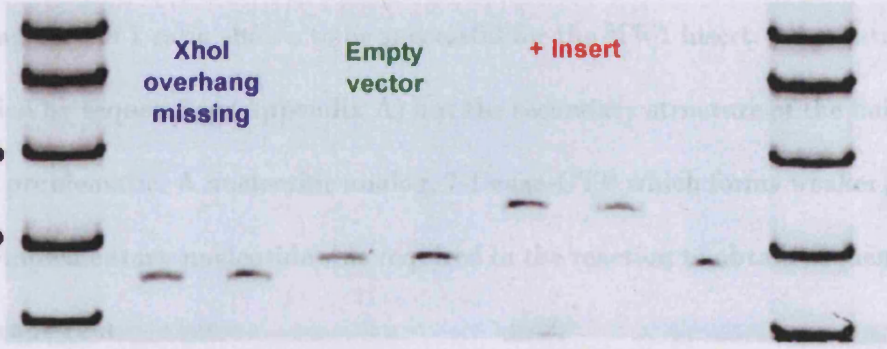

100ng of diagnostic digest reactions were run on a 6% TBE polyacrylamide gel. Empty vector was run in lanes 4, 5 and 8 to provide a size comparison for unknown samples. Bands were visualised as before.

5.2.5 Sequence-verification of constructs

A selection of plasmid preparations that yielded all 3 different sizes of bands in the diagnostic digest were sequenced using the following primer within the Flap sequence upstream of the U6 promoter in pLL3.7:

5'-CAGTGCAGGGGAAAGAATAGTAGAC-3'

Sequencing confirmed the presence of the desired insert in the 2 suspected positive constructs indicating that the 10:1 insert: vector ligation had been successful. The constructs yielding smaller bands than the empty vector were shown to be missing the 3' overhang of the *Xho* I site verifying there was over-digestion of 5-10% of the plasmids by this enzyme.

The remaining short hairpin inserts, MW2 and MW3, were ligated into the pLL3.7 vector using the 10: 1 ratio shown to be successful for the MW1 insert. All constructs were verified by sequencing (Appendix A) but the secondary structure of the hairpin insert was problematic. A nucleotide analog, 7-Deaza-GTP which forms weaker bonds with its complementary nucleotide was required in the reaction to obtain sequences for the MW3 construct.

5.3 Production of lentivirus

5.3.1 Confirming integrity of helper plasmids

Prior to lentiviral construction, each component of the system was transfected individually into HEK293T cells to ensure the plasmids expressed the anticipated proteins. Integrity of the lentiviral plasmid, pLL3.7, was demonstrated by the fluorescence of the GFP reporter in transfected cells (Figure: 5.8A). Western blotting confirmed expression of the viral coat protein, VSV-G, from the pMD2G plasmid and the Gag polyprotein and its cleaved capsid product from the pCMV_dR8_74 vector (Figure: 5.8B and C).

Figure 5.7 Vectors required for lentivirus production are functional

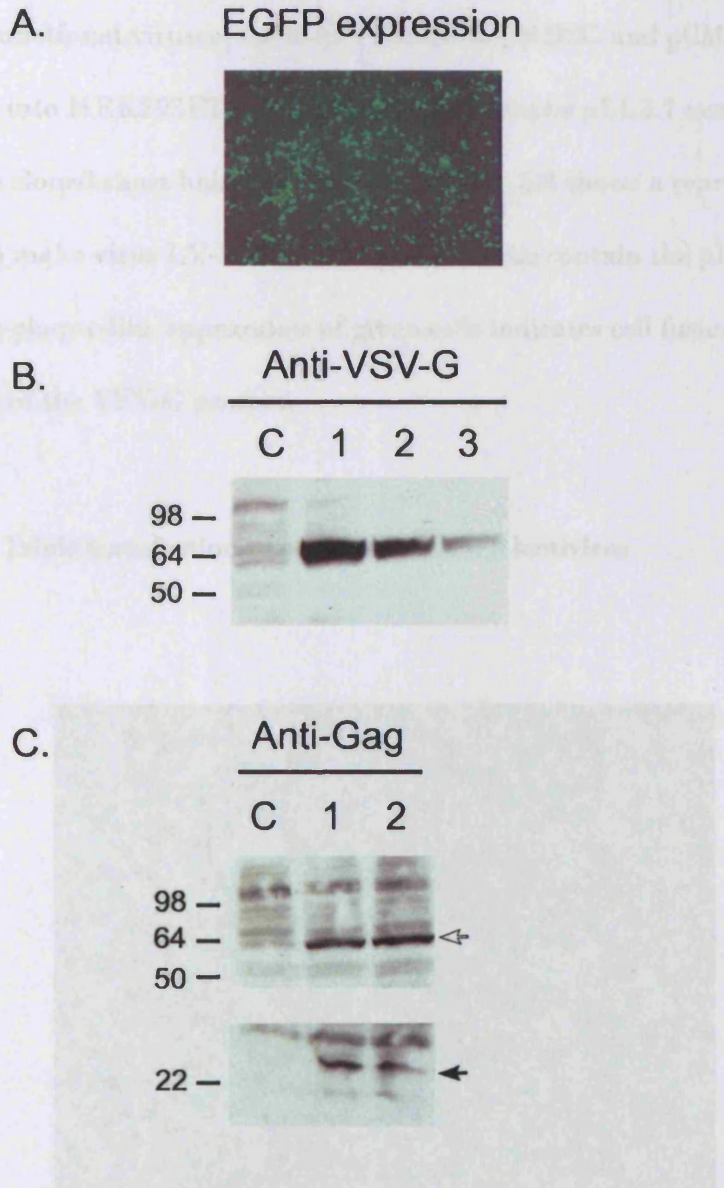

(A) Expression of the GFP reporter gene from pLL3.7 was confirmed by visualisation of fluorescence in transfected cells under UV light 72 hours post-transfection using a Axiovert 200 microscope (Zeiss) with a Nikon Coolpix 995 digital camera. Cells transfected with the helper plasmids were harvested 72 hours post-transfection, lysates made and 25µl of each was run on a 16% polyacrylamide gel. (B) Expression of the VSV-G coat protein from pMD2.G was detected by western blotting with a primary anti-VSV-G antibody (Roche) at 0.5µg/ml. (C) Expression of the *Gag* polyprotein (open arrow) and its cleaved capsid product (closed arrow) was detected with a primary anti-Gag antibody (Abcam) at 1:2000 dilution. Binding of both primary antibodies was visualised with a HRP-conjugated goat anti-mouse secondary antibody and ECL reagents. C = control: untransfected HEK293 cells.

5.3.2 Triple transfection to produce lentivirus

To construct functional viruses, the helper plasmids, pMD2G and pCMV_dR8.74 were co-transfected into HEK293FT cells with either the empty pLL3.7 vector or pLL3.7 containing the cloned short hairpin constructs. Figure 5.8 shows a representative triple transfection to make virus LV-MW3. GFP-positive cells contain the pLL3.7-MW3 vector and the plaque-like appearance of green cells indicates cell fusion resulting from the expression of the VSV-G protein.

Figure 5.8 Triple transfection to produce LV-MW3 lentivirus

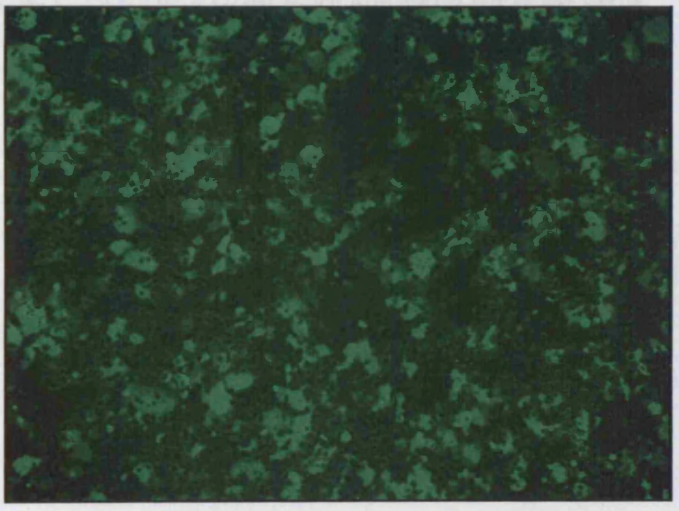

GFP expression in triple-transfected HEK293 cells was visualised under UV light 48 hours post-transfection as before.

5.3.3 Titering lentiviruses

To ensure consistency in subsequent experiments, the titre was calculated for all viruses produced. Serial dilutions of virus were added to fresh HEK293FT cells and FACS analysis for GFP expression was performed. The percentage of GFP-positive cells was double-checked by fluorescence microscopy and always confirmed the FACS result (Figure 5.9). The titre was then calculated by correcting for the number of cells plated and the viral dilution factor using the following equation:

Titre = (% GFP-positive) x (virus dilution factor) x (number of cells plated)

Titres in the range of 1 - 5 x 10^8 TU/ml were achieved for each virus.

Figure 5.9 Determination of viral titre by FACS and immunofluorescence

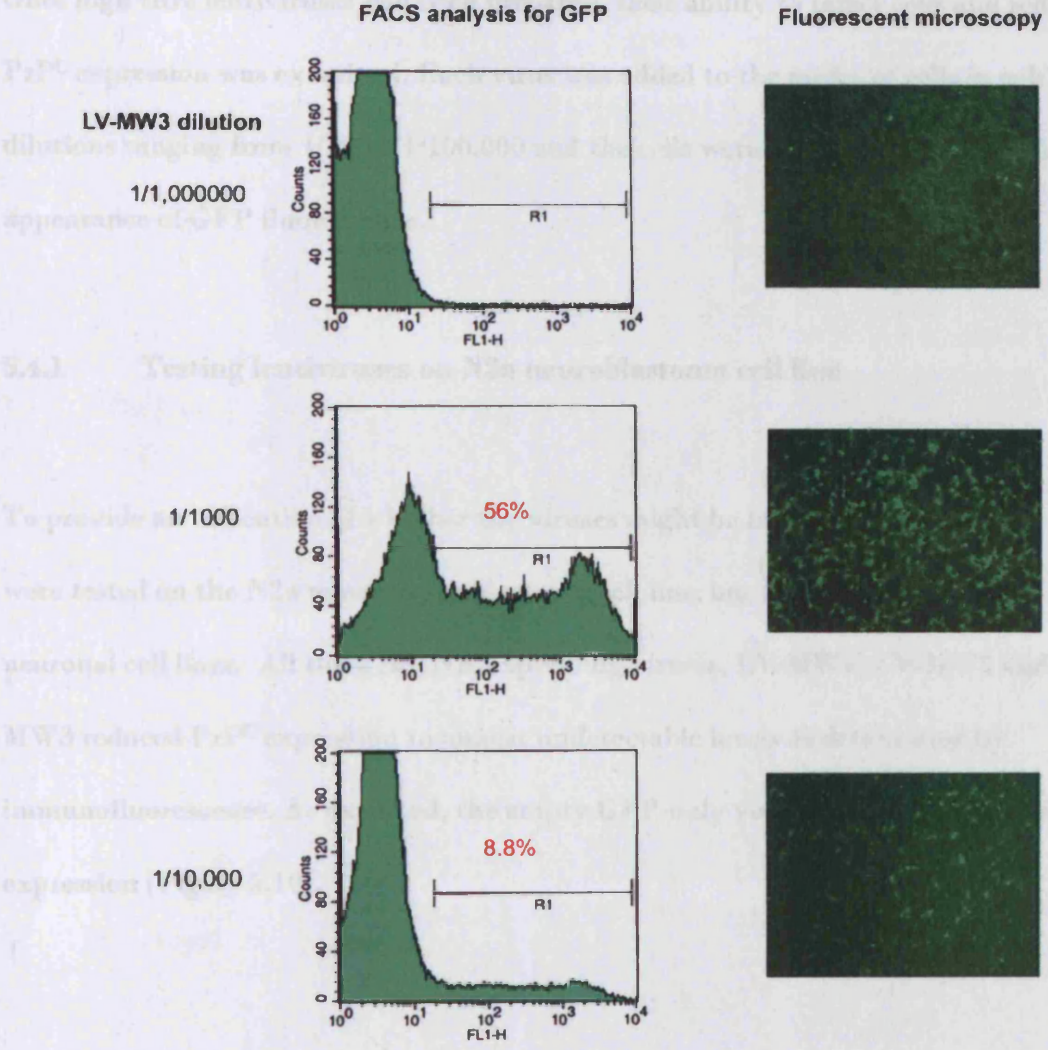

Titre = %GFP+ve x Dilution Factor x Number of cells plated

= 0.088 x 10,000 x 2 x 10^5

= 1.8 x 10^8 TU/ml

Cells infected with LV-MW3 at dilutions ranging from 1:1,000 – 1:1,000,000 were viewed under UV light to estimate percent positive for GFP expression 48 hours post-transduction. They were then harvested, fixed and GFP fluorescence detected by FACS on a FACSCalibur (Becton Dickinson). BD Cellquest software was used to measure the percentage of the population positive for GFP (R1).

5.4 Testing lentiviruses *in vitro*

Once high titre lentiviruses had been prepared, their ability to infect cells and reduce PrP^C expression was examined. Each virus was added to the media of cells in culture at dilutions ranging from 1/100 – 1/100,000 and the cells were monitored daily for the appearance of GFP fluorescence.

5.4.1 Testing lentiviruses on N2a neuroblastoma cell line

To provide an indication of whether the viruses might be functional in the brain, they were tested on the N2a mouse neuroblastoma cell line, one of very few available neuronal cell lines. All three shRNA-expressing viruses, LV-MW1, LV-MW2 and LV-MW3 reduced PrP^C expression to almost undetectable levels as determined by immunofluorescence. As expected, the empty GFP-only virus had no effect on PrP^C expression (Figure 5.10).

Figure 5.10 shRNA-expressing lentiviruses reduce PrP^C expression in N2a cells

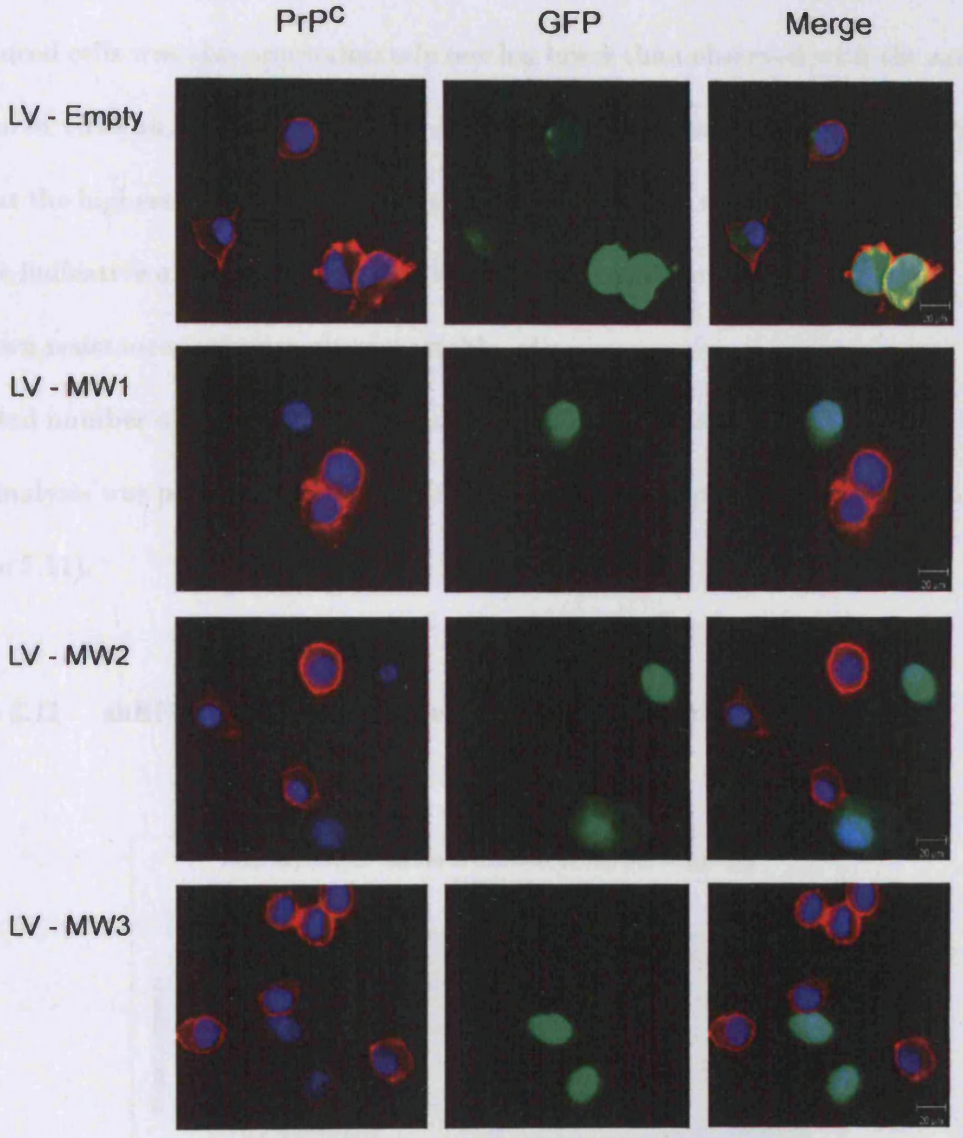

Four days post infection with the lentiviruses, N2a cells on glass coverslips were fixed and immunostained with primary antibody ICSM18 at 10µg/ml. Detection of antibody binding was performed with secondary antibody, Alexa Fluor®568 goat anti-mouse IgG (H+L) (Molecular Probes) at 1:800 dilution. Coverslips were mounted onto slides with DAKO fluorescent mounting medium containing 1 µg/ml 4',6-diamidino-2-phenylindole (DAPI; Sigma) and cells were viewed on an Axioplan 2 MOT microscope (Zeiss) with an AxioCam MRm camera and Axiovision Control software (Zeiss). The cell nuclei are shown in blue, the green signal represents GFP fluorescence in virally transduced cells and red labelling indicates PrP^C staining.

GFP fluorescence was not maximal in virally transduced N2a cells until 4 days post-infection, possibly reflecting the previously reported lower activity of the CMV promoter in rodent cells than in human cells (Ikeda et al., 2002). The proportion of transduced cells was also approximately one log lower than observed with the same dilution of virus on HEK293T cells, revealing the lower permissiveness of the N2a cells. Even at the highest concentrations administered, some cells remained uninfected which may be indicative of quiescence at the time of infection or development of other unknown resistance factors in these unstable cells.

A limited number of transduced cells were manually picked and RNA extracted. RT-PCR analysis was performed to determine the extent of *Prnp* mRNA knockdown (Figure 5.11).

Figure 5.11 shRNA-expressing lentiviruses reduce *Prnp* mRNA expression

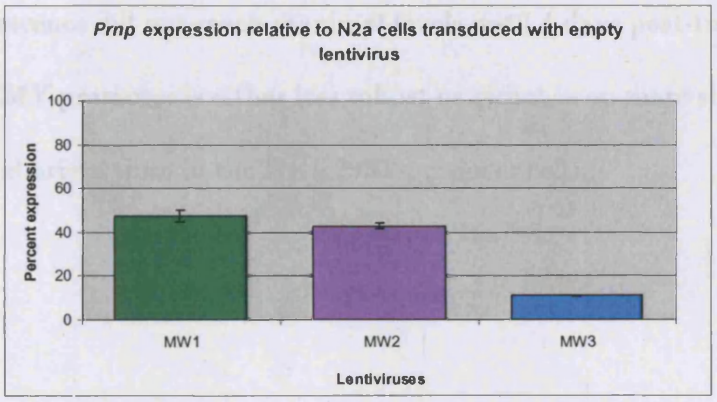

Transduced cells positive for GFP fluorescence under UV light were manually picked and total RNA extracted. One-step RT-PCR amplification of Prnp and β-actin was performed using commercially available ABI assays: Mm00448389_m1 (with FAM labeled probe) for Prnp and Mouse ACTB Endogenous control, VIC® labeled MGB probe. All reactions were performed in triplicate and negative controls included H_2O only and omission of Reverse Transcriptase. *Prnp* expression was normalized to β-actin and expression is shown as a percentage of that in N2a cells transduced with the empty lentivirus. Error bars represent s.e.m.

Transduction with the MW1 and MW2 lentiviruses resulted in ~60% knockdown of PrP mRNA relative to cells transduced with the empty lentivirus. The MW3 lentivirus was more effective, producing ~90% knockdown.

5.4.2 Testing lentiviruses on GT1 hypothalamic cell line

Although the N2a cell line is a useful model in studies of prion disease due to its ability to propagate mouse-adapted scrapie prions, the cells are undifferentiated and therefore do not represent the *in vivo* situation. The GT1 cell line is a well-differentiated neuronal cell line established from hypothalamic neurons which has many characteristics of neurons *in vivo* (Mellon et al., 1990). Following transduction with the shRNA-expressing lentiviruses, PrP^C expression was reduced to nearly undetectable levels in the GT1 cells (Figure 5.12). As before, the negative control GFP-expressing virus, LV-Empty, had no effect on PrP^C. In concordance with the previous transduction of N2a cells, GFP fluorescence did not reach maximal levels until 4 days post-infection suggesting the CMV promoter is either less robust or switches on more slowly in murine cells of a neuronal origin than in the HEK293T producer cells.

Figure 5.12 shRNA-expressing lentiviruses reduce PrP^C expression in GT1 cells

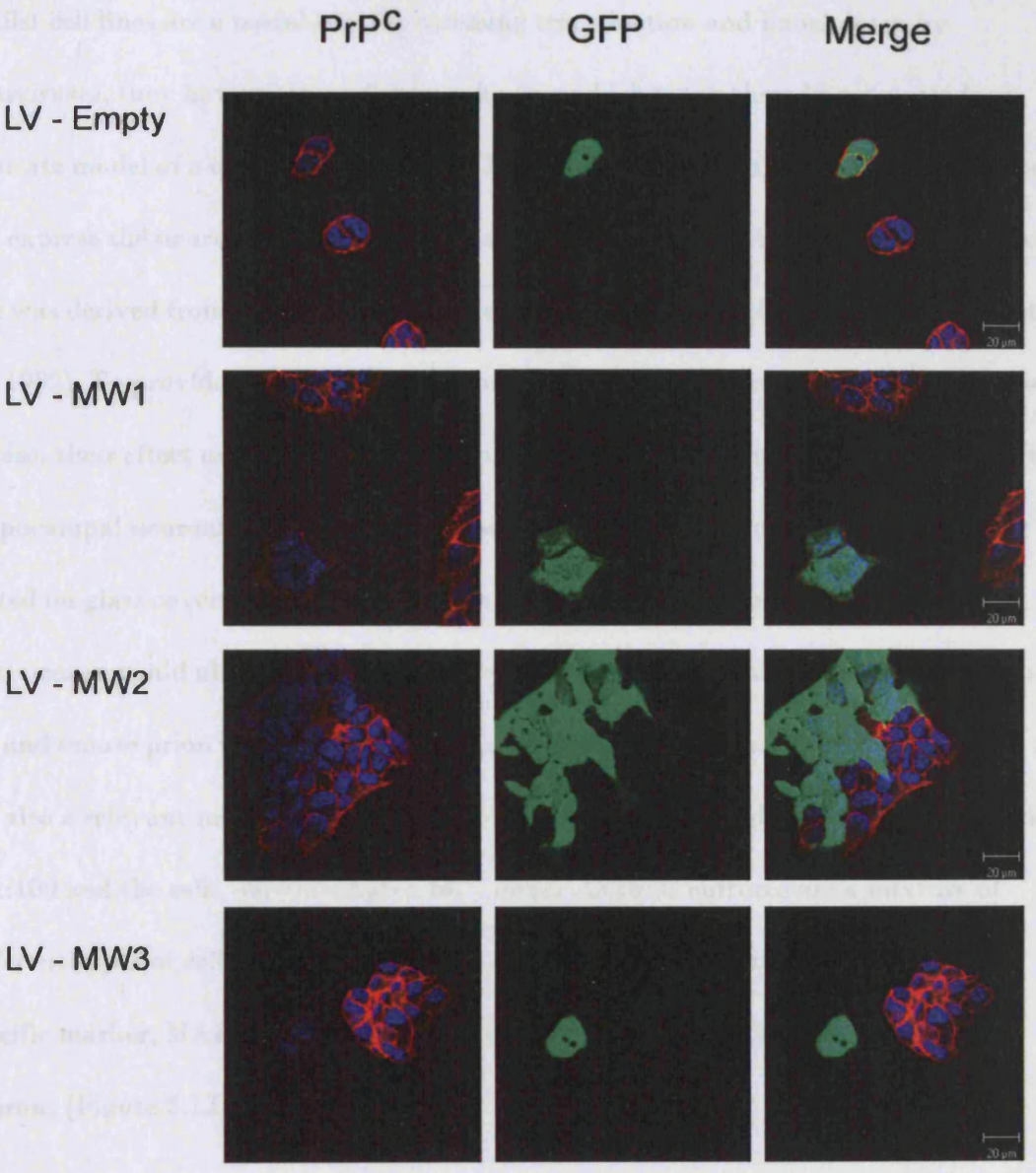

Four days post infection with the lentiviruses, GT1 cells on glass coverslips were fixed and immunostained as before (see Figure 5.10). The cell nuclei are shown in blue, the green signal represents GFP fluorescence in virally transduced cells and red labelling indicates PrP^C staining.

5.4.3 Testing lentiviruses on primary neuronal cultures

Whilst cell lines are a useful tool for assessing transduction and knockdown by lentiviruses, they have often undergone changes which mean they do not provide an accurate model of a cells function *in vivo*. For example, the N2a cell line used here does not express the neuronal marker MAP2 (Izant and McIntosh, 1980) and the GT1-1 cell line was derived from an artificially induced tumour in a transgenic mouse (Weiner et al., 1992). To provide a better indication of whether the lentiviruses would be effective *in vivo*, their effect on primary hippocampal neurons was examined. Freshly dissociated hippocampal neurons from newborn rats were kindly provided on glial feeder layers plated on glass coverslips by Joost Heeroma (Institute of Neurology). Although the lentiviruses would ultimately be administered to mice, the target sequences within the rat and mouse prion proteins are homologous enough that primary neurons from the rat are also a relevant model. The lentiviruses were added to the culture media at a dilution of 1:100 and the cells were incubated for 7 days. As these cultures are a mixture of different types of cells from the brain, the cells were immunostained with a neuron-specific marker, MAP2, to show that the lentiviruses were able to infect primary neurons (Figure 5.13).

Figure 5.13 MAP2 immunofluorescence confirms lentiviruses infect primary neurons

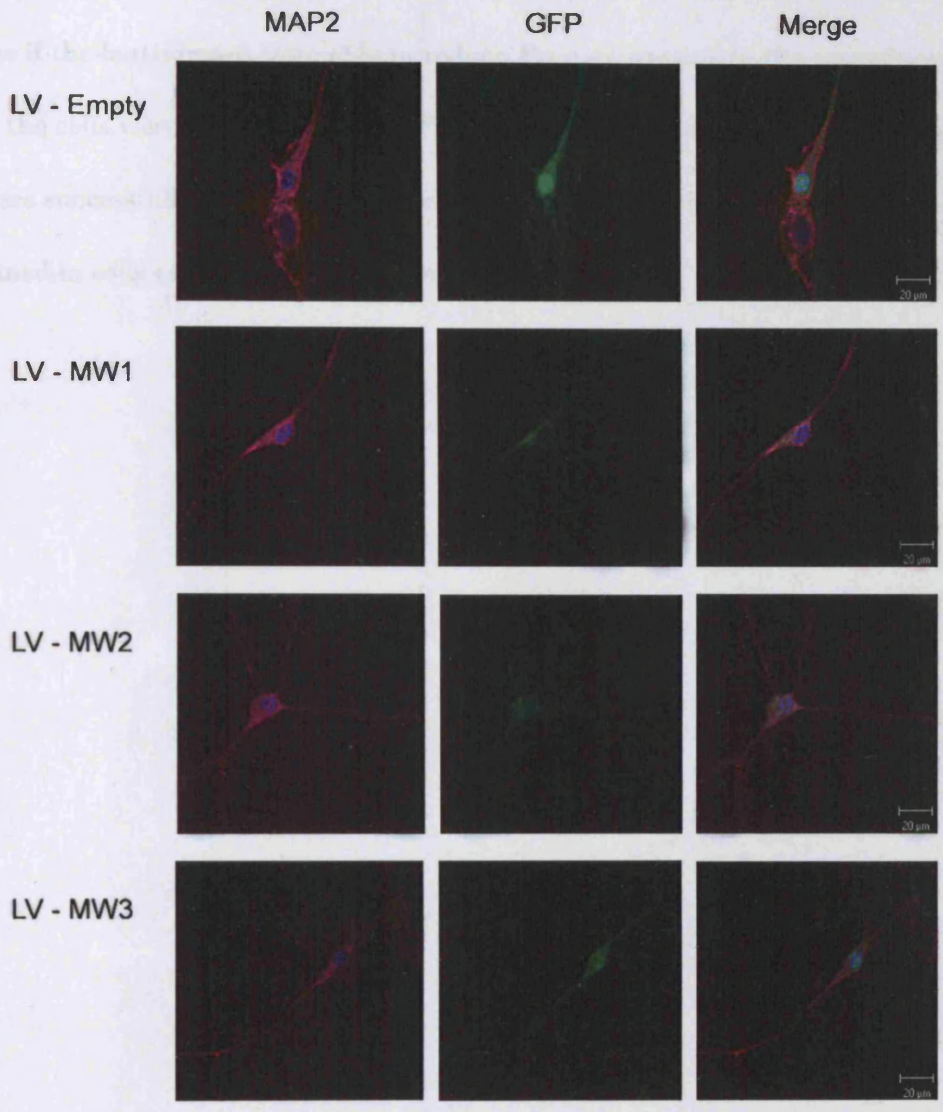

One week post infection with the lentiviruses, primary neurons with glial feeder layers on glass coverslips were fixed and immunostained with primary antibody MAP2 at 1:500 (Abcam). Detection of antibody binding was performed with secondary antibody, Alexa Fluor® 568 goat anti-chicken IgG (Molecular Probes) at 1:1000 dilution. Coverslips were mounted onto slides with DAKO fluorescent mounting medium containing 1 µg/ml 4',6-diamidino-2-phenylindole (DAPI; Sigma) and cells were viewed using a confocal microscope (Zeiss microscope LSM510 META) equipped with a "plan-Apochromat" _63/1.40 oil differential interference contrast objective at room temperature and controlled by Zeiss LSM software. The cell nuclei are shown in blue, the green signal represents GFP fluorescence in virally transduced cells and purple labelling indicates MAP2 staining.

The co-localisation of MAP2 staining and GFP expression in virally transduced cells demonstrates the ability of the lentiviruses to infect primary hippocampal neurons. To determine if the lentiviruses were able to reduce *Prnp* expression in the transduced neurons, the cells were stained for PrP^C. Figure 5.14 shows the shRNA-expressing lentiviruses successfully knocked down PrP^C expression in primary neurons, whereas it was retained in cells transduced by the empty lentivirus.

Figure 5.14 shRNA-expressing lentiviruses reduce PrP^C protein in primary neurons

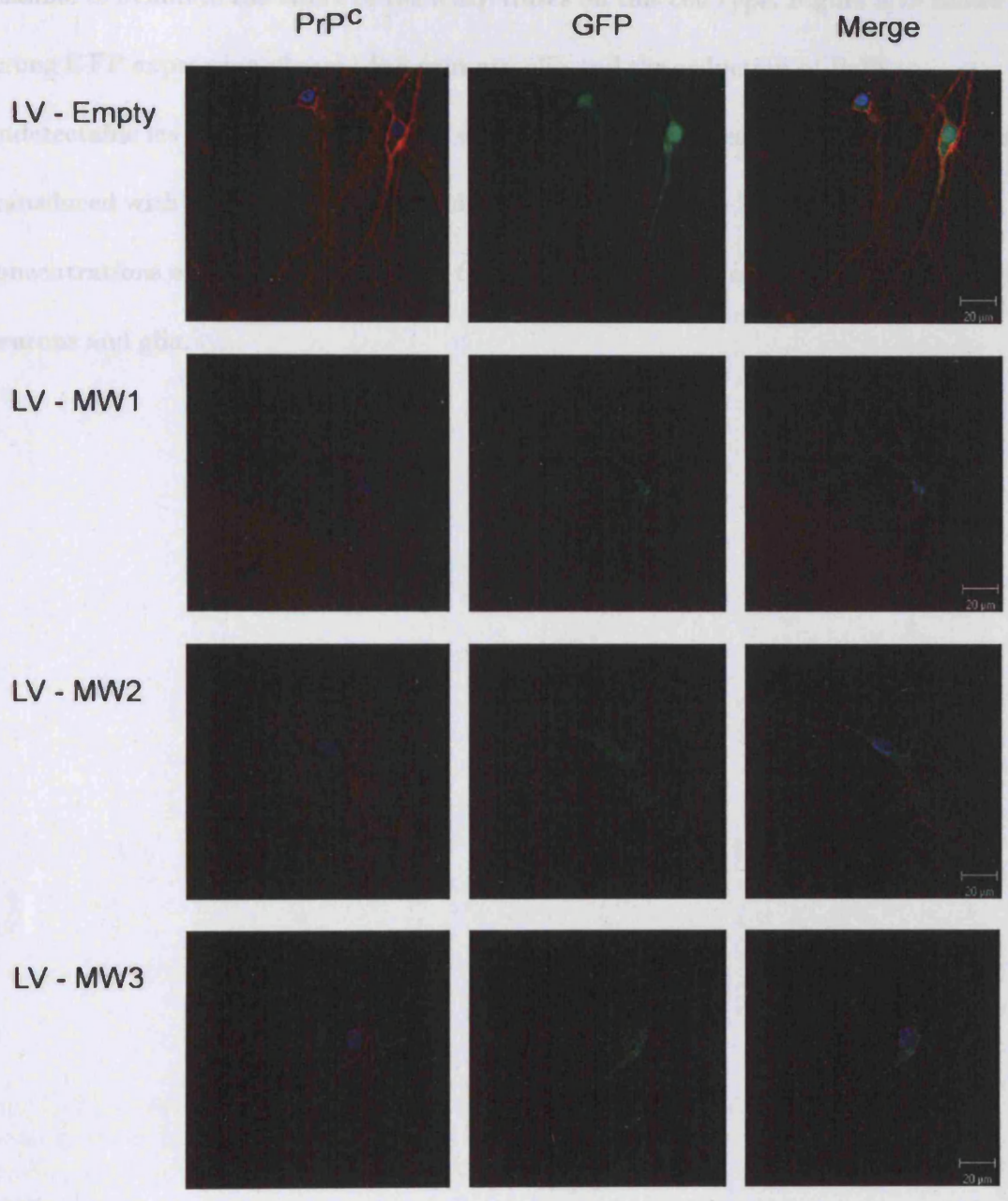

One week post infection with the lentiviruses at 1:100 dilution, primary neurons with glial feeder layers on glass coverslips were fixed and immunostained with primary antibody ICSM18 at 10μg/ml. Detection of antibody binding was performed with secondary antibody, Alexa Fluor®568 goat anti-mouse IgG (H+L) (Molecular Probes) at 1:800 dilution. Coverslips were mounted onto slides and cells were viewed as before. The cell nuclei are shown in blue, the green signal represents GFP fluorescence in virally transduced cells and red labelling indicates PrP^C staining.

As the primary neurons were maintained on feeder layers of glial cells, it was also possible to evaluate the effect of the lentiviruses on this cell type. Figure 5.15 shows the strong GFP expression observed in primary glia and the reduction of PrP^C to undetectable levels in cells transduced with the shRNA-expressing lentiviruses. Cells transduced with the empty lentivirus showed no reduction in PrP^C. At higher concentrations of virus it was possible to transduce all of the cells in the culture - both neurons and glia.

Figure 5.15 shRNA-expressing lentiviruses knockdown PrP^C protein in primary glia

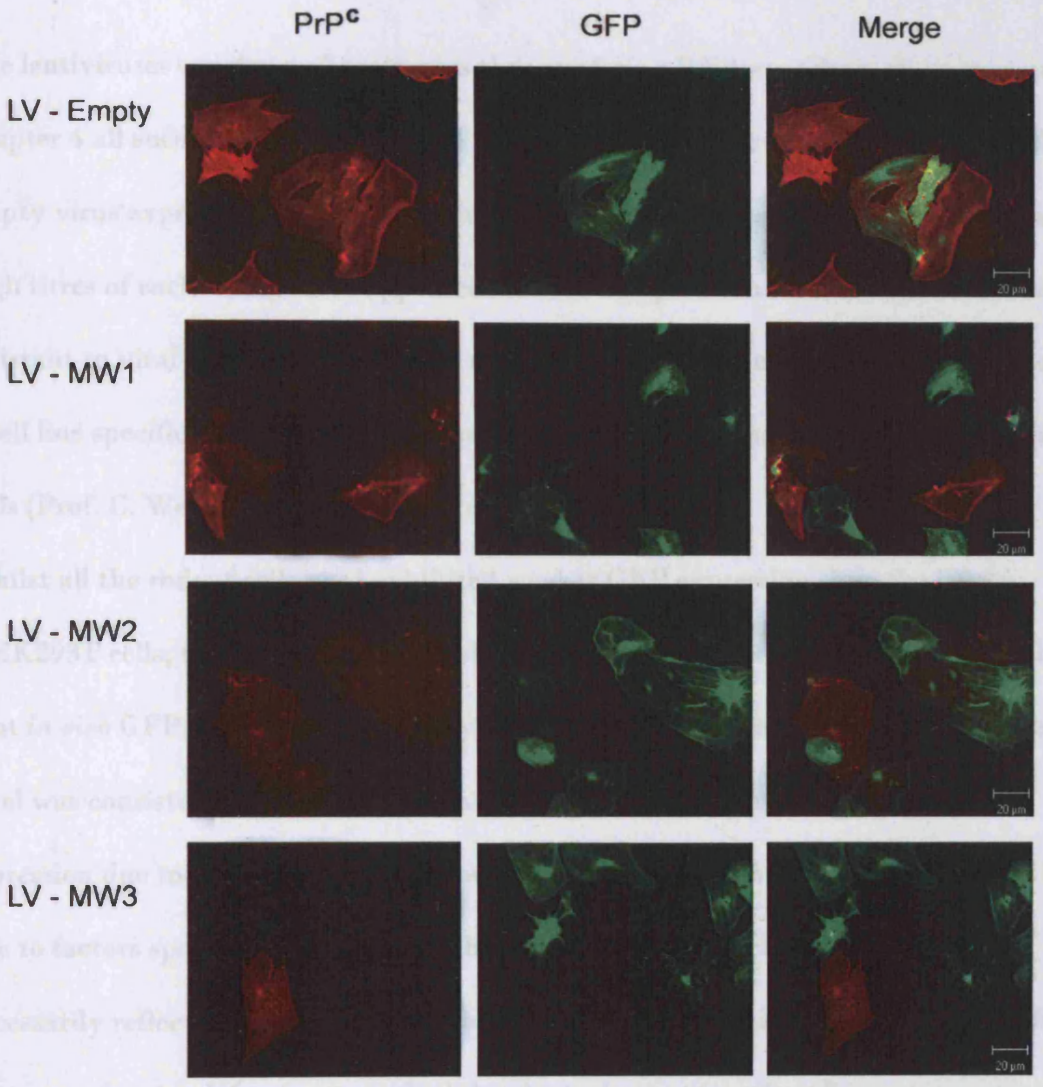

One week post-infection with the lentiviruses at 1:100 dilution, primary neurons with glial feeder layers on glass coverslips were fixed and immunostained as in Figure 5.13. The green signal represents GFP fluorescence in virally transduced cells and red labelling indicates PrP^C staining.

5.5 Discussion

The lentiviruses constructed to express the interfering RNA sequences characterized in chapter 4 all successfully reduced PrP^C expression levels following viral infection. The empty virus expressed GFP only and had no effect on PrP^C levels. Despite achieving high titres of each virus, there appeared to be sub-populations of N2a cells that were resistant to viral infection. As this did not occur with the primary cells, it seemed to be a cell line specific phenomenon, perhaps arising due to the unstable karyotype of these cells (Prof. C. Weissman, unpublished data).

Whilst all the rodent cells used exhibited weaker GFP expression than the human HEK293T cells, the primary neurons showed the lowest fluorescence of all, indicating that *in vivo* GFP expression levels may also be low in neurons. That the GFP expression level was consistently lower in neurons than glia suggests that it is probably not repression due to the integration site (which would vary from cell to cell), but may be due to factors specific to the neurons themselves. Low GFP expression does not necessarily reflect low shRNA expression as the interfering hairpins are expressed from a separate murine U6 promoter which has been shown to work well in various mouse tissues including brain (Rubinson et al., 2003).

Although viruses coated with the VSV-G envelope protein have previously been shown to preferentially infect neurons over glia (Duale et al., 2005), this was not apparent here. When virus was added to a culture of primary neurons on glial feeder layers, the glia were more readily infected with higher proportions of transduced cells at each dilution than the neurons. It is, however, also possible that transduced neurons were

simply more likely to die, resulting in fewer positive cells, or that addition of virus to the culture media killed some neurons. It is unlikely that the effect is due to removal of PrP^C as the same proportions of transduced neurons were also observed with the negative control virus, LV-Empty. Accurate neuronal counts could establish whether the lentiviruses actually infected more glia than neurons.

The coding sequence of the rat *Prnp* gene is ~94% identical to the mouse gene so rat primary cells are an acceptable model system for assessing knockdown of murine *Prnp*. Interestingly, two of the sequences utilized here, MW1 and MW3, target areas which contain a single nucleotide difference in that region of the rat gene. As some mismatches between a siRNA sequence and its target mRNA may block cleavage by RISC it was possible the single nucleotide difference may have abrogated knockdown. The position and type of the mismatch within the siRNA sequence is central to its effect, with maximal disruption of silencing occurring with purine:purine mismatches at the 10^{th} or 16^{th} position from the 5' end of the antisense strand (Schwarz et al., 2006). The mismatches between the shRNAs and the rat *Prnp* gene were both pyrimidine:pyrimidine changes occurring at position 7 for MW1 and position 11 for MW3. These changes have been shown to be well tolerated and did not affect the silencing ability of the lentiviruses used here.

All three shRNA-expressing lentiviruses gave excellent knockdown of PrP^C *in vitro* with LV-MW1 subjectively appearing to yield the greatest knockdown in primary neurons. *In vivo* delivery of the lentiviruses to the brains of prion-infected mice would be required to determine if reduction of *Prnp* expression in this way can be of therapeutic benefit in prion disease.

LENTIVIRAL KNOCKDOWN OF PRP *IN VIVO*

6.1 Introduction

In Chapter 5, lentiviruses expressing shRNAs directed against *Prnp* were shown to be effective at reducing levels of both PrP protein and mRNA in neuronal cell lines and primary neuronal cultures. Reduction of neuronal PrP^{C} expression is known to reduce pathology and prolong survival in prion-infected mice (Mallucci et al., 2003), but an extrinsic mechanism to achieve this is not currently available. To determine if extraneous reduction of PrP^{C} expression through lentivirally-mediated RNAi could be an effective therapy for prion disease, the efficacy of the viruses must be tested *in vivo*. This chapter describes testing of the lentiviruses in mice and preliminary data from therapeutic lentiviral injection of prion-infected mice.

6.1.1 Previous use of lentiviral-mediated RNAi against the prion protein

The first published use of lentiviral gene therapy in prion disease was the demonstration that lentiviruses encoding *Prnp* containing naturally occurring 'prion-resistant' polymorphisms could inhibit the formation of PrP^{Sc} in prion-infected cells (Crozet et al., 2004). The transgenic PrP^{C} acted in a dominant-negative fashion to inhibit conversion of endogenous PrP^{C} into PrP^{Sc}. Although this may have a therapeutic effect *in vivo*, the consequences of expressing this additional PrP^{C} in prion-infected animals still remain unknown.

Another study validated the use of lentiviral-mediated RNAi against the prion protein as a method for engineering transgenic livestock which would potentially be resistant to prion disease (Golding et al., 2006). Although demonstrating a significant reduction of PrP^C expression, this strategy is obviously not applicable to the therapeutic situation where germline manipulations are not relevant.

A more recent paper by Pfiefer and colleagues also describes the use of lentiviral-mediated RNAi against the prion protein (Pfeifer et al., 2006). They tested 6 shRNA sequences for reduction of PrP^C in N2a cells and showed that 1 of them suppressed accumulation of PrP^{Sc} in prion-infected N2a cells in agreement with the RNAi-mediated reduction of PrP^{Sc} and infectivity demonstrated in the IPK1 cell line here (Chapter 4). Stereotaxic injection of their lentivirus into the brains of uninfected mice resulted in localised reduction of PrP^C expression around the injection site, but the virus was not administered to prion-infected mice. Instead, chimeric mice transgenic for the shRNA targeting *Prnp* were made and it was found that 64% of these animals with variable chimerism survived longer than controls after prion infection. Whilst this study demonstrated the safe use of a stably expressed shRNA against the prion protein *in vivo*, it was not administered in a therapeutic form that can be translated into a viable therapy. The chimeric mice created are essentially another transgenic model of PrP^C depletion. It still remains to be determined if reduction of PrP^C expression by stereotaxic delivery of lentiviruses for RNAi can be used to treat prion disease.

6.2 Optimising stereotaxic coordinates for hippocampal targeting of lentiviruses

Intravenous injection of VSV-G coated lentiviruses does not result in efficient transduction of the brain (Pan et al., 2002), meaning the viruses must be injected directly into the desired region. To achieve precise targeting of structures in the brain, stereotaxic surgery is used. To enable comparison of the effects on prion pathology following RNAi-mediated *Prnp* knockdown with the reversal seen after Cre-mediated knockout (Mallucci et al., 2003), the same strain of RML prions would be used. In mice, RML causes severe neuropathology in the hippocampus so this structure was selected as the target for lentiviral transduction. In order to identify the best coordinates for hippocampal targeting, a series of pilot injections was conducted using trypan blue dye injected into freshly culled mice. Tg37 mice were used, as therapeutic treatment would eventually be tested in models of prion disease in this mouse strain.

Figure 6.1 Optimisation of stereotaxic coordinates by trypan blue injection

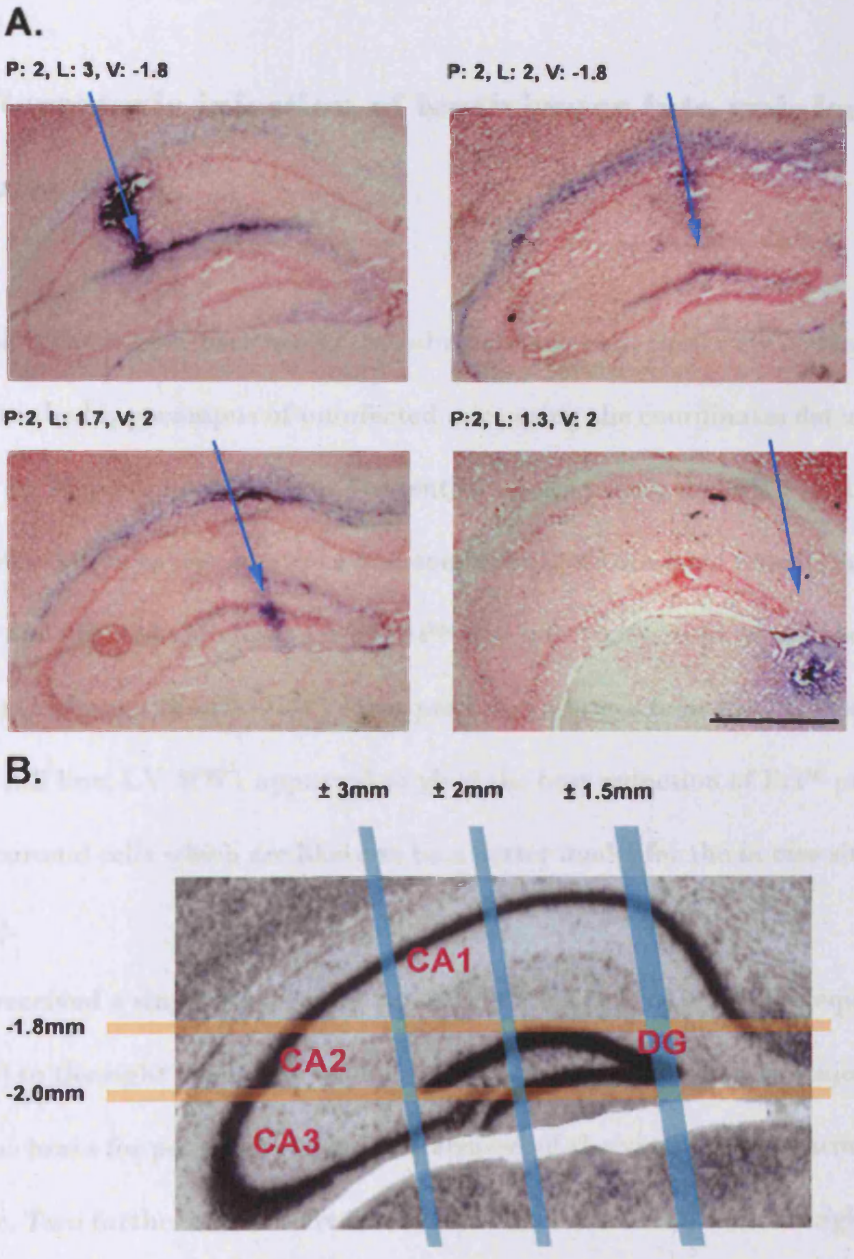

A. Cryostat sections demonstrating representative trypan blue injections into the hippocampus at a range of coordinates. The arrow indicates the path of the needle. Measurements are given in millimetres relative to bregma. P = posterior, L = lateral, V = ventral. B. Schematic illustrating the coordinates targeting the hippocampus identified by the series of trypan blue injections. Scale bar = 1mm.

Optimal targeting of the hippocampus was achieved at coordinates 2mm posterior to bregma, 1.5 – 3mm lateral and 1.8 – 2mm ventral.

6.3 Stereotaxic injection of lentiviruses into uninfected mice

To establish if the lentiviruses would transduce cells *in vivo*, they were stereotaxically injected into the hippocampus of uninfected mice using the coordinates determined previously by trypan blue injection. The lentivirus expressing the MW1 shRNA sequence was chosen as this sequence had consistently shown good reduction of PrP^{C} expression and allowed the clearance of PrP^{Sc} and infectivity from prion-infected cells (Chapter 4). Although the LV-MW3 virus produced a larger reduction of *Prnp* mRNA in the N2a cell line, LV-MW1 appeared to yield the best reduction of PrP^{C} protein in primary neuronal cells which are likely to be a better model for the *in vivo* situation (Chapter 5).

Two mice received a single injection of 2µl of LV-MW1 at 5×10^{8} TU/ml (equivalent to 1×10^{6} TU) to the right hippocampus only, to control for effects of virus injection and examine the brain for possible retrograde transport of the virus to the contralateral hemisphere. Two further mice received two injections of LV-MW1 to the right hippocampus and two injections of LV-Empty at 2×10^{8} TU/ml (equivalent to 4×10^{5} TU/injection) to the left hippocampus to compare transduction efficiencies of the two viruses. Seven days later, they were culled and the brains fixed and embedded in

paraffin. Coronal sections were cut through the hippocampus and every 7th section was stained with an anti-GFP antibody to detect transduced cells. Sections showing positive staining are shown in Figure 6.2.

Figure 6.2 Lentivirally transduced cells in the hippocampus of uninfected mice

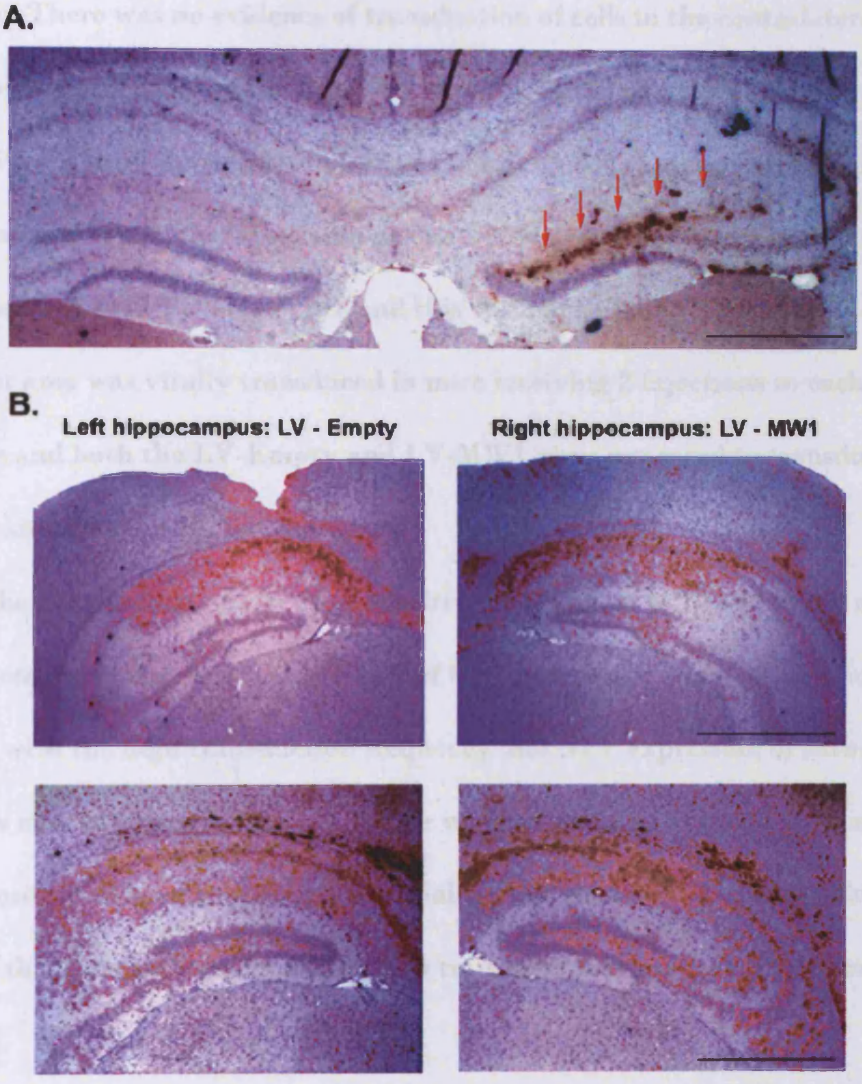

Coronal sections of paraffin-embedded brains were dewaxed and stained with an Anti-GFP antibody (Abcam) at 1:200. Primary antibody binding was detected with a HRP conjugated Goat Anti-mouse antibody (Sigma) on a Ventana automated staining machine (Ventana Medical Systems) according to manufacturers instructions. Sections were counterstained with haematoxylin and mounted in DPX. A. Representative section showing GFP positive cells (brown, indicated by red arrows) in the right hippocampus and lack of staining in the uninjected left hippocampus. Coordinates for injection were: P = 2mm, L = -2mm, V = -2mm. B. Sections from the bilaterally injected mice showing positive GFP staining for LV-Empty in the left hippocampus and LV-MW1 in the right hippocampus. Coordinates for the injections were: P = 2mm, L = ± 2mm, V = -1.8mm and P = 2mm, L = ± 3mm, V = -2mm. Scale bar = 1mm. P = posterior, L = lateral, V = ventral.

The initial set of injections demonstrated transduction of cells in the injected hippocampi. There was no evidence of transduction of cells in the contralateral hippocampus or any other brain structures (remote from the needle track) in the mice which received a single injection of virus to the right hippocampus. A single mouse showed neuronal loss in the hippocampus but TUNEL staining revealed no evidence for neuronal loss in any of the other mice and this was not observed in any other animals. A much larger area was virally transduced in mice receiving 2 injections to each hemisphere and both the LV-Empty and LV-MW1 virus appeared to transduce cells with approximately equal efficiency.

Based on the morphology, many of the positive cells appear to be astrocytic and in general, these cells expressed higher levels of GFP than the neurons. This is in agreement with the high transduction frequency and GFP expression of astrocytes observed *in vitro* in Chapter 5.4.3. At higher magnification however, it was possible to see GFP-positive cells with neuronal morphology and processes that resemble axons, suggesting the lentiviruses were also able to transduce neurons *in vivo* (red arrows, Figure 6.3).

Figure 6.3 **Transduction of neurons and astrocytes by lentiviruses *in vivo***

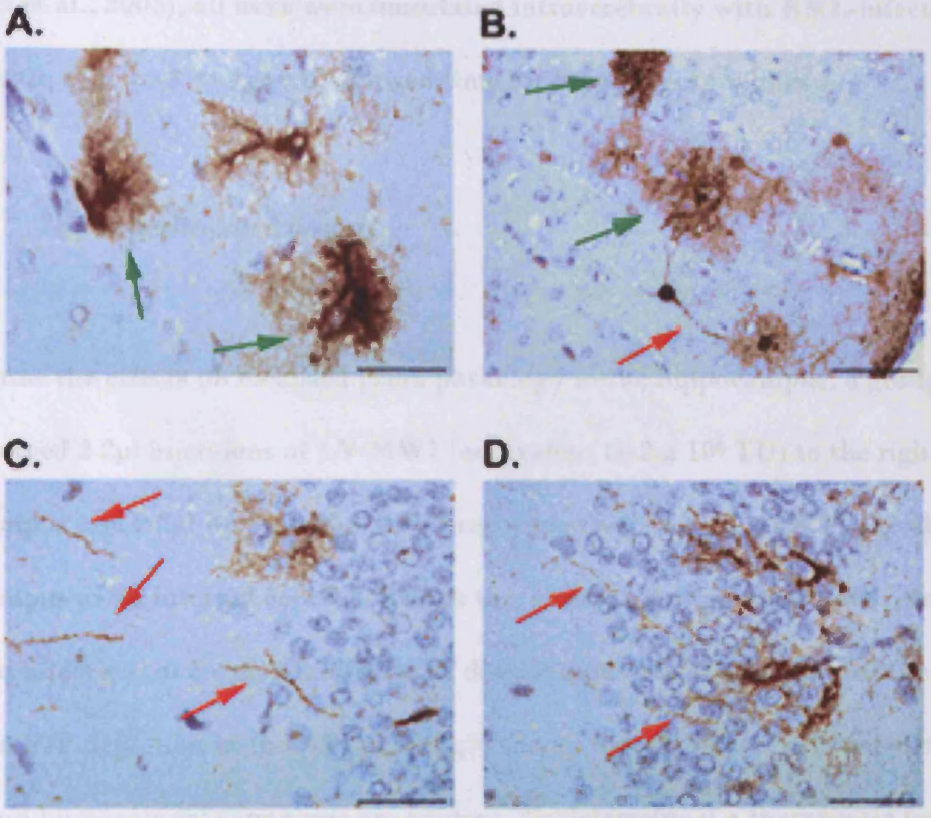

Higher magnification images of sections from uninfected mice injected with LV-MW1. Green arrows indicate GFP-positive cells with astrocytic morphology. Red arrows indicate probable neuronal processes from lentivirally transduced neurons. All images show regions of the hippocampus except for section B which shows virally transduced cells near the top of the needle track in the cortex. Scale bar = 100μm for A, C and D, and 200μm for B.

6.4 Stereotaxic injection of lentiviruses into the hippocampus of RML-infected mice

Following the successful demonstration of lentiviral transduction in uninfected mice, an experiment was designed to examine the effects of the lentiviruses on pathology in mice

with established prion disease. In accordance with the study by Mallucci and colleagues (Mallucci et al., 2003), all mice were inoculated intracerebrally with RML-infected brain homogenate at 1 week of age and allowed time for the prions to replicate.

6.4.1 The experimental design

To examine the effects on localised prion pathology in the hippocampus, a group of mice received 2 2μl injections of LV-MW1 (equivalent to 2 x 10^6 TU) to the right hippocampus and 2 2μl injections of LV-Empty (equivalent to 8 x 10^5 TU) to the left hippocampus as an internal control. Within this group, 1 sub-group of mice received the lentiviral injections at 8wpi, a mid-stage of disease equivalent to the time of Cre-mediated PrP depletion in the NFH-Cre/Tg37 mouse model, when PrP^{Sc} deposition, gliosis and hippocampal spongiosis are evident. To determine if a therapeutic benefit is possible further into the disease course, a 2nd sub-group received the lentiviral injections at 10wpi, a late-stage of disease when neuronal loss is occurring and the mice display early clinical symptoms. All mice were culled 2 weeks after lentivirus administration and their brains taken for analysis of hippocampal *Prnp* mRNA or histological examination. Figure 6.4 shows a schematic illustrating this experimental design.

Figure 6.4 **Schematic illustrating the experiment for comparison of LV-MW1 and LV-Empty in prion-infected mice.**

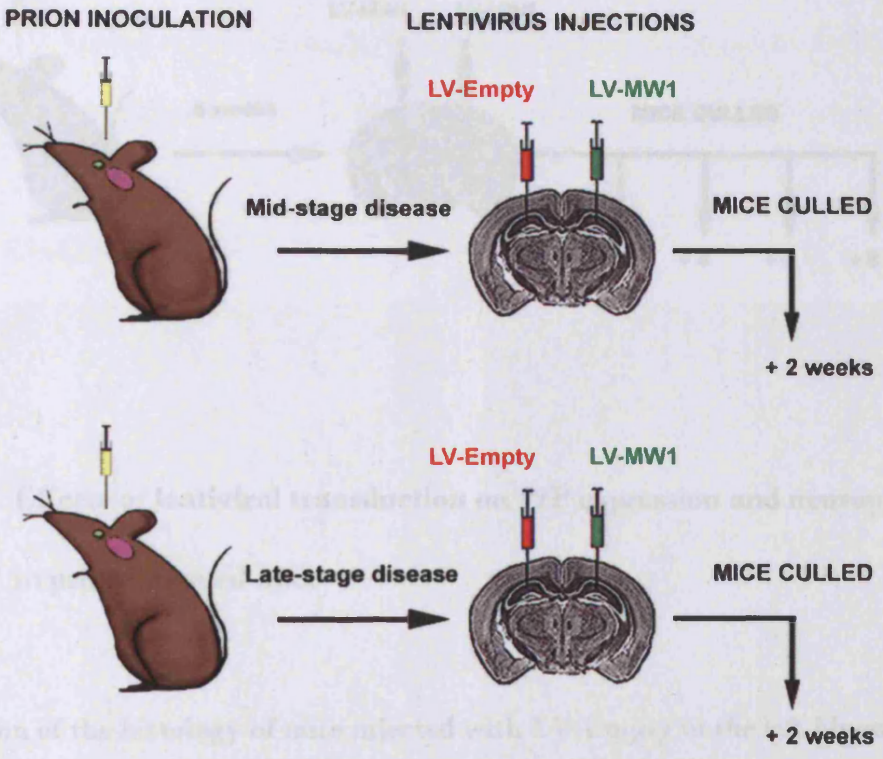

To confirm the lentiviral expression cassette was able to integrate into the host cell genome and produce stable expression and to examine the duration of viral expression in prion-infected mice, a timecourse study was performed. RML-infected mice received 2 2µl injections of LV-MW1 (equivalent to 2 x 10^6 TU) to each hippocampus at 6wpi. Mice were then culled at 2 week intervals and their brains collected for analysis of hippocampal *Prnp* expression and histological examination. A schematic illustrating this experimental design is shown in Figure 6.5.

Figure 6.5 **Schematic illustrating study of duration of LV-MW1 expression *in vivo***

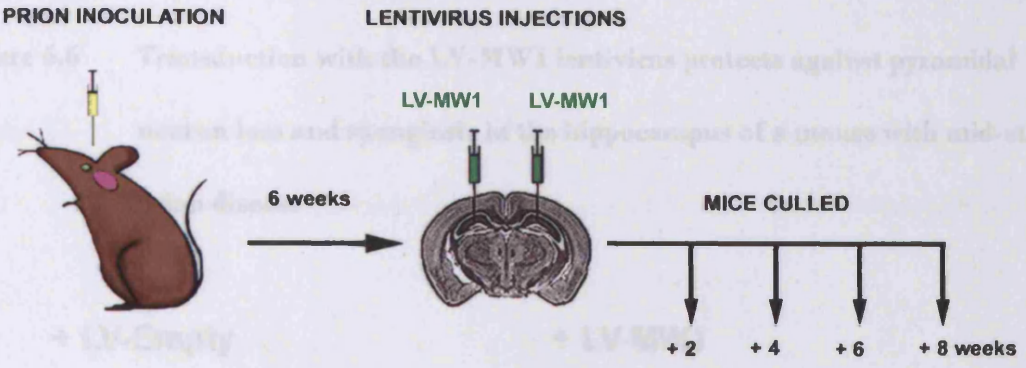

6.4.2 Effects of lentiviral transduction on PrP expression and neuropathology in prion-infected mice

Comparison of the histology of mice injected with LV-Empty in the left hippocampus and LV-MW1 in the right hippocampus 8 weeks post-inoculation with prions revealed local neuroprotective effects in the area transduced with LV-MW1 (Figure 6.6). There was less spongiosis and a more intact stratum pyramidale layer (black arrows, Figure 6.6) in the hippocampus treated with the shRNA-expressing lentivirus. The hippocampus transduced with LV-Empty appeared shrunken with respect to the treated one as indicated by the black, red and blue lines showing the combined depth of the layers from the top of the stratum pyramidale layer to the top of the dentate gyrus.

This is most likely due to loss of cells, projections and interneurons in the LV-Empty treated hippocampus.

Figure 6.6 **Transduction with the LV-MW1 lentivirus protects against pyramidal neuron loss and spongiosis in the hippocampus of a mouse with mid-stage prion disease**

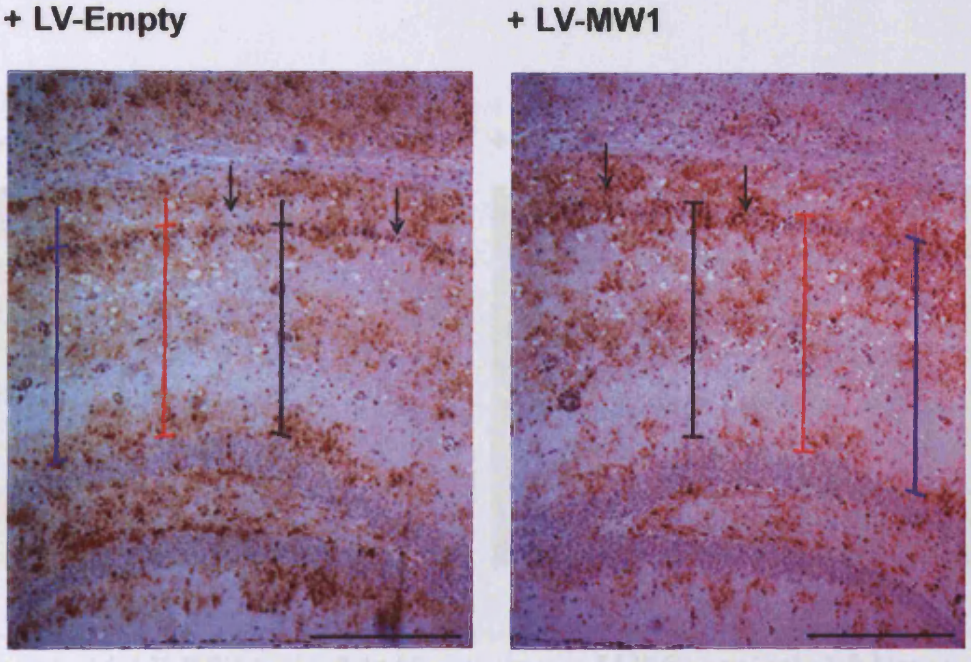

Mice injected with LV-MW1 in the right hippocampus and LV-Empty in the left hippocampus at 8wpi were culled 2 weeks later and stained for GFP expression as before. Image shows left and right hippocampi from the same section of 1 mouse. Brown staining indicates virally transduced cells in the hippocampus. The black arrows highlight the stratum pyramidale and the combined depth of cell layers between the stratum oriens and the dentate gyrus is indicated by the vertical bars. Scale bar = 1mm.

Protection of the stratum pyramidale layer by LV-MW1 was even attainable in mice which received the lentivirus at 10wpi, a late stage of disease when clinical symptoms were evident (Figure 6.7).

Figure 6.7 Transduction with the LV-MW1 lentivirus protects against loss of pyramidal neurons in the hippocampus of a mouse with late-stage prion disease

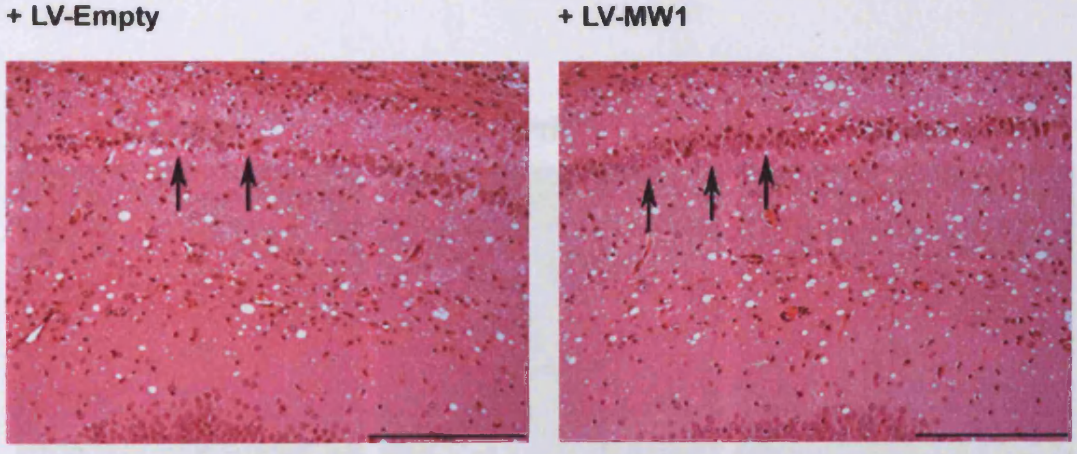

Mice injected with LV-MW1 in the right hippocampus and LV-Empty in the left hippocampus at 10wpi were culled 2 weeks later and stained with haematoxylin and eosin. Image shows left and right hippocampi from the same section of 1 mouse. The black arrows highlight the stratum pyramidale. Scale bar = 500μm.

The protection of the stratum pyramidale conferred by transduction with LV-MW1 appears to be even greater than that attained when the virus was administered 8wpi but this may reflect the fact that these mice were allowed to progress 2 weeks further into the disease course when the majority of neuronal loss may normally occur. It is still

significant however, that neuronal protection can be achieved even in late-stage prion disease.

Double-immunofluorescence for virally expressed GFP and PrP^{Sc} showed little or no colocalisation in the brains of mice injected with LV-MW1 (Figure 6.8). This suggests that stable expression of the MW1 sequence *in vivo* in prion-infected mice prevents accumulation of PrP^{Sc} in a similar manner to that seen *in vitro* in prion-infected cells in Chapter 4.

Figure 6.8 LV-MW1 reduces PrP^{Sc} deposition in prion-infected mice

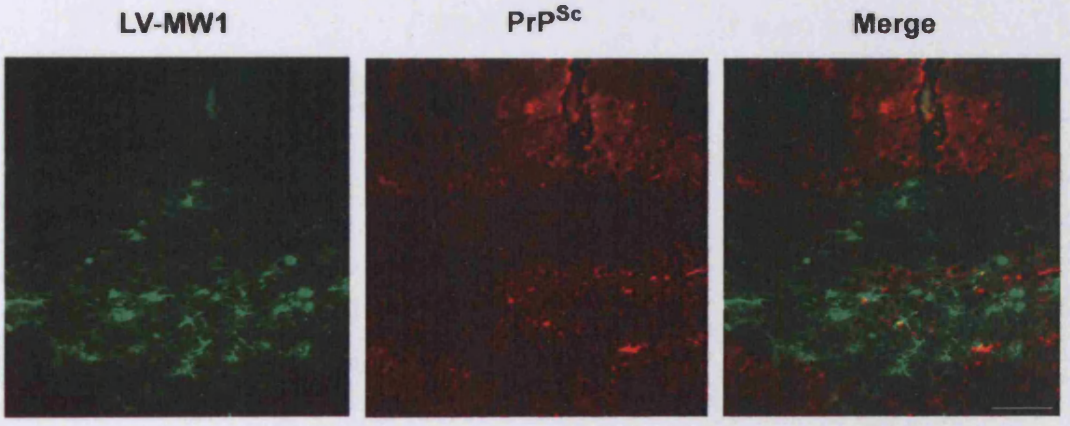

Sections from prion-infected mice injected with LV-MW1 at 8wpi and culled 2 weeks later were dewaxed as usual. They were incubated in 98% formic acid for 3 minutes to remove PrP^{C} and stained with Anti-GFP antibody (Abcam) at 1:150 dilution overnight to detect virally transduced cells. PrP^{Sc} deposition was detected with ICSM35 at 1:1500 dilution. Primary antibody binding was detected with Alexa Fluor®488 goat anti-rabbit IgG (H+L) (Molecular Probes) secondary antibody at 1:400 for GFP and Alexa Fluor®546 goat anti-mouse IgG (H+L) (Molecular Probes) for PrP^{Sc}. Scale bar = 500μm.

Ongoing analysis is expected to verify that the empty lentivirus does not prevent PrP^{Sc} deposition as it has been shown to have no effect on *Prnp* mRNA expression in the hippocampus (Figure 6.9), and no effect on PrP^{C} protein expression in primary hippocampal neurons (Chapter 5.4.3).

RT-PCR analysis confirmed LV-MW1 reduced *Prnp* expression in the hippocampus relative to RML-infected Tg37 mice, whereas LV-Empty did not (Figure 6.9). The knockdown was detectable 2 weeks after administration of the lentivirus and lasted for at least 1 month, signifying the hippocampal cells were stably transduced.

Figure 6.9 Stereotaxic injection of LV-MW1 results in reduction of hippocampal *Prnp* mRNA expression for at least 4 weeks

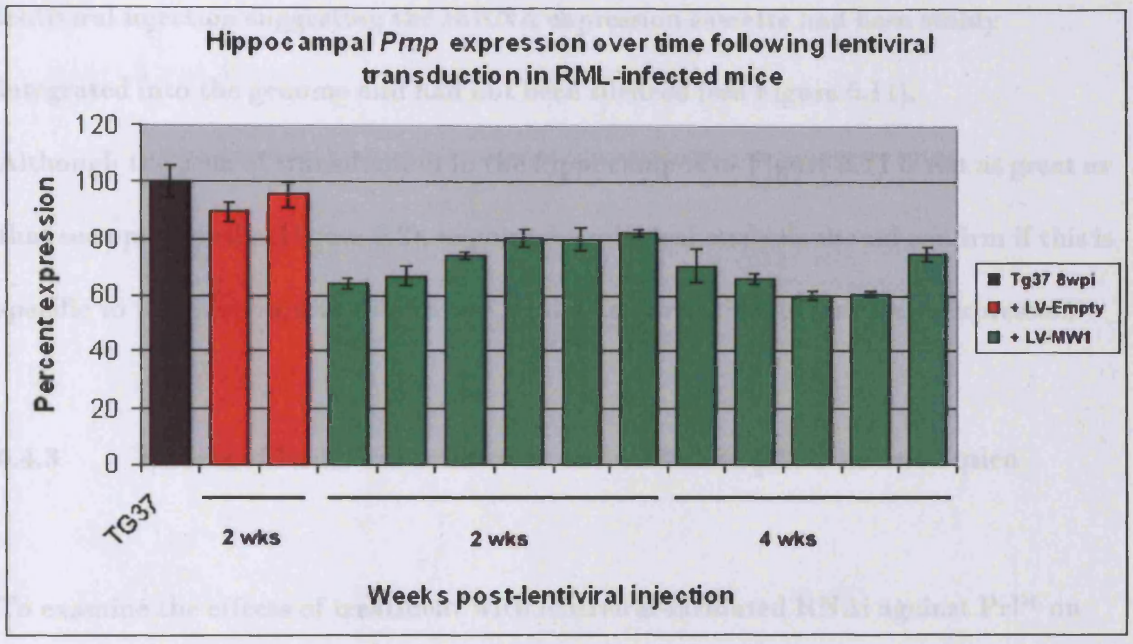

RML-infected mice were culled at the indicated timepoints following lentiviral administration. The hippocampi were dissected out and total RNA extracted. One-step RT-PCR amplification of the MloxP transgene mRNA and β-actin was performed. Primers and probes for the *Prnp* transgene were as follows. Forward primer, 50-GCCCATGATCCATTTTGG-30; reverse primer, 50-CGGTACATGTTTTCACGGTAGT-30; probe, 50-FAM-AACGACTGGGAGGACC-30. β-actin was amplified using a commercially available ABI assay: Mouse ACTB Endogenous control, VIC labeled MGB probe. All reactions were performed in triplicate, and negative controls included H_2O only and omission of Reverse Transcriptase. *Prnp* expression was normalized to β-actin and expression levels in lentivirally injected mice were compared to a pool of 3 Tg37 mice at 8wpi. Error bars represent s.e.m.

The extent of knockdown attained suggested a high rate of lentiviral transduction of a minimum of 20 - 40% of the hippocampus. It was not possible to analyse the mRNA levels 6 weeks after lentiviral injection as the group number was reduced due to loss of animals during surgery and from fighting. Mice were due to be culled 8 weeks after the

lentiviral injection but had become scrapie sick at this time. As this was in excess of the standard incubation time for Tg37 mice however, their brains were taken for histological analysis.

Immunohistological staining confirmed continued GFP expression at 8 weeks post-lentiviral injection suggesting the shRNA expression cassette had been stably integrated into the genome and had not been silenced (see Figure 6.11).

Although the area of transduction in the hippocampus in Figure 6.11 is not as great as that seen previously (Figure 6.2), ongoing histological analysis should confirm if this is specific to the injections in this mouse, or due to partial loss of transgene expression.

6.4.3 Effects of lentiviral treatment on survival in prion-infected mice

To examine the effects of treatment with lentiviral-mediated RNAi against PrP^C on incubation time in mice with established prion disease, a group of mice received 2 2μl injections of either LV-MW1 (equivalent to 2 x 10^6 TU) to each hippocampus or 2 2μl injections of LV-Empty (equivalent to 8 x 10^5 TU) to each hippocampus as a negative control, 8 weeks post-inoculation with RML (Figure 6.10). Treatment was not given to mice with late-stage prion disease due to the difficulty of performing successful surgery on animals with such advanced illness.

Figure 6.10 **Schematic illustrating experimental design to examine the effect of treatment with LV-MW1 on incubation time in mice with mid-stage prion disease**

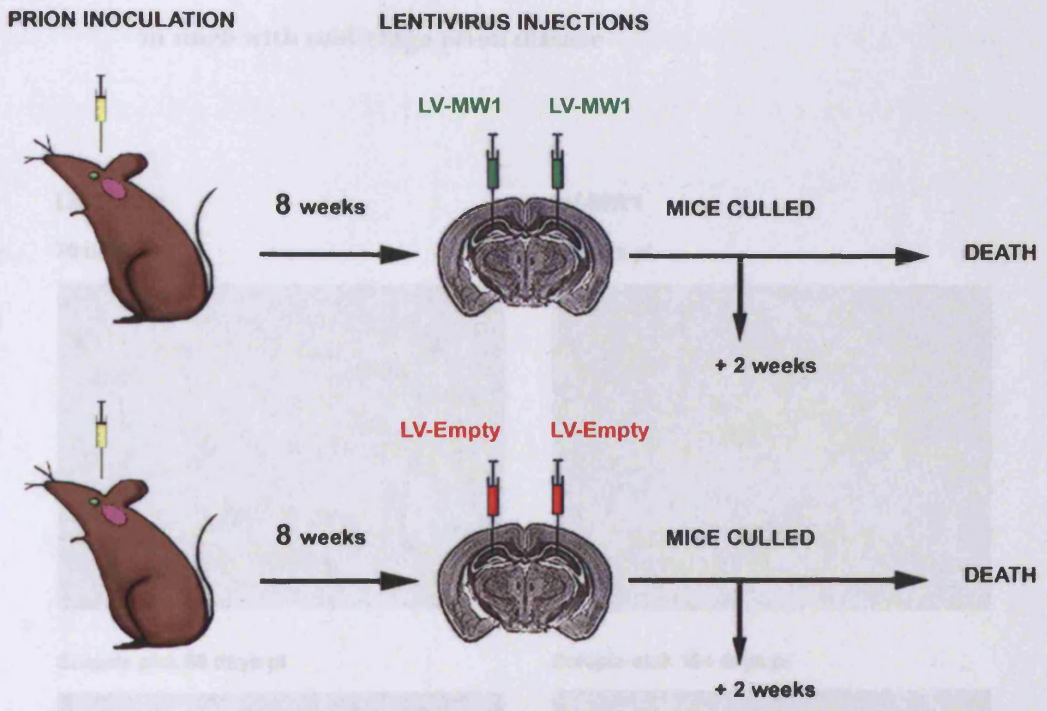

Two weeks after the administration of the lentivirus, 3 - 4 animals from each condition were culled and their brains collected for analysis to determine if bilateral injection affected prion pathology differently to the unilateral treatment administered in the left-right comparison experiment (Figure 6.6). This analysis is currently ongoing.

As the results of the initial timecourse experiment had suggested transduction of the hippocampus alone may be sufficient to impact on incubation time in this model, the

remaining animals were allowed to progress to end-stage disease, were culled according to local rules and their brains collected for histological analysis.

Figure 6.11 Bilateral injection of LV-MW1 protects against hippocampal neuronal loss in mice with mid-stage prion disease

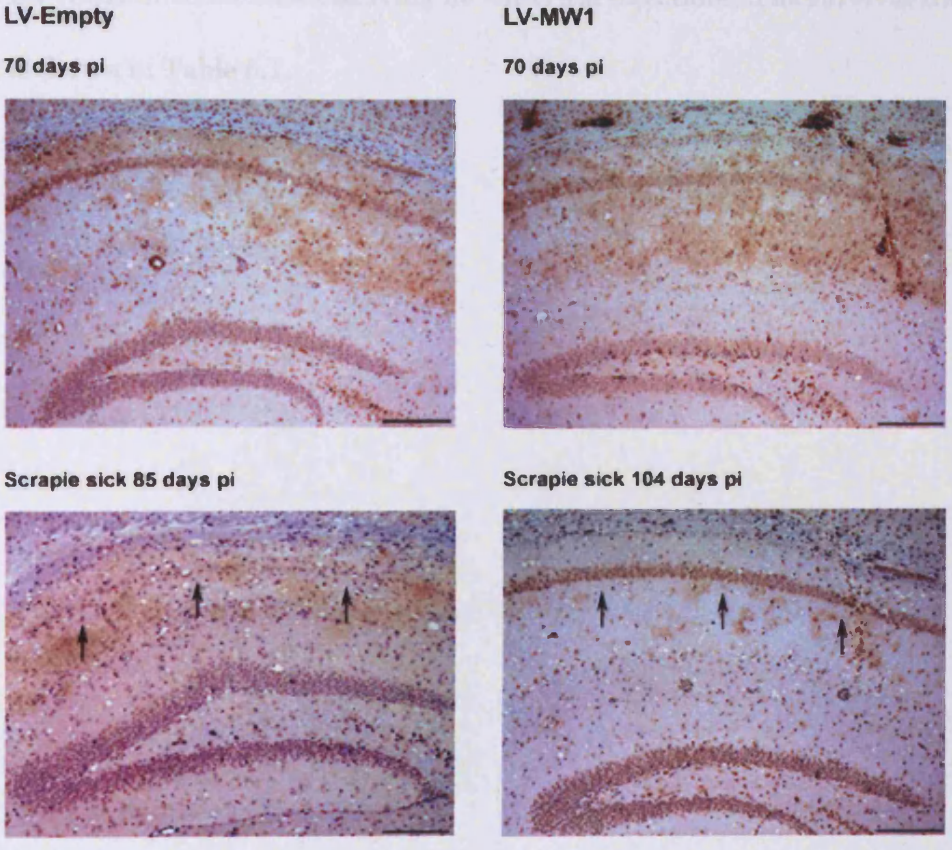

Prion-infected mice injected bilaterally with LV-MW1 or LV-Empty at 8wpi were culled 2 weeks post-injection or when scrapie sick and their brains were stained for GFP expression as before. Brown staining indicates virally transduced cells in the hippocampus. The black arrows highlight the stratum pyramidale layer in the scrapie sick mice. The needle track is evident in both mice injected with LV-MW1. Scale bar = 500μm.

Immunohistochemical analysis confirmed bilateral transduction of the hippocampi with LV-MW1 protected against hippocampal neuronal loss in mice receiving the lentivirus at 8wpi. The stratum pyramidale layer (black arrows, Figure 6.11) was remarkably intact in the longest-surviving mice injected with LV-MW1 which were culled due to scrapie sickness at 104 days post-inoculation. These mice survived 16 days longer than the average for mice injected bilaterally with LV-Empty and 19 days longer than the average for RML-infected mice receiving no lentiviral injections. The survival times of all mice is shown in Table 6.1.

Table 6.1 **Survival times of RML-infected Tg37 mice with and without bilateral lentiviral injections at mid-stage prion disease**

Condition	Survival time (dpi)	Mean survival time (dpi) ± sd
RML-only	81	
	83	
	84	
	84	
	91	85 ± 4
+ LV-Empty	85	
	85	
	85	
	91	
	91	
	91	88 ± 3
+ LV-MW1	91	
	91	
	97	
	98	
	98	
	104	
	104	98 ± 5

A single administration of 2 injections of LV-MW1 to the dorsal hippocampus was sufficient to significantly prolong the survival time of prion-infected mice by 15% compared to RML-infected controls ($p = 0.009$, Mann-Whitney test, 2 tailed). These mice also survived significantly longer than the mice injected with the empty lentivirus ($p = 0.012$, Mann-Whitney test, 2 tailed). There was no significant difference in survival time between mice receiving LV-Empty and uninfected controls ($p = 0.066$, Mann-Whitney test, 2 tailed). Figure 6.12 shows a survival curve for all mice.

Figure 6.12 Mice injected bilaterally with LV-MW1 in mid-stage prion disease survive significantly longer than controls

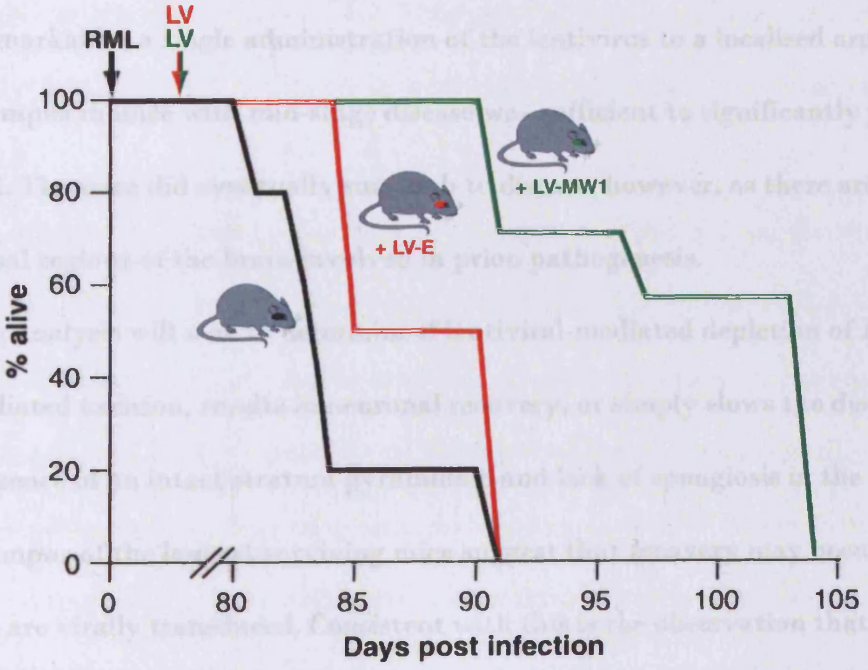

Survival of prion-infected Tg37 mice following lentiviral injection compared to mice receiving no injection. n = 5 for RML only, 6 for LV-Empty and 7 for LV-MW1.

6.5 Discussion

The data presented here strongly support a therapeutic role for RNAi-mediated reduction of PrP^C expression in prion disease. A lentivirus expressing a shRNA directed against *Prnp* reduced PrP mRNA expression *in vivo*, prevented accumulation of PrP^{Sc} in transduced cells, protected against neuronal loss in the hippocampus and prolonged survival in a mouse model of prion disease relative to treatment with an empty lentivirus and RML-infected controls. Furthermore, administration of the lentivirus at a late stage of disease, when clinical symptoms are already present and neuropathological change is established, was able to protect against neuronal loss in the hippocampus demonstrating the rapid action of this intervention.

Most remarkably, a single administration of the lentivirus to a localised area of the hippocampus in mice with mid-stage disease was sufficient to significantly prolong survival. The mice did eventually succumb to disease, however, as there are clearly additional regions of the brain involved in prion pathogenesis.

Ongoing analysis will seek to determine if lentiviral-mediated depletion of PrP^C, like Cre-mediated excision, results in neuronal recovery, or simply slows the disease process. The presence of an intact stratum pyramidale and lack of spongiosis in the hippocampus of the longest surviving mice suggest that recovery may occur if enough neurons are virally transduced. Consistent with this is the observation that the mouse with the most prominent expression of GFP in the pyramidal neurons survived the

longest. This would imply that targeting the lentivirus to neuronal cells may be crucial to the success of such a therapy.

Further analysis will also be required to ascertain whether there was any silencing of the transgene over time. Some of the mice culled 6 - 8 weeks after administration of the lentivirus did appear to have reduced GFP expression. Detection of the virally expressed GFP, however, was problematic, unreliable and apparently underestimated the true extent of viral transduction. RT-PCR analysis of the injected hippocampi suggested that even assuming 100% knockdown of *Prnp* in all transduced cells, a minimum of 20 - 40% of the hippocampus should have been positive for GFP. As LV-MW1 is unlikely to completely remove PrP^C expression *in vivo*, the true figure would be even higher, but this degree of GFP expression was seldom detected by immunohistochemistry. This may have been due to poor detection sensitivity or low expression from the CMV promoter *in vivo*, in accordance with the *in vitro* results in Chapter 5.

The experiments described in this chapter were designed to replicate the transgene-mediated knockout of PrP^C achieved in the NFH-Cre/Tg37 mouse model during prion disease. This method of PrP^C depletion results in complete rescue of pathology and normal survival of the mice due to total knockout of PrP expression in all neuronal cells. It is not surprising therefore, that lentiviral-mediated RNAi against the prion protein did not achieve the same extraordinary result, as only a fraction of all neuronal cells were virally transduced. It is, however, an important proof-of-principle that reduction of PrP expression through extrinsic means can protect those areas which have been targeted.

GENERAL DISCUSSION

The work described in this thesis strongly validates the use of lentiviral-mediated RNA interference as a therapeutic approach in prion disease: a single administration of this treatment in established prion disease prolongs survival and protects against neuronal loss in the targeted area. First it was demonstrated that reducing PrP^{C} expression with siRNA duplexes enabled clearance of PrP^{Sc} and infectivity from prion-infected cells *in vitro*. It was then confirmed that stable expression of the interfering RNA molecules through lentiviral transduction of the hippocampus reduced local pathology and significantly prolonged survival in a mouse model of prion disease. This represents an important and novel advance in the treatment of established prion disease.

7.1 Results and possible improvements on methodology

Previously, the only exogenously delivered agents which have been of therapeutic benefit in mice with established prion neuropathology are amphotericin B, its derivative MS-8209 (Demaimay et al., 1994), and pentosan polysulphate (Doh-ura et al., 2004).

Intraperitoneal administration of amphotericin B or MS-8209 to prion-infected mice starting ~70% of the way through the incubation period (an approximately equivalent stage of disease to those injected with lentivirus here) prolonged survival times by 14% and 19% respectively at the highest doses given (Demaimay et al., 1997). This resulted from an extension of the incubation time, but, following disease onset, pathology and

clinical signs were unchanged. The effect has been shown to be dependent on the prion strain however, with a loss of efficacy in mice infected with BSE compared to scrapie prions (Adjou et al., 1996). Furthermore, the only known treatment of a human CJD patient with amphotericin B was unsuccessful (Masullo et al., 1992).

The most promising results published to date have been achieved through intra-ventricular infusion of pentosan polysulphate in prion-infected mice (Doh-ura et al., 2004). A 141% prolongation of survival was observed with continuous, high dose infusion into the ventricles starting 10 days after infection of transgenic mice (expressing hamster PrP), with the 263K hamster prion strain. This fell to 71%, however, when the treatment began 70% of the way through the incubation period. The increased incubation times were accompanied by a decrease in PrP^{Sc} deposition and neurodegenerative changes in the treated hemisphere and a reduction in infectivity upon subsequent passage to mice. There was no evidence of reduction of pre-existing PrP^{Sc} in the brain, however, implying that endogenous clearance mechanisms were inhibited. Again, the effect was strain-dependent in murine PrP-overexpressing Tg20a mice infected with the RML (mouse-adapted scrapie) and Fukuoka-1 (mouse-adapted GSS) prion strains. The therapeutic effects of pentosan polysulphate were considerably reduced, giving only 46% longer survival in RML-infected Tg20a mice when administered 70% of the way through the incubation period.

The anti-coagulant action of pentosan polysulphate caused haemorrhaging in 80% of animals around the pump insertion site in mice and continuous high dose infusion caused fatal seizures in 4/5 dogs (Doh-ura et al., 2004). Despite these adverse side effects, pentosan polysulphate has been administered to human prion disease sufferers

on compassionate grounds in the absence of other available treatments. The effectiveness of this treatment in humans remains unclear due to small sample sizes, the different prion diseases involved, varying treatment schedules, and due to complications arising from increasing disability as a result of the disease process itself. A Medical Research Council monitoring study of pentosan polysulphate treatment in CJD patients found that although long-term infusion was well-tolerated, it did not appear to halt loss of brain function or disease progression (Bone, 2006). Further experimental work to confirm and elaborate on the findings of Doh-Ura and colleagues was recommended.

The effects of lentiviral-mediated reduction in *Prnp* expression in prion-infected mice achieved here are comparable in terms of survival to treatment with amphotericin B or MS-8209, and superior in terms of neuropathological protection. Although the prolongation of survival was not as great as that attained in RML-infected mice infused with the highest dose of pentosan polysulphate, only a single administration of lentivirus was given to a very restricted area of the dorsal hippocampus. Increasing the area of transduction, either through multiple injections or more efficient delivery methods, should offer improved protection. Indeed, recent reports have shown that the use of convection-enhanced delivery methods can significantly improve the area of viral transduction within the brain (Bankiewicz et al., 2000;Chen et al., 2005;Cunningham et al., 2000;Hadaczek et al., 2006). As incubation times in prion disease are known to be correlated with PrP^C expression levels, transducing a larger area of the brain would be expected to improve the therapeutic outcome.

Furthermore, it may be possible to identify regions of the brain in which reduction of *Prnp* expression may have a relatively greater effect on disease course. Previous

research in a mouse model of Spinocerebellar Ataxia 1 demonstrated that reduction of pathogenic protein by viral-mediated RNAi in only 5 - 10% of cerebellar Purkinje cells was sufficient to mediate a significant improval in motor function (Xia et al., 2004). By defining and targeting areas of the brain in which prion replication or pathology is the highest, a greater prolongation of survival may be attainable. This idea is also supported by the observation that the degree of chimerism in mice transgenic for an shRNA targeting *Prnp* expression did not always correlate with the survival time following prion infection (Pfeifer et al., 2006). Some mice with only 10 - 20% chimerism survived as long as mice which were 90 - 95% chimeric, indicating that the regions of the brain in which *Prnp* expression is reduced are important contributors to the therapeutic outcome.

In addition to targeting specific structures within the brain, further increasing the efficiency of lentiviral transduction of the most vulnerable cell types may improve the therapeutic effect. It has been demonstrated that PrP^{C} conversion must occur within neurons to be neurotoxic (Chesebro et al., 2005;Mallucci et al., 2003), so improving transduction efficiency of this cell type should be investigated. Pseudotyping the viral particles with a coat protein that preferentially infects neurons, thereby improving the ratio of transduced neurons to glia, may facilitate a greater therapeutic benefit from the same amount of virus.

It still remains to be determined if lentiviral-mediated reduction of *Prnp* expression assisted clearance of PrP^{Sc} or simply prevented its deposition, but the *in vitro* results using siRNA duplexes in a prion-infected cell line (Chapter 4) suggest that clearance may occur.

7.1.1 Functional recovery in prion disease

It has only recently been demonstrated that the early stages of prion disease are characterised by cognitive and behavioural deficits which precede neuronal and synaptic loss (Mallucci et al., 2007). This impairment is independent of PrP^{Sc} deposition and appears to be related to presynaptic axonal dysfunction. Remarkably, depletion of neuronal PrP^{C} rapidly reverses these deficits, demonstrating that the morphological recovery previously observed upon Cre-mediated PrP depletion in prion-infected mice is also accompanied by a functional recovery. This suggests that there is a window during which time it may be possible to not only halt clinical progression, but also reverse initial cognitive and behavioural abnormalities associated with prion disease. Early reduction of PrP^{C} expression in human prion disease may allow some degree of functional recovery in addition to prolonging survival.

7.1.2 RNAi as a therapy for all classes of prion disease

A significant advantage of the RNAi therapeutic approach in prion disease is a lack of strain specificity. As all prion diseases involve conversion of endogenous PrP^{C}, removing this substrate through RNAi should be an effective general treatment for all strains. This should also apply to familial prion diseases which arise from a coding mutation in *PRNP*. It is likely that allele-specific silencing strategies to reduce expression of the mutant *PRNP* allele, as has been achieved in models of other neurodegenerative

diseases (Gonzalez-Alegre et al., 2005;Sapru et al., 2006;Xia et al., 2006) would be effective here. As the familial prion diseases are the only ones for which there is currently an early diagnostic test available, successful treatment of this category may be possible through reduction of mutant PrP^C expression prior to development of pathology.

A further category of prion disease patients that may benefit from RNAi-mediated silencing of *PRNP* are those individuals known to have been peripherally infected, such as recipients of contaminated blood products. Systemic delivery of VSV-G pseudotyped lentiviruses has been shown to efficiently transduce the spleen and bone marrow (Croyle et al., 2004;Pan et al., 2002), which are crucial for peripheral prion spread and neuroinvasion (reviewed in (Aguzzi and Heikenwalder, 2006)). Reduction of *PRNP* expression in these organs may significantly prolong the incubation period. Selective targeting of routes of neuroinvasion such as the sympathetic nerves within the vertebral column may also significantly extend incubation time and perhaps even prevent neuroinvasion.

7.1.3 The therapeutic potential of siRNA duplexes in prion disease

RNAi-mediated reduction of *PRNP* expression is not restricted to the use of viruses. siRNA duplexes such as those characterised in Chapter 3 may also be of therapeutic use. Systemic delivery results in efficient gene silencing in peripheral organs in mice (Lewis et al., 2002), and may represent a possible treatment to manage peripheral prion levels,

effectively maintaining a subclinical state. It has also recently been demonstrated that systemic delivery of siRNA in non-human primates is well tolerated and results in up to 90% silencing of the target gene for as long as 11 days following a single administration (Zimmermann et al., 2006). Intraventricular infusion can mediate widespread knockdown in the brain (Thakker et al., 2004) and may be a valid approach following prion neuroinvasion. Preclinical research is already underway to investigate the use of this technology in other neurodegenerative diseases such as Parkinson's, Huntington's and Alzheimer's Diseases (www.alnylam.com/therapeutic-programs/programs.asp). As the effect is transient, treatment for prion disease would need to involve ongoing administration to remove PrP^C and potentially allow clearance of infectivity to a sub-pathological threshold.

7.1.4 Combinational therapy for prion disease

To further improve the chances of a therapeutic gain, combinational therapy should be investigated. It is possible that administration of another agent, such as pentosan polysulphate, in conjunction with RNAi-mediated reduction of PrP^C expression may have a synergistic effect. This has already been observed in combinational therapy for Hepatitis B Virus using siRNA with currently available treatments (www.sirna.com/wt/page/anti_viral). Lowering the level of PrP^C available for conversion may enhance the ability of pentosan polysulphate to inhibit the disease process. Lentiviral-mediated RNAi may be more amenable to combinational therapy as

expression of the shRNA is driven by constructs stably integrated into the genome whereas the effects of another drug on the uptake and action of siRNA duplexes would need to be carefully assessed.

7.1.5 The use of RNAi in humans

Although the use of lentiviruses for gene therapy is still largely at the experimental stage, the recent results of the first clinical trial using a lentivirus in HIV-infected humans were very encouraging (Levine et al., 2006). No adverse clinical effects were observed for 2 years following administration of the lentivirus, providing initial optimistic data on the clinical suitability of lentiviral gene therapy.

Clinical trials utilising RNAi against a variety of diseases are currently underway. Several Phase I clinical trials have demonstrated safety of RNAi targeting Respiratory Syncytial Virus in healthy volunteers (www.alnylam.com/therapeutic-programs/programs.asp). Positive Phase II results have been reported in patients suffering from wet age-related macular degeneration (www.acuitypharma.com/press/release15.pdf), and an siRNA that demonstrated therapeutic benefit in mouse models of this condition (Shen et al., 2006) has also translated to effective treatment in human patients (www.sirna.com/wt/page/ocular). It is possible that mouse models of disease may be more relevant for RNAi-based therapies than traditional drug treatment as the effects of drug metabolism in different biological systems are difficult to predict.

The interfering RNA sequences used here only provide partial knockdown of *Prnp* expression. It is highly probable that still more effective sequences could be identified, however the demonstration of a therapeutic benefit resulting from incomplete knockdown suggests this may not be necessary. As the normal function of PrP^C remains unclear and the effects of depletion in humans unexamined, it may be prudent to only reduce its expression enough to tip the balance between conversion and clearance of prion infectivity towards a subclinical disease state.

7.2 Future work

Future work should aim to translate this proof-of-principle demonstration into a viable therapy for prion disease. The *in vivo* experiments described here were performed in PrP^C-overexpressing mice to provide a direct comparison with previous results using Cre-mediated depletion in this model (Mallucci et al., 2003). Further experiments in wild-type mice are planned to assess the effects of the treatment at physiological levels of PrP^C. Identifying the therapeutic window in which recovery of cognitive and behavioural deficits is possible is important and experiments aimed at this are also planned.

As mentioned previously, experiments aimed at optimising the transduction of larger areas and specific cell types should be performed. Lentiviral reduction of *Prnp* expression in different restricted structures within the brain could provide information on which regions are most vulnerable to prion pathology and therefore merit

therapeutic targeting. Identification of allele-specific sequences capable of silencing familial mutations in *PRNP* should be attempted because early intervention in this category of prion disease is possible due to the availability of diagnostic testing. Investigations into RNAi-mediated reduction of peripheral PrP^C expression should also be conducted as slowing or preventing neuroinvasion offers the best therapeutic hope for peripherally-infected patients. The recent demonstrations of prion infection through contaminated blood products (Llewelyn et al., 2004;Peden et al., 2004;Wroe et al., 2006), and the current lack of an effective screening method mean an unknown number of people are still at risk of contracting prion disease in this manner.

Finally, the siRNA duplexes and lentiviruses characterised in this thesis can also be used as tools for investigation into the function of PrP^C and kinetics of prion infection. Reducing *Prnp* expression transiently through the use of siRNA may help further elucidate the cellular pathways PrP^C normally functions within. The creation of stable cell lines expressing PrP^C knocked down to varying levels through lentiviral transduction may help identify the cellular threshold below which prion replication is not supported. This could be used to inform therapeutic development and provide information on the kinetics of the conversion reaction.

7.3 Conclusions

This thesis provides a proof-of-principle demonstration that the use of RNA interference to reduce PrP^C expression may be of therapeutic benefit in prion disease.

Reduction of focal neuropathology and a significant prolongation of survival were attained following a single treatment in mice with established prion disease. Further optimisation of delivery and targeting to pathologically important areas may translate this approach into a viable therapy for all classes of the currently fatal neurodegenerative prion diseases.

Sequence of LV-Empty

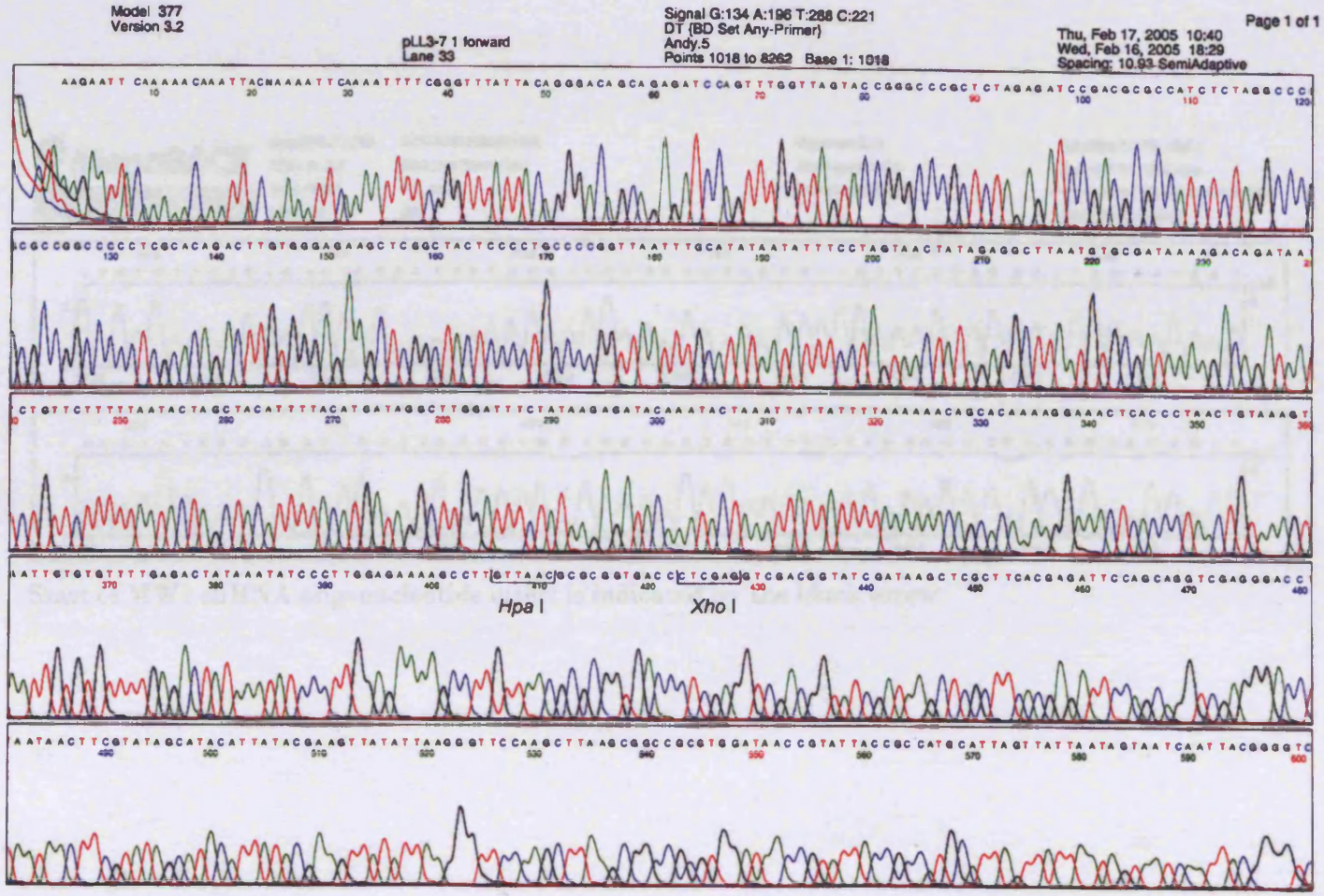

Cloning sites as indicated

Sequence of LV-MW1

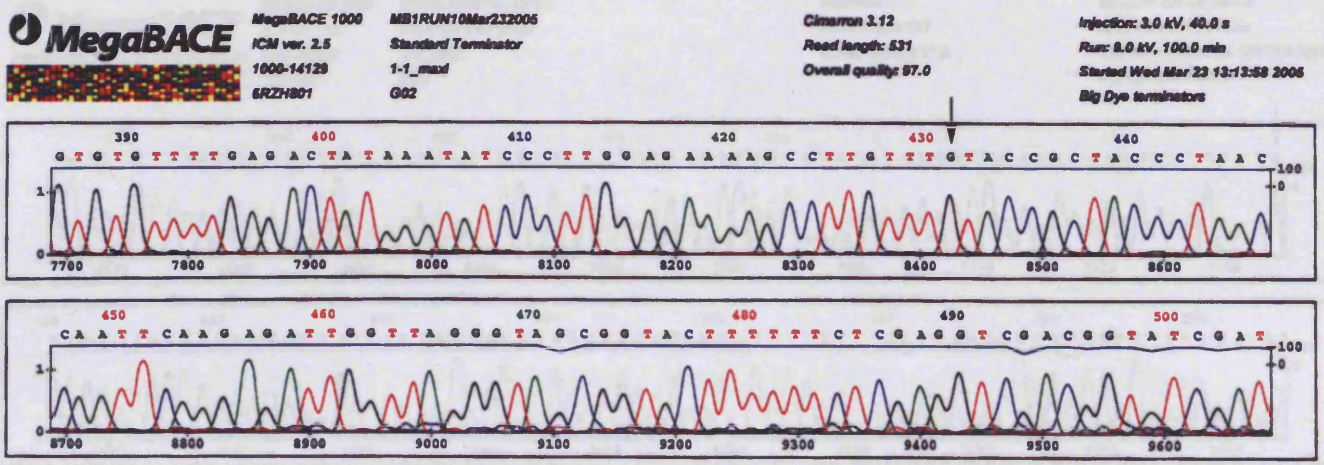

Start of MW1 shRNA oligonucleotide insert is indicated by the black arrow

Sequence of LV-MW2

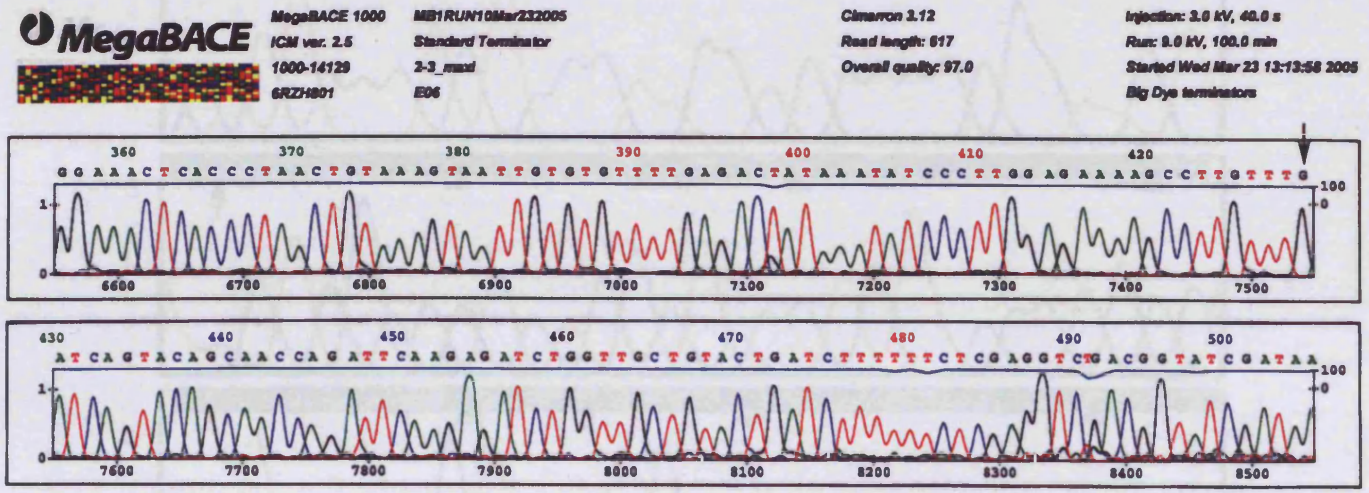

Start of MW2 shRNA oligonucleotide insert is indicated by the black arrow

Sequence of LV-MW3

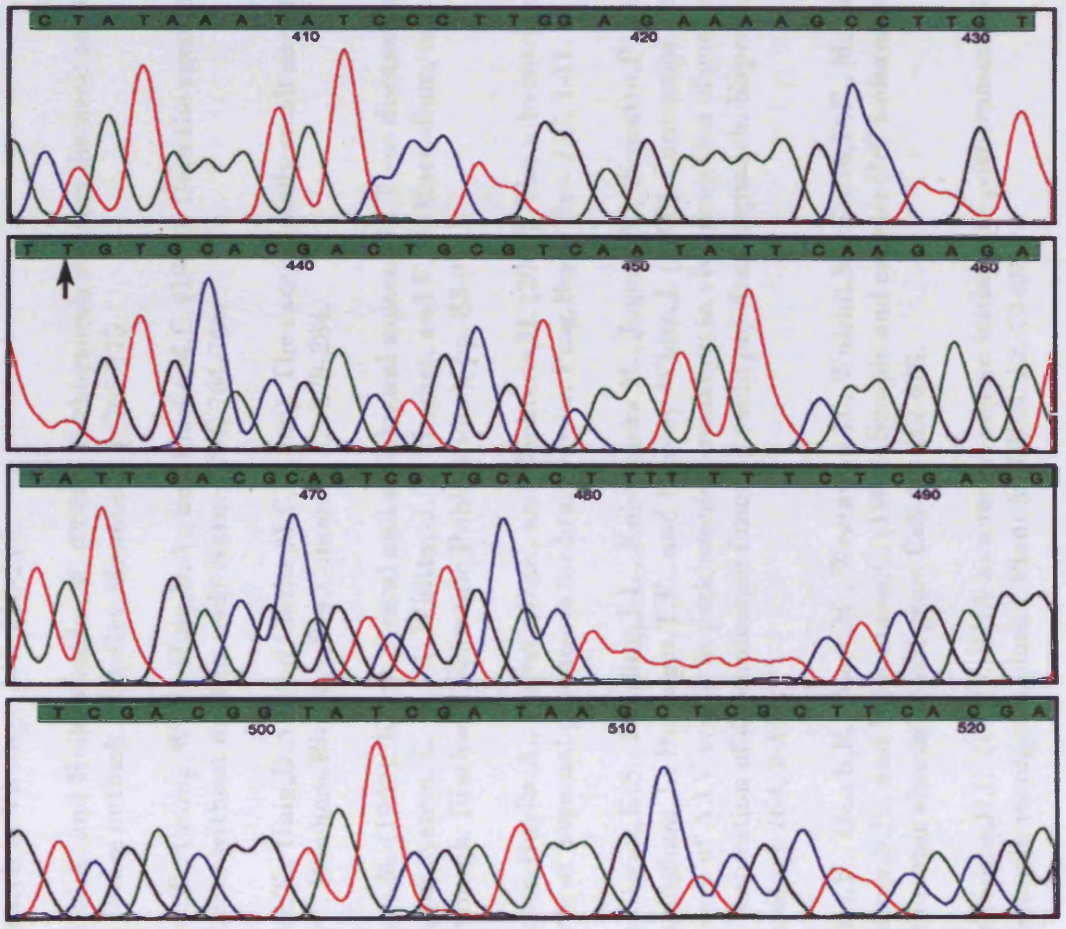

Start of MW3 shRNA oligonucleotide insert is indicated by the black arrow

REFERENCES

Adjou,K.T., Demaimay,R., Lasmézas,C.I., Seman,M., Deslys,J.P., and Dormont,D. (1996). Differential effects of a new amphotericin B derivative, MS-8209, on mouse BSE and scrapie: Implications for the mechanism of action of polyene antibiotics. Research in Virology *147*, 213-218.

Aguzzi,A. and Heikenwalder,M. (2006). Pathogenesis of prion diseases: current status and future outlook. Nat.Rev.Microbiol. *4*, 765-775.

Alper,T., Cramp,W.A., Haig,D.A., and Clarke,M.C. (1967). Does the agent of scrapie replicate without nucleic acid? Nature *214*, 764-766.

Alper,T., Haig,D.A., and Clarke,M.C. (1966). The exceptionally small size of the scrapie agent. Biochem.Biophys.Res.Commun. *22*, 278-284.

Alpers,M. (1969). Kuru: clinical and aetiological aspects. In Virus diseases and the nervous system, C. W. M. Whitty, J. T. Hughes, and F. O. MacCallum, eds. (Oxford & Edinburgh: Blackwell Scientific Publications), pp. 83-97.

Alvarez-Buylla,A., Herrera,D.G., and Wichterle,H. (2000). The subventricular zone: source of neuronal precursors for brain repair. Prog.Brain Res. *127*, 1-11.

Bankiewicz,K.S., Eberling,J.L., Kohutnicka,M., Jagust,W., Pivirotto,P., Bringas,J., Cunningham,J., Budinger,T.F., and Harvey-White,J. (2000). Convection-enhanced delivery of AAV vector in parkinsonian monkeys; in vivo detection of gene expression and restoration of dopaminergic function using pro-drug approach. Experimental Neurology *164*, 2-14.

Basler,K., Oesch,B., Scott,M., Westaway,D., Walchli,M., Groth,D.F., McKinley,M.P., Prusiner,S.B., and Weissmann,C. (1986). Scrapie and cellular PrP isoforms are encoded by the same chromosomal gene. Cell *46*, 417-428.

Baulcombe,D.C. (1996). RNA as a target and an initiator of post-transcriptional gene silencing in transgenic plants. Plant Mol.Biol. *32*, 79-88.

Berger-Sweeney,J., Zearfoss,N.R., and Richter,J.D. (2006). Reduced extinction of hippocampal-dependent memories in CPEB knockout mice. Learn.Mem. *13*, 4-7.

Bernstein,E., Caudy,A.A., Hammond,S.M., and Hannon,G.J. (2001). Role for a bidentate ribonuclease in the initiation step of RNA interference. Nature *409*, 363-366.

Bieschke,J., Weber,P., Sarafoff,N., Beekes,M., Giese,A., and Kretzschmar,H. (2004). Autocatalytic self-propagation of misfolded prion protein. Proc.Natl.Acad Sci U.S.A.

REFERENCES

Billette de Villemeur,T.B., Beauvais,P., Gourmelen,M., and Richardet,J.M. (1991). Creutzfeldt-Jakob disease in children treated with growth hormone. Lancet *337*, 864-865.

Bingham,P.M. (1997). Cosuppression comes to the animals. Cell *90*, 385-387.

Blomer,U., Naldini,L., Kafri,T., Trono,D., Verma,I.M., and Gage,F.H. (1997). Highly efficient and sustained gene transfer in adult neurons with a lentivirus vector. J Virol. *71*, 6641-6649.

Bolton,D.C. and Bendheim,P.E. (1991). Purification of scrapie agents: How far have we come. Curr.Top.Microbiol.Immunol. *172*, 39-55.

Bone,I. Intraventricular Pentosan Polysulphate in Human Prion Diseases: A study of experience in the United Kingdom. MRC New Therapies Scrutiny Group for Prion Disease , 1-211. 2006. Medical Research Council.

Borchelt,D.R., Scott,M., Taraboulos,A., Stahl,N., and Prusiner,S.B. (1990). Scrapie and cellular prion proteins differ in their kinetics of synthesis and topology in cultured cells. J Cell Biology *110*, 743-752.

Bosque,P.J. and Prusiner,S.B. (2000). Cultured cell sublines highly susceptible to prion infection. J.Virol. *74*, 4377-4386.

Bounhar,Y., Zhang,Y., Goodyer,C.G., and LeBlanc,A. (2001). Prion protein protects human neurons against Bax-mediated apoptosis. Journal of Biological Chemistry *276*, 39145-39149.

Brandner,S., Isenmann,S., Raeber,A., Fischer,M., Sailer,A., Kobayashi,Y., Marino,S., Weissmann,C., and Aguzzi,A. (1996). Normal host prion protein necessary for scrapie-induced neurotoxicity. Nature *379*, 339-343.

Bridge,A.J., Pebernard,S., Ducraux,A., Nicoulaz,A.L., and Iggo,R. (2003). Induction of an interferon response by RNAi vectors in mammalian cells. Nat.Genet. *34*, 263-264.

Brown,D.R. (1999). Prion protein expression aids cellular uptake and veratridine-induced release of copper. Journal of Neuroscience Research *58*, 717-725.

Brown,D.R. (2001). Copper and prion disease. Brain Research Bulletin *55*, 165-173.

Brown,D.R., Qin,K., Herms,J.W., Madlung,A., Manson,J., Strome,R., Fraser,P.E., Kruck,T., von Bohlen,A., Schulz-Schaeffer,W., Giese,A., Westaway,D., and Kretzschmar,H. (1997a). The cellular prion protein binds copper in vivo. Nature *390*, 684-687.

REFERENCES

Brown,D.R., Schulz-Schaeffer,W.J., Schmidt,B., and Kretzschmar,H.A. (1997b). Prion protein-deficient cells show altered response to oxidative stress due to decreased SOD-1 activity. Exp.Neurol *146*, 104-112.

Brown,K.L., Stewart,K., Ritchie,D.L., Mabbott,N.A., Williams,A., Fraser,H., Morrison,W.I., and Bruce,M.E. (1999). Scrapie replication in lymphoid tissues depends on prion protein-expressing follicular dendritic cells. Nature Medicine *5*, 1308-1312.

Brown,P., Gajdusek,D.C., Gibbs,C.J.Jr., and Asher,D.M. (1985). Potential epidemic of Creutzfeldt-Jakob disease from human growth hormone therapy. New England Journal of Medicine *313*, 728-731.

Bruce,M., Chree,A., McConnell,I., Brown,K., and Fraser,H. (1996). Transmission and strain typing studies of scrapie and bovine spongiform encephaolpathy. In Transmissible Subacute Spongiform Encephalopathies: Prion Diseases, L. Court and A. Dodge, eds. (Paris: Elsevier), pp. 259.

Bruce,M.E., Fraser,H., McBride,P.A., Scott,J.R., and Dickinson,A.G. (1992). The Basis of Strain Variation in Scrapie. In Prion Diseases in Human and Animals, S. B. Prusiner, J. Collinge, J. Powell, and B. Anderton, eds. (London: Ellis Horwood).

Bruce,M.E., Will,R.G., Ironside,J.W., McConnell,I., Drummond,D., Suttie,A., McCardle,L., Chree,A., Hope,J., Birkett,C., Cousens,S., Fraser,H., and Bostock,C.J. (1997). Transmissions to mice indicate that 'new variant' CJD is caused by the BSE agent. Nature *389*, 498-501.

Brummelkamp,T.R., Bernards,R., and Agami,R. (2002). A system for stable expression of short interfering RNAs in mammalian cells. Science *296*, 550-553.

Bueler,H., Aguzzi,A., Sailer,A., Greiner,R.A., Autenried,P., Aguet,M., and Weissmann,C. (1993). Mice devoid of PrP are resistant to scrapie. Cell *73*, 1339-1347.

Bueler,H., Fischer,M., Lang,Y., Bluethmann,H., Lipp,H.-P., DeArmond,S.J., Prusiner,S.B., Aguet,M., and Weissmann,C. (1992). Normal development and behaviour of mice lacking the neuronal cell-surface PrP protein. Nature *356*, 577-582.

Bueler,H., Raeber,A., Sailer,A., Fischer,M., Aguzzi,A., and Weissmann,C. (1994). High prion and PrPSc levels but delayed onset of disease in scrapie-inoculated mice heterozygous for a disrupted PrP gene. Mol.Med. *1*, 19-30.

Butler,D.A., Scott,M.R., Bockman,J.M., Borchelt,D.R., Taraboulos,A., Hsiao,K.K., Kingsbury,D.T., and Prusiner,S.B. (1988). Scrapie-infected murine neuroblastoma cells produce protease- resistant prion proteins. J Virol. *62*, 1558-1564.

Caplen,N.J., Fleenor,J., Fire,A., and Morgan,R.A. (2000). dsRNA-mediated gene silencing in cultured Drosophila cells: a tissue culture model for the analysis of RNA interference. Gene *252*, 95-105.

REFERENCES

Carthew,R.W. (2006). Gene regulation by microRNAs. Curr.Opin.Genet.Dev. *16*, 203-208.

Castilla,J., Saa,P., Hetz,C., and Soto,C. (2005). In vitro generation of infectious scrapie prions. Cell *121*, 195-206.

Caughey,B., Kocisko,D.A., Raymond,G.J., and Lansbury,P.T., Jr. (1995). Aggregates of scrapie-associated prion protein induce the cell-free conversion of protease-sensitive prion protein to the protease-resistant state. Current Biology *2*, 807-817.

Caughey,B., Neary,K., Buller,R., Ernst,D., Perry,L.L., Chesebro,B., and Race,R.E. (1990). Normal and scrapie-associated forms of prion protein differ in their sensitivities to phospholipase and proteases in intact neuroblastoma cells. J Virol. *64*, 1093-1101.

Caughey,B., Race,R.E., and Chesebro,B. (1988). Detection of prion protein mRNA in normal and scrapie-infected tissues and cell lines. J Gen.Virol. *69*, 711-716.

Caughey,B., Race,R.E., Ernst,D., Buchmeier,M.J., and Chesebro,B. (1989). Prion protein biosynthesis in scrapie-infected and uninfected neuroblastoma cells. J Virol. *63*, 175-181.

Caughey,B.W., Dong,A., Bhat,K.S., Ernst,D., Hayes,S.F., and Caughey,W.S. (1991). Secondary structure analysis of the scrapie-associated protein PrP 27-30 in water by infrared spectroscopy. Biochemistry *30*, 7672-7680.

Cavanagh,H.D. and Hogan,R.N. (1999). Preventing prion transmission in corneal transplants. Journal of the American Medical Association *282*, 2211.

Chan,D.C. and Kim,P.S. (1998). HIV entry and its inhibition. Cell *93*, 681-684.

Chen,M.Y., Hoffer,A., Morrison,P.F., Hamilton,J.F., Hughes,J., Schlageter,K.S., Lee,J., Kelly,B.R., and Oldfield,E.H. (2005). Surface properties, more than size, limiting convective distribution of virus-sized particles and viruses in the central nervous system. J.Neurosurg. *103*, 311-319.

Chesebro,B., Race,R., Wehrly,K., Nishio,J., Bloom,M., Lechner,D., Bergstrom,S., Robbins,K., Mayer,L., Keith,J.M., and Raeber,A.J. (1985). Identification of scrapie prion protein-specific mRNA in scrapie- infected and uninfected brain. Nature *315*, 331-333.

Chiesa,R., Pestronk,A., Schmidt,R.E., Tourtellotte,W.G., Ghetti,B., Piccardo,P., and Harris,D.A. (2001). Primary myopathy and accumulation of PrP^{Sc}-like molecules in peripheral tissues of transgenic mice expressing a prion protein insertional mutation. Neurobiology of Disease *8*, 279-288.

Chiu,Y.L. and Rana,T.M. (2002). RNAi in human cells: basic structural and functional features of small interfering RNA. Molecular Cell *10*, 549-561.

REFERENCES

Coitinho,A.S., Freitas,A.R.O., Lopes,M.H., Hajj,G.N.M., Roesler,R., Walz,R., Rossato,J.I., Cammarota,M., Izquierdo,I., Martins,V.R., and Brentani,R.R. (2006). The interaction between prion protein and laminin modulates memory consolidation. European Journal of Neuroscience *24*, 3255-3264.

Colling,S.B., King,T.M., Collinge,J., and Jefferys,J.G.R. Prion protein null mice: abnormal intrinsic properties of hippocampal CA1 pyramidal cells. Brain Res.Assoc.Abstr 12[49]. 1995.

Collinge,J. (1998). Human prion diseases: aetiology and clinical features. In The Dementias, J. H. Growdon and M. Rossor, eds. (Newton, MA: Butterworth-Heinemann), pp. 113-148.

Collinge,J. (2001). Prion diseases of humans and animals: their causes and molecular basis. Annu.Rev Neurosci. *24*, 519-550.

Collinge,J. (2005). Molecular neurology of prion disease. J Neurol Neurosurg.Psychiatry *76*, 906-919.

Collinge,J., Brown,J., Hardy,J., Mullan,M., Rossor,M.N., Baker,H., Crow,T.J., Lofthouse,R., Poulter,M., Ridley,R., Owen,F., Bennett,C., Dunn,G., Harding,A.E., Quinn,N., Doshi,B., Roberts,G.W., Honavar,M., Janota,I., and Lantos,P.L. (1992). Inherited prion disease with 144 base pair gene insertion: II: Clinical and pathological features. Brain *115*, 687-710.

Collinge,J., Palmer,M.S., and Dryden,A.J. (1991). Genetic predisposition to iatrogenic Creutzfeldt-Jakob disease. Lancet *337*, 1441-1442.

Collinge,J., Palmer,M.S., Sidle,K.C.L., Gowland,I., Medori,R., Ironside,J., and Lantos,P.L. (1995). Transmission of fatal familial insomnia to laboratory animals. Lancet *346*, 569-570.

Collinge,J., Sidle,K.C.L., Meads,J., Ironside,J., and Hill,A.F. (1996). Molecular analysis of prion strain variation and the aetiology of 'new variant' CJD. Nature *383*, 685-690.

Collinge,J., Whitfield,J., McKintosh,E., Beck,J., Mead,S., Thomas,D.J., and Alpers,M.P. (2006). Kuru in the 21st century-an acquired human prion disease with very long incubation periods. Lancet *367*, 2068-2074.

Collinge,J., Whittington,M.A., Sidle,K.C.L., Smith,C.J., Palmer,M.S., Clarke,A.R., and Jefferys,J.G.R. (1994). Prion protein is necessary for normal synaptic function. Nature *370*, 295-297.

Cronier,S., Laude,H., and Peyrin,J.M. (2004). Prions can infect primary cultured neurons and astrocytes and promote neuronal cell death. Proc.Natl.Acad Sci U.S.A.

REFERENCES

Croyle,M.A., Callahan,S.M., Auricchio,A., Schumer,G., Linse,K.D., Wilson,J.M., Brunner,L.J., and Kobinger,G.P. (2004). PEGylation of a vesicular stomatitis virus G pseudotyped lentivirus vector prevents inactivation in serum. J.Virol. *78*, 912-921.

Crozet,C., Lin,Y.L., Mettling,C., Mourton-Gilles,C., Corbeau,P., Lehmann,S., and Perrier,V. (2004). Inhibition of PrPSc formation by lentiviral gene transfer of PrP containing dominant negative mutations. J Cell Sci *117*, 5591-5597.

Cuillé,J. and Chelle,P.L. (1936). La maladie dite tremblante du mouton est-elle inocuable? Compte rendu de l'Academie des Sciences *203*, 1552-1554.

Cunningham,C., Deacon,R., Wells,H., Boche,D., Waters,S., Diniz,C.P., Scott,H., Rawlins,J.N., and Perry,V.H. (2003). Synaptic changes characterize early behavioural signs in the ME7 model of murine prion disease. Eur.J Neurosci. *17*, 2147-2155.

Cunningham,J., Oiwa,Y., Nagy,D., Podsakoff,G., Colosi,P., and Bankiewicz,K.S. (2000). Distribution of AAV-TK following intracranial convection-enhanced delivery into rats. Cell Transplant. *9*, 585-594.

Daude,N., Marella,M., and Chabry,J. (2003). Specific inhibition of pathological prion protein accumulation by small interfering RNAs. J Cell Sci *116*, 2775-2779.

Davidson,T.J., Harel,S., Arboleda,V.A., Prunell,G.F., Shelanski,M.L., Greene,L.A., and Troy,C.M. (2004). Highly efficient small interfering RNA delivery to primary mammalian neurons induces MicroRNA-like effects before mRNA degradation. Journal of Neuroscience *24*, 10040-10046.

de Veer,M.J., Sledz,C.A., and Williams,B.R. (2005). Detection of foreign RNA: implications for RNAi. Immunol.Cell Biol. *83*, 224-228.

DeArmond,S.J., Sánchez,H., Yehiely,F., Qiu,Y., Ninchak-Casey,A., Daggett,V., Camerino,A.P., Cayetano,J., Rogers,M., Groth,D., Torchia,M., Tremblay,P., Scott,M.R., Cohen,F.E., and Prusiner,S.B. (1997). Selective neuronal targeting in prion disease. Neuron *19*, 1337-1348.

Demaimay,R., Adjou,K., Lasmézas,C., Lazarini,F., Cherifi,K., Seman,M., Deslys,J.-P., and Dormont,D. (1994). Pharmacological studies of a new derivative of amphotericin B, MS-8209, in mouse and hamster scrapie. J.Virol. *75*, 2499-2503.

Doh-ura,K., Ishikawa,K., Murakami-Kubo,I., Sasaki,K., Mohri,S., Race,R., and Iwaki,T. (2004). Treatment of Transmissible Spongiform Encephalopathy by Intraventricular Drug Infusion in Animal Models. J Virol. *78*, 4999-5006.

Dorn,G., Patel,S., Wotherspoon,G., Hemmings-Mieszczak,M., Barclay,J., Natt,F.J., Martin,P., Bevan,S., Fox,A., Ganju,P., Wishart,W., and Hall,J. (2004). siRNA relieves chronic neuropathic pain. Nucleic Acids Res. *32*, e49.

REFERENCES

Drisaldi,B., Stewart,R.S., Adles,C., Stewart,L.R., Quaglio,E., Biasini,E., Fioriti,L., Chiesa,R., and Harris,D.A. (2003). Mutant PrP is delayed in its exit from the endoplasmic reticulum, but neither wild-type nor mutant PrP undergoes retrotranslocation prior to proteasomal degradation. J Biol.Chem.

Dron,M., Bailly,Y., Beringue,V., Haeberle,A.M., Griffond,B., Risold,P.Y., Tovey,M.G., Laude,H., and Dandoy-Dron,F. (2005). Scrg1 is induced in TSE and brain injuries, and associated with autophagy. Eur J Neurosci. *22*, 133-146.

Dron,M., Bailly,Y., Beringue,V., Haeberle,A.M., Griffond,B., Risold,P.Y., Tovey,M.G., Laude,H., and Dandoy-Dron,F. (2006). SCRG1, a potential marker of autophagy in transmissible spongiform encephalopathies. Autophagy. *2*, 58-60.

Duale,H., Kasparov,S., Paton,J.F., and Teschemacher,A.G. (2005). Differences in transductional tropism of adenoviral and lentiviral vectors in the rat brainstem. Exp.Physiol *90*, 71-78.

Elbashir,S.M., Harborth,J., Lendeckel,W., Yalcin,A., Weber,K., and Tuschl,T. (2001a). Duplexes of 21-nucleotide RNAs mediate RNA interference in cultured mammalian cells. Nature *411*, 494-498.

Elbashir,S.M., Harborth,J., Weber,K., and Tuschl,T. (2002). Analysis of gene function in somatic mammalian cells using small interfering RNAs. Methods *26*, 199-213.

Elbashir,S.M., Lendeckel,W., and Tuschl,T. (2001b). RNA interference is mediated by 21- and 22-nucleotide RNAs. Genes Dev. *15*, 188-200.

Elbashir,S.M., Martinez,J., Patkaniowska,A., Lendeckel,W., and Tuschl,T. (2001c). Functional anatomy of siRNAs for mediating efficient RNAi in Drosophila melanogaster embryo lysate. EMBO Journal *20*, 6877-6888.

Enari,M., Flechsig,E., and Weissmann,C. (2001). Scrapie prion protein accumulation by scrapie-infected neuroblastoma cells abrogated by exposure to a prion protein antibody. Proc.Natl.Acad Sci U.S.A *98*, 9295-9299.

Ertmer,A., Gilch,S., Yun,S.W., Flechsig,E., Klebl,B., Stein-Gerlach,M., Klein,M.A., and Schatzl,H.M. (2004). The tyrosine kinase inhibitor STI571 induces cellular clearance of PrPSc in prion-infected cells. J.Biol.Chem. *279*, 41918-41927.

Ferrer,I. (1999). Nuclear DNA fragmentation in Creutzfeldt-Jakob disease: does a mere positive in situ nuclear end-labeling indicate apoptosis? Acta Neuropathologica *97*, 5-12.

Fioriti,L., Dossena,S., Stewart,L.R., Stewart,R.S., Harris,D.A., Forloni,G., and Chiesa,R. (2005). Cytosolic prion protein (PrP) is not toxic in N2a cells and primary neurons expressing pathogenic PrP mutations. J Biol chem. *280*, 11320-8.

REFERENCES

Fire,A., Xu,S., Montgomery,M.K., Kostas,S.A., Driver,S.E., and Mello,C.C. (1998). Potent and specific genetic interference by double-stranded RNA in Caenorhabditis elegans. Nature *391*, 806-811.

Fischer,M., Rulicke,T., Raeber,A., Sailer,A., Moser,M., Oesch,B., Brandner,S., Aguzzi,A., and Weissmann,C. (1996). Prion protein (PrP) with amino-proximal deletions restoring susceptibility of PrP knockout mice to scrapie. EMBO Journal *15*, 1255-1264.

Flechsig,E., Hegyi,I., Leimeroth,R., Zuniga,A., Rossi,D., Cozzio,A., Schwarz,P., Rulicke,T., Gotz,J., Aguzzi,A., and Weissmann,C. (2003). Expression of truncated PrP targeted to Purkinje cells of PrP knockout mice causes Purkinje cell death and ataxia. EMBO Journal *22*, 3095-3101.

Flechsig,E., Shmerling,D., Hegyi,I., Raeber,A.J., Fischer,M., Cozzio,A., von Mering,C., Aguzzi,A., and Weissmann,C. (2000). Prion protein devoid of the octapeptide repeat region restores susceptibility to scrapie in PrP knockout mice. Neuron *27*, 399-408.

Ford,M.J., Burton,L.J., Morris,R.J., and Hall,S.M. (2002). Selective expression of prion protein in peripheral tissues of the adult mouse. Neuroscience *113*, 177-192.

Forloni,G., Angeretti,N., Chiesa,R., Monzani,E., Salmona,M., Bugiani,O., and Tagliavini,F. (1993). Neurotoxicity of a prion protein fragment. Nature *362*, 543-546.

Foster,J.D., Parnham,D., Chong,A., Goldmann,W., and Hunter,N. (2001). Clinical signs, histopathology and genetics of experimental transmission of BSE and natural scrapie to sheep and goats. Veterinary Record *148*, 165-171.

Frigg,R., Klein,M.A., Hegyi,I., Zinkernagel,R.M., and Aguzzi,A. (1999). Scrapie pathogenesis in subclinically infected B-Cell-deficient mice. J.Virol. *73*, 9584-9588.

Gage,F.H. (2000). Mammalian neural stem cells. Science *287*, 1433-1438.

Gajdusek,D.C. and Gibbs,C.J.Jr. (1971). Transmission of two subacute spongiform encephalopathies of man (kuru and Creutzfeldt-Jakob disease) to New World monkeys. Nature *230*, 588-591.

Gajdusek,D.C., Gibbs,C.J.Jr., and Alpers,M.P. (1966). Experimental transmission of a kuru-like syndrome to chimpanzees. Nature *209*, 794-796.

Gajdusek,D.C. and Zigas,V. (1957). Degenerative disease of the central nervous system in New Guinea. N.Engl.J Med. *257*, 974-978.

Gasset,M., Baldwin,M.A., Fletterick,R.J., and Prusiner,S.B. (1993). Perturbation of the secondary structure of the scrapie prion protein under conditions that alter infectivity. Proc.Natl.Acad.Sci.U.S A. *90*, 1-5.

REFERENCES

Gibbs,C.J.Jr., Gajdusek,D.C., Asher,D.M., Alpers,M.P., Beck,E., Daniel,P.M., and Matthews,W.B. (1968). Creutzfeldt-Jakob Disease (Spongiform Encephalopathy): Transmission to the Chimpanzee. Science *161*, 388-389.

Gibbs,C.J.Jr., Joy,A., Heffner,R., Franko,M., Miyazaki,M., Asher,D.M., Parisi,J.E., Brown,P.W., and Gajdusek,D.C. (1985). Clinical and pathological features and laboratory confirmation of Creutzfeldt-Jakob disease in a recipient of pituitary-derived human growth hormone. N.Engl.J Med. *313*, 734-738.

Glatzel,M., Heppner,F.L., Albers,K.M., and Aguzzi,A. (2001). Sympathetic innervation of lymphoreticular organs is rate limiting for prion neuroinvasion. Neuron *31*, 25-34.

Golding,M.C., Long,C.R., Carmell,M.A., Hannon,G.J., and Westhusin,M.E. (2006). Suppression of prion protein in livestock by RNA interference. Proc.Natl.Acad.Sci.U.S.A *103*, 5285-5290.

Gomez,C. and Hope,T.J. (2005). The ins and outs of HIV replication. Cell Microbiol. *7*, 621-626.

Gonzalez-Alegre,P., Bode,N., Davidson,B.L., and Paulson,H.L. (2005). Silencing primary dystonia: lentiviral-mediated RNA interference therapy for DYT1 dystonia. Journal of Neuroscience *25*, 10502-10509.

Gordon,W.S. (1946). Advances in veterinary research: louping ill, tick-borne fever and scrapie. Veterinary Record *58*, 516-525.

Gorodinsky,A. and Harris,D.A. (1995). Glycolipid-anchored proteins in neuroblastoma cells form detergent-resistant complexes without caveolin. J Cell Biology *129*, 619-627.

Graner,E., Mercadante,A.F., Zanata,S.M., Forlenza,O.V., Cabral,A.L.B., Veiga,S.S., Juliano,M.A., Roesler,R., Walz,R., Minetti,A., Izquierdo,I., Martins,V.R., and Brentani,R.R. (2000a). Cellular prion protein binds laminin and mediates neuritogenesis. Molecular Brain Research *76*, 85-92.

Graner,E., Mercadante,A.F., Zanata,S.M., Martins,V.R., Jay,D.G., and Brentani,R.R. (2000b). Laminin-induced PC-12 cell differentiation is inhibited following laser inactivation of cellular prion protein. FEBS Letters *482*, 257-260.

Griffith,J.S. (1967). Self Replication and Scrapie. Nature *215*, 1043-1044.

Grishok,A., Pasquinelli,A.E., Conte,D., Li,N., Parrish,S., Ha,I., Baillie,D.L., Fire,A., Ruvkun,G., and Mello,C.C. (2001). Genes and mechanisms related to RNA interference regulate expression of the small temporal RNAs that control C. elegans developmental timing. Cell *106*, 23-34.

Hadaczek,P., Kohutnicka,M., Krauze,M.T., Bringas,J., Pivirotto,P., Cunningham,J., and Bankiewicz,K. (2006). Convection-enhanced delivery of adeno-associated virus type 2 (AAV2) into the striatum and transport of AAV2 within monkey brain. Human Gene Therapy *17*, 291-302.

Hadlow,W.J. (1959). Scrapie and kuru. Lancet *ii*, 289-290.

Hamilton,A.J. and Baulcombe,D.C. (1999). A species of small antisense RNA in posttranscriptional gene silencing in plants. Science *286*, 950-952.

Haraguchi,T., Fisher,S., Olofsson,S., Endo,T., Groth,D., Tarentino,A., Borchelt,D.R., Teplow,D., Hood,L.E., Burlingame,A.L., Lycke,E., Kobata,A., and Prusiner,S.B. (1989). Asparagine-linked glycosylation of the Scrapie and cellular prion proteins. Arch Biochem.Biophys. *274*, 1-13.

Hardy,J. and Selkoe,D.J. (2002). The amyloid hypothesis of Alzheimer's disease: progress and problems on the road to therapeutics Science *297*, 353-356.

Harper,S.Q., Staber,P.D., He,X., Eliason,S.L., Martins,I.H., Mao,Q., Yang,L., Kotin,R.M., Paulson,H.L., and Davidson,B.L. (2005). RNA interference improves motor and neuropathological abnormalities in a Huntington's disease mouse model. Proc.Natl.Acad.Sci.U.S.A *102*, 5820-5825.

Hassani,Z., Lemkine,G.F., Erbacher,P., Palmier,K., Alfama,G., Giovannangeli,C., Behr,J.P., and Demeneix,B.A. (2005). Lipid-mediated siRNA delivery down-regulates exogenous gene expression in the mouse brain at picomolar levels. J Gene Med *7*, 198-207.

Hegde,R.S., Mastrianni,J.A., Scott,M.R., DeFea,K.A., Tremblay,P., Torchia,M., DeArmond,S.J., Prusiner,S.B., and Lingappa,V.R. (1998). A transmembrane from of the prion protein in neurodegenerative disease. Science *279*, 827-834.

Hegde,R.S., Tremblay,P., Groth,D., DeArmond,S.J., Prusiner,S.B., and Lingappa,V.R. (1999). Transmissible and genetic prion diseases share a common pathway of neurodegeneration. Nature *402*, 822-826.

Heinen,E., Bosseloir,A., and Bouzahzah,F. (1995). Follicular dendritic cells: origin and function. Curr.Top.Microbiol.Immunol. *201*, 15-47.

Hetz,C., Russelakis-Carneiro,M., Maundrell,K., Castilla,J., and Soto,C. (2003). Caspase-12 and endoplasmic reticulum stress mediate neurotoxicity of pathological prion protein. EMBO Journal *22*, 5435-5445.

Hetz,C. and Soto,C. (2003). Protein misfolding and disease: the case of prion disorders. Cell Mol.Life Sci *60*, 133-143.

Hill,A.F., Antoniou,M., and Collinge,J. (1999). Protease-resistant prion protein produced *in vitro* lacks detectable infectivity. J Gen Virol. *80*, 11-14.

Hill,A.F. and Collinge,J. (2003). Subclinical prion infection. Trends in Microbiology *11*, 578-584.

Hill,A.F., Desbruslais,M., Joiner,S., Sidle,K.C.L., Gowland,I., and Collinge,J. (1997). The same prion strain causes vCJD and BSE. Nature *389*, 448-450.

REFERENCES

Hill,A.F., Joiner,S., Linehan,J., Desbruslais,M., Lantos,P.L., and Collinge,J. (2000). Species barrier independent prion replication in apparently resistant species. Proc.Natl.Acad Sci U.S.A *97*, 10248-10253.

Hope,J., Ritchie,L., Farquhar,C., Somerville,R., and Hunter,N. (1989). Bovine spongiform encephalopathy: a scrapie-like disease of British cattle. Prog.Clin.Biol.Res. *317*, 659-667.

Hosszu,L.L.P., Baxter,N.J., Jackson,G.S., Power,A., Clarke,A.R., Waltho,J.P., Craven,C.J., and Collinge,J. (1999). Structural mobility of the human prion protein probed by backbone hydrogen exchange. Nature Structural Biology *6*, 740-743.

Huang,F.P., Farquhar,C.F., Mabbott,N.A., Bruce,M.E., and MacPherson,G.G. (2002). Migrating intestinal dendritic cells transport PrP(Sc) from the gut. J Gen Virol. *83*, 267-271.

Hutvagner,G., McLachlan,J., Pasquinelli,A.E., Balint,E., Tuschl,T., and Zamore,P.D. (2001). A cellular function for the RNA-interference enzyme Dicer in the maturation of the let-7 small temporal RNA. Science *293*, 834-838.

Ikeda,Y., Collins,M.K., Radcliffe,P.A., Mitrophanous,K.A., and Takeuchi,Y. (2002). Gene transduction efficiency in cells of different species by HIV and EIAV vectors. Gene Ther. *9*, 932-938.

Ingelbrecht,I., Van Houdt,H., Van Montagu,M., and Depicker,A. (1994). Posttranscriptional silencing of reporter transgenes in tobacco correlates with DNA methylation. Proc.Natl.Acad.Sci.U.S.A *91*, 10502-10506.

Izant,J.G. and McIntosh,J.R. (1980). Microtubule-associated proteins: a monoclonal antibody to MAP2 binds to differentiated neurons. Proc.Natl.Acad.Sci.U.S.A *77*, 4741-4745.

Jackson,A.L., Bartz,S.R., Schelter,J., Kobayashi,S.V., Burchard,J., Mao,M., Li,B., Cavet,G., and Linsley,P.S. (2003). Expression profiling reveals off-target gene regulation by RNAi. Nature Biotechnology *21*, 635-637.

Jackson,G.S., Murray,I., Hosszu,L.L.P., Gibbs,N., Waltho,J.P., Clarke,A.R., and Collinge,J. (2001). Location and properties of metal-binding sites on the human prion protein. Proc.Natl.Acad.Sci.U.S.A *98*, 8531-8535.

James,T.L., Liu,H., Ulyanov,N.B., Farr-Jones,S., Zhang,H., Donne,D.G., Kaneko,K., Groth,D., Mehlhorn,I., Prusiner,S.B., and Cohen,F.E. (1997). Solution structure of a 142-residue recombinant prion protein corresponding to the infectious fragment of the scrapie isoform. Proc.Natl.Acad Sci U.S.A *94*, 10086-10091.

Jarrett,J.T. and Lansbury,P.T.J. (1993). Seeding "one-dimensional crystallization" of amyloid: a pathogenic mechanism in Alzheimer's disease and scrapie? Cell *73*, 1055-1058.

Jorgensen,R. (1990). Altered gene expression in plants due to trans interactions between homologous genes. Trends Biotechnol. *8*, 340-344.

Kavi,H.H., Fernandez,H.R., Xie,W., and Birchler,J.A. (2005). RNA silencing in Drosophila. FEBS Lett. *579*, 5940-5949.

Kayed,R., Head,E., Thompson,J.L., McIntire,T.M., Milton,S.C., Cotman,C.W., and Glabe,C.G. (2003). Common structure of soluble amyloid oligomers implies common mechanism of pathogenesis. Science *300*, 486-489.

Kennerdell,J.R. and Carthew,R.W. (1998). Use of dsRNA-mediated genetic interference to demonstrate that frizzled and frizzled 2 act in the wingless pathway. Cell *95*, 1017-1026.

Keshet,G.I., Ovadia,H., Taraboulos,A., and Gabizon,R. (1999). Scrapie-infected mice and PrP knockout mice share abnormal localization and activity of neuronal nitric oxide synthase. Journal of Neurochemistry *72*, 1224-1231.

Ketting,R.F., Fischer,S.E., Bernstein,E., Sijen,T., Hannon,G.J., and Plasterk,R.H. (2001). Dicer functions in RNA interference and in synthesis of small RNA involved in developmental timing in C. elegans. Genes Dev. *15*, 2654-2659.

Khalili-Shirazi,A., Summers,L., Linehan,J., Mallinson,G., Anstee,D., Hawke,S., Jackson,G.S., and Collinge,J. (2005). PrP glycoforms are associated in a strain-specific ratio in native PrPSc. J Gen Virol. *86*, 2635-2644.

Khvorova,A., Reynolds,A., and Jayasena,S.D. (2003). Functional siRNAs and miRNAs exhibit strand bias. Cell *115*, 209-216.

Kim,B.H., Lee,H.G., Choi,J.K., Kim,J.I., Choi,E.K., Carp,R.I., and Kim,Y.S. (2004). The cellular prion protein (PrP(C)) prevents apoptotic neuronal cell death and mitochondrial dysfunction induced by serum deprivation. Brain Res.Mol.Brain Res. *124*, 40-50.

Kim,V.N. (2003). RNA interference in functional genomics and medicine. J.Korean Med.Sci. *18*, 309-318.

Kirkwood,J.K. and Cunningham,A.A. (1994). Epidemiological observations on spongiform encephalopathies in captive wild animals in the British Isles. Vet.Rec. *135*, 296-303.

Kirkwood,J.K., Wells,G.A., Wilesmith,J.W., Cunningham,A.A., and Jackson,S.I. (1990). Spongiform encephalopathy in an arabian oryx (Oryx leucoryx) and a greater kudu (Tragelaphus strepsiceros). Vet.Rec. *127*, 418-420.

Kitamoto,T., Muramoto,T., Mohri,S., Doh-ura,K., and Tateishi,J. (1991). Abnormal isoform of prion protein accumulates in follicular dendritic cells in mice with Creutzfeldt-Jakob disease. J Virol. *65*, 6292 6295.

REFERENCES

Klein,M., Frigg,R., Raeber,A., Flechsig,E., Hegyi,I., Zinkernagel,R.M., Weissmann,C., and Aguzzi,A. (1998). PrP expression in B-lymphocytes is not required for prion neuroinvasion. Nature Medicine *4*, 1429-1433.

Klohn,P.C., Stoltze,L., Flechsig,E., Enari,M., and Weissmann,C. (2003). A quantitative, highly sensitive cell-based infectivity assay for mouse scrapie prions. Proc.Natl.Acad.Sci U.S.A *100*, 11666-11671.

Kocisko,D.A., Come,J.H., Priola,S.A., Chesebro,B., Raymond,G.J., Lansbury,P.T., and Caughey,B. (1994). Cell-free formation of protease-resistant prion protein. Nature *370*, 471-474.

Kocisko,D.A., Priola,S.A., Raymond,G.J., Chesebro,B., Lansbury,P.T., Jr., and Caughey,B. (1995). Species specificity in the cell-free conversion of prion protein to protease-resistant forms: a model for the scrapie species barrier. Proc.Natl.Acad.Sci.U.S A. *92*, 3923-3927.

Kocisko,D.A., Vaillant,A., Lee,K.S., Arnold,K.M., Bertholet,N., Race,R.E., Olsen,E.A., Juteau,J.M., and Caughey,B. (2006). Potent antiscrapie activities of degenerate phosphorothioate oligonucleotides. Antimicrob.Agents Chemother. *50*, 1034-1044.

Kretzschmar,H.A., Stowring,L.E., Westaway,D., Stubblebine,W.H., Prusiner,S.B., and DeArmond,S.J. (1986). Molecular cloning of a human prion protein cDNA. DNA *5*, 315-324.

Kristiansen,M., Messenger,M.J., Klohn,P.C., Brandner,S., Wadsworth,J.D., Collinge,J., and Tabrizi,S.J. (2005). Disease-related prion protein forms aggresomes in neuronal cells leading to caspase-activation and apoptosis. J Biol Chem.

Kumar,P., Lee,S.K., Shankar,P., and Manjunath,N. (2006). A single siRNA suppresses fatal encephalitis induced by two different flaviviruses. PLoS.Med. *3*, e96.

Kushnirov,V.V. and Ter-Avanesyan,M.D. (1998). Structure and replication of yeast prions. Cell *94*, 13-16.

Kuwahara,C., Takeuchi,A.M., Nishimura,T., Haraguchi,K., Kubosaki,A., Matsumoto,Y., Saeki,K., Yokoyama,T., Itohara,S., and Onodera,T. (1999). Prions prevent neuronal cell-line death. Nature *400*, 225-226.

Lagos-Quintana,M., Rauhut,R., Lendeckel,W., and Tuschl,T. (2001). Identification of novel genes coding for small expressed RNAs. Science *294*, 853-858.

Lasmézas,C.I., Deslys,J.-P., Demaimay,R., Adjou,K.T., Lamoury,F., Dormont,D., Robain,O., Ironside,J., and Hauw,J.-J. (1996). BSE transmission to macaques. Nature *381*, 743-744.

Lau,N.C., Lim,L.P., Weinstein,E.G., and Bartel,D.P. (2001). An abundant class of tiny RNAs with probable regulatory roles in Caenorhabditis elegans. Science *294*, 858-862.

REFERENCES

Lazarini,F., Deslys,J.-P., and Dormont,D. (1991). Regulation of the glial fibrillary acidic protein, beta actin and prion protein mRNAs during brain development in mouse. Molecular Brain Research *10*, 343-346.

Lee,H.S., Brown,P., Cervenáková,L., Garruto,R.M., Alpers,M.P., Gajdusek,D.C., and Goldfarb,L.G. (2001). Increased susceptibility to Kuru of carriers of the *PRNP* 129 methionine/methionine genotype. Journal of Infectious Diseases *183*, 192-196.

Lee,R.C. and Ambros,V. (2001). An extensive class of small RNAs in Caenorhabditis elegans. Science *294*, 862-864.

Legname,G., Baskakov,I.V., Nguyen,H.O., Riesner,D., Cohen,F.E., DeArmond,S.J., and Prusiner,S.B. (2004). Synthetic mammalian prions. Science *305*, 673-676.

Levine,B.L., Humeau,L.M., Boyer,J., MacGregor,R.R., Rebello,T., Lu,X., Binder,G.K., Slepushkin,V., Lemiale,F., Mascola,J.R., Bushman,F.D., Dropulic,B., and June,C.H. (2006). Gene transfer in humans using a conditionally replicating lentiviral vector. Proc.Natl.Acad.Sci.U.S.A *103*, 17372-17377.

Lewis,D.L., Hagstrom,J.E., Loomis,A.G., Wolff,J.A., and Herweijer,H. (2002). Efficient delivery of siRNA for inhibition of gene expression in postnatal mice. Nat Genet *32*, 107-108.

Lewis,P.A., Tattum,M.H., Jones,S., Bhelt,D., Batchelor,M., Clarke,A.R., Collinge,J., and Jackson,G.S. (2006). Codon 129 polymorphism of the human prion protein influences the kinetics of amyloid formation. J Gen Virol. *87*, 2443-2449.

Li,A. and Harris,D.A. (2005). Mammalian prion protein suppresses Bax-induced cell death in yeast. J Biol Chem.

Liebman,S.W. and Derkatch,I.L. (1999). The yeast [*PSI*$^+$] prion: Making sense of nonsense. J Biol.Chem *274*, 1181-1184.

Liu,H., Farr-Jones,S., Ulyanov,N.B., Llinas,M., Marqusee,S., Groth,D., Cohen,F.E., Prusiner,S.B., and James,T.L. (1999). Solution structure of syrian hamster prion protein (90-231). Biochemistry *38*, 5362-5377.

Liu,J., Carmell,M.A., Rivas,F.V., Marsden,C.G., Thomson,J.M., Song,J.J., Hammond,S.M., Joshua-Tor,L., and Hannon,G.J. (2004). Argonaute2 is the catalytic engine of mammalian RNAi. Science *305*, 1437-1441.

Llewelyn,C.A., Hewitt,P.E., Knight,R.S., Amar,K., Cousens,S., Mackenzie,J., and Will,R.G. (2004). Possible transmission of variant Creutzfeldt-Jakob disease by blood transfusion. Lancet *363*, 417-421.

Locht,C., Chesebro,B., Race,R., and Keith,J.M. (1986). Molecular cloning and complete sequence of prion protein cDNA from mouse brain infected with the scrapie agent. Proc.Natl.Acad.Sci.U.S A. *83*, 6372-6376.

REFERENCES

Luhr,K.M., Nordstrom,E.K., Low,P., and Kristensson,K. (2004a). Cathepsin B and L are involved in degradation of prions in GT1-1 neuronal cells. Neuroreport *15*, 1663-1667.

Luhr,K.M., Nordstrom,E.K., Low,P., Ljunggren,H.G., Taraboulos,A., and Kristensson,K. (2004b). Scrapie Protein Degradation by Cysteine Proteases in CD11c(+) Dendritic Cells and GT1-1 Neuronal Cells. J Virol. *78*, 4776-4782.

Luo,M.C., Zhang,D.Q., Ma,S.W., Huang,Y.Y., Shuster,S.J., Porreca,F., and Lai,J. (2005). An efficient intrathecal delivery of small interfering RNA to the spinal cord and peripheral neurons. Mol.Pain *1*, 29.

Ma,J., Wollmann,R., and Lindquist,S. (2002). Neurotoxicity and Neurodegeneration When PrP Accumulates in the Cytosol. Science *298*, 1781-1785.

Ma,J.Y. and Lindquist,S. (2001). Wild-type PrP and a mutant associated with prion disease are subject to retrograde transport and proteasome degradation. Proc.Natl.Acad Sci U.S.A *98*, 14955-14960.

Mabbott,N.A., Young,J., McConnell,I., and Bruce,M.E. (2003). Follicular dendritic cell dedifferentiation by treatment with an inhibitor of the lymphotoxin pathway dramatically reduces scrapie susceptibility. J Virol. *77*, 6845-6854.

Madore,N., Smith,K.L., Graham,C.H., Jen,A., Brady,K., Hall,S., and Morris,R. (1999). Functionally different GPI proteins are organized in different domains on the neuronal surface. EMBO Journal *18*, 6917-6926.

Mallucci,G.R., Campbell,T.A., Dickinson,A., Beck,J., Holt,M., Plant,G., De Pauw,K.W., Hakin,R.N., Clarke,C.E., Howell,S., Davies-Jones,G.A.B., Lawden,M., Smith,C.M.L., Ince,P., Ironside,J.W., Bridges,L.R., Dean,A., Weeks,I., and Collinge,J. (1999). Inherited prion disease with an alanine to valine mutation at codon 117 in the prion protein gene. Brain *122*, 1823-1837.

Mallucci,G.R., Ratté,S., Asante,E.A., Linehan,J., Gowland,I., Jefferys,J.G.R., and Collinge,J. (2002). Post-natal knockout of prion protein alters hippocampal CA1 properties, but does not result in neurodegeneration. EMBO Journal *21*, 202-210.

Mallucci,G.R., Dickinson,A., Linehan,J., Klohn,P.C., Brandner,S., and Collinge,J. (2003). Depleting neuronal PrP in prion infection prevents disease and reverses spongiosis. Science *302*, 871-874.

Mallucci,G.R., White,M.D., Farmer,M., Dickinson,A., Khatun,H., Powell,A.D., Brandner,S., Jefferys,J.G., and Collinge,J. (2007). Targeting cellular prion protein reverses early cognitive deficits and neurophysiological dysfunction in prion-infected mice. Neuron *53*, 325-335.

Mange,A., Milhavet,O., Umlauf,D., Harris,D., and Lehmann,S. (2002). PrP-dependent cell adhesion in N2a neuroblastoma cells. FEBS Lett. *514*, 159-162.

REFERENCES

Manson,J., West,J.D., Thomson,V., McBride,P., Kaufman,M.H., and Hope,J. (1992). The prion protein gene: a role in mouse embryogenesis? Development *115*, 117-122.

Manson,J.C., Clarke,A.R., Hooper,M.L., Aitchison,L., McConnell,I., and Hope,J. (1994a). 129/Ola mice carrying a null mutation in PrP that abolishes mRNA production are developmentally normal. Mol.Neurobiol. *8*, 121-127.

Manson,J.C., Clarke,A.R., McBride,P.A., McConnell,I., and Hope,J. (1994b). PrP gene dosage determines the timing but not the final intensity or distribution of lesions in scrapie pathology. Neurodegeneration *3*, 331-340.

Manson,J.C., Hope,J., Clarke,A.R., Johnston,A., Black,C., and MacLeod,N. (1995). PrP gene dosage and long term potentiation. Neurodegeneration *4*, 113-114.

Manuelidis,L., Fritch,W., and Xi,Y.-G. (1997). Evolution of a strain of CJD that induces BSE-like plaques. Science *277*, 94-98.

Martinez,J., Patkaniowska,A., Urlaub,H., Luhrmann,R., and Tuschl,T. (2002). Single-stranded antisense siRNAs guide target RNA cleavage in RNAi. Cell *110*, 563-574.

Martinez-Lage,J.F., Poza,M., Sola,J., Tortosa,J.G., Brown,P., Cervenakova,L., Esteban,J.A., and Mendoza,A. (1994). Accidental transmission of Creutzfeldt-Jakob disease by dural cadaveric grafts. J. Neurol. Neurosurg.Psychiatry *57*, 1091-1094.

Masullo,C., Macchi,G., Xi,Y.G., and Pocchiari,M. (1992). Failure to ameliorate Creutzfeldt-Jakob disease with amphotericin B therapy. J.Infect.Dis. *165*, 784-785.

Matranga,C., Tomari,Y., Shin,C., Bartel,D.P., and Zamore,P.D. (2005). Passenger-strand cleavage facilitates assembly of siRNA into Ago2-containing RNAi enzyme complexes. Cell *123*, 607-620.

Matzke,M.A., Matzke,A.J., Pruss,G.J., and Vance,V.B. (2001). RNA-based silencing strategies in plants. Curr.Opin.Genet.Dev. *11*, 221-227.

McKay,R. (1997). Stem cells in the central nervous system. Science *276*, 66-71.

McKinley,M.P., Bolton,D.C., and Prusiner,S.B. (1983). A protease-resistant protein is a structural component of the scrapie prion. Cell *35*, 57-62.

McKinley,M.P., Lingappa,V.R., and Prusiner,S.B. (1988). Developmental regulation of prion protein mRNA in brain. Ciba.Found.Symp. *135*, 101-116.

McManus,M.T. and Sharp,P.A. (2002). Gene silencing in mammals by small interfering RNAs. Nat.Rev.Genet. *3*, 737-747.

Mead,S. (2006). Prion Disease Genetics. European Journal of Human Genetics *14*, 273-281.

REFERENCES

Meister,G. and Tuschl,T. (2004). Mechanisms of gene silencing by double-stranded RNA. Nature *431*, 343-349.

Mellon,P.L., Windle,J.J., Goldsmith,P.C., Padula,C.A., Roberts,J.L., and Weiner,R.I. (1990). Immortalization of hypothalamic GnRH neurons by genetically targeted tumorigenesis. Neuron *5*, 1-10.

Merlin,G., Chebath,J., Benech,P., Metz,R., and Revel,M. (1983). Molecular cloning and sequence of partial cDNA for interferon-induced (2'-5')oligo(A) synthetase mRNA from human cells. Proc.Natl.Acad.Sci.U.S.A *80*, 4904-4908.

Meyer,P. (1996). Repeat-induced gene silencing: common mechanisms in plants and fungi. Biological Chemistry Hoppe-Seyler *377*, 87-95.

Miyoshi,H., Blomer,U., Takahashi,M., Gage,F.H., and Verma,I.M. (1998). Development of a self-inactivating lentivirus vector. J.Virol. *72*, 8150-8157.

Mobley,W.C., Neve,R.L., Prusiner,S.B., and McKinley,M.P. (1988). Nerve growth factor increases mRNA levels for the prion protein and the beta-amyloid protein precursor in developing hamster brain. Proc.Natl.Acad.Sci.U.S.A. *85*, 9811-9815.

Montgomery,M.K., Xu,S., and Fire,A. (1998). RNA as a target of double-stranded RNA-mediated genetic interference in Caenorhabditis elegans. Proc.Natl.Acad.Sci.U.S.A *95*, 15502-15507.

Moore,R.A., Vorberg,I., and Priola,S.A. (2005). Species barriers in prion diseases--brief review. Arch.Virol.Suppl 187-202.

Moore,R.C., Lee,I.Y., Silverman,G.L., Harrison,P.M., Strome,R., Heinrich,C., Karunaratne,A., Pasternak,S.H., Chishti,M.A., Liang,Y., Mastrangelo,P., Wang,K., Smit,A.F.A., Katamine,S., Carlson,G.A., Cohen,F.E., Prusiner,S.B., Melton,D.W., Tremblay,P., Hood,L.E., and Westaway,D. (1999). Ataxia in prion protein (PrP)-deficient mice is associated with upregulation of the novel PrP-like protein Doppel. Journal of Molecular Biology *292*, 797-817.

Mouillet-Richard,S., Ermonval,M., Chebassier,C., Laplanche,J.L., Lehmann,S., Launay,J.M., and Kellermann,O. (2000). Signal transduction through prion protein. Science *289*, 1925-1928.

Naldini,L., Blomer,U., Gage,F.H., Trono,D., and Verma,I.M. (1996a). Efficient transfer, integration, and sustained long-term expression of the transgene in adult rat brains injected with a lentiviral vector. Proc.Natl.Acad.Sci.U.S.A *93*, 11382-11388.

Naldini,L., Blomer,U., Gallay,P., Ory,D., Mulligan,R., Gage,F.H., Verma,I.M., and Trono,D. (1996b). In vivo gene delivery and stable transduction of nondividing cells by a lentiviral vector. Science *272*, 263-267.

REFERENCES

Napoli,C., Lemieux,C., and Jorgensen,R. (1990). Introduction of a Chimeric Chalcone Synthase Gene into Petunia Results in Reversible Co-Suppression of Homologous Genes in trans. Plant Cell *2*, 279-289.

Nykanen,A., Haley,B., and Zamore,P.D. (2001). ATP requirements and small interfering RNA structure in the RNA interference pathway. Cell *107*, 309-321.

O'Donovan,C.N., Tobin,D., and Cotter,T.G. (2001). Prion protein fragment PrP-(106-126) induces apoptosis via mitochondrial disruption in human neuronal SH-SY5Y cells. J Biol.Chem *276*, 43516-43523.

Oates,A.C., Bruce,A.E., and Ho,R.K. (2000). Too much interference: injection of double-stranded RNA has nonspecific effects in the zebrafish embryo. Developmental Biology *224*, 20-28.

Oesch,B., Westaway,D., Walchli,M., McKinley,M.P., Kent,S.B., Aebersold,R., Barry,R.A., Tempst,P., Teplow,D.B., Hood,L.E., and Raeber,A.J. (1985). A cellular gene encodes scrapie PrP 27-30 protein. Cell *40*, 735-746.

Paddison,P.J., Caudy,A.A., and Hannon,G.J. (2002). Stable suppression of gene expression by RNAi in mammalian cells. Proc.Natl.Acad.Sci.U.S.A *99*, 1443-1448.

Palmer,M.S., Dryden,A.J., Hughes,J.T., and Collinge,J. (1991). Homozygous prion protein genotype predisposes to sporadic Creutzfeldt-Jakob disease. Nature *352*, 340-342.

Pan,D., Gunther,R., Duan,W., Wendell,S., Kaemmerer,W., Kafri,T., Verma,I.M., and Whitley,C.B. (2002). Biodistribution and toxicity studies of VSVG-pseudotyped lentiviral vector after intravenous administration in mice with the observation of in vivo transduction of bone marrow. Mol Ther. *6*, 19-29.

Pan,K.-M., Baldwin,M.A., Nguyen,J., Gasset,M., Serban,A., Groth,D., Mehlhorn,I., Huang,Z., Fletterick,R.J., Cohen,F.E., and Prusiner,S.B. (1993). Conversion of α-helices into β-sheets features in the formation of the scrapie prion proteins. Proc Natl Acad Sci U.S.A *90*, 10962-10966.

Parchi,P., Zou,W.Q., Wang,W., Brown,P., Capellari,S., Ghetti,B., Kopp,N., Schulz-Schaeffer,W.J., Kretzschmar,H.A., Head,M.W., Ironside,J.W., Gambetti,P., and Chen,S.G. (2000). Genetic influence on the structural variations of the abnormal prion protein. Proc.Natl.Acad Sci U.S.A *97*, 10168-10172.

Pasquinelli,A.E., Reinhart,B.J., Slack,F., Martindale,M.Q., Kuroda,M.I., Maller,B., Hayward,D.C., Ball,E.E., Degnan,B., Muller,P., Spring,J., Srinivasan,A., Fishman,M., Finnerty,J., Corbo,J., Levine,M., Leahy,P., Davidson,E., and Ruvkun,G. (2000). Conservation of the sequence and temporal expression of let-7 heterochronic regulatory RNA. Nature *408*, 86-89.

REFERENCES

Pauly,P.C. and Harris,D.A. (1998). Copper stimulates endocytosis of the prion protein. J Biol.Chem *273*, 33107-33110.

Pebernard,S. and Iggo,R.D. (2004). Determinants of interferon-stimulated gene induction by RNAi vectors. Differentiation *72*, 103-111.

Peden,A.H., Head,M.W., Ritchie,D.L., Bell,J.E., and Ironside,J.W. (2004). Preclinical vCJD after blood transfusion in a *PRNP* codon 129 heterozygous patient. Lancet *364*, 527-529.

Peretz,D., Williamson,R.A., Kaneko,K., Vergara,J., Leclerc,E., Schmitt-Ulms,G., Mehlhorn,I.R., Legname,G., Wormald,M.R., Rudd,P.M., Dwek,R.A., Burton,D.R., and Prusiner,S.B. (2001). Antibodies inhibit prion propagation and clear cell cultures of prion infectivity. Nature *412*, 739-743.

Persengiev,S.P., Zhu,X., and Green,M.R. (2004). Nonspecific, concentration-dependent stimulation and repression of mammalian gene expression by small interfering RNAs (siRNAs). RNA. *10*, 12-18.

Pfeifer,A., Eigenbrod,S., Al Khadra,S., Hofmann,A., Mitteregger,G., Moser,M., Bertsch,U., and Kretzschmar,H. (2006). Lentivector-mediated RNAi efficiently suppresses prion protein and prolongs survival of scrapie-infected mice. J.Clin.Invest *116*, 3204-3210.

Prinz,M., Heikenwalder,M., Junt,T., Schwarz,P., Glatzel,M., Heppner,F.L., Fu,Y.X., Lipp,M., and Aguzzi,A. (2003). Positioning of follicular dendritic cells within the spleen controls prion neuroinvasion. Nature.

Prusiner,S.B. (1982). Novel proteinaceous infectious particles cause scrapie. Science *216*, 136-144.

Prusiner,S.B. (1989). Scrapie Prions. Annual Review Microbiology *43*, 345-374.

Prusiner,S.B. (1991). Molecular Biology of Prion Diseases. Science *252*, 1515-1522.

Prusiner,S.B. (1997). Prion diseases and the BSE crisis. Science *278*, 245-251.

Prusiner,S.B. (1998). Prions. Proc Natl Acad Sci U.S.A. *95*, 13363-13383.

Prusiner,S.B., Groth,D.F., Bolton,D.C., Kent,S.B., and Hood,L.E. (1984). Purification and structural studies of a major scrapie prion protein. Cell *38*, 127-134.

Prusiner,S.B., Scott,M., Foster,D., Pan,K.M., Groth,D., Mirenda,C., Torchia,M., Yang,S.L., Serban,D., Carlson,G.A., and Raeber,A.J. (1990). Transgenetic studies implicate interactions between homologous PrP isoforms in scrapie prion replication. Cell *63*, 673-686.

Puckett,C., Concannon,P., Casey,C., and Hood,L. (1991). Genomic Structure of the Human Prion Protein Gene. Am.J Hum.Genet. *49*, 320-329.

Race,R. and Chesebro,B. (1998). Scrapie infectivity found in resistant species. Nature *392*, 770.

Ralph,G.S., Radcliffe,P.A., Day,D.M., Carthy,J.M., Leroux,M.A., Lee,D.C., Wong,L.F., Bilsland,L.G., Greensmith,L., Kingsman,S.M., Mitrophanous,K.A., Mazarakis,N.D., and Azzouz,M. (2005). Silencing mutant SOD1 using RNAi protects against neurodegeneration and extends survival in an ALS model. Nat Med *11*, 429-433.

Rand,T.A., Petersen,S., Du,F., and Wang,X. (2005). Argonaute2 cleaves the anti-guide strand of siRNA during RISC activation. Cell *123*, 621-629.

Rane,N.S., Yonkovich,J.L., and Hegde,R.S. (2004). Protection from cytosolic prion protein toxicity by modulation of protein translocation. EMBO Journal. *23*, 4550-4559.

Raoul,C., Abbas-Terki,T., Bensadoun,J.C., Guillot,S., Haase,G., Szulc,J., Henderson,C.E., and Aebischer,P. (2005). Lentiviral-mediated silencing of SOD1 through RNA interference retards disease onset and progression in a mouse model of ALS. Nature Medicine *11*, 423-428.

Raymond,G.J., Hope,J., Kocisko,D.A., Priola,S.A., Raymond,L.D., Bossers,A., Ironside,J., Will,R.G., Chen,S.G., Petersen,R.B., Gambetti,P., Rubenstein,R., Smits,M.A., Lansbury,P.T.Jr., and Caughey,B. (1997). Molecular assessment of the potential transmissibilities of BSE and scrapie to humans. Nature *388*, 285-288.

Reinhart,B.J., Slack,F.J., Basson,M., Pasquinelli,A.E., Bettinger,J.C., Rougvie,A.E., Horvitz,H.R., and Ruvkun,G. (2000). The 21-nucleotide let-7 RNA regulates developmental timing in Caenorhabditis elegans. Nature *403*, 901-906.

Reynolds,A., Leake,D., Boese,Q., Scaringe,S., Marshall,W.S., and Khvorova,A. (2004a). Rational siRNA design for RNA interference
Nat Biotechnol. *22*, 326-330.

Riek,R., Hornemann,S., Wider,G., Billeter,M., Glockshuber,R., and Wuthrich,K. (1996). NMR structure of the mouse prion protein domain PrP (121-231). Nature *382*, 180-182.

Riek,R., Hornemann,S., Wider,G., Glockshuber,R., and Wüthrich,K. (1997). NMR characterization of the full-length recombinant murine prion protein, *m*PrP(23-231). FEBS Lett. *413*, 282-288.

Riek,R., Wider,G., Billeter,M., Hornemann,S., Glockshuber,R., and Wuthrich,K. (1998). Prion protein NMR structure and familial human spongiform encephalopathies. Proc Natl Acad Sci U.S.A. *95*, 11667-11672.

Riesner,D., Kellings,K., Post,K., Wille,H., Serban,H., Groth,D., Baldwin,M.A., and Prusiner,S.B. (1996). Disruption of prion rods generates 10-nm spherical particles having high α-helical content and lacking scrapie infectivity. J.Virol. *70*, 1714-1722.

REFERENCES

Rivas,F.V., Tolia,N.H., Song,J.J., Aragon,J.P., Liu,J., Hannon,G.J., and Joshua-Tor,L. (2005). Purified Argonaute2 and an siRNA form recombinant human RISC. Nat.Struct.Mol.Biol. *12*, 340-349.

Rodriguez-Lebron,E., Denovan-Wright,E.M., Nash,K., Lewin,A.S., and Mandel,R.J. (2005). Intrastriatal rAAV-mediated delivery of anti-huntingtin shRNAs induces partial reversal of disease progression in R6/1 Huntington's disease transgenic mice. Mol.Ther. *12*, 618-633.

Rossi,D., Cozzio,A., Flechsig,E., Klein,M.A., Rülicke,T., Aguzzi,A., and Weissmann,C. (2001). Onset of ataxia and Purkinje cell loss in PrP null mice inversely correlated with Dpl level in brain. EMBO Journal *20*, 694-702.

Roucou,X., Guo,Q., Zhang,Y., Goodyer,C.G., and LeBlanc,A.C. (2003). Cytosolic prion protein is not toxic and protects against Bax-mediated cell death in human primary neurons. J Biol.Chem.

Rubenstein,R., Carp,R.I., and Callahan,S.M. (1984). In vitro replication of scrapie agent in a neuronal model: infection of PC12 cells. J Gen.Virol. *65*, 2191-2198.

Rubinson,D.A., Dillon,C.P., Kwiatkowski,A.V., Sievers,C., Yang,L., Kopinja,J., Rooney,D.L., Ihrig,M.M., McManus,M.T., Gertler,F.B., Scott,M.L., and Van Parijs,L. (2003). A lentivirus-based system to functionally silence genes in primary mammalian cells, stem cells and transgenic mice by RNA interference
Nat Genet *33*, 401-406.

Rudd,P.M., Wormald,M.R., Wing,D.R., Prusiner,S.B., and Dwek,R.A. (2001). Prion glycoprotein: Structure, dynamics, and roles for the sugars. Biochemistry *40*, 3759-3766.

Safar,J.G., DeArmond,S.J., Kociuba,K., Deering,C., Didorenko,S., Bouzamondo-Bernstein,E., Prusiner,S.B., and Tremblay,P. (2005). Prion clearance in bigenic mice. J Gen Virol. *86*, 2913-2923.

Sakaguchi,S., Katamine,S., Nishida,N., Moriuchi,R., Shigematsu,K., Sugimoto,T., Nakatani,A., Kataoka,Y., Houtani,T., Shirabe,S., Okada,H., Hasegawa,S., Miyamoto,T., and Noda,T. (1996). Loss of cerebellar Purkinje cells in aged mice homozygous for a disrupted PrP gene. Nature *380*, 528-531.

Samuel,C.E. (2001). Antiviral actions of interferons. Clinical Microbiology Reviews *14*, 778-809.

Sapru,M.K., Yates,J.W., Hogan,S., Jiang,L., Halter,J., and Bohn,M.C. (2006). Silencing of human alpha-synuclein in vitro and in rat brain using lentiviral-mediated RNAi. Experimental Neurology *198*, 382-390.

Sarafoff,N.I., Bieschke,J., Giese,A., Weber,P., Bertsch,U., and Kretzschmar,H.A. (2005). Automated PrPres amplification using indirect sonication. J Biochem.Biophys.Methods.

REFERENCES

Scacheri,P.C., Rozenblatt-Rosen,O., Caplen,N.J., Wolfsberg,T.G., Umayam,L., Lee,J.C., Hughes,C.M., Shanmugam,K.S., Bhattacharjee,A., Meyerson,M., and Collins,F.S. (2004). Short interfering RNAs can induce unexpected and divergent changes in the levels of untargeted proteins in mammalian cells. Proc.Natl.Acad.Sci.U.S.A *101*, 1892-1897.

Schmitt-Ulms,G., Legname,G., Baldwin,M.A., Ball,H.L., Bradon,N., Bosque,P.J., Crossin,K.L., Edelman,G.M., DeArmond,S.J., Cohen,F.E., and Prusiner,S.B. (2001). Binding of neural cell adhesion molecules (N-CAMs) to the cellular prion protein. Journal of Molecular Biology *314*, 1209-1225.

Schwarz,A., Kratke,O., Burwinkel,M., Riemer,C., Schultz,J., Henklein,P., Bamme,T., and Baier,M. (2003). Immunisation with a synthetic prion protein-derived peptide prolongs survival times of mice orally exposed to the scrapie agent. Neurosci.Lett. *350*, 187-189.

Schwarz,D.S., Ding,H., Kennington,L., Moore,J.T., Schelter,J., Burchard,J., Linsley,P.S., Aronin,N., Xu,Z., and Zamore,P.D. (2006). Designing siRNA that distinguish between genes that differ by a single nucleotide. PLoS.Genet. *2*, e140.

Scott,M.R., Will,R., Ironside,J., Nguyen,H.O.B., Tremblay,P., DeArmond,S.J., and Prusiner,S.B. (1999). Compelling transgenetic evidence for transmission of bovine spongiform encephalopathy prions to humans. Proc.Natl.Acad Sci U.S.A *96*, 15137-15142.

Shen,J., Samul,R., Silva,R.L., Akiyama,H., Liu,H., Saishin,Y., Hackett,S.F., Zinnen,S., Kossen,K., Fosnaugh,K., Vargeese,C., Gomez,A., Bouhana,K., Aitchison,R., Pavco,P., and Campochiaro,P.A. (2006). Suppression of ocular neovascularization with siRNA targeting VEGF receptor 1. Gene Ther. *13*, 225-234.

Shmerling,D., Hegyi,I., Fischer,M., Blättler,T., Brandner,S., Götz,J., Rülicke,T., Flechsig,E., Cozzio,A., von Mering,C., Hangartner,C., Aguzzi,A., and Weissmann,C. (1998). Expression of amino-terminally truncated PrP in the mouse leading to ataxia and specific cerebellar lesions. Cell *93*, 203-214.

Shyng,S.-L., Huber,M.T., and Harris,D.A. (1993). A prion protein cycles between the cell surface and an endocytic compartment in cultured neuroblastoma cells. J Biol.Chem. *268 (21)*, 15922-15928.

Si,K., Lindquist,S., and Kandel,E.R. (2003). A Neuronal Isoform of the Aplysia CPEB Has Prion-Like Properties. Cell *115*, 879-891.

Sigurdsson,E.M., Brown,D.R., Daniels,M., Kascsak,R.J., Kascsak,R., Carp,R., Meeker,H.C., Frangione,B., and Wisniewski,T. (2002). Immunization delays the onset of prion disease in mice. Am.J.Pathol. *161*, 13-17.

REFERENCES

Sikorska,B., Liberski,P.P., Giraud,P., Kopp,N., and Brown,P. (2004). Autophagy is a part of ultrastructural synaptic pathology in Creutzfeldt-Jakob disease: a brain biopsy study. Int.J Biochem.Cell Biol *36*, 2563-2573.

Silveira,J.R., Raymond,G.J., Hughson,A.G., Race,R.E., Sim,V.L., Hayes,S.F., and Caughey,B. (2005). The most infectious prion protein particles. Nature *437*, 257-261.

Singer,O., Marr,R.A., Rockenstein,E., Crews,L., Coufal,N.G., Gage,F.H., Verma,I.M., and Masliah,E. (2005). Targeting BACE1 with siRNAs ameliorates Alzheimer disease neuropathology in a transgenic model. Nat Neurosci. *8*, 1343-1349.

Sirven,A., Ravet,E., Charneau,P., Zennou,V., Coulombel,L., Guetard,D., Pflumio,F., and Dubart-Kupperschmitt,A. (2001). Enhanced transgene expression in cord blood CD34(+)-derived hematopoietic cells, including developing T cells and NOD/SCID mouse repopulating cells, following transduction with modified trip lentiviral vectors. Mol.Ther. *3*, 438-448.

Sledz,C.A., Holko,M., de Veer,M.J., Silverman,R.H., and Williams,B.R. (2003). Activation of the interferon system by short-interfering RNAs. Nat.Cell Biol. *5*, 834-839.

Solforosi,L., Criado,J.R., McGavern,D.B., Wirz,S., Sanchez-Alavez,M., Sugama,S., DeGiorgio,L.A., Volpe,B.T., Wiseman,E., Abalos,G., Masliah,E., Gilden,D., Oldstone,M.B., Conti,B., and Williamson,R.A. (2004). Cross-Linking Cellular Prion Protein Triggers Neuronal Apoptosis in Vivo. Science *303*, 1514-1516.

Song,J.J., Smith,S.K., Hannon,G.J., and Joshua-Tor,L. (2004). Crystal structure of Argonaute and its implications for RISC slicer activity. Science *305*, 1434-1437.

Sontheimer,E.J. (2005). Assembly and function of RNA silencing complexes. Nat.Rev.Mol.Cell Biol. *6*, 127-138.

Sparkes,R.S., Simon,M., Cohn,V.H., Fournier,R.E., Lem,J., Klisak,I., Heinzmann,C., Blatt,C., Lucero,M., Mohandas,T., and Raeber,A.J. (1986). Assignment of the human and mouse prion protein genes to homologous chromosomes. Proc.Natl.Acad.Sci.U.S.A. *83*, 7358-7362.

Spielhaupter,C. and Schatzl,H.M. (2001). PrPC directly interacts with proteins involved in signaling pathways. J.Biol.Chem. *276*, 44604-44612.

Stahl,N., Baldwin,M.A., Teplow,D.B., Hood,L., Gibson,B.W., Burlingame,A.L., and Prusiner,S.B. (1993). Structural Studies of the scrapie prion protein using mass spectrometry and amino acid sequencing. Biochemistry *32*, 1991-2002.

Stahl,N., Borchelt,D.R., Hsiao,K., and Prusiner,S.B. (1987). Scrapie prion protein contains a phosphatidylinositol glycolipid. Cell *51*, 229-240.

Stahl,N. and Prusiner,S.B. (1991). Prions and prion proteins. FASEB Journal *5*, 2799-2807.

Stark,G.R., Kerr,I.M., Williams,B.R., Silverman,R.H., and Schreiber,R.D. (1998). How cells respond to interferons. Annual Review of Biochemistry *67*, 227-264.

Stewart,R.S., Piccardo,P., Ghetti,B., and Harris,D.A. (2005). Neurodegenerative illness in transgenic mice expressing a transmembrane form of the prion protein. J Neurosci. *25*, 3469-3477.

Sui,G., Soohoo,C., Affar,e.B., Gay,F., Shi,Y., Forrester,W.C., and Shi,Y. (2002). A DNA vector-based RNAi technology to suppress gene expression in mammalian cells. Proc.Natl.Acad.Sci.U.S.A *99*, 5515-5520.

Supattapone,S., Nguyen,H.O.B., Cohen,F.E., Prusiner,S.B., and Scott,M.R. (1999). Elimination of prions by branched polyamines and implications for therapeutics. Proc.Natl.Acad Sci U.S.A *96*, 14529-14534.

Svoboda,P., Stein,P., Hayashi,H., and Schultz,R.M. (2000). Selective reduction of dormant maternal mRNAs in mouse oocytes by RNA interference. Development *127*, 4147-4156.

Tan,P.H., Yang,L.C., Shih,H.C., Lan,K.C., and Cheng,J.T. (2005). Gene knockdown with intrathecal siRNA of NMDA receptor NR2B subunit reduces formalin-induced nociception in the rat. Gene Ther. *12*, 59-66.

Taraboulos,A., Raeber,A., Borchelt,D.R., Serban,D., and Prusiner,S.B. (1992). Synthesis and trafficking of prion proteins in cultured cells. Molecular Biology of the Cell *3*, 851-863.

Tateishi,J., Brown,P., Kitamoto,T., Hoque,Z.M., Roos,R., Wollman,R., Cervenakova,L., and Gajdusek,D.C. (1995). First experimental transmission of fatal familial insomnia. Nature *376*, 434-435.

Taylor,D.M., McConnell,I., and Ferguson,C.E. (2000). Closely similar values obtained when the ME7 strain of scrapie agent was titrated in parallel by two individuals in separate laboratories using two sublines of C57BL mice. Journal of Virological Methods *86*, 35-40.

Thackray,A.M., Klein,M.A., Aguzzi,A., and Bujdoso,R. (2002). Chronic subclinical prion disease induced by low-dose inoculum in the brain. J.Virol. *76*, 2510-2517.

Thackray,A.M., Klein,M.A., and Bujdoso,R. (2003). Subclinical prion disease induced by oral inoculation. J Virol. *77*, 7991-7998.

Thakker,D.R., Natt,F., Husken,D., Maier,R., Muller,M., van der,P.H., Hoyer,D., and Cryan,J.F. (2004). Neurochemical and behavioral consequences of widespread gene knockdown in the adult mouse brain by using nonviral RNA interference. Proc Natl Acad Sci U S A *101*, 17270-17275.

Thomas,C.E., Ehrhardt,A., and Kay,M.A. (2003). Progress and problems with the use of viral vectors for gene therapy. Nat.Rev.Genet. *4*, 346-358.

Tilly,G., Chapuis,J., Vilette,D., Laude,H., and Vilotte,J.L. (2003). Efficient and specific down-regulation of prion protein expression by RNAi. Biochem.Biophys.Res.Commun. *305*, 548-551.

Tobler,I., Gaus,S.E., Deboer,T., Achermann,P., Fischer,M., Rulicke,T., Moser,M., Oesch,B., McBride,P.A., and Manson,J.C. (1996). Altered circadian activity rhythms and sleep in mice devoid of prion protein. Nature *380*, 639-642.

Todd,N.V., Morrow,J., Doh-ura,K., Dealler,S., O'hare,S., Farling,P., Duddy,M., and Rainov,N.G. (2005). Cerebroventricular infusion of pentosan polysulphate in human variant Creutzfeldt-Jakob disease. J Infect. *50*, 394-396.

Tomari,Y., Matranga,C., Haley,B., Martinez,N., and Zamore,P.D. (2004). A protein sensor for siRNA asymmetry. Science *306*, 1377-1380.

Tranchant,C., Doh-ura,K., Warter,J.M., Steinmetz,G., Chevalier,Y., Hanauer,A., Kitamoto,T., and Tateishi,J. (1992). Gerstmann-Sträussler-Scheinker disease in an Alsatian family: Clinical and genetic studies. Journal of Neurology, Neurosurgery and Psychiatry *55*, 185-187.

Tranulis,M.A. (2002). Influence of the prion protein gene, Prnp, on scrapie susceptibility in sheep. APMIS *110*, 33-43.

Tremblay,P., Meiner,Z., Galou,M., Heinrich,C., Petromilli,C., Lisse,T., Cayetano,J., Torchia,M., Mobley,W., Bujard,H., DeArmond,S.J., and Prusiner,S.B. (1998). Doxycycline control of prion protein transgene expression modulates prion disease in mice. Proc Natl Acad Sci U.S.A *95*, 12580-12585.

Trevitt,C.R. and Collinge,J. (2006). A systematic review of prion therapeutics in experimental models. Brain *129*, 2241-2265.

Tsuchiya,S., Okuno,Y., and Tsujimoto,G. (2006). MicroRNA: biogenetic and functional mechanisms and involvements in cell differentiation and cancer. J.Pharmacol.Sci. *101*, 267-270.

Tuschl,T., Zamore,P.D., Lehmann,R., Bartel,D.P., and Sharp,P.A. (1999). Targeted mRNA degradation by double-stranded RNA in vitro. Genes Dev. *13*, 3191-3197.

Vance,V. and Vaucheret,H. (2001). RNA silencing in plants--defense and counterdefense. Science *292*, 2277-2280.

Vey,M., Pilkuhn,S., Wille,H., Nixon,R., DeArmond,S.J., Smart,E.J., Anderson,R.G.W., Taraboulos,A., and Prusiner,S.B. (1996). Subcellular colocalization of the cellular and scrapie prion proteins in caveolae-like membranous domains. Proc.Natl.Acad Sci U.S.A *93*, 14945-14949.

Wang,X., Wang,F., Sy,M.S., and Ma,J. (2004). Calpain and other cytosolic proteases can contribute to the degradation of retro-translocated prion protein in the cytosol. J Biol chem.

Wang,Y.L., Liu,W., Wada,E., Murata,M., Wada,K., and Kanazawa,I. (2005). Clinico-pathological rescue of a model mouse of Huntington's disease by siRNA. Neurosci.Res. *53*, 241-249.

Waterhouse,P.M., Wang,M.B., and Finnegan,E.J. (2001). Role of short RNAs in gene silencing. Trends Plant Sci. *6*, 297-301.

Weiner,R.I., Wetsel,W., Goldsmith,P., Martinez,d.l.E., Windle,J., Padula,C., Choi,A., Negro-Vilar,A., and Mellon,P. (1992). Gonadotropin-releasing hormone neuronal cell lines. Front Neuroendocrinol. *13*, 95-119.

Weissmann,C. (1996). Molecular biology of transmissible spongiform encephalopathies. FEBS Lett. *389*, 3-11.

Westaway,D., Cooper,C., Turner,S., Da Costa,M., Carlson,G.A., and Prusiner,S.B. (1994). Structure and polymorphism of the mouse prion protein gene. Proc.Natl.Acad Sci U.S.A *91*, 6418-6422.

Westaway,D., Goodman,P.A., Mirenda,C.A., McKinley,M.P., Carlson,G.A., and Prusiner,S.B. (1987). Distinct prion proteins in short and long scrapie incubation period mice. Cell *51*, 651-662.

Westaway,D. and Prusiner,S.B. (1986). Conservation of the cellular gene encoding the scrapie prion protein. Nucleic.Acids.Res. *14*, 2035-2044.

White,A.R., Enever,P., Tayebi,M., Mushens,R., Linehan,J., Brandner,S., Anstee,D., Collinge,J., and Hawke,S. (2003). Monoclonal antibodies inhibit prion replication and delay the development of prion disease. Nature *422*, 80-83.

Whittle,I.R., Knight,R.S., and Will,R.G. (2006). Unsuccessful intraventricular pentosan polysulphate treatment of variant Creutzfeldt-Jakob disease. Acta Neurochir.(Wien.) *148*, 677-679.

Wianny,F. and ernicka-Goetz,M. (2000). Specific interference with gene function by double-stranded RNA in early mouse development. Nature Cell Biology *2*, 70-75.

Will,R.G., Ironside,J.W., Zeidler,M., Cousens,S.N., Estibeiro,K., Alperovitch,A., Poser,S., Pocchiari,M., Hofman,A., and Smith,P.G. (1996). A new variant of Creutzfeldt-Jakob disease in the UK. Lancet *347*, 921-925.

Williams,B.R. (1999). PKR; a sentinel kinase for cellular stress. Oncogene *18*, 6112-6120.

Williams,E.S. and Young,S. (1993). Neuropathology of chronic wasting disease of mule deer (Odocoileus hemionus) and elk (Cervus elaphus nelsoni). Vet Pathology *30*, 36-45.

Wroe,S.J., Pal,S., Siddique,D., Hyare,H., Macfarlane,R., Joiner,S., Linehan,J.M., Brandner,S., Wadsworth,J.D., Hewitt,P., and Collinge,J. (2006). Clinical presentation and pre-mortem diagnosis of variant Creutzfeldt-Jakob disease associated with blood transfusion: a case report. Lancet *368*, 2061-2067.

Wyatt,J.M., Pearson,G.R., Smerdon,T.N., Gruffydd-Jones,T.J., Wells,G.A.H., and Wilesmith,J.W. (1991). Naturally occurring scrapie-like spongiform encephalopathy in five domestic cats. Vet.Rec. *129*, 233-236.

Xia,H., Mao,Q., Eliason,S.L., Harper,S.Q., Martins,I.H., Orr,H.T., Paulson,H.L., Yang,L., Kotin,R.M., and Davidson,B.L. (2004). RNAi suppresses polyglutamine-induced neurodegeneration in a model of spinocerebellar ataxia. Nature Medicine *10*, 816-820.

Xia,H., Mao,Q., Paulson,H.L., and Davidson,B.L. (2002). siRNA-mediated gene silencing in vitro and in vivo. Nat Biotechnol. *20*, 1006-1010.

Xia,X., Zhou,H., Huang,Y., and Xu,Z. (2006). Allele-specific RNAi selectively silences mutant SOD1 and achieves significant therapeutic benefit in vivo. Neurobiol.Dis. *23*, 578-586.

Zahn,R., Liu,A.Z., Lührs,T., Riek,R., Von Schroetter,C., García,F.L., Billeter,M., Calzolai,L., Wider,G., and Wüthrich,K. (2000). NMR solution structure of the human prion protein. Proc.Natl.Acad Sci U.S.A *97*, 145-150.

Zamore,P.D., Tuschl,T., Sharp,P.A., and Bartel,D.P. (2000). RNAi: double-stranded RNA directs the ATP-dependent cleavage of mRNA at 21 to 23 nucleotide intervals. Cell *101*, 25-33.

Zanata,S.M., Lopes,M.H., Mercadante,A.F., Hajj,G.N., Chiarini,L.B., Nomizo,R., Freitas,A.R., Cabral,A.L., Lee,K.S., Juliano,M.A., De Oliveira,E., Jachieri,S.G., Burlingame,A., Huang,L., Linden,R., Brentani,R.R., and Martins,V.R. (2002). Stress-inducible protein 1 is a cell surface ligand for cellular prion that triggers neuroprotection 27. EMBO Journal *21*, 3307-3316.

Zennou,V., Serguera,C., Sarkis,C., Colin,P., Perret,E., Mallet,J., and Charneau,P. (2001). The HIV-1 DNA flap stimulates HIV vector-mediated cell transduction in the brain. Nature Biotechnology *19*, 446-450.

Zhang,H., Kolb,F.A., Jaskiewicz,L., Westhof,E., and Filipowicz,W. (2004). Single processing center models for human Dicer and bacterial RNase III. Cell *118*, 57-68.

Zhao,Z., Cao,Y., Li,M., and Meng,A. (2001). Double-stranded RNA injection produces nonspecific defects in zebrafish. Developmental Biology *229*, 215-223.

Zheng,Y.H., Lovsin,N., and Peterlin,B.M. (2005). Newly identified host factors modulate HIV replication. Immunol.Lett. *97*, 225-234.

REFERENCES

Zimmermann,T.S., Lee,A.C., Akinc,A., Bramlage,B., Bumcrot,D., Fedoruk,M.N., Harborth,J., Heyes,J.A., Jeffs,L.B., John,M., Judge,A.D., Lam,K., McClintock,K., Nechev,L.V., Palmer,L.R., Racie,T., Rohl,I., Seiffert,S., Shanmugam,S., Sood,V., Soutschek,J., Toudjarska,I., Wheat,A.J., Yaworski,E., Zedalis,W., Koteliansky,V., Manoharan,M., Vornlocher,H.P., and MacLachlan,I. (2006). RNAi-mediated gene silencing in non-human primates. Nature *441*, 111-114.